

MICROFOSSIL TAPHONOMIC ANALYSIS OF OVERWASH DEPOSITS

**FORAMINIFERAL TAPHONOMY AS A PALEO-TSUNAMI AND
OVERWASH INDICATOR IN COASTAL ENVIRONMENTS -
EVIDENCE FROM OMAN AND THE BRITISH VIRGIN ISLANDS**

By

Jessica Erin Pilarczyk, B.Sc.

A Thesis

Submitted to the School of Graduate Studies

in Partial Fulfilment of the Requirements

for the Degree

Doctor of Philosophy

McMaster University

© Copyright by Jessica Erin Pilarczyk, April 2011

DOCTOR OF PHILOSOPHY (2011)
(Geography & Earth Sciences)

McMaster University
Hamilton, Ontario

TITLE: Foraminiferal taphonomy as a paleo-tsunami and overwash
indicator in coastal environments - evidence from Oman
and the British Virgin Islands

AUTHOR: Jessica E. Pilarczyk, B.Sc.
(McMaster University, Hamilton, Ontario, Canada, 2004)

SUPERVISOR: Professor Eduard G. Reinhardt

NUMBER OF PAGES: xix, 151 pp.

ABSTRACT

Historical records suggest that the coastlines of the British Virgin Islands (BVI) and the Sultanate of Oman have been subjected to catastrophic storm and tsunami events throughout recorded history. In 1945, a 7.8 magnitude earthquake ~100 km south of Karachi, Pakistan generated a tsunami that impacted the coast of Oman and resulted in over 4000 deaths. Although the 1945 tsunami deposit has been documented, no other paleo-tsunami deposits have been identified despite the fact that historical and paleo-seismic records suggest the contrary. Similarly, the north-eastern islands of the Caribbean, particularly Anegada, BVI, have been subjected to intense hurricane strikes over the past 300 years. Due to its position relative to the Atlantic Ocean and the Puerto Rico Trench, Anegada is a potential recorder of local (e.g. 1690, 1867) and trans-oceanic tsunami events (e.g. 1755 Lisbon) as well. Potential tsunami overwash events at both locations are expected to be intermingled with marine incursions resulting from major storms and Holocene sea level change.

Discerning between storm and tsunami overwash is problematic and usually favours a storm interpretation due to their frequency in the geologic record. This bias and lack of properly constrained geologic evidence has hindered the accuracy of tsunami prediction models, and subsequently, the assessment of seismic and tsunami hazards at both locations. Several studies employ the use of foraminifera to distinguish between storm and tsunami deposition; however, they are traditionally conducted in contrasting settings where differences between the terrestrial and marine realms are easily detected. Marine influenced settings lack the same degree of contrast; therefore, microfossil analysis alone is not effective.

This dissertation investigates the use of foraminiferal taphonomy as an overwash indicator in two types of coastal settings: 1. a siliclastic arid system lagoon (Sur, Sultanate of Oman), and 2. semi-tropical carbonate marine ponds (Anegada, British Virgin Islands). Although traditional microfossil taphonomic characteristics have been reported in some overwash studies, no multi-variate investigation into their usefulness as tsunami or storm indicators has previously been conducted. This dissertation shows that the surface condition (e.g. angularity, color, size, fragmentation, etc.) of foraminifera provides important information regarding the origin of overwash deposits and is useful in detecting older deposits at both locations when combined with other proxies.

Several important contributions have resulted from this research: 1. Taphofacies analysis helped to constrain sediment provenance and modern

nearshore hydrodynamics in an arid system lagoon that could not be achieved with traditional foraminiferal analysis alone. 2. The combined use of foraminiferal provenance and taphonomy was effective in identifying the 1945 Makran Trench tsunami at Sur Lagoon and will be a good indicator of older events at this location; a point which is particularly significant since no geologic evidence of previous tsunami events has ever been recorded. High abundances of predominantly marine taxa coupled with high abundances of large test sizes, fragments and fossil specimens were found to be indicators of tsunami deposition in contrast to lagoon deposition which was characterized by smaller test sizes and less robust lagoon taxa. 3. The preservation of the reefal dwelling *Homotrema rubrum*, a common encrusting foraminifer in Caribbean reef settings, provided the direction of origin of an overwash event deposited in marine ponds at Anegada and constrained the list of potential overwash candidates. Large and highly preserved *Homotrema* fragments that are typical of modern reef and storm wrack sediment were found in high abundances within Sand and Shell Sheet in three marine ponds at Anegada. A decrease in the abundance of highly preserved specimens from north to south throughout the ponds, coupled with mollusc taphonomic data strengthens a tsunami interpretation for the deposit.

This dissertation shows that taphofacies analysis has broad application to event stratigraphy in a variety of coastal systems. Although the application of taphonomic analysis between the two contrasting environments was widely different, in both cases, taphonomic data provided indicative information regarding the origin of deposition of overwash units at Anegada, BVI and Sur, Sultanate of Oman.

ACKNOWLEDGEMENTS

First and foremost I would like to thank my supervisor Dr. Eduard Reinhardt for not only offering much appreciated encouragement, direction and assistance throughout my PhD, but also for providing me my first introduction to SCUBA diving and shawarma. Multiple field seasons to Oman, as well as various other excursions provided unique research experiences that I will never forget. Thanks to you I will always remember the way to Masirah.

I also wish to express my sincere gratitude to my committee members, Dr. Joe Boyce and Dr. Henry Schwarcz; both of whom provided generous feedback on several manuscripts during the course of this thesis. Dr. Boyce is especially thanked for his involvement in field data collection and the creation of a DEM and surface PSD plots which appear in several chapters of this dissertation. This thesis was also greatly improved through many insightful comments by Dr. Jim Smith and Dr. Lisa Park.

Several people provided technical and logistical support, both in lab and in the field. Dr. Richard Rothaus and Dr. Simon Donato are greatly acknowledged for their involvement in data collection while on site in Oman, while Dr. Brian Atwater is sincerely thanked for providing significant guidance, editing and encouragement with both Anegada manuscripts. Martin Knyf provided assistance with isotopic analysis and Dr. Lisa Sonnenburg offered her expertise in plotting PSDs in Oasis Montaj™ on numerous occasions.

I was very fortunate to have had the help of three amazing undergraduate research assistants over the years. Alyson Brown assisted in petrographic analysis on the Anegada project, while Tomas Kosciuch and Shawn Kovacs each endured long hours running particle size data for the Oman work. For their commitment, insightful questions and most of all, enthusiasm, I am very thankful.

Several members of the Department of Geography and Earth Sciences provided immeasurable support. Past and present members of the McMaster MicroPaleo Laboratory (Simon, Pete, Jeremy, Shawn, Samira and Shakeel) are greatly acknowledged for their insight, conversations and friendship over the years. Dr. Jack Rink, my former Honours thesis supervisor, maintained a mentoring role during my years as a graduate student. His advice and support are greatly appreciated. Also, I cannot thank LouAnne Disher and Ann Wallace enough for their continued assistance.

I would like to thank friends and family who offered their unwavering support and encouragement over the years. Mom, Dad and Ryan always took interest in my academic endeavours and always let me know how proud they were. Laura Watt, Bianca Laudadio, Sonya Sidorkewicz and Rebecca Hewitson were also amazing sources of support throughout my time as a graduate student. Special mention goes out to my grandfather for making it to every one of my past graduations and for teaching me at an early age that doing well in school would open many doors. You were right.

Finally, I gratefully acknowledge the various sources of funding that supported this PhD research: (1) Natural Sciences and Engineering Research Council of Canada (NSERC) for a Post-Graduate Scholarship (CGM), (2) The Ontario Graduate Scholarship (OGS), (3) The Canadian Meteorological and Oceanographic Society (CMOS) Scholarship, (4) The Cushman Foundation for Foraminiferal Research (Loeblich and Tappan Student Research Award), (5) The Geological Society of America (GSA) for a Student Research Grant, and (6) The United Nations for a Student Research Grant.

TABLE OF CONTENTS

ABSTRACT	iii
ACKNOWLEDGEMENTS	v
TABLE OF CONTENTS	vii
LIST OF FIGURES	xi
LIST OF TABLES	xvii
PREFACE	xviii
CHAPTER 1: INTRODUCTION	1
1.1 Site selection	2
1.2 Research objectives	2
1.3 Dissertation structure	3
References	4
CHAPTER 2: ASSESSING SURFICIAL FORAMINIFERAL DISTRIBUTIONS AS AN OVERWASH INDICATOR IN SUR LAGOON, SULTANATE OF OMAN	6
Abstract	7
2.1 Introduction	8
2.1.1 Foraminifera and taphonomy	8
2.1.2 Regional setting	9
2.1.3 Tsunami overwash in Sur Lagoon	10
2.2 Materials and methods	11
2.2.1 Foraminiferal analysis	11
2.2.2 Stable isotopic analysis	12
2.2.3 Particle size analysis	13
2.3 Results	13
2.3.1 Bio- and taphofacies	13
2.3.1.1 Distal Lagoon Basin (BF _A , TF _A)	13
2.3.1.2 Main Lagoon Basin (BF _B , TF _B)	14
2.3.1.3 Shallow Marine Area (BF _C , TF _C)	15
2.3.2 Stable isotopes	15
2.3.3 Particle size	16
2.4 Discussion	16
2.4.1 Foraminiferal and taphonomic trends	16
2.4.2 Foraminiferal taphonomy as a potential overwash indicator	17
2.5 Conclusions	18

Acknowledgements	18
References	18
Appendices	23
2.A.1 Systematics of foraminifera	23
Chapter 2 Figures	24
Chapter 2 Tables	35
Chapter 2 Online supplementary data	37

CHAPTER 3: TESTING FORAMINIFERAL TAPHONOMY AS A TSUNAMI INDICATOR IN A SHALLOW ARID SYSTEM LAGOON: SUR, SULTANATE OF OMAN

	51
Abstract	52
3.1 Introduction	53
3.1.1 The 1945 Makran Trench tsunami	53
3.2 Regional setting	54
3.2.1 Sur Lagoon physiography	54
3.2.2 Recent cyclonic activity	55
3.2.3 Arabian Sea environments as tsunami indicators	56
3.3 Methods	56
3.4 Results	57
3.4.1 Previous shell and particle-size results	57
3.4.2 Previous foraminiferal results from surface samples	58
3.4.3 Foraminiferal character of the tsunami unit	58
3.5 Discussion	59
3.5.1 Allochthonous tests and size-sorting	60
3.5.2 Fragmentation	60
3.5.3 Relationships with bed geometry	61
3.5.4 The potential for documenting older events	62
3.6 Conclusions	63
Acknowledgements	63
References	63
Chapter 3 Figures	67
Chapter 3 Online supplementary data	73
Chapter 3 Tables	80

CHAPTER 4: *HOMOTREMA RUBRUM* (LAMARCK) TAPHONOMY AS AN OVERWASH INDICATOR IN MARINE PONDS ON ANEGADA, BRITISH VIRGIN ISLANDS

	88
Abstract	90

4.1 Introduction	91
4.1.1 <i>Homotrema rubrum</i> taphonomy	91
4.2 Site description	92
4.3 Event history	93
4.4 Methodology	94
4.4.1 Sample collection	94
4.4.2 Taphonomic analysis	94
4.4.3 Particle-size analysis (PSD)	95
4.5 Results	95
4.5.1 Stratigraphy and particle-size distributions (PSDs)	95
4.5.2 <i>Homotrema</i> taphonomy	97
4.6 Discussion	98
4.7 Conclusions	99
Acknowledgements	100
References	100
Chapter 4 Figures	104
Chapter 4 Tables	112

CHAPTER 5: PROBABLE TSUNAMI ORIGIN FOR A SHELL AND SAND SHEET FROM MARINE PONDS ON ANEGADA, BRITISH VIRGIN ISLANDS

Abstract	118
5.1 Introduction	120
5.2 Setting	121
5.3 Shell taphonomy	122
5.4 Methods	123
5.5 Results	124
5.5.1 Stratigraphy and molluskan ecology	125
5.5.2 Former marine pond shell bed and reef-flat storm wrack comparisons	126
5.5.3 Pond taphonomic and stratigraphic trends	127
5.5.4 Radiocarbon dates	128
5.6 Discussion	129
5.6.1 Pond taphonomic processes	129
5.6.2 Does the Shell and Sand Sheet represent an event bed?	129
5.6.3 Shell and Sand Sheet characteristics and a tsunami origin	130
5.6.4 Hurricane considerations	132
5.6.5 Stratigraphic comparisons	133
5.7 Conclusions	133
Acknowledgements	134

References	134
Chapter 5 Figures	139
Chapter 5 Tables	145
CHAPTER 6: SUMMARY AND CONCLUSIONS	147
6.1 Addressing the central research questions	147
References	150

LIST OF FIGURES

All figures are located in consecutive manner at the end of each chapter, as per the general style required for manuscript submission to peer-reviewed journals.

CHAPTER 2

Figure 2.1: Location of Sur Lagoon relative to the Makran Subduction Zone (MSZ). Epicentre of the 28 November 1945 tsunamigenic earthquake (M_w 8.1; black star) and broad-scale geologic features within Oman indicated.....24

Figure 2.2: **a)** Satellite image of Sur Lagoon obtained from Google Earth. **b)** Digital Elevation Model (DEM) of the study area using data collected with a Trimble R3 unit and a Lowrance SONAR. **c)** Sedimentary sub-environments within the lagoon. Colors correspond to varying lithofacies identified during field survey, DEM analysis, and satellite imagery. **d)** Location of surface samples used in the foraminiferal analysis. Nodes at the base of the entrance channel and at the Main – Distal Lagoon boundary were used to calculate the distance of each sample location relative to the marine source (Figs. 2.7 - 2.9).....25

Figure 2.3: Particle-size distribution (PSD) plots for Sur Lagoon based on percent abundance of particle size fraction (0-11 ϕ). Sample locations (n = 111) used for the particle-size analysis are represented by black circles.....26

Figure 2.4: Q-Mode versus R-Mode cluster analysis using Ward's method indicating three biofacies.....27

Figure 2.5: Q-Mode versus R-Mode cluster analysis using Ward's method indicating three taphofacies.....28

Figure 2.6: Distribution of biofacies (**a**) and taphofacies (**b**) showing relationship with geographic boundaries (Distal Lagoon Basin, Main Lagoon Basin and Shallow Marine Area).....29

Figure 2.7: **a)** Elevation along a transect from the Shallow Marine Area through the Main and Distal Lagoon Basins using nodes shown in Fig. 2.2d. **b)** Stable isotope data for sample locations along the transect. **c)** Particle-size plots for the transect (D.V. % = differential volume percent).....30

Figure 2.8: Abundances of significant taxa and Shannon-Weaver Diversity Index (SDI) vs. distance from the Shallow Marine Area outside the lagoon using nodes shown in Fig. 2.2d.....31

Figure 2.9: Dominant taphonomic characters vs. distance from the Shallow Marine Area outside the lagoon using nodes shown in Fig. 2.2d.....32

Plate 2.1: All scale bars are equal to 100 μm . 1. *Ammonia tepida* ventral view. 2. *Ammonia tepida* dorsal view. 3. *Ammonia parkinsoniana* ventral view. 4. *Ammonia parkinsoniana* dorsal view. 5. *Ammonia inflata* ventral view. 6. *Ammonia inflata* dorsal view. 7. *Elphidium gerthi* side view. 8. *Elphidium craticulatum* side view. 9. *Elphidium striatopunctatum* side view. 10. *Elphidium advenum* side view. 11. *Porosonion granosa* side view. 12. *Amphistegina lessonii* ventral view. 13. *Amphistegina lobifera* ventral view....33

Plate 2.2: All scale bars represent 100 μm . 1-3. Minimally corraded recent individuals (recent only). 4-6. Moderately corraded individuals (recent and fossil). 7-9. Maximally corraded fossil individuals (fossil only). 10. Fragmented individual (recent and fossil). 11. Taphonomically unaltered individual (recent only). 12. Bioeroded individual (recent only).....34

CHAPTER 3

Figure 3.1: a. Location of Sur, Oman. b. Makran Subduction Zone (MSZ), broad-scale plate tectonics and the 1945 earthquake epicentre are indicated (after Donato et al., 2009 and Heidarzadeh et al., 2008).....67

Figure 3.2: a. Google Earth image of Sur Lagoon indicating the lagoon entrance, tidal channels, wadi entrance and location of cores 1 – 8 (circles). b. Digital Elevation Model (DEM) of Sur Lagoon. The node used to measure core distances from the lagoon entrance is indicated by a square (Fig. 3.4).....68

Figure 3.3: Photographic record of Core 1 showing the stratigraphic units designated by bivalve taphonomy and particle-size data as shown in Donato et al. (2009). Details of the tsunami unit shows articulated bivalves out of life position with angular fragmented shells. Note the red-orange color of the shell unit vs. the sand above and below. Recent pop bottle label which shows reworking of the upper sediments. Compare exposure with trench section in Fig. 3.4d.....69

Figure 3.4: a. Tidal channel erosion of the tsunami shell unit. b. shells exposed

in tidal channel become edge rounded, bioeroded (microboring) and encrusted. **c.** accumulation of shells at the bottom of tidal channels. **d.** exposure of the shell unit in a trench section close to core 1.....70

Figure 3.5: **a.** Lithologic (PSD), shell and foraminiferal data for cores 1 – 8. Foraminifera and taphonomic characters that best reflect tsunami overwash are indicated. For all taxonomic and taphonomic data see Online Figs. 3.1 – 3.5. Tsunami and lagoon units are based the PSD and shell taphonomy (Donato et al., 2008; Donato et al., 2009). **b.** PSD facies. **c.** Core locations within Sur Lagoon.....71

Figure 3.6: **a.** Foraminiferal data from surface samples (after Pilarczyk et al., submitted) and major stratigraphic units in Sur Lagoon. Core locations are arranged in order of increasing distance into the lagoon. Percentages on the y-axis reflect relative abundances. **b.** A generalized stratigraphic section indicating an older more restricted lagoon system evolving into a more open system by way of tsunami inundation. **c.** Core locations within Sur Lagoon. **d.** Correlation of cores through two north-south transect lines (eastern and western) indicating a slight thinning trend in tsunami bed thickness.....72

Online Supplementary Figure 3.1: Lithologic, PSD and foraminiferal data for cores 1 and 2. Core elevation (E) is indicated. Total individuals per 1 cm³, Shannon Diversity Index (SDI), foraminiferal taxa, test size (small: <150 µm; medium: 150-250 µm; large: >250 µm), taphonomic characters (modern corroded, modern fragmented, modern unaltered, total fossil specimens and fossil fragments) are indicated. Foraminiferal based tsunami indicators are highlighted in green. Tsunami and lagoon units are based the PSD and shell taphonomy (Donato et al., 2008; Donato et al., 2009). Black circles indicate sampling intervals.....75

Online Supplementary Figure 3.2: Lithologic, PSD and foraminiferal data for cores 3 and 4. Core elevation (E) is indicated. Total individuals per 1 cm³, Shannon Diversity Index (SDI), foraminiferal taxa, test size (small: <150 µm; medium: 150-250 µm; large: >250 µm), taphonomic characters (modern corroded, modern fragmented, modern unaltered, total fossil specimens and fossil fragments) are indicated. Foraminiferal based tsunami indicators are highlighted in green. Tsunami and lagoon units are based the PSD and shell taphonomy (Donato et al., 2008; Donato et al., 2009). Black circles indicate sampling intervals.....76

Online Supplementary Figure 3.3: Lithologic, PSD and foraminiferal data for

cores 5 and 8. Core elevation (E) is indicated. Total individuals per 1 cm³, Shannon Diversity Index (SDI), foraminiferal taxa, test size (small: <150 μm; medium: 150-250 μm; large: >250 μm), taphonomic characters (modern corroded, modern fragmented, modern unaltered, total fossil specimens and fossil fragments) are indicated. Foraminiferal based tsunami indicators are highlighted in green. Tsunami and lagoon units are based the PSD and shell taphonomy (Donato et al., 2008; Donato et al., 2009). Black circles indicate sampling intervals.....77

Online Supplementary Figure 3.4: Lithologic, PSD and foraminiferal data for core 6. Core elevation (E) is indicated. Total individuals per 1 cm³, Shannon Diversity Index (SDI), foraminiferal taxa, test size (small: <150 μm; medium: 150-250 μm; large: >250 μm), taphonomic characters (modern corroded, modern fragmented, modern unaltered, total fossil specimens and fossil fragments) are indicated. Foraminiferal based tsunami indicators are highlighted in green. Tsunami and lagoon units are based the PSD and shell taphonomy (Donato et al., 2008; Donato et al., 2009). Black circles indicate sampling intervals.....78

Online Supplementary Figure 3.5: Lithologic, PSD and foraminiferal data for core 7. Core elevation (E) is indicated. Total individuals per 1 cm³, Shannon Diversity Index (SDI), foraminiferal taxa, test size (small: <150 μm; medium: 150-250 μm; large: >250 μm), taphonomic characters (modern corroded, modern fragmented, modern unaltered, total fossil specimens and fossil fragments) are indicated. Foraminiferal based tsunami indicators are highlighted in green. Tsunami and lagoon units are based the PSD and shell taphonomy (Donato et al., 2008; Donato et al., 2009). Black circles indicate sampling intervals.....79

CHAPTER 4

Figure 4.1a: a) Map of Anegada showing major geomorphic features (modified from Atwater et al. 2010). b) Detailed map of study area showing site locations of trenches (sites 5, 11, 13, 14, 15, 16, 19) and surface samples (1–5) depicted in (c).104

Figure 4.1b: c) *Homotrema* taphonomic data from surface samples and major stratigraphic units in the ponds. Two north–south transects (western and eastern) are compared. The western transect runs through Red and Point Peter Ponds, while the eastern transect encompasses Bumber Well Pond. A generalized stratigraphic section based on all trench sections is indicated at the top right.

MMP Microbial-Mat Peat, MC Mud Cap, SSS Shell and Sand Sheet, SM Shelly Mud.....	105
--	-----

Figure 4.2: Taphonomic condition of *Homotrema* specimens. (1) Exceptionally preserved (red, angular, well preserved chambers); (2–5) Well preserved (pink, angular, hollowed chambers); (6–8) Moderately preserved (pink, rounded, hollowed chambers); (9) Highly altered (whitish, rounded, hollowed chambers); (10–12) *Homotrema* encrusted on *Ammonia beccari*, (10) Exceptionally preserved, (11) Well preserved (12) Moderately preserved; (13) Unaltered holothuridian spicule; (14) *Homotrema* encrusted holothuridian. Scale bars represent 100 μm.....106

Figure 4.3: a) Detailed lithological, PSD, and *Homotrema* taphonomic data for core sites 5, 11, 13, 14, 15, 16 and 19. Event horizon designation is based on *Homotrema* concentration peak. Circles indicate sampling intervals (black) and radiocarbon dating intervals (orange; see Atwater et al. 2010 for details on the radiocarbon dates). b) Trench site locations for gutter cores. c) Generalized stratigraphic section based on all trench sections.....107

Figure 4.4: a) Core PSD plots for pond sections (gutter cores). Facies designations are based on field observations (see Fig. 4.3). b) Location of core sites (adapted from Atwater et al. 2010). c) Average PSD statistical data for facies.....110

Figure 4.5: PSD plots of modern environments for comparison with the Mud Cap, Shell and Sand Sheet and Shelly Mud from pond stratigraphy. Statistical data (mean, mode, and SD) of each environment (modern samples) and unit (core samples) is indicated.....111

CHAPTER 5

Figure 5.1: Physiography of the northeastern Caribbean showing tectonic plates and the path of Hurricane Donna in 1960 (Modified from Fig. 1, Atwater et al. 2011; Lopez et al. 2006; Dunn 1961).....139

Figure 5.2: Map showing geomorphic and geological features of Anegada (Modified from Fig. 2, Atwater et al. 2011).....140

Figure 5.3: Molluskan species, taphonomic and clast data from the Shell and Sand Sheet and the storm wrack deposit on Windlass Bight Beach. Eleven

samples were analyzed from the Shell and Sand Sheet and two samples from the Storm Wrack Deposit—average values are reported with 1 σ and the range of values. For the clast data, bars represent 1 σ141

Figure 5.4: a) Location of trenches in Bumber Well and Red Pond and their stratigraphic logs showing sample resolution. b) Mean values of dominant taphonomic and petrographic characters for the idealized stratigraphic section. c) Distribution of radiocarbon dates in the analyzed stratigraphic sections (for details see Atwater et al. 2011).....142

Figure 5.5: Articulated *Anomalocardia* radiocarbon dates for the Shell and Sand Sheet illustrating the range in dates and the lack of taphonomic correlation.....143

Figure 5.6: Distribution of the dominant taphonomic and petrographic characters of the Sand and Shell Sheet in Bumber Well Pond showing spatial trends. Stratigraphic cross-section from Atwater et al. (2011).....144

LIST OF TABLES

All tables are located in consecutive manner at the end of each chapter following the corresponding figures, as per the general style required for manuscript submission to peer-reviewed journals.

CHAPTER 2

Table 2.1: Biofacies elevation, exposure time, average Shannon Diversity Index (SDI) and foraminiferal abundances ($\% \pm 1$ std.) for the three biofacies determined with cluster analysis.....35

Table 2.2: Taphofacies elevation, exposure time, and average foraminiferal taphonomic characteristics ($\% \pm 1$ std.) for the three taphofacies determined with cluster analysis.....36

Table 2.S1: Textural and geochemical data by biofacies.....37

Table 2.S2: Foraminiferal data (Shannon-Weaver diversity index, fractional abundances and standard error).....39

Table 2.S3: Taphonomic data (fractional abundances).....44

CHAPTER 3

Table 3.1: Taphonomic data (fractional abundances).....80

CHAPTER 4

Table 4.1: *Homotrema* taphonomic data for cores.....112

Table 4.2: *Homotrema* taphonomic data for surface samples.....114

Table 4.3: Textural data.....115

CHAPTER 5

Table 5.1: Mollusc and petrographic data.....145

PREFACE

This dissertation is a compilation of four individual research papers that are currently either published, submitted or in preparation. Research objectives and the relationship among these papers are described in the introductory chapter. Chapter six summarizes the major contributions these papers have made to the discipline of tsunami geology. Different levels of collaboration existed on each paper and are outlined in detail below. In each case all authors reviewed the manuscripts prior to submission and Dr. Eduard Reinhardt provided valuable guidance concerning research direction, interpretation of results, editing and submission to peer-reviewed journals. The individual research papers presented herein include:

Chapter 2:

PILARCZYK, J.P., REINHARDT, E.G., BOYCE, J.I., SCHWARCZ, H.P., DONATO, S.V., (*submitted*). Assessing surficial foraminiferal distributions as an overwash indicator in Sur Lagoon, Sultanate of Oman. Submitted to *Marine Micropaleontology* April 2010.

Surface sediment samples were collected by Simon Donato and Dr. Eduard Reinhardt. Dr. Joe Boyce provided a Digital Elevation Model (DEM) and Particle-size Distribution (PSD) maps. Stable isotopic analysis was conducted in collaboration with Dr. Henry Schwarcz. The dissertation author completed all foraminiferal, taphonomic and stable isotope analyses. Data compilation, critical analysis, interpretation, figures and manuscript writing were also conducted by the dissertation author.

Chapter 3:

PILARCZYK, J.P., REINHARDT, E.G., (*in preparation*). Testing foraminiferal taphonomy as a tsunami indicator in a shallow arid system lagoon: Sur, Sultanate of Oman. *Marine Geology*.

Cores were previously collected by Simon Donato and Dr. Eduard Reinhardt. Core PSD plots from Donato et al. (2009) were used to supplement foraminiferal data. Dr. Joe Boyce provided a DEM of the study area as well as comments on the final version of this manuscript. The dissertation author was

involved in field data collection and completed all laboratory and data analysis, interpretations and manuscript preparation.

Chapter 4:

PILARCZYK, J.P., REINHARDT, E.G., 2011. *Homotrema rubrum* (Lamarck) taphonomy as an overwash indicator in Marine Ponds on Anegada, British Virgin Islands. *Natural Hazards*, doi: 10.1007/s11069-010-9706-3.

Field sampling was conducted by Dr. Brian Atwater (USGS) and Dr. Eduard Reinhardt. Brian Atwater provided edits for the final version of this manuscript. All laboratory analyses (e.g. foraminiferal, taphonomic and particle-size analyses), data interpretation and manuscript preparation were completed by the dissertation author. In addition, the dissertation author independently developed a method of documenting and assessing the taphonomic condition of *Homotrema* tests.

Chapter 5:

REINHARDT, E.G., PILARCZYK, J.E., BROWN, A., 2011. Probable tsunami origin for a shell and sand sheet from marine ponds on Anegada, British Virgin Islands. *Natural Hazards*, doi:10.1007/s11069-011-9730-y.

Field sampling was conducted by Dr. Brian Atwater (USGS) and Dr. Eduard Reinhardt. Dr. Eduard Reinhardt wrote the manuscript. The dissertation author oversaw the supervision of an undergraduate research assistant (Alyson Brown), provided guidance at all stages of analysis (e.g. methodological approach, species identification, etc.). The dissertation author also tabulated and graphed all results for the paper and significantly contributed to the overall conclusions of the final manuscript.

The chapters in this dissertation utilized varying formatting styles reflective of the requirements for the journals in which they were submitted. This dissertation is presented in a 'sandwich style' and readers may notice unavoidable overlap in content throughout the chapters, particularly in sections describing methodology and previous research. McMaster University copyright regulations require permission to reproduce research papers already published and/or in press. As required, reproduction permissions were requested for published manuscripts.

CHAPTER 1

INTRODUCTION

Tsunami deposits have been shown to contain diagnostic bivalve taphonomic trends (e.g. articulation, fragmentation; Reinhardt et al., 2006; Donato et al., 2008; Massari et al., 2009). This method is effective when examining tsunami deposits in large exposed beds; however, it cannot always be applied in core studies. Since microfossils exhibit similar trends and are more abundant, they can be used to identify tsunami deposits when shells are in limited quantities (e.g. cores). Studies using foraminifera to identify tsunamis are traditionally conducted in contrasting settings where differences between the terrestrial and marine realms are easily detected. Marine influenced settings lack the same degree of contrast; therefore, microfossil analysis alone is not effective. Tsunami deposits have previously been recognized by the presence of allochthonous marine microfossils and sediments in a non-marine setting (e.g. terrestrial, fresh water; Kortekaas and Dawson, 2007). Sedimentological and microfossil differences between the fresh- and saltwater realms are easily distinguished in these types of settings. However, tsunami deposits in non-marine settings are often discontinuous, influenced by vegetation, and infrequent. In contrast, marine settings are more ubiquitous, but the sedimentological and microfossil signature of a tsunami deposit exhibits less contrast. Marine settings have received little research attention because: (1) differentiating between storms and tsunamis is deemed problematic (Kortekaas and Dawson, 2007), and (2) of the perceived difficulty in identifying tsunami deposits amongst more frequent background geologic processes (Mandic et al., 2004). Reinhardt et al. (2006) and Donato et al. (2008) demonstrate that tsunami deposits can be identified in marine settings when using shell taphonomy as an indicator. This technique is limited to situations where allochthonous shells are available in sufficient quantities. Together with mollusc taphonomy and sedimentological analysis, this dissertation examines the usefulness of foraminiferal taphonomy (allochthonous vs. autochthonous specimens, breakage patterns, etc.) in ascribing depositional origin to catastrophic event beds in coastal sequences at Anegada, BVI and Sur, Sultanate of Oman. This research has implications for event chronology which can be used to qualify risk assessment for these locations; which to date remains largely undocumented.

1.1 SITE SELECTION

The seismically active Makran Subduction Zone (MSZ) located off the coast of Pakistan has been known to produce tsunamigenic earthquakes that have catastrophically impacted the coasts of Iran, Pakistan, India and Oman. Little is known about the MSZ, and models of potential future events are based on historical information as no geologic (i.e. tsunami deposit) evidence has been available. Donato et al. (2008, 2009) were the first to identify and document a laterally extensive shell unit emplaced by the most recent MSZ tsunami which struck the Omani coastline on 28 November 1945 killing over 4000 people. Donato et al. (2008) based their tsunami interpretation largely on the abundance of articulated offshore marine taxa and angular fragments intermingled with lagoon sediment. In addition to the most recent tsunami, historical records indicate that several MSZ tsunamis have impacted Northern Arabian Sea coastlines and could potentially be archived within lagoon stratigraphy at Sur (e.g. 325 B. C, 1483, 1851, 1765, etc.; Ambraseys and Melville, 1982; Heidarzadeh et al., 2008). Using the 1945 Makran tsunami deposit as a reference, this dissertation tests the use of foraminiferal taphonomy (allochthonous vs. autochthonous specimens, breakage patterns, etc.) as a tsunami indicator in an effort to establish a method for detecting event deposits deeper in the geologic record that contain little or no shell signature so that a chronology of tsunami events can be established.

Anegada, British Virgin Islands, due to its position relative to the Atlantic Ocean and the Puerto Rico Trench, may be a good tsunami recorder of local (e.g. 1690, 1867; Reid & Taber 1920; Zahibo 2003) and trans-oceanic events (e.g. 1755 Lisbon; O'Loughlin & Lander 2003). These events, as well as major storms impacting the island in 1713 (Pickering 1983), 1819 (Millás & Pardue 1968; Pickering 1983) and 1960 (Hurricane Donna; Dunn 1961), are candidates for the origin of a laterally extensive Shell and Sand Sheet found in marine ponds from central Anegada. The overwash unit contains abundant foraminifera including *Homotrema rubrum* (Lamarck) a common encrusting foraminifer in reefal settings that bleaches from red to light pink after death (Emiliani 1951). Taphonomic condition of *Homotrema* has previously been used as a transport but has never been applied to overwash deposits like the ones identified at Anegada (MacKenzie et al. 1965; Machado & Moreas 2002).

1.2 RESEARCH OBJECTIVES

The main objective of this dissertation is to further the collective understanding of tsunami impact on coastlines through the identification and

characterization of tsunami overwash using a combined paleontological (mollusc and foraminiferal taphonomy) and sedimentological (high resolution particle size distributions) technique. More specifically, this dissertation investigated three central research questions:

1. What are the modern spatial distributions and controls on foraminiferal taphonomy in a marine-influenced arid system lagoon?
2. Can foraminiferal taphonomy be used to document overwash in an arid siliciclastic (Sultanate of Oman) and a semi-tropical carbonate (British Virgin Islands) coastal setting?
3. Does foraminiferal taphonomic analysis provide insight into the origin of overwash deposits and can it be used to infer hydrodynamic regimes? Does it match up with other proxies?

1.3 DISSERTATION STRUCTURE

The structure of this thesis is a compilation of four manuscripts that address the central research questions concerning previously identified event beds. Chapters two and three focus on documenting tsunami overwash within Sur Lagoon, Oman; while chapters four and five deal with Anegada, BVI. Chapter one examines the modern baseline distributions of foraminifera (taxa and taphonomy), grain size and stable isotopes ($\delta^{13}\text{C}$, $\delta^{18}\text{O}$) in surface samples ($n = 54$) throughout Sur Lagoon. This study indicates that large specimens, offshore taxa (e.g. planktics, *Amphistegina* sp., *Ammonia inflata*) and sediment in-filled fossil specimens are the best indicators of marine incursions into the Sur Lagoon. Taphofacies analysis provided insight into provenance assessment of lagoonal sediment and shows promise in assessing hydrodynamics associated with event beds. Chapter two uses the baseline data documented in chapter one to interpret down-core trends within a series ($n = 8$) of cores containing the 1945 Makran Trench tsunami. This chapter investigates the potential of a taphonomic overwash indicator for tsunami detection so that older events may be documented; and a tsunami chronology for the Omani coastline established.

Chapter four provides evidence for a probable tsunami that impacted Anegada sometime between A.D. 1650 – 1700. Foraminiferal provenance using the ecology and taphonomy (e.g. color, fragmentation, edge rounding, chamber preservation) of *Homotrema rubrum* (Lamarck) proved useful in assessing event

beds in a series of marine ponds. Anegeda's ponds with their close proximity to reef source regions and their low-lying topography make it difficult to distinguish hurricane versus tsunami deposits; however, a marked decrease in highly preserved fragments from north to south supports a tsunami interpretation. Chapter 5 uses mollusc taphonomy and petrographic analysis on the same overwash bed. Contrary to similar studies where concentrated beds of allochthonous articulated species indicated tsunami deposition (Reinhardt et al., 2006; Donato et al., 2008), this study provided evidence of widespread overwash that likely eroded and winnowed the former marine pond's substrate into a shell hash with sheet-like geometry consisting of autochthonous lagoon molluscs.

REFERENCES

- Ambraseys, N.N., Melville, C.P., 1982. A history of Persian earthquakes. New York: Cambridge University Press, 219 p
- Donato, S.V., Reinhardt, E.G., Boyce, J.I., Pilarczyk, J.E., Jupp, B.P., 2009. Particle-size distribution of inferred tsunami deposits in Sur Lagoon, Sultanate of Oman. *Marine Geology*, 257: 54-64
- Donato, S.V., Reinhardt, E.G., Boyce, J.I., Rothaus, R., Vosmer, T., 2008. Identifying tsunami deposits using bivalve shell taphonomy. *Geology*, 36: 199-202
- Dunn, G.E., 1961. The hurricane season of 1960. *Monthly Weather Review*, 89: 99-108
- Emiliani, C., 1951. On the species *Homotrema rubrum* (Lamarck). *Cushman Foundation for Foraminiferal Research Special Contribution*, 2: 143-147
- Heidarzadeh, M., Pirooz, M.D., Zaker, N.H., Yalciner, A.C., Mokhtari, M., Esmaily, A., 2008. Historical tsunami in the Makran Subduction Zone off the southern coasts of Iran and Pakistan and results of numerical modeling. *Ocean Engineering*, 35: 774-786
- Kortekaas, S., Dawson, A.G., 2007. Distinguishing tsunami and storm deposits: an example from Martinhal, SW Portugal. *Sedimentary Geology*, 200: 208-221
- Machado, A.J., Moraes, S.S., 2002. A note on the occurrence of the encrusting foraminifera *Homotrema rubrum* in reef sediments from two distinctive hydrodynamic settings. *Annals of the Brazilian Academy of Science*, 74: 727-735
- MacKenzie, F.T., Kulm, L.D., Cooley, R.L., Barnhart, J.T., 1965. *Homotrema rubrum* (Lamarck), a sediment transport indicator. *Journal of Sedimentary Research*, 35: 265-272
- Massari, F., D'Alessandro, A., Davaud, E., 2009. A coquinoid tsunamite from the Pliocene of Salento (SE Italy). *Sedimentary Geology*, 221: 7-18

- Millás, J.C., Pardue, L., 1968. Hurricanes of the Caribbean and adjacent regions, 1492 – 1800. Academy of the Arts and Sciences of the Americas, Miami, Fla.
- O’Loughlin, K.F., Lander, J.F., 2003. Caribbean tsunamis: A 500-year history from 1498 – 1998. Kluwer Academic, Dordrecht, Boston, pp 263
- Pickering, V.W., 1983. Early history of the British Virgin Islands: from Columbus to emancipation. Falcon Publications International, pp 248
- Reid, H.F., Taber, S., 1920. The Virgin Islands earthquakes of 1867-1868. Bulletin of the Seismological Society of America, 10: 9-20
- Reinhardt, E.G., Goodman, B.N., Boyce, J.I., Lopez, G., van Hengstum, P., Rink, W.J., Mart, Y., Raban, A., 2006. The tsunami of 13 December A.D. 115 and the destruction of Herod the Great’s harbour at Caesarea Maritima, Israel. *Geology* 34, 1061-1064
- Zahibo, N., Pelinovsky, E., Yalciner, A.C., Kurkin, A., Koselkov, A., Zaitsev, A., 2003. The 1867 Virgin Island Tsunami. *Natural Hazards and Earth System Sciences*, 3: 367-376

CHAPTER 2

ASSESSING SURFICIAL FORAMINIFERAL DISTRIBUTIONS AS AN OVERWASH INDICATOR IN SUR LAGOON, SULTANATE OF OMAN

Jessica E. Pilarczyk*

Eduard G. Reinhardt

Joseph I. Boyce

Henry P. Schwarcz

School of Geography and Earth Sciences, McMaster University, Hamilton, ON,
Canada, L8S 4K1

Simon V. Donato

Imperial Oil Resources, 237 4th Avenue Southwest, P.O. Box 2480 Station M,
Calgary, AB, Canada, T2P 3M9

*Corresponding author: J.E. Pilarczyk (pilarcje@mcmaster.ca)

Citation: Pilarczyk, J.E., Reinhardt, E.G., Boyce, J.I., Schwarcz, H.P., Donato, S.V., *submitted*. Assessing surficial foraminiferal distributions as an overwash indicator in Sur Lagoon, Sultanate of Oman. *Marine Micropaleontology*.

Status: submitted April 2010

ABSTRACT

This study provides baseline data assessing foraminifera as an overwash indicator in a small intertidal lagoon located at Sur, Sultanate of Oman. The lagoon is shallow, tidally-controlled and communicates with the open sea through a narrow subtidal entrance channel. The lagoon is largely composed of intertidal sand and mud flats with fringing mangroves. A total of three wadis empty into the lagoon occasionally supplying freshwater and sediment during the monsoon season (May to September). Foraminiferal (taxa and taphonomy), particle-size and stable isotopic analyses were conducted on surface sediment samples to determine modern spatial trends within the lagoon. Q-mode cluster analysis of the foraminiferal data ($n = 54$) reveals three main biofacies which follow lagoon sub-environments: Shallow Marine Area, Main Lagoon Basin, and Distal Lagoon Basin. The Shallow Marine Area is mainly subtidal with higher wave energy, the Main Lagoon Basin is predominantly intertidal with moderate wave energy, whereas the Distal Lagoon Basin is isolated and mainly intertidal with low wave energy.

The most useful parameters for assessing overwash events in Sur Lagoon are the foraminifera taxa rather than the taphonomic characters themselves. The most useful taxa for recognizing an overwash (e.g. tsunami or storm) was the abundance of *Amphistegina* spp., *Ammonia inflata*, *Elphidium advenum* and planktics. These species have higher r^2 values with distance into the lagoon, and a distinct transition from the Shallow Marine Area to the Main and Distal Lagoon Basins. Taphonomically there is a predominance of larger specimens in the Shallow Marine Area along with a higher abundance of fossil specimens which will also be useful.

2.1 INTRODUCTION

2.1.1 Foraminifera and taphonomy

After the 2004 Indian Ocean tsunami there is increased interest in the Makran Subduction Zone on the northern margin of the Arabian Sea and its potential to generate large tsunamis, but there is little geological data to assess its past history. The coastlines around the Arabian Sea may contain evidence of these past events, but they are predominantly arid and there are few tsunami indicators developed for these settings.

Foraminifera have been used as an overwash indicator in numerous studies by documenting allochthonous tests in coastal lagoons, ponds and marshes but most of these studies have been conducted in temperate or tropical settings. A recent assessment of foraminifera as a tsunami indicator emphasized the importance of understanding contemporary taphonomic trends for interpreting overwash in the stratigraphic record (Mamo et al., 2009 and references therein). However, in the case of the Arabian Sea, there are few foraminiferal studies for background information and comparisons with other areas in the world may not be valid (e.g. sabkhas). Most studies from the Arabian Sea are from western India, Iran and the Persian Gulf, with few from Oman (e.g. Murray, 1965; Murray, 1966a; Murray, 1966b; Murray, 1966c; Reddy and Rao, 1984; El-Nakhal, 1990; Nigam and Khare, 1995; Cherif et al., 1997; Lezine et al., 2002; Bhalla et al., 2007; Moghaddasi et al., 2008; Ghosh et al., 2009). Of these studies, there are few that have examined foraminiferal distributions within lagoons (e.g. Murray, 1965; Murray, 1966a; Murray, 1966b; Murray, 1966c; Cherif et al., 1997).

Taphonomic evidence has been used to document paleo-environmental trends in the geological record (e.g. Parsons-Hubbard, 2005; Reinhardt et al., 2006; De Francesco and Hassan, 2008; Donato et al., 2008) and is often referred to as taphofacies analysis (Martin, 1999). Fragmentation, edge preservation, luster, encrustation, bioerosion and articulation are among the taphonomic characters often used (e.g. Martin et al., 1996; Best and Kidwell, 2000; Parsons-Hubbard, 2005; Reinhardt et al., 2006; Donato et al., 2008; Berkeley et al., 2009). The majority of the research has focussed on mollusc shells, with foraminiferal studies mostly examining vertical time averaging or lateral transport (Martin et al., 1995; Culver et al., 1996; Martin et al., 1996; Murray and Alve, 1999; Hippensteel et al., 2000). Foraminiferal provenance is a well recognized tool for determining overwash events (e.g. from open marine to lagoon) from hurricanes (e.g. Hippensteel and Martin, 1999; Hippensteel and Martin, 2000; Scott et al., 2003) or tsunamis (e.g. Luque et al., 2002; Hawkes et al., 2007, Kortekaas and Dawson, 2007). However, very little

research has been devoted to recognizing specific taphonomic features of these event beds. Berkeley et al. (2009) document the taphonomic character of individual intertidal foraminifera, demonstrating that foraminiferal taphonomic analysis, which has been associated with information loss, can be used to provide additional information concerning depositional environment and subsequent transport histories. Recent research from Anegada, British Virgin Islands has shown foraminiferal provenance using the ecology and taphonomy (color, fragmentation and edge rounding) of *Homotrema rubrum* to be useful and important for assessing overwash beds in hypersaline lagoons (Pilarczyk and Reinhardt, 2011).

2.1.2 Regional setting

The Sultanate of Oman has an arid, subtropical continental climatic regime. Seasonal weather changes are notably severe; in summer, temperatures peak to ~45-50°C, whereas in winter, temperatures commonly dip to 0°C (Lezine et al., 2002). Rainfall occurs predominantly in the winter due to eastern Mediterranean troughs which follow the Zagros Mountains and penetrate the Persian Gulf along the north of the Arabian Peninsula with less rainfall in the summer months due to the south-western monsoon circulation (Deil, 1996). Average annual precipitation in Sur (Fig. 1) is 114.7 mm with the highest amount of precipitation falling between November and April. Humidity also peaks in the winter months (February = 70%) and drops significantly in the summer (May = 53%). Average mean monthly temperatures range from 21.7°C in January to 34.1°C in June (Lezine et al., 2002).

Sur Lagoon is a small (~12 km²) tidally-dominated, micro-tidal lagoon (mean tidal amplitude ~1.2 m) situated approximately 100 km south of the capital city Muscat on the western coast of Oman (Fig. 2.1; Fig. 2.2). The lagoon is divided into Distal and Main Lagoon Basins and it communicates with the Shallow Marine Area (Gulf of Oman) through a narrow (103 - 209 m wide) entrance channel along its eastern edge, which connects a 2.5 km network of tidal channels in the lagoon. Paleocene-Eocene aged highlands border and define most of the extent of the lagoon with the entrance channel further restricted by a low relief sand spit (~2 – 3 m.s.l.; Fig. 2.2b). Probable overwash during a storm or tsunami would follow the existing lagoon channel and possibly overtop the sand spit. Four wadi channels empty into the lagoon, the largest of which is Wadi Shamah that culminates in a ~1 km wide delta. The interior of the lagoon is made up of a series of intertidal sand and mudflats which are exposed and submerged through daily tidal cycles. At low tide ~90% of the lagoon surface is exposed, while at high tide only ~10% is exposed. Mangroves fringe most of the lagoon with the highest density along the NE tip of the Distal Basin and the SW section of the Main Basin (Fig. 2.2c).

The Shallow Marine Area outside of the lagoon has a narrow shelf which drops off to depths of over 200 m after ~5 km (Szuman et al., 2006). The coastline of north-eastern Oman supplies continuous sediment to the Gulf of Oman through erosion of prominent rocky headlands and ephemeral wadis. Wave action in the nearshore environment is high due to the large fetch associated with the Gulf of Oman. In contrast, the restricted lagoon basins experience little wave action and are predominantly tidal. Wadi systems (e.g. Wadi Shamah) provide poorly sorted sediment (muds - gravels) to the lagoon; whereas, predominantly fine to medium sands come from the Gulf of Oman. During Cyclone Gonu (June 1st to 7th 2007) heavy rainfall (up to 610 mm) washed away the road and eroded much of the delta in the southeastern wadi (Wadi Shamah; Donato et al., 2009). However, most of the sediment moved seaward into the Shallow Marine Area bypassing the Main Lagoon Basin although lesser events would likely contribute sediment directly to the lagoon.

Field observations and a Digital Elevation Model (DEM) were used to determine 12 sub-environments (Donato et al., 2008; 2009; Fig. 2.2c). These include: wadi, mangrove, mud flat, lagoon shoreface, sand flat, lagoon creek (intertidal), flood delta, shelly firm ground, lagoon channel (subtidal), wadi delta, entrance channel and marine shoreface (Fig. 2.2c).

2.1.3 Tsunami overwash in Sur Lagoon

Previous research from Sur Lagoon focused on the identification and characterization of a tsunami deposit from the November 28, 1945 Makran Trench earthquake (Donato et al., 2008; Donato et al., 2009). The seismically active Makran Subduction Zone (MSZ) located off the coast of Pakistan has been known to produce tsunamigenic earthquakes that have impacted the coasts of Iran, Pakistan, India and Oman (e.g. Heidarzadeh et al., 2008; Okal and Synolakis, 2008). Little is known about the MSZ, and predictions of future events are based on historical information as no geologic (i.e. tsunami deposit) evidence has been available (Ambraseys and Melville, 1982). Donato et al. (2008) documented an event horizon in Sur Lagoon, Oman inferred to be from the 1945 Makran Trench event. This deposit consisted of a coarse shell-rich layer with distinctive taphonomic characteristics and particle-size trends: thick (5 - 25 cm), laterally extensive (>1 km²), sheet-like geometry which thinned and became finer grained with distance inland from the lagoon entrance, and contained whole and fragmented lower-shore offshore bivalves (Donato et al., 2008; Donato et al., 2009).

2.2 MATERIALS AND METHODS

One hundred and eleven surface sediment samples (upper 2 cm) were collected in February 2006 along 12 transect lines spaced ~300 m apart (Fig. 2.3). Sample locations used in the microfossil analysis are shown in Fig. 2.2d. Nearshore marine samples were collected by free-diving along similar grid lines. All sub-environments within the lagoon and marine embayment were sampled (e.g. entrance channel, intertidal, subtidal, mangrove, sandflat, mudflat, beach, shallow marine, wadi).

A Trimble R3 differential GPS unit was used to create a digital elevation model (DEM; Fig. 2.2b; Donato et al., 2009). The DEM was produced by walking a differential GPS (D-GPS) in north-south transects spaced 100 m apart, and east-west lines at 300 m spacing. A single-beam echo sounder was used to survey depths greater than 1.5 m within the lagoon, the entrance channel, and the Shallow Marine Area ~1 km out from the coastline. Both datasets were combined using Geosoft Oasis TM software to create the DEM and were levelled to a mean sea level datum (see Donato et al., 2008).

2.2.1 Foraminiferal analysis

Samples (n = 54) were selected for foraminiferal analysis based on the facies and spatial distribution within the lagoon (Figure 2.2c). Samples ranged in volume from 5 - 20 cm³ and were sieved (>63 µm) and dried for foraminiferal analysis. Samples were randomly split to provide specimen counts of ~300 and analyzed using an Olympus SZX12® microscope. A total of 22 foraminifera taxa (Pl. 2.1; Table 2.1; Online Table 2.S2) were identified using the taxonomy of Hottinger et al. (1993) and Hayward et al. (2004). Scanning Electron Microscopy (SEM) was conducted at the Brockhouse Institute for Materials Research at McMaster University.

Q-Mode (statistically similar populations) and R-mode (statistically affiliated populations) cluster analysis of the foraminiferal data (% species) was performed in the statistical software package PAST™ (Fig. 2.4). Q-Mode cluster analysis used Ward's Minimum variance and is reported as squared Euclidean distances (Fishbein and Patterson, 1993). Standard error was calculated on the fractional abundances following Patterson and Fishbein (1989) and species that had standard errors greater than relative fractional abundances in all samples were eliminated from the cluster analysis. A total of 16 species were found to be statistically significant in at least one sample: *Ammonia inflata*, *Ammonia parkinsoniana*, *Ammonia tepida*,

Amphistegina spp., *Patellinella* sp., *Brizalina striatula*, *Cibicides pseudolobatus*, *Elphidium advenum*, *Elphidium craticulatum*, *Elphidium gerthi*, *Elphidium striatopunctatum*, *Peneroplis planatus*, *Porosononion granosa*, *Rosalina orientalis*, miliolids and planktics (Fig. 2.5; Table 2.1; Online Table 2.S2). *Amphistegina lessonii* and *Amphistegina lobifera* were combined as were *Cycloforina carinata*, *Pseudotriloculina laevigata*, *Quinqueloculina multimarginata*, *Quinqueloculina patagonica* and *Quinqueloculina seminulum* as they share similar ecological constraints and combining them produced better cluster results (Fig. 2.4).

Taphonomic analysis used the following characters: (1) unaltered, (2) degree of fragmentation (small fragment: <49% of specimen, large fragment: >50% of specimen), (3) degree of corrasion (combined influence of corrosion and abrasion; minimal, moderate, maximal), (4) size (>500 μm , 250-500 μm , 150-250 μm , <150 μm). In addition, the abundance of in-filled fossil specimens were recorded although, they were heavily altered and could not be reliably identified to the species level (Pl. 2.2; Table 2.2; Online Table 2.S3). This taphonomic data was clustered using the same method as described previously (Fig. 2.6).

Plots of taxa and taphonomic characters vs. linear distance into lagoon used measurement nodes in the entrance channel (0 km) and at the transition (2.5 km) between the Distal and Main Lagoon Basins (Fig. 2.2d). Distances (line of sight) from the nodal point (after Donato et al., 2009) were measured in a westerly direction for points in the lagoon while samples outside the lagoon have negative distances and were measured in a N-NW direction. These measurement nodes were selected to reflect a probable transport path for a marine incursion (storm or tsunami).

2.2.2 Stable isotopic analysis

Unaltered *Ammonia parkinsoniana* specimens ($n = 3$ to 5 ; 85-100 μg) were selected for stable isotopic analysis ($\delta^{18}\text{O}$, $\delta^{13}\text{C}$) from 22 of the surface samples obtained along a transect within the lagoon. *A. parkinsoniana* was chosen due to its abundance in all samples and because it has been reported to have minimal microhabitat effects (Chandler et al., 1996). Prior to analysis, samples were washed in an ultrasonic bath of distilled water to remove any sediment particles. SEM analysis showed that the selected specimens were free from any encrustation or sediment in-filling. Stable isotopic analysis was performed on the Finnigan Delta Plus XP® mass spectrometer ($\delta^{13}\text{C}$ precision = ± 0.10 ; $\delta^{18}\text{O}$ precision = ± 0.07) at McMaster University's Stable Isotope Research Laboratory (MSIRL). Values are reported relative to VPDB and are the average of two trials for each sample location.

2.2.3 Particle size analysis

Sediment samples (n=110) were treated with 10% HCl to remove carbonates and 40% H₂O₂ to remove organic material. The remaining siliciclastic fraction was sieved using an 1800 µm mesh before analysis with a Beckman Coulter LS 230 laser diffraction particle size analyzer. Samples were stirred as a moist paste to homogenize the sediment, then ultrasonically disaggregated with hexametaphosphate (NaPO₃)₆ to reduce flocculation. Particle size values were calculated using the Fraunhofer Optical Model (Murray, 2002; van Hengstum et al., 2007; Online Table S1) and are the average of two replicates. Particle sizes were converted to the Wentworth Phi Scale, interpolated and gridded using a Triangular Irregular Network (TIN) algorithm according to Sambridge et al. (1995), and plotted as Particle Size Distribution (PSD) plots in Geosoft Oasis TM.

2.3 RESULTS

2.3.1 Bio- and taphofacies

R-Mode cluster analysis shows that populations of *A. tepida*, *A. parkinsoniana*, *E. gerthi*, *P. planatus* and miliolids are closely associated and are predominantly found in the lagoon basins (Distal and Main); whereas *A. inflata*, *Amphistegina* sp., *P. hanzawai*, *B. striatula*, *C.pseudolobatulus*, *E. advenum*, *E. craticulatum*, *E. striatopunctatum*, *P. granosa*, *R. orientalis*, and planktics are mostly found in the Shallow Marine areas. Q-mode cluster analysis of taxonomic and taphonomic data produced dendrograms with three biofacies and taphofacies: Biofacies A (BF_A), BF_B and BF_C; Taphofacies A (TF_A), TF_B and TF_C (Fig. 2.4; Fig. 2.5). Generally, the biofacies corresponds well with lagoon areas although inter-sample variabilities are quite high with high standard-deviations (Fig. 2.6).

2.3.1.1 Distal Lagoon Basin (BF_A, TF_A)

BF_A is predominantly found in the Distal Lagoon Basin located in the westernmost arm of the lagoon (Fig. 2.6a), which has the highest mean elevation (n = 17; E_{avg} = 0.6 ± 0.5 m.s.l.) and the most subaerial exposure time over tidal cycles (e_x = 11 hr/day; Table 1). BF_A is characterized by high proportions of miliolids (37 ± 8%), *A. parkinsoniana* (14 ± 5%), *A. tepida* (13 ± 5%), *E. gerthi* (11 ± 6%) and *P. planatus* (9 ± 5%) and a near absence of open marine benthics including *A. inflata*, *Amphistegina* spp. and planktics (<2%). Main Lagoon Basin samples 44 and 28 cluster with BF_A likely because their elevations were relatively high for this part of

the basin. Mean Shannon Diversity Index (SDI) values at 1.8 ± 0.1 (Table 2.1) indicate that the Distal Lagoon Basin is a transitional (SDI = 1.5 - 2.5) environment rather than stable (SDI = 2.5-3.5) or stressed (SDI = 0.1 – 1.5; e.g. Patterson and Kumar, 2000; Patterson and Kumar, 2002). In fact, all sample locations within the lagoon exhibited SDIs within the transitional range (1.5 – 2.4), except sample 57 (SDI = 1.4) which reflects a stressed environment at the mouth of Wadi Shamah (Fig. 2.7; Table 2.1). Generally, the diversity decreases with increased tidal exposure time (Shallow Marine Area = 2.0 ± 0.2 ; Main Lagoon Basin = 1.9 ± 0.1 ; Distal Lagoon Basin = 1.8 ± 0.1 ; Table 2.1), although there is considerable overlap in these values. It is questionable as to whether the SDIs are a true reflection of conditions within the lagoon as transport of allochthonous tests is likely quite high.

The Distal Lagoon Basin is predominantly made up of TF_A (n = 16; Fig. 2.6b; Table 2.2). The TF_A has the highest abundance of recent relative to fossil specimens ($84 \pm 8\%$), the most unaltered recent foraminifera ($51 \pm 22\%$) with the highest values of corrosion ($31 \pm 14\%$) and bioerosion ($11 \pm 7\%$). Fossil specimens are low in abundance ($16 \pm 8\%$) and did not seem to have any distinctive characteristics (Table 2.2).

2.3.1.2 Main Lagoon Basin (BF_B, TF_B)

Biofacies B (n = 20) is predominantly found in the Main Lagoon Basin with a mean elevation and tidal exposure time slightly lower than that of the Distal Lagoon ($E_{\text{avg}} = 0.3 \pm 0.6$ m.s.l., $e_x = 8$ hr/day; Table 1; Fig. 2.6a). There are only minor differences in the biofacies composition relative to BF_A, miliolids ($28 \pm 10\%$), *A. parkinsoniana* ($17 \pm 5\%$), *E. gerthi* ($15 \pm 6\%$) and *A. tepida* ($12 \pm 7\%$) are still the dominant taxa. However, the presence of minor allochthonous species (planktics: $6 \pm 3\%$; *Amphistegina* spp.: $2 \pm 2\%$; and *A. inflata*: $<1\%$) distinguishes it from BF_A in the cluster analysis (Fig. 2.4; Table 2.1). The network of intertidal channels connecting the Main Lagoon Basin with the Shallow Marine Area is the likely source for these taxa which would be transported into the lagoon via storms and tidal currents (e.g. *Amphistegina* spp. = $12 \pm 13\%$). These taxa are virtually absent in the Distal Lagoon Basin (Table 2.1).

TF_B is predominantly made up of recent specimens ($78 \pm 14\%$) which is slightly lower than TF_A ($84 \pm 8\%$) but higher than TF_C ($68 \pm 25\%$; Table 2.2; Fig. 2.6b). The other taphonomic characters are very similar to those in TF_A with only minor differences (e.g. corrosion and bioerosion; Table 2.2), although, there are larger differences with the Shallow Marine Area.

2.3.1.3 Shallow Marine Area (BF_C, TF_C)

Biofacies C (n = 15) is mainly found in the Shallow Marine Area in the embayment and also subtidal regions of the lagoon and has the lowest elevations (-0.8 ± 1.1 m.s.l.; i.e. open marine, entrance channel, main subtidal channel; Table 2.1; Fig. 2.6a). BF_C is characterized by lower abundances of miliolids ($22 \pm 12\%$) and *A. tepida* ($6 \pm 11\%$), and higher abundances of planktics ($14 \pm 10\%$), *Amphistegina* spp. ($12 \pm 13\%$), *Patellinella* sp., ($5 \pm 7\%$) and *A. inflata* ($2 \pm 2\%$). *A. inflata* abundances are low but important, as it is absent to very low in the lagoon basins. In general, the largest and most robust species (e.g. *Amphistegina* spp.) tend to dominate the Shallow Marine Area which has higher wave and current energies. The taphonomic characters show similar trends with high abundances of robust fossil specimens ($32 \pm 25\%$), and large sized foraminifera ($>500\mu\text{m} = 4 \pm 8\%$; $250\text{--}500\mu\text{m} = 13 \pm 12\%$), compared to the Distal and Main Lagoon Basins (Table 2.1; Table 2.2; Peebles and Lewis, 1991).

2.3.2 Stable isotopes

The stable isotopic data shows minor variations and is not useful in distinguishing subenvironments (Fig. 2.7). Generally, the subtidal Shallow Marine Area and the Main Lagoon Basin have slightly more negative $\delta^{18}\text{O}$ values ($\delta^{18}\text{O}_{\text{avg}} = -1.7 \pm 0.1\text{‰}$) than the intertidal environments in the Distal Lagoon Basin ($\delta^{18}\text{O}_{\text{avg}} = -1.3 \pm 0.4\text{‰}$). This lack of contrast seems unusual since the intertidal areas would have higher average temperatures, and evaporation rates with the 8 - 10 hr/day subaerial exposure (Fig. 2.7). The Gulf of Oman off Sur has sea surface temperatures of $\sim 27^\circ\text{C}$ and salinities of ~ 36.5 ppt (Sultan and Elghribi, 1996; Schils and Wilson, 2006). Measured salinity and temperature from mangroves in the lagoon are higher ($41.7 - 44.2$ ppt; $26 - 29^\circ\text{C}$) than the open sea, so some effect would be expected. The lack of contrast in values may be due to taphonomic biases due to reworking of older tests or transport of tests from subtidal areas of the lagoon.

Similarly the $\delta^{13}\text{C}$ values follow no trend and are more variable within the lagoon, likely due to the taphonomic issues already pointed out but also due to the complexity of factors affecting the dissolved inorganic carbon of the water (e.g. salinity, productivity and OM decomposition; Mackensen et al., 2001; Bickert and Mackensen, 2004; Peros et al., 2007).

2.3.3 Particle size

Generally, the fine silt and clay sized sediment is found in the mangrove areas on the southern lagoon margin as well as the Wadi Shamah deltaic area. Sandy sediments dominate the rest of the Lagoon (Main and Distal) and Shallow Marine Area. The Shallow Marine Area tends to have very coarse sand which transitions to medium sand in the Main Lagoon and fine to very fine sand in the Distal Lagoon (Fig. 2.3). The PSD transect with increasing penetration distance into the lagoon (Fig. 2.7), shows a coarse PSD tail (0 phi) in the Main Lagoon area but not in the Distal Lagoon Basin. This transition from coarse to fine particle sizes separates the subtidal and intertidal regions and is likely a reflection of reduced tidal current competence deeper into the lagoon.

2.4 DISCUSSION

2.4.1 Foraminiferal and taphonomic trends

Sediment inputs for Sur Lagoon predominantly come from three ephemeral wadis that occasionally flood during the rainy season, but do not provide a constant source of sediment. Wadi Shamah in particular, with its bird's foot delta, is likely one of the main inputs of new sediment into the lagoon (Fig. 2.2). Sediment is transported in and out of the lagoon via storms and tidal currents, with sediment removed from the shallow marine source due to longshore transport or export to the steeply sloping shelf. The coastline to the NW and SE of Sur is very rocky with one large wadi to the NW of Sur that is also a potential sediment source.

The transport of sediment in and out of the lagoon, with residence time in both areas, is supported by foraminiferal results. Overall, there is not a large difference in the foraminiferal biofacies or taphofacies between the Shallow Marine Area and the Lagoon Basins (Main and Distal), even though there is considerable environmental difference with tidal exposure and wave climate inside and outside of the lagoon. The greatest difference is between the Distal Lagoon Basin and Shallow Marine Area, with the Main Lagoon Basin acting as a transitional zone (Figs. 2.6, 2.8, 2.9; Table 2.1; Table 2.2). This similarity suggests that sediment spends residence time inside and outside of the lagoon inheriting taphonomic characteristics from both environments.

The abundance of miliolids, *A. tepida*, *A. parkinsoniana* and *E. gerthi* suggests they are the dominant taxa living in the lagoon and are found in similar coastal environments (e.g. Ghosh et al., 2009; Debenay et al., 2001; Murray 1991;

Lezine et al., 2002). The less-calcified specimens (e.g. *A. tepida*) are likely destroyed quickly in the Shallow Marine Area if exported from the lagoon, while the heavily calcified and larger *Amphistegina* spp. make their way into the Main Lagoon through storms, but not into the Distal Lagoon Basin (Fig. 2.8). This is supported by particle size data showing a slight fining trend into the distal areas, and fossil fragment size which gets smaller into the Distal Lagoon (Figs. 2.3, 2.7, 2.9). Likewise, the abundance of fossil specimens is greatest in the Shallow Marine Area likely due to their robustness and resistance to fragmentation and abrasion in the more energetic wave-dominated regime (i.e. vs. the modern specimens; Table 2.1; Table 2.2; Fig. 2.9). Fossil specimens are likely eroding out of Tertiary rocks outcropping on the coast and shelf areas as there is not an increased abundance of them in the wadi channels.

The degree of corrasion also shows some relationships with distance into the lagoon but it is only expressed in the fossil foraminifera. Maximal corrasion is highest in the Main and Distal Lagoon Basins but this maybe a size effect. The inner confines of the lagoon have higher quantities of fossil fragments which may have been exposed to corrasion for a longer period vs. the whole fossils which are found in the outer marine areas (Fig. 2.9).

Corrasion with modern specimens did not show a predictable trend; it was present, but was highly variable within the basins (Table 2.2). The lack of a clear trend maybe due to transport as discussed, or may relate to our ability to distinguish between dissolution and abrasion which would be correspondingly high inside vs. outside the lagoon.

2.4.2 Foraminiferal taphonomy as a potential overwash indicator

Based on the transect data, the most useful parameters for assessing an overwash event in Sur Lagoon will be the foraminifera taxa rather than the taphonomic characters per se (Fig. 2.5; Fig. 2.7). The most useful taxa for recognizing a marine incursion (e.g. tsunami or storm) will be the abundance of *Amphistegina* spp., *A. inflata*, *E. advenum* and planktics and we would expect them to be highly concentrated through transport and sorting in an event bed. These species have higher r^2 values with distance into the lagoon, and a distinct transition from the Shallow Marine Area to the Main and Distal Lagoon Basins. Taphonomically, large specimen sizes (>250 μm) and high proportions of fossil specimens were also closely associated with the Shallow Marine Area and therefore may be useful as a potential overwash indicator. Of note is the presence of planktic taxa and large sized specimens, which have been used previously (e.g. Hawkes et

al., 2007) with respect to the 2004 Indian Ocean tsunami, and based on this study will also prove important here.

2.5 CONCLUSIONS

In this arid intertidal lagoon at Sur, full taphonomic analysis is of limited value as the different environments are not causing a significant taphonomic imprint on the foraminifera. By far the most useful character is the foraminiferal assemblage itself and the enumeration of the number of fossil specimens. An overwash event at Sur Lagoon is expected to contain poorly sorted, heterogenous sand with relatively high abundances of *A. inflata*, *Amphistegina* spp., *E. advenum* and planktics, as well as large specimen sizes (>250 µm) and high proportions of fossil specimens. The best location to detect the overwash beds with foraminifera will be in the inner areas of the lagoon where the number of robust specimens (recent or fossil) is low or non-existent. This study illustrates the necessity of these types of studies to understand the sediment transport dynamics in order to assess event-beds and determine where the best sediment records can be sought.

ACKNOWLEDGEMENTS

The authors gratefully acknowledge (1) Richard Rothaus for field support, (2) Tom Vosmer and Barry Jupp for their assistance while on site in Oman, (3) Martin Knyf for technical assistance in McMaster's biogeochemistry laboratory, and (4) St. Cloud State University for the use of their Lowrance SONAR and Trimble R3. Funding was provided by NSERC research grants to Eduard Reinhardt (Discovery) and Jessica Pilarczyk (CGSM). This manuscript was greatly improved by comments from Ron Martin and two anonymous reviewers.

REFERENCES

- Ambraseys, N. N., Melville, C. P., 1982. A history of Persian earthquakes. Cambridge University Press, Cambridge, 219 pp.
- Berkeley, A., Perry, C. T., Smithers, S. G., 2009. Taphonomic signatures and patterns of test degradation on tropical, intertidal benthic foraminifera. *Mar Micropaleontol.* 73, 148-163.
- Best, M.M.R., Kidwell, S.M., 2000. Bivalve taphonomy in tropical mixed siliciclastic-carbonate settings: environmental variation in shell condition. *Paleobiology* 26, 80-102.

- Bhalla, S.N., Khare, N., Shanmukha, D.H., Henriques, P.J., 2007. Foraminiferal studies in nearshore regions of western coast of India and Laccadives Islands: A review. *Indian J. Mar. Sci.* 36, 272-287.
- Bickert, T., Mackensen, A., 2004. Last glacial Holocene changes in South Atlantic deep water circulation. In: Wefer, G., Mulitza, S., Ratmeyer, V. (Eds.), *The South Atlantic in the Late Quaternary: Reconstruction of material budgets and current systems*. Springer-Verlag, pp. 671-695.
- Chandler, G. T., Williams, D. F., Spero, H. J., Xiaodong, G., 1996. Sediment microhabitat effects on carbon stable isotopic signatures of microcosm-cultured benthic foraminifera. *Limnol. Oceanogr.* 41, 680-688.
- Cherif, O.H., Al-Ghadban, A., Al-Rifaiy, I.A., 1997. Distribution of foraminifera in the Arabian Gulf. *Micropaleontology* 43, 253-280.
- Culver, S.J., Woo, H.J., Oertel, G.F., Buzas, M.A., 1996. Foraminifera of coastal depositional environments, Virginia, U.S.A.: distribution and taphonomy. *Palaios* 11, 459-486.
- Debenay, J-P., Geslin, E., Eichler, B.B., Duleba, W., Sylvestre, F., Eichler, P., 2001. Foraminiferal assemblages in a hypersaline lagoon, Araruama (R. J.) Brazil. *J. Foramin. Res.* 31, 133-151.
- De Francesco, C.G., Hassan, G.S., 2008. Dominance of reworked fossil shells in modern estuarine environments: implications for paleoenvironmental reconstructions based on biological remains. *Palaios* 23, 14-23.
- Deil, U., 1996. Zur Kenntnis der Adiantetea-Gesellschaften des Mittelmeerraumes und umliegender Gebiete. *Phytocoenologia* 26, 481-536.
- Donato, S. V., Reinhardt, E. G., Boyce, J. I., Pilarczyk, J. E., Jupp, B. P., 2009. Particle-size distribution of inferred tsunami deposits in Sur Lagoon, Sultanate of Oman. *Mar. Geol.* 257, 54-64.
- Donato, S. V., Reinhardt, E. G., Boyce, J. I., Rothaus, R., Vosmer, T., 2008. Identifying tsunami deposits using bivalve shell taphonomy. *Geology* 36, 199-202.
- El-Nakhal, H., 1990. Geographical distribution of the foraminiferal genus *Agglutinella*. *Micropaleontology* 36, 86-87.
- Fishbein, E., Patterson, R.T., 1993. Error-weighted maximum likelihood (EWML): a new statistically based method to cluster quantitative micropaleontological data. *J. Paleontol.* 67, 475-486.
- Ghosh, A., Saha, S., Saraswati, P. K., Banerjee, S., Burley, S., 2009. Intertidal foraminifera in the macro-tidal estuaries of the Gulf of Cambay: Implications for interpreting sea-level change in palaeo-estuaries. *Mar. Petrol. Geol.* 26, 1592-1599.
- Hawkes, A.D., Bird, M., Cowie, S., Grundy-Warr, C., Horton, B.P., Tan Shau Hwai, A., Law, L., Macgregor, C., Nott, J., Eong Ong, J., Rigg, J., Robinson, R., Tan-Mullins, M., Tiong, T., Yasin, Z., Wan Aik, L., 2007. *Sediments*

- deposited by the 2004 Indian Ocean tsunami along the Malaysia-Thailand Peninsula. *Mar. Geol.* 242: 169-190.
- Hayward, B. W., Holzmann, M., Grenfell, H. R., Pawlowski, J., Triggs, C. M., 2004. Morphological distinction of molecular types in *Ammonia* - towards a taxonomic revision of the world's most commonly misidentified foraminifera. *Mar. Micropaleontol.* 50, 237-271.
- Heidarzadeh, M., Pirooz, M. D., Zaker, N. H., Yalciner, A. C., Mokhtari, M., Esmaeily, A., 2008. Historical tsunami in the Makran Subduction Zone off the southern coasts of Iran and Pakistan and results of numerical modeling. *Ocean Eng.* 35, 774-786.
- Hippensteel, S. P., Martin, R. E., 1999. Foraminifera as an indicator of overwash deposits, Barrier Island sediment supply, and Barrier Island evolution: Folly Island, South Carolina. *Palaeogeogr. Palaeoclimatol.* 149, 115-125.
- Hippensteel, S. P., Martin, R. E., 2000. Foraminifera of storm-generated washover fans: implications for determining storm frequency in relation to sediment supply and barrier island evolution, Folly Island, South Carolina. In: Martin, R. E. (ed.), *Environmental Micropaleontology: Topics in Geobiology*. Kluwer Academic/Plenum Publication, New York, 351-369.
- Hippensteel, S. P., Martin, R. E., Nikitina, D., Pizzuto, J. E., 2000. The formation of Holocene marsh foraminiferal assemblages, middle Atlantic Coast, U.S.A.: Implications for Holocene sea-level change. *J. Foramin. Res.* 30, 272-293.
- Hottinger, L., Halicz, E., Reiss, Z., 1993. Recent foraminifera from the Gulf of Aqaba, Red Sea. *Slovenska Akademija Znanosti in Umenosti (Ljubljana), classis IV, dela, 33*, 179, 230 pp.
- Kortekaas, S., Dawson, A. G., 2007. Distinguishing tsunami and storm deposits: an example from Martinhal, SW Portugal. *Sediment. Geol.* 200: 208-221.
- Lézine, A., Saliège, J., Mathieu, R., Tagliatela, T., Mery, S., Charpentier, V., Cleuziou, S., 2002. Mangroves of Oman during the late Holocene: climatic implications and impact on human settlements. *Veg. Hist. Archaeobot.* 11, 221-232.
- Loeblich, A. R., Tappan, H., 1987. *Foraminiferal Genera and their Classification*. Van Nostrand Reinhold Co., New York.
- Luque, L., Lario, J., Civis, J., Silva, P. G., Zazo, C., Goy, J. L., Dabrio, C. J., 2002. Sedimentary record of a tsunami during Roman times, Bay of Cadiz, Spain. *J. Quaternary Sci.* 17, 623-631.
- Mackensen, A., Rudolph, M., Kuhn, G., 2001. Late Pleistocene deepwater circulation in the subantarctic eastern Atlantic. *Global Planet. Change* 30, 197-229.
- Mamo, B., Strotz, L., Dominey-Howes, D., 2009. Tsunami sediments and their foraminiferal assemblages. *Earth-Sci. Rev.* 96, 263-278.
- Martin, R. E., 1999. *Taphonomy: A Process Approach*. Cambridge University

- Press, Cambridge, 508 pp.
- Martin, R.E., Harris, M.S., Liddell, W.D., 1995. Taphonomy and time-averaging of foraminiferal assemblages in Holocene tidal flat sediments, Bahia La Choya, Sonora, Mexico (Northern Gulf of California). *Mar. Micropaleontol.* 26, 187-206.
- Martin, R.E., Wehmiller, J.F., Harris, M.S., Liddell, W.D., 1996. Comparative taphonomy of bivalves and foraminifera from Holocene tidal flat sediments, Bahia la Choya, Sonora, Mexico (Northern Gulf of California): taphonomic grades and temporal resolution. *Paleobiology* 22, 80-90.
- Moghaddasi, B., Nabavi, S. M. B., Vosoughi, G., Fatemi, S. M. R., Jamili, S., 2008. Abundance and distribution of benthic foraminifera in the Northern Oman Sea (Iranian Side) continental shelf sediments. *Res. J. Environ. Sci.* 3, 210-217.
- Murray, J.W., 1965. The foraminiferida of the Persian Gulf. 2. The Abu Dhabi Region. *Palaeogeogr. Palaeocl.* 1, 307-332.
- Murray, J.W., 1966a. The foraminiferida of the Persian Gulf. 3. The Halat Al Bahrani region. *Palaeogeogr. Palaeocl.* 2, 59-68.
- Murray, J.W., 1966b. The foraminiferida of the Persian Gulf. 4. Khor Al Bazam. *Palaeogeogr. Palaeocl.* 2, 153-169.
- Murray, J.W., 1966c. The foraminiferida of the Persian Gulf. 5. The shelf off the Trucial Coast. *Palaeogeogr. Palaeocl.* 2, 267-278.
- Murray, J.W., 1991. Ecology and paleoecology of benthic foraminifera. John Wiley & Sons, Inc., 397p.
- Murray, J.W., Alve, E., 1999. Taphonomic experiments on marginal marine foraminiferal assemblages: how much ecological information is preserved? *Palaeogeogr. Palaeocl.* 149, 183-197.
- Murray, M.R., 2002. Is laser particle size determination possible for carbonate-rich lake sediments? *J. Paleolimnol.* 27, 173-183.
- Nigam, R., Khare, N., 1995. Recent foraminifera along west coast of India: Retrospect, perspect and prospect. *Journal of the Indian Academy of Geoscience* 38, 7-24.
- Okal, E. A., Synolakis, C. E., 2008. Far-field tsunami hazard from mega-thrust earthquakes in the Indian Ocean. *Geophys. J. Int.* 172, 995-1015.
- Parsons-Hubbard, K.M., 2005. Molluscan taphofacies in recent carbonate reef/lagoon systems and their application to sub-fossil samples from reef cores. *Palaios.* 20, 175-191.
- Patterson, R. T., Fishbein, E., 1989. Re-examination of the statistical methods used to determine the number of point counts needed for micropaleontological quantitative research. *J. Paleontol.* 63, 245-248.
- Patterson, R. T., Kumar, A., 2000. Use of arcellacea to gauge levels of pollution and remediation of industrially polluted lakes. In: Martin, R. E. (Ed.),

- Environmental Micropaleontology, v. 15 of Topics in Geobiology. Kluwer Academic/Plenum Publication, New York. Pp. 257-278.
- Patterson, R.T., Kumar, A., 2002. A review of current testate rhizopod (thecamoebian) research in Canada. *Palaeogeogr. Palaeoclimatol.* 180, 225-251.
- Peebles, M. W., Lewis, R. D., 1991. Surface textures of benthic foraminifera from San-Salvador, Bahamas. *J. Foramin. Res.* 21, 285-292.
- Peros, M.C., Reinhardt, E.G., Davis, A.M., 2007. High-resolution paleosalinity reconstruction from Laguna de la Leche, north coastal Cuba, using Sr, O, and C isotopes. *Palaeogeogr. Palaeoclimatol.* 245, 535-550.
- Pilarczyk, J. E., Reinhardt, E. G., 2011. *Homotrema rubrum* (Lamarck) taphonomy as an overwash indicator in marine ponds on Anegada, British Virgin Islands. *Nat. Hazards*. doi: 10.1007/s11069-010-9706-3.
- Reddy, K. R., Rao, R. J., 1984. Foraminifera-salinity relationship in the Pennar Estuary, India. *J. Foramin. Res.* 14, 115-119.
- Reinhardt, E.G., Goodman, B.E., Boyce, J.I., Lopez, G., van Hengstum, P., Rink, W., Mart, Y., Raban, A., 2006. The Tsunami of December 13, 115 A.D. and the destruction of Herod the Great's Harbor at Caesarea Maritima, Israel. *Geology* 34, 1061-1064.
- Sambridge, M., Braun, J., McQueen, H., 1995. Geophysical parametrization and interpolation of irregular data using natural neighbors. *Geophys. J. Int.* 122, 837-857.
- Schils, T., Wilson, S. C., 2006. Temperature threshold as a biogeographic barrier in northern Indian Ocean macroalgae. *J. Phycol.* DOI: 10.1111/j.1529-8817.2006.00242.x
- Scott, D. B., Collins, E. S., Gayes, P. T., Wright, E., 2003. Records of prehistoric hurricanes on the South Carolina coast based on micropaleontological and sedimentological evidence, with comparison to other Atlantic Coast records. *Geol. Soc. Am. Bull.* 115, 1027-1039.
- Sultan, S. A. R., Elghribi, N. M., 1996. Temperature inversion in the Arabian Gulf and the Gulf of Oman. *Cont. Shelf Res.* 16, 1521-1544.
- Szuman, M., Berndt, C., Jacobs, C., Best, A., 2006. Seabed characterization through a range of high-resolution acoustic systems - a case study offshore Oman. *Mar. Geophys. Res.* 27, 167-180.
- van Hengstum, P.J., Reinhardt, E.G., Boyce, J.I., Clark, C., 2007. Changing sedimentation patterns due to historical land-use change in Frenchman's Bay, Pickering, Canada: evidence from high-resolution textural analysis. *J. Paleolimnol.* 37, 603-618.

APPENDICES

2.A.1: Systematics of Foraminifera

Faunal reference list for dominant taxa. The classification follows that of Hottinger et al. (1993), Hayward et al. (2004) and Loeblich and Tappan (1987). Systematics of individual species are from Hottinger et al. (1993) and references therein.

Amphistegina lessonii D'ORBIGNY, 1826

Amphistegina lobifera LARSEN, 1976

Ammonia inflata = *Rosalina inflata* SEGUENZA, 1862

Ammonia parkinsoniana = *Rosalina parkinsoniana* D'ORBIGNY, 1839

Ammonia tepida = *Rotalia beccarii* var. *tepida* CUSHMAN, 1936

Cibicides pseudolobatus PERELIS & REISS, 1976

Elphidium advenum CUSHMAN, 1930

Elphidium craticulatum = *Nautilus craticulatus* FICHTEL & MOLL, 1798

Elphidium gerthi VAN VOORTHUYSEN, 1957

Elphidium striatopunctatum = *Nautilus striatopunctatus* FICHTEL & MOLL, 1798

Peneroplis planatus = *Nautilus planatus* FICHTEL & MOLL, 1798

Porosonion granosa = *Noionina granosa* D'ORBIGNY, 1846

CHAPTER 2 FIGURES

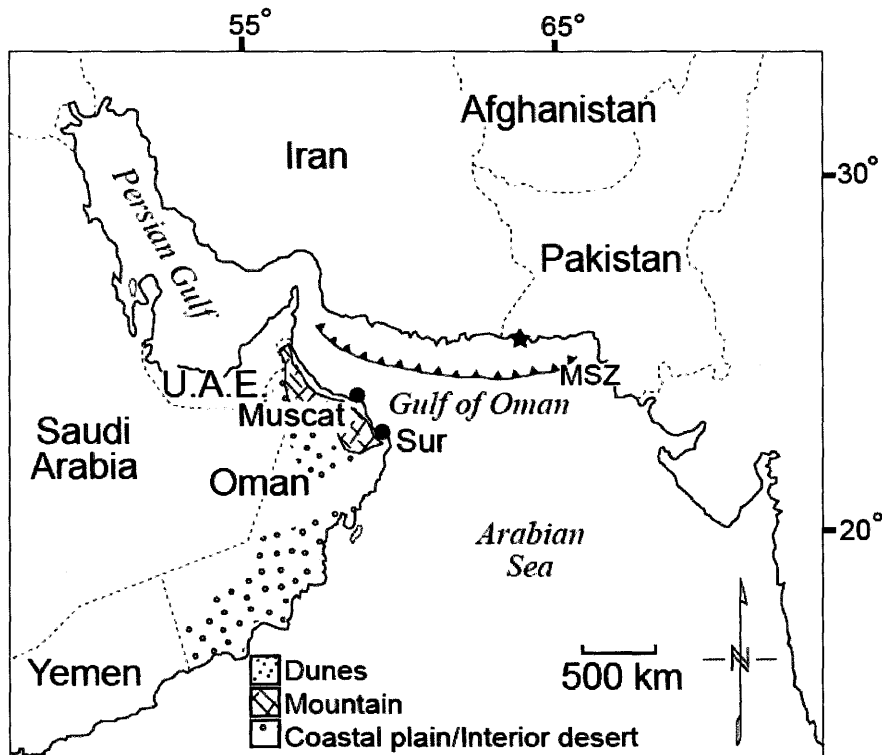
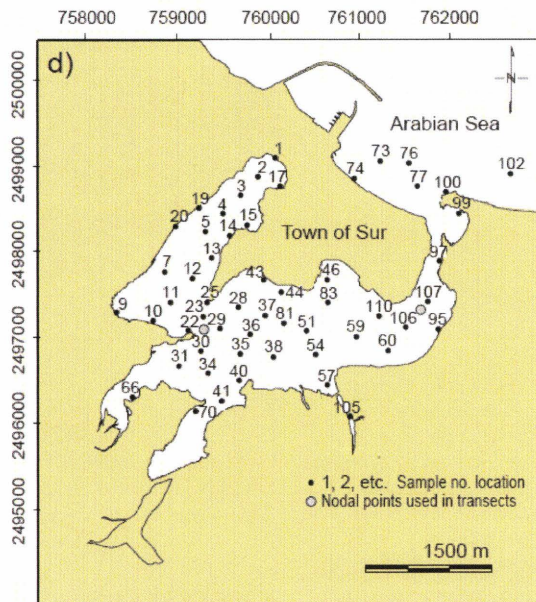
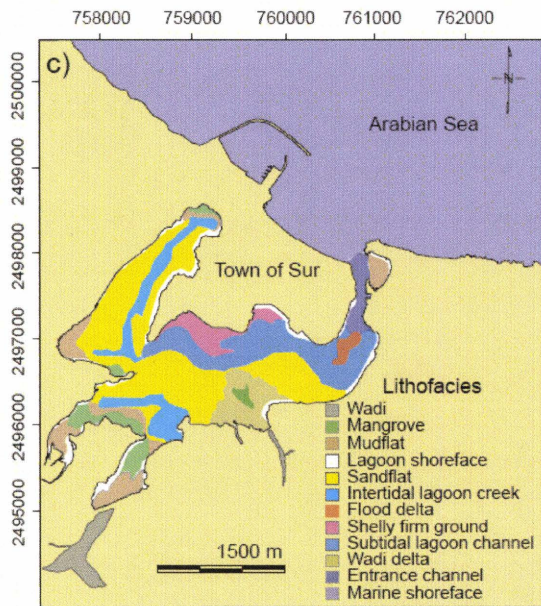
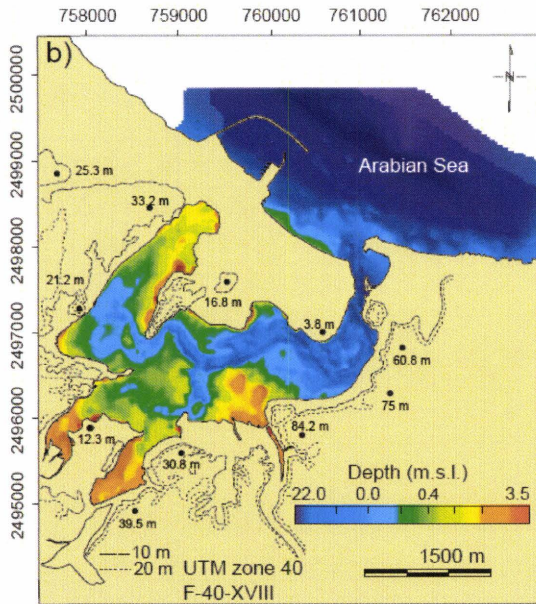
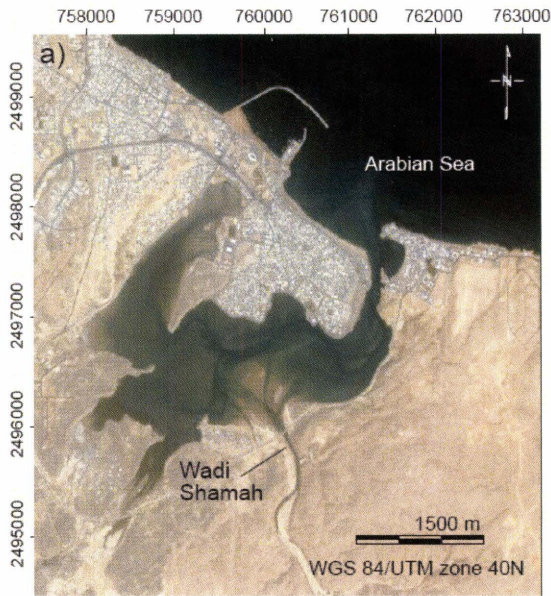


Figure 2.1: Location of Sur Lagoon relative to the Makran Subduction Zone (MSZ). Epicentre of the 28 November 1945 tsunamigenic earthquake (M_w 8.1; black star) and broad-scale geologic features within Oman indicated.

Figure 2.2: a) Satellite image of Sur Lagoon obtained from Google Earth. b) Digital Elevation Model (DEM) of the study area using data collected with a Trimble R3 unit and a Lowrance SONAR. c) Sedimentary sub-environments within the lagoon. Colors correspond to varying lithofacies identified during field survey, DEM analysis, and satellite imagery. d) Location of surface samples used in the foraminiferal analysis. Nodes at the base of the entrance channel and at the Main – Distal Lagoon boundary were used to calculate the distance of each sample location relative to the marine source (Figs. 2.7 - 2.9). (see following page)



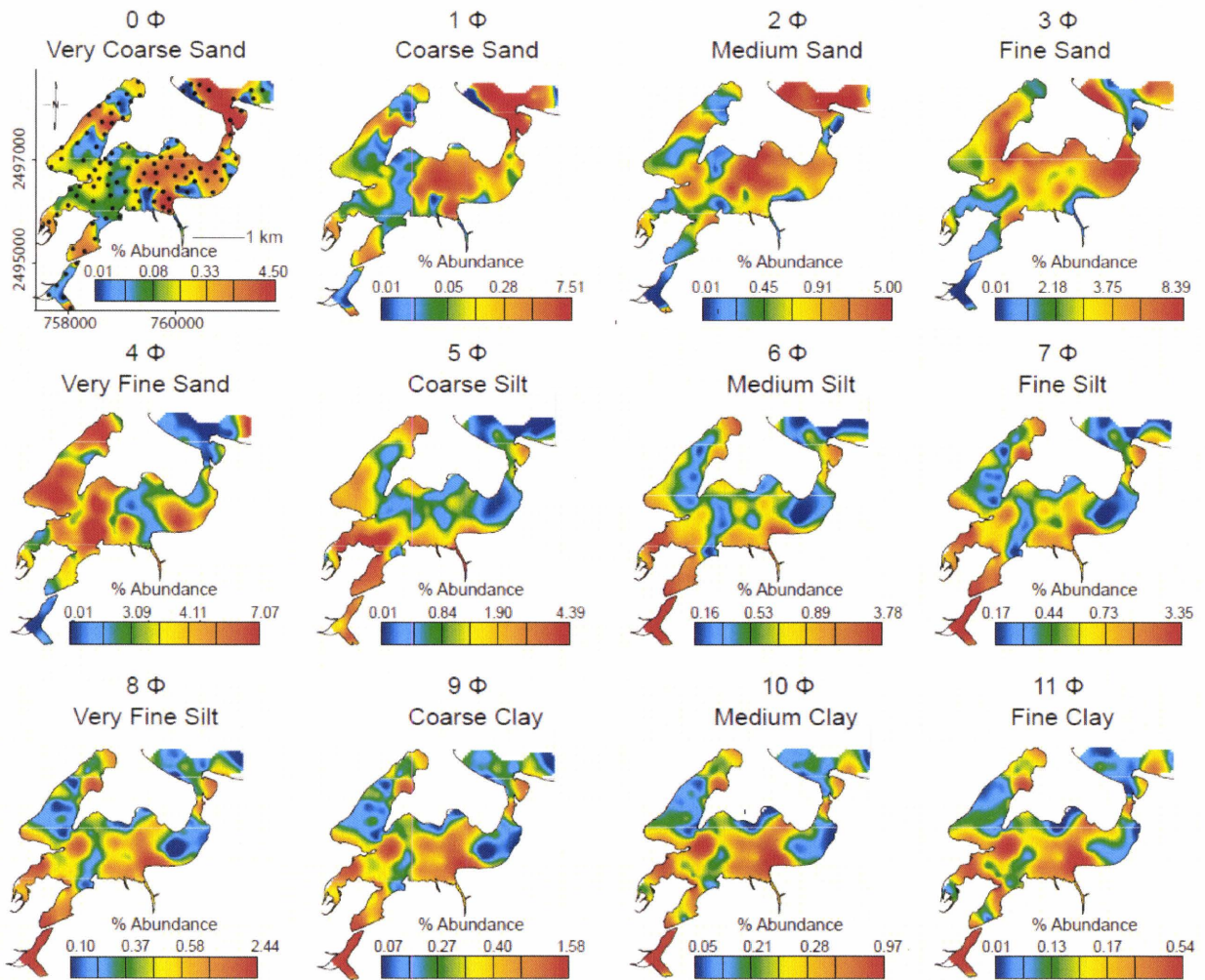
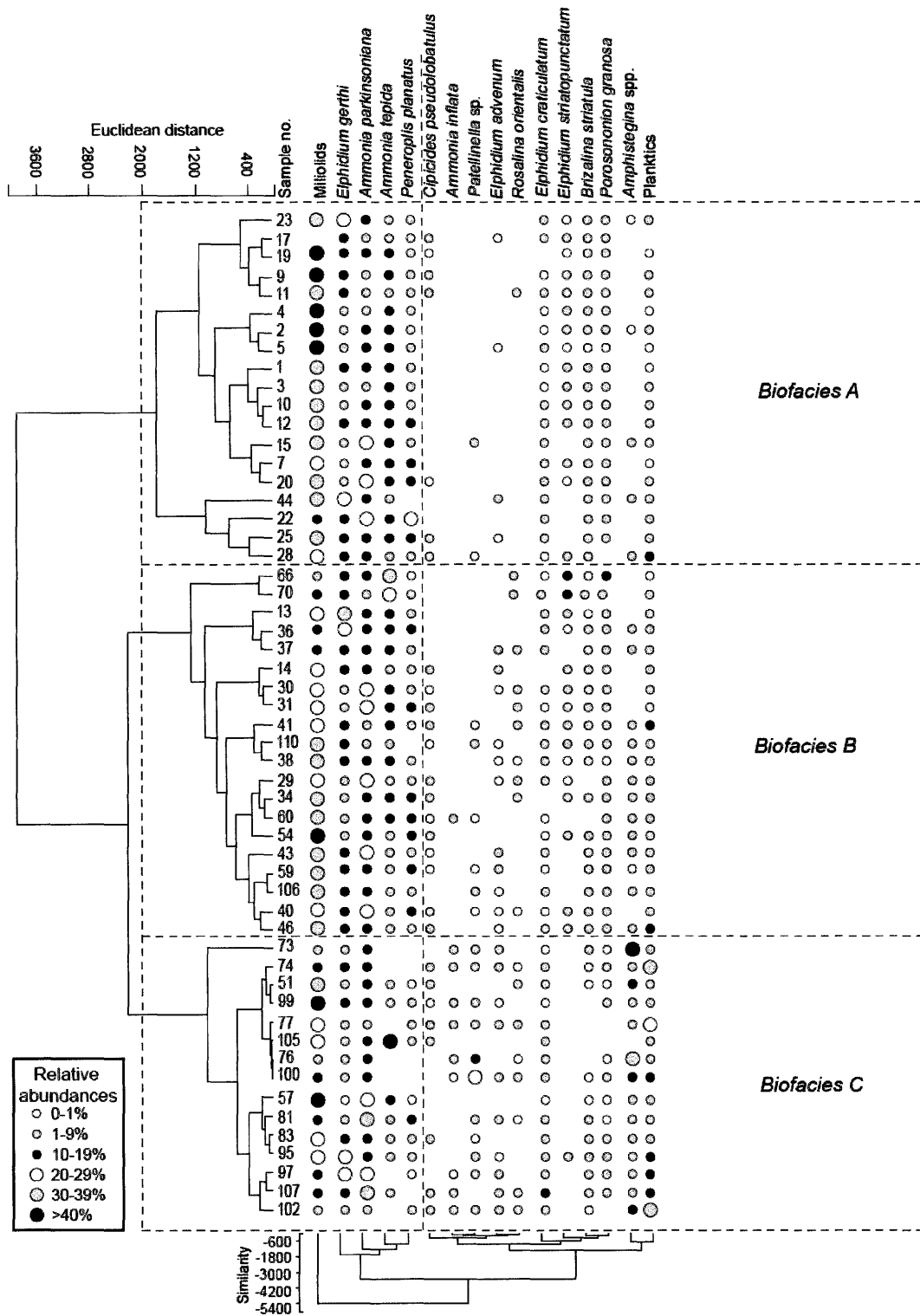


Figure 2.3: Particle-size distribution (PSD) plots for Sur Lagoon based on percent abundance of particle size fraction (0-11 ϕ). Sample locations ($n = 111$) used for the particle-size analysis are represented by black circles.

Figure 2.4: Q-Mode versus R-Mode cluster analysis using Ward's method indicating three biofacies (*See following page*).



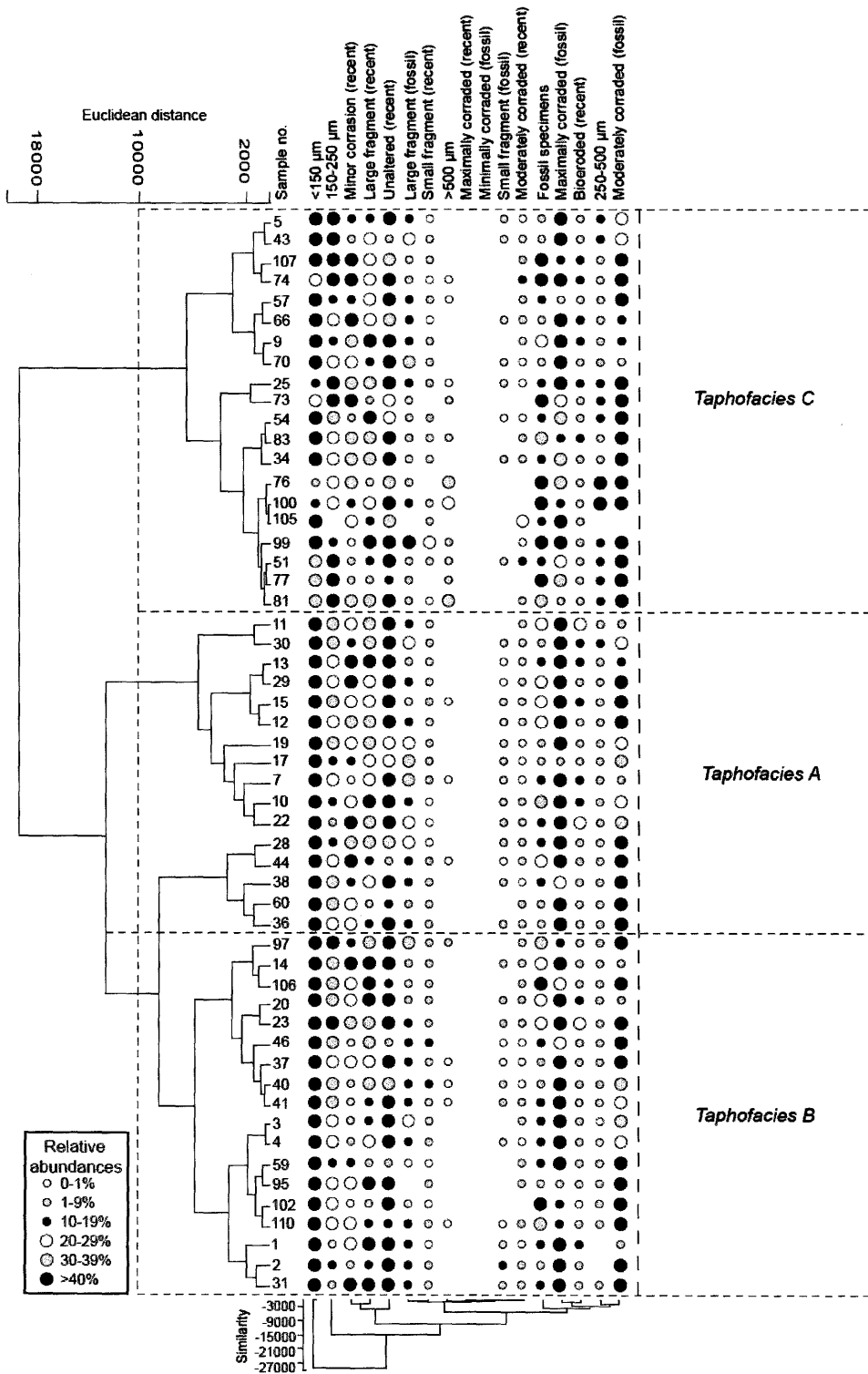


Figure 2.5: Q-Mode versus R-Mode cluster analysis using Ward's method indicating three taphofacies (See previous page).

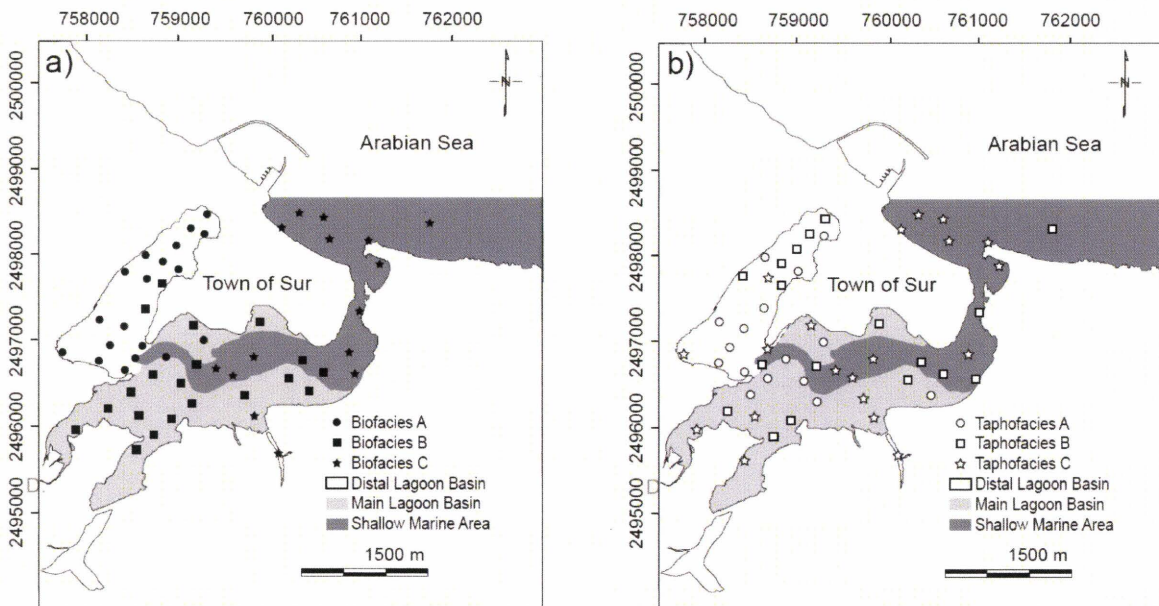


Figure 2.6: Distribution of biofacies (a) and taphofacies (b) showing relationship with geographic boundaries (Distal Lagoon Basin, Main Lagoon Basin and Shallow Marine Area).

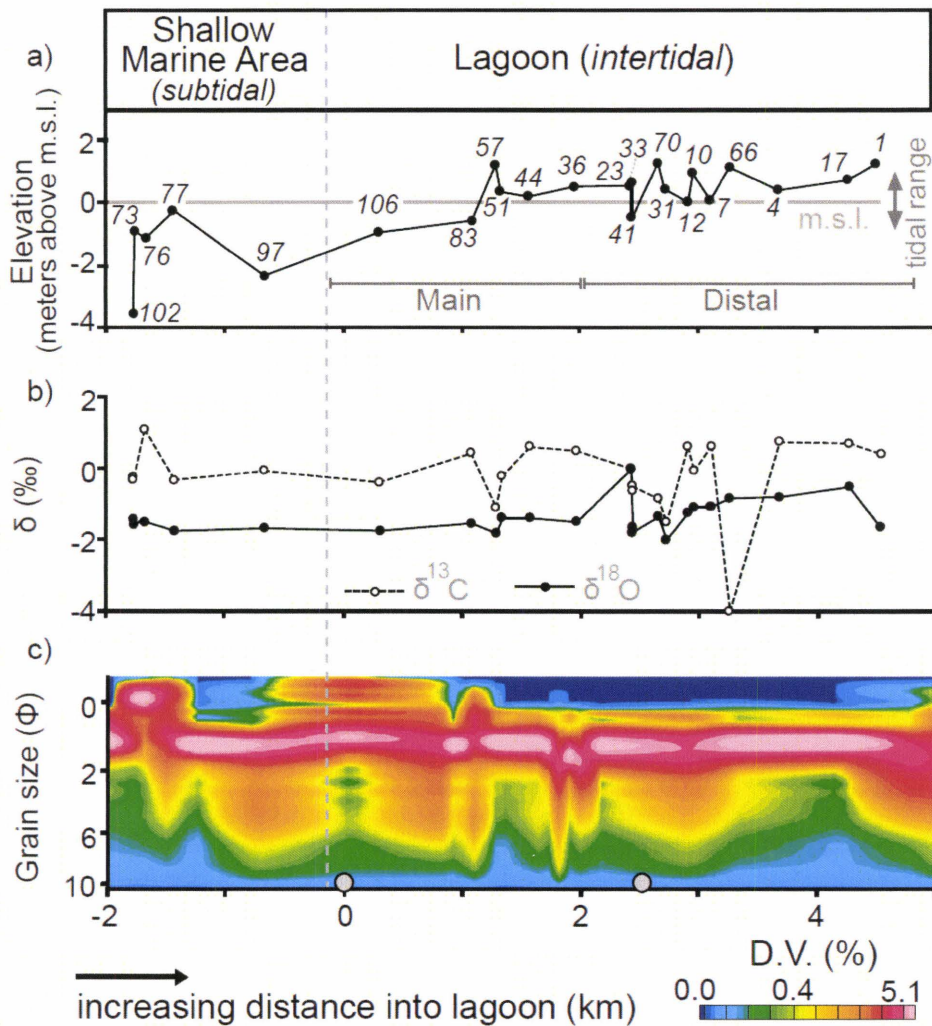
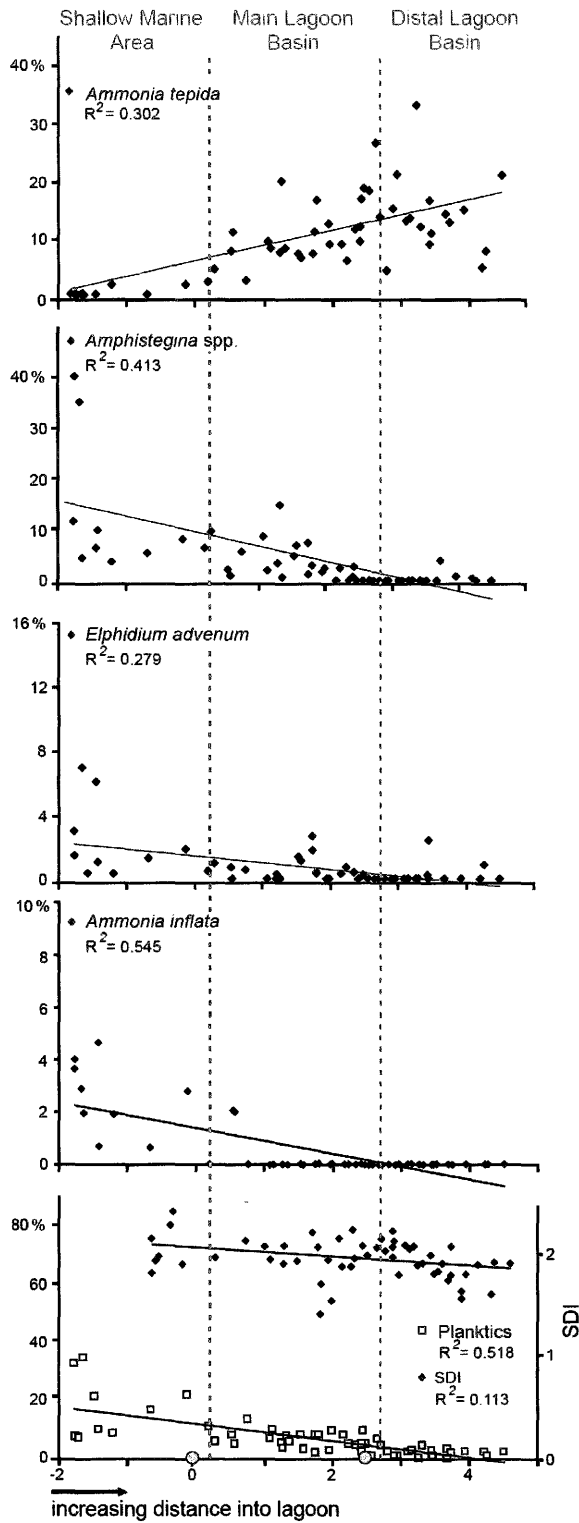


Figure 2.7: **a)** Elevation along a transect from the Shallow Marine Area through the Main and Distal Lagoon Basins using nodes shown in Fig. 2.2d. **b)** Stable isotope data for sample locations along the transect. **c)** Particle-size plots for the transect (D.V. % = differential volume percent).

Figure 2.8: Abundances of significant taxa and Shannon-Weaver Diversity Index (SDI) vs. distance from the Shallow Marine Area outside the lagoon using nodes shown in Fig. 2.2d (See following page).



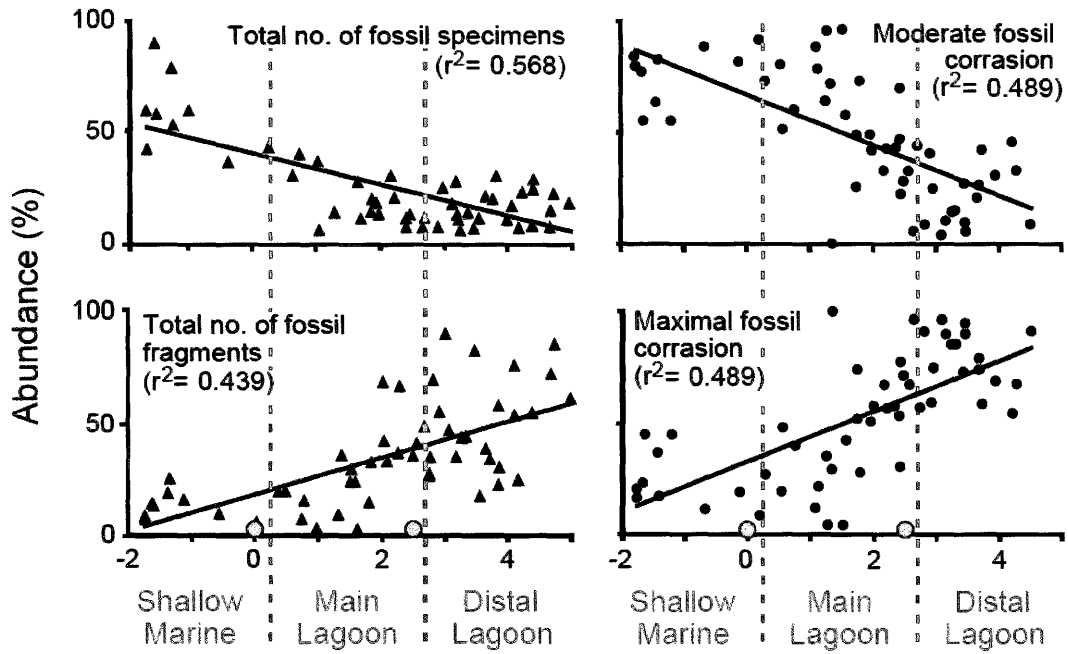


Figure 2.9: Dominant taphonomic characters vs. distance from the Shallow Marine Area outside the lagoon using nodes shown in Fig. 2.2d.

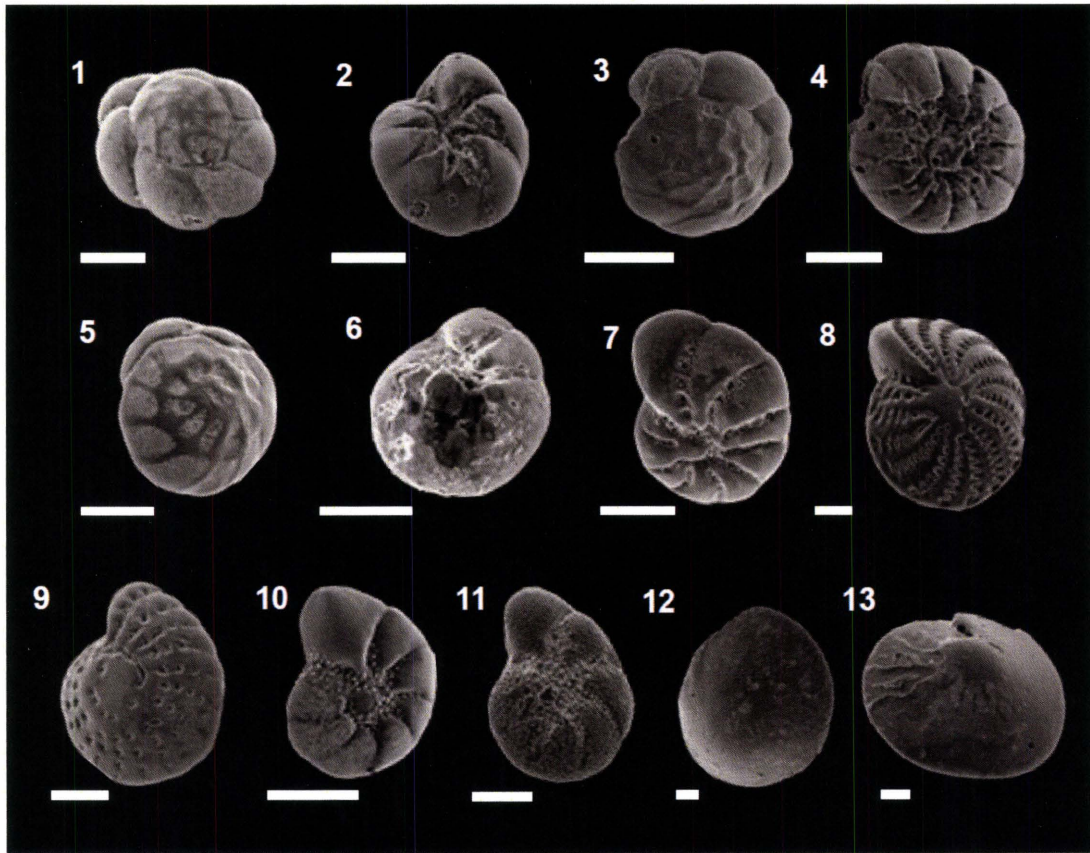


Plate 2.1: All scale bars are equal to 100 μm . 1. *Ammonia tepida* ventral view. 2. *Ammonia tepida* dorsal view. 3. *Ammonia parkinsoniana* ventral view. 4. *Ammonia parkinsoniana* dorsal view. 5. *Ammonia inflata* ventral view. 6. *Ammonia inflata* dorsal view. 7. *Elphidium gerthi* side view. 8. *Elphidium craticulatum* side view. 9. *Elphidium striatopunctatum* side view. 10. *Elphidium advenum* side view. 11. *Porosonion granosa* side view. 12. *Amphistegina lessonii* ventral view. 13. *Amphistegina lobifera* ventral view.

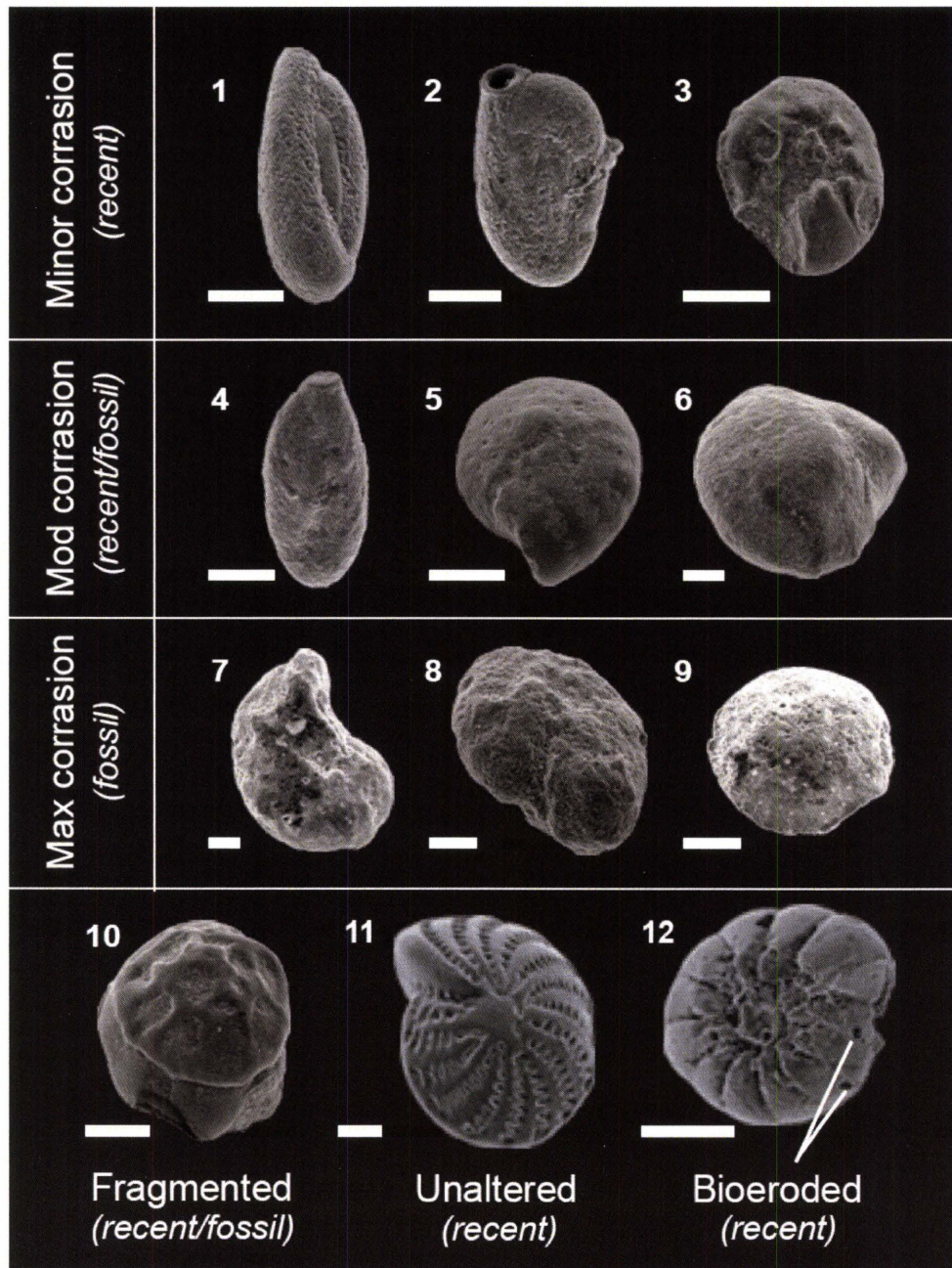


Plate 2.2: All scale bars represent 100 μm . 1-3. Minimally corroded recent individuals (recent only). 4-6. Moderately corroded individuals (recent and fossil). 7-9. Maximally corroded fossil individuals (fossil only). 10. Fragmented individual (recent and fossil). 11. Taphonomically unaltered individual (recent only). 12. Bioeroded individual (recent only).

CHAPTER 2 TABLES

Biofacies	BF_A	BF_B	BF_C
Elevation (m.s.l.)	0.6 ± 0.5	0.3 ± 0.6	-0.8 ± 1.1
Exposure time (hr/day)	11	8	0
Shannon-Weaver diversity (SDI)	1.8 ± 0.1	1.9 ± 0.1	2.0 ± 0.2
<i>Ammonia inflata</i>	0	<1	2 ± 2
<i>Ammonia parkinsoniana</i>	14 ± 5	17 ± 5	18 ± 7
<i>Ammonia tepida</i>	13 ± 5	12 ± 7	6 ± 11
<i>Amphistegina</i> spp.	<1	2 ± 2	12 ± 13
<i>Patellinella</i> sp.	<1	<1	5 ± 7
<i>Brizalina striatula</i>	4 ± 2	3 ± 1	1 ± 1
<i>Cibicides pseudobatulus</i>	1 ± 2	1 ± 2	1 ± 2
<i>Elphidium gerthi</i>	11 ± 6	15 ± 6	10 ± 6
<i>Elphidium craticulatum</i>	2 ± 2	2 ± 2	2 ± 2
<i>Elphidium advenum</i>	<1	<1	2 ± 2
<i>Peneroplis planatus</i>	9 ± 5	7 ± 4	2 ± 3
<i>Elphidium striatopunctatum</i>	2 ± 2	2 ± 4	<1
<i>Porosononion granosa</i>	4 ± 2	3 ± 3	2 ± 2
<i>Milliolids</i>	37 ± 8	28 ± 10	22 ± 12
Planktics	2 ± 2	6 ± 3	14 ± 10

Table 2.1: Biofacies elevation, exposure time, average Shannon Diversity Index (SDI) and foraminiferal abundances (% ± 1 std.) for the three biofacies determined with cluster analysis.

Taphofacies	TF_A	TF_B	TF_C
Taphofacies elevation (m.s.l.)	0.4 ± 0.3	0.2 ± 1.1	-0.1 ± 1.4
Exposure time (hr/day)	11	8	0
Specimen size:			
>500µm	<1	<1	4 ± 8
250-500µm	6 ± 3	4 ± 3	13 ± 12
150-250µm	27 ± 9	26 ± 10	35 ± 17
<150µm	67 ± 11	69 ± 13	48 ± 25
Recent foraminifera:			
Total recent	84 ± 8	78 ± 14	68 ± 25
Minor corrosion	29 ± 13	21 ± 19	25 ± 17
Moderate corrosion	2 ± 1	2 ± 2	4 ± 6
Maximal corrosion	0	0	0
Total corrosion	31 ± 14	22 ± 19	29 ± 19
Small fragment	3 ± 2	4 ± 5	3 ± 5
Large fragment	29 ± 10	28 ± 15	26 ± 18
Total fragments	32 ± 10	32 ± 17	30 ± 23
Bioeroded	11 ± 7	6 ± 6	7 ± 4
Unaltered	51 ± 22	45 ± 28	49 ± 21
Fossil foraminifera:			
Total fossil	16 ± 8	22 ± 14	32 ± 25
Minor corrosion	0	0	0
Moderate corrosion	34 ± 20	49 ± 29	56 ± 31
Maximal corrosion	66 ± 20	51 ± 29	45 ± 31
Small fragment	2 ± 1	3 ± 5	1 ± 2
Large fragment	17 ± 9	11 ± 6	10 ± 8
Total fragments	19 ± 9	14 ± 10	12 ± 10

Table 2.2: Taphofacies elevation, exposure time, and average foraminiferal taphonomic characteristics (% ± 1 std.) for the three taphofacies determined with cluster analysis.

CHAPTER 2 ONLINE SUPPLEMENTARY DATA

Sample No.	UTM easting	UTM northing	Distance (km)	Elevation (m.s.l.)	Mean (μm)	Mode (μm)	σ (μm)	$\delta^{13}\text{C}$ (‰)	$\delta^{18}\text{O}$ (‰)	Environment	* Taphofacies	
Biofacies A - Distal Lagoon Basin												
1	759327	2498526	4.5	1.2	116.1	87.9	73.9	0.4	-1.6	Mangrove	ML	
2	759114	2498315	4.2	0.8	91.5	87.9	73.9	-	-	Sand flat	ML	
3	758910	2498097	3.9	0.5	116.6	127.6	68.6	-	-	Intertidal channel	ML	
4	758721	2497898	3.7	0.4	132.4	140.1	73.2	0.7	-0.8	Intertidal channel	ML	
5	758517	2497693	3.4	0.3	140.6	153.8	98.0	-	-	Intertidal channel	SM	
7	758100	2497277	3.1	0.1	98.5	101.2	74.6	0.6	-1.1	Sand flat	DL	
9	757644	2496825	3.3	1.4	90.1	99.9	106.1	-	-	Sand flat	SM	
10	758012	2496738	3.0	0.9	101.8	106.2	108.7	-0.1	-1.1	Mangrove	DL	
11	758181	2496941	2.8	0.1	95.1	87.9	69.1	-	-	Sand flat	DL	
12	758400	2497178	2.9	0.0	121.9	140.1	81.4	0.6	-1.2	Sand flat	DL	
15	759013	2497833	3.7	1.5	92.5	127.6	78.9	-	-	Intertidal channel	DL	
17	759384	2498225	4.3	0.7	82.3	85.3	103.6	0.7	-0.5	Mangrove edge	DL	
19	758484	2497955	3.7	0.7	166.9	144.7	185.5	-	-	Sand flat	DL	
20	758265	2497718	3.5	1.5	202.3	149.2	250.3	-	-	Sand flat	ML	
22	758401	2496632	2.6	0.6	132.3	127.6	84.6	-	-	Sand flat	DL	
23	758545	2496820	2.4	0.5	116.8	127.6	77.4	-	-	Intertidal channel	ML	
25	758615	2496906	2.4	0.0	145.2	153.8	84.5	-	-	Sand flat	SM	
28	758966	2496878	2.0	0.4	125.5	127.6	81.6	-	-	Subtidal channel	DL	
44	759415	2497016	1.6	0.2	134.1	140.1	79.0	0.6	-1.4	Sand flat	DL	
				Average	0.6	121.2	121.2	103.3	0.5	-1.1		
				σ	0.5	29.7	26.7	49.1	0.3	0.4		
Biofacies B - Main Lagoon Basin												
13	758605	2497394	3.2	0.5	127.9	140.1	61.9	-	-	Sand flat	DL	
14	758807	2497613	3.5	1.1	120.3	140.1	85.3	-	-	Sand flat	ML	
29	758725	2496647	2.2	0.4	154.5	153.8	161.2	-	-	Sand flat	DL	
30	758507	2496440	2.5	0.4	92.4	80.1	79.5	-	-	Sand flat	DL	
31	758298	2496234	2.7	0.4	76.3	66.4	72.7	-1.5	-2.0	Sand flat	ML	
33	758482	2496030	2.5	0.7	73.5	66.4	72.9	-0.6	-1.7	Sand flat	-	
34	758603	2496160	2.4	0.3	93.1	87.9	79.8	-	-	Intertidal channel	SM	
36	759006	2496581	2.0	0.5	126.2	140.1	88.8	0.5	-1.5	Sand flat	DL	
37	759208	2496793	1.8	-0.5	148.6	140.1	106.1	-	-	Subtidal channel	ML	
38	759197	2496383	1.8	-0.2	103.6	116.3	56.9	-	-	Subtidal channel	DL	
40	758898	2496083	2.2	0.4	123.9	127.7	82.9	-	-	Intertidal channel	ML	
41	758690	2495885	2.4	-0.5	123.9	127.6	82.8	-0.5	-1.8	Mangrove edge	ML	
43	759276	2497188	1.7	0.6	160.6	147.0	121.9	-	-	Mud flat	SM	
46	759900	2497164	1.1	-0.3	165.5	140.1	107.0	-	-	Sand flat	ML	
54	759746	2496408	1.3	1.1	44.9	72.9	39.5	-	-	Wadi delta	SM	
59	760239	2496550	0.8	0.0	106.1	116.3	57.2	-	-	Sand flat	ML	
60	760502	2496436	0.6	-0.2	113.2	127.6	62.7	-	-	Sand flat	DL	
66	757803	2495985	3.3	1.1	65.7	50.2	76.4	-4.0	-0.8	Mangrove	SM	
70	758477	2495798	2.7	1.3	65.7	55.1	84.8	-0.9	-1.3	Mangrove	SM	
106	760713	249624	0.3	-1.0	122.7	140.1	56.1	-0.4	-1.8	Subtidal channel	ML	
110	760421	2496736	0.5	-0.2	131.8	140.1	81.6	-	-	Intertidal channel	ML	
				Average	0.3	113.4	115.5	82.3	-1.1	-1.6		
				σ	0.6	32.9	33.5	26.9	1.4	0.4		

* DL = Distal Lagoon Basin, ML = Main Lagoon Basin, SM = Shallow Marine Area

Table 2.S1: Textural and geochemical data by biofacies.

Table 2.S1 continued...

WP	UTM easting	UTM northing	Distance (km)	Elevation (m.s.l.)	Mean (μm)	Mode (μm)	σ (μm)	$\delta^{13}\text{C}$ (‰)	$\delta^{18}\text{O}$ (‰)	Environment	* Taphofacies
Biofacies C - Shallow Marine Area											
51	759630	2496678	1.3	0.3	217.2	153.8	243.8	-0.2	-1.4	Wadi delta edge	SM
57	759859	2496114	1.3	1.2	50.2	50.3	68.4	-1.1	-1.8	Wadi	SM
73	760392	2498441	-1.8	-0.9	213.1	203.5	144.3	-0.2	-1.7	Shallow marine	SM
74	760213	2498236	-1.6	0.4	173.2	213.5	105.4	-	-	Beach	SM
76	760643	2498418	-1.7	-1.1	642.6	751.1	376.9	1.1	-1.5	Shallow marine	SM
77	760763	2498195	-1.4	-0.2	434.2	905.1	445.0	-0.3	-1.7	Shallow marine	SM
81	759429	2496720	1.5	-0.9	209.3	169.6	263.8	-	-	Subtidal channel	SM
83	759885	2496880	1.1	-0.6	185.7	127.6	280.0	0.4	-1.5	Subtidal channel	SM
95	761093	2496624	0.2	-1.1	126.2	140.1	79.1	-	-	Lagoon shoreface	ML
97	761142	2497418	-0.7	-2.3	126.2	120.1	92.6	-0.1	-1.7	Subtidal channel	ML
99	761310	2497919	-1.2	-0.3	75.3	80.1	95.4	-	-	Mud flat	SM
100	761189	2498170	-1.4	-0.2	473.0	517.2	258.1	-	-	Beach	SM
102	761857	2498303	-1.8	-3.6	121.2	127.6	62.0	-0.3	-1.6	Shallow marine	ML
105	760157	2495677	1.4	1.5	69.9	72.9	61.7	-	-	Wadi edge	SM
107	760936	2496884	-0.1	-1.0	164.7	168.9	90.5	-	-	Subtidal channel	SM
			Average	-0.8	243.2	282.9	195.1	-0.1	-1.6		
			σ	1.1	167.4	266.3	124.8	0.6	0.1		

* DL = Distal Laoon Basin, ML = Main Lagoon Basin, SM = Shallow Marine Area

Sample ID	WP 1	WP 2	WP 3	WP 4	WP 5	WP 7	WP 9	WP 10	WP 11
Total count (benthics)	269	559	541	339	416	269	283	280	278
Specimens per 1 cc	2765	2378	2456	2470	2650	2643	2372	2730	2658
Shannon-Weaver diversity	1.9	1.6	1.9	1.6	1.7	1.9	1.9	1.9	2.0
Elevation (m.s.l.)	2.1	0.8	0.5	0.2	0.3	0.1	2.7	0.4	0.1
Biofacies*	DL	DL	DL	DL	DL	DL	DL	DL	DL
<i>Ammonia inflata</i>	-	-	-	-	-	-	-	-	-
Standard error ±	-	-	-	-	-	-	-	-	-
<i>Ammonia parkinsoniana</i>	0.104	0.014	0.049	0.028	0.144	0.207	0.091	0.109	0.067
Standard error ±	0.037	0.010	0.018	0.017	0.033	0.048	0.033	0.036	0.029
<i>Ammonia tepida</i>	0.193	0.042	0.139	0.131	0.153	0.120	0.111	0.197	0.039
Standard error ±	0.048	0.016	0.029	0.035	0.034	0.038	0.036	0.046	0.022
<i>Amphistegina</i> sp.	-	0.005	-	-	-	-	-	-	-
Standard error ±	-	0.006	-	-	-	-	-	-	-
<i>Assilina ammonoides</i>	-	-	-	-	-	-	-	-	-
Standard error ±	-	-	-	-	-	-	-	-	-
<i>Patellinella</i> cf. <i>P. hanzawai</i>	-	-	-	-	-	-	-	0.035	-
Standard error ±	-	-	-	-	-	-	-	0.021	-
<i>Brizalina striatula</i>	0.066	0.007	0.023	0.023	0.005	0.051	0.020	0.021	0.133
Standard error ±	0.030	0.007	0.013	0.016	0.007	0.026	0.016	0.017	0.039
<i>Cipicides pseudolobatus</i>	-	-	-	-	-	-	0.077	-	0.049
Standard error ±	-	-	-	-	-	-	0.030	-	0.025
<i>Cornispira</i> sp.	-	-	-	-	-	-	-	-	-
Standard error ±	-	-	-	-	-	-	-	-	-
<i>Elphidium gerthi</i>	0.162	0.031	0.052	0.097	0.078	0.033	0.104	0.088	0.147
Standard error ±	0.045	0.014	0.019	0.031	0.025	0.021	0.035	0.033	0.041
<i>Elphidium craticulatum</i>	0.008	0.002	0.005	0.006	0.094	0.018	0.007	0.014	0.011
Standard error ±	0.011	0.003	0.006	0.008	0.028	0.016	0.009	0.014	0.012
<i>Elphidium advenum</i>	-	-	-	-	0.002	-	-	-	-
Standard error ±	-	-	-	-	0.005	-	-	-	-
<i>Peneroplis planatus</i>	0.023	0.003	0.007	0.017	0.075	0.254	0.094	0.056	0.067
Standard error ±	0.018	0.005	0.007	0.014	0.025	0.051	0.033	0.027	0.029
<i>Elphidium striatopunctatum</i>	0.058	0.007	0.023	0.020	0.009	0.025	0.020	0.021	0.011
Standard error ±	0.028	0.007	0.013	0.015	0.009	0.019	0.016	0.017	0.012
<i>Porosonion granosa</i>	0.035	0.014	0.038	0.034	0.009	0.043	0.027	0.056	0.063
Standard error ±	0.022	0.010	0.016	0.019	0.009	0.024	0.018	0.027	0.028
<i>Miliamina fusca</i>	-	-	-	-	-	-	-	-	-
Standard error ±	-	-	-	-	-	-	-	-	-
<i>Miliolids</i>	0.313	0.848	0.622	0.585	0.405	0.225	0.383	0.380	0.379
Standard error ±	0.056	0.029	0.040	0.051	0.047	0.049	0.055	0.056	0.056
<i>Rosalina orientalis</i>	-	-	-	-	-	-	-	-	0.011
Standard error ±	-	-	-	-	-	-	-	-	0.012
<i>Spirillina</i> sp.	-	-	0.002	-	-	-	-	-	-
Standard error ±	-	-	0.004	-	-	-	-	-	-
<i>Textularia</i> sp.	-	-	-	-	-	-	-	-	-
Standard error ±	-	-	-	-	-	-	-	-	-
Planktics	0.027	0.026	0.025	0.037	0.021	0.025	0.050	0.014	0.025
Standard error ±	0.020	0.013	0.013	0.020	0.014	0.019	0.025	0.014	0.018

* DL = Distal Lagoon Basin, ML = Main Lagoon Basin, SM = Shallow Marine Area

Table 2.S2: Foraminiferal data (Shannon-Weaver diversity index, fractional abundances and standard error).

Table 2.S2 continued...

WP 12	WP 13	WP 14	WP 15	WP 17	WP 19	WP 20	WP 22	WP 23	WP 25	WP 28	WP 29
297	310	285	297	343	317	247	293	283	262	243	264
2802	1984	1195	2500	2170	1984	2108	3648	2406	3354	3085	1664
1.9	1.8	2.0	1.8	1.9	1.6	1.8	1.8	1.9	2.0	2.0	2.1
0.2	0.7	1.2	1.2	2.2	0.5	0.2	0.7	0.2	0.2	0.3	0.4
DL	ML	ML	DL	DL	DL	DL	DL	DL	DL	DL	ML
-	-	-	-	-	-	-	-	-	-	-	-
-	-	-	-	-	-	-	-	-	-	-	-
0.189	0.184	0.180	0.240	0.089	0.132	0.204	0.242	0.103	0.163	0.189	0.211
0.044	0.042	0.044	0.048	0.030	0.037	0.050	0.049	0.035	0.044	0.047	0.048
0.140	0.125	0.082	0.118	0.069	0.129	0.100	0.168	0.086	0.105	0.081	0.054
0.039	0.036	0.031	0.036	0.027	0.037	0.037	0.043	0.032	0.036	0.033	0.026
-	-	-	0.043	-	-	-	-	0.007	-	0.026	0.025
-	-	-	0.023	-	-	-	-	0.010	-	0.019	0.018
-	-	-	-	-	-	-	-	-	-	0.007	-
-	-	-	-	-	-	-	-	-	-	0.010	-
-	-	-	0.013	-	-	-	-	-	-	0.007	-
-	-	-	0.013	-	-	-	-	-	-	0.010	-
0.063	0.006	0.031	0.020	0.055	0.028	0.036	0.010	0.076	0.033	0.019	-
0.027	0.009	0.020	0.016	0.024	0.018	0.023	0.011	0.030	0.021	0.016	-
-	-	0.071	-	0.014	0.009	0.008	-	-	0.022	0.011	0.050
-	-	0.029	-	0.013	0.011	0.011	-	-	0.017	0.013	0.026
-	-	-	-	-	-	-	-	0.003	-	-	-
-	-	-	-	-	-	-	-	0.007	-	-	-
0.156	0.306	0.153	0.063	0.109	0.116	0.076	0.104	0.221	0.101	0.148	0.082
0.041	0.051	0.041	0.027	0.033	0.035	0.033	0.035	0.048	0.036	0.042	0.032
0.010	0.019	-	0.030	0.052	-	0.012	0.027	0.024	0.036	0.004	0.061
0.011	0.015	-	0.019	0.023	-	0.013	0.018	0.018	0.022	0.007	0.028
-	-	0.024	-	0.009	-	-	-	-	0.004	-	0.007
-	-	0.017	-	0.010	-	-	-	-	0.007	-	0.010
0.086	0.047	0.071	0.033	0.037	0.047	0.108	0.205	0.083	0.156	0.078	0.104
0.032	0.023	0.029	0.020	0.020	0.023	0.038	0.046	0.032	0.043	0.032	0.036
0.020	0.022	0.017	-	0.043	0.009	0.008	-	0.003	-	0.015	0.007
0.016	0.016	0.015	-	0.021	0.011	0.011	-	0.007	-	0.014	0.010
0.043	0.025	0.031	0.013	0.046	0.038	0.024	0.010	0.038	0.029	-	0.018
0.023	0.017	0.020	0.013	0.022	0.021	0.019	0.011	0.022	0.020	-	0.016
-	-	-	-	-	-	-	-	-	-	-	0.004
-	-	-	-	-	-	-	-	-	-	-	0.007
0.279	0.231	0.293	0.372	0.451	0.465	0.392	0.192	0.314	0.301	0.281	0.290
0.051	0.046	0.052	0.054	0.052	0.055	0.061	0.045	0.053	0.054	0.054	0.053
-	0.003	-	-	-	-	-	-	0.017	-	-	0.022
-	0.006	-	-	-	-	-	-	0.015	-	-	0.017
-	-	-	-	-	-	-	-	-	-	-	-
-	-	-	-	-	-	-	-	-	-	-	-
-	-	-	-	0.011	0.019	-	-	-	-	-	-
-	-	-	-	0.011	0.015	-	-	-	-	-	-
0.013	0.031	0.031	0.023	0.014	0.003	0.012	0.013	0.024	0.051	0.100	0.054
0.013	0.019	0.020	0.017	0.013	0.006	0.013	0.013	0.018	0.026	0.036	0.026

Table 2.S2 continued...

WP 30	WP 31	WP 34	WP 36	WP 37	WP 38	WP 40	WP 41	WP 43	WP 44	WP 46	WP 51
383	257	240	303	264	286	295	248	256	259	303	258
1304	1244	1517	1926	1664	1779	1888	1536	1632	3315	1933	202
2.1	2.0	2.0	2.0	2.2	1.9	2.0	2.2	1.8	1.9	2.0	1.9
0.3	0.4	0.5	0.3	0.2	0.4	0.7	0.4	0.3	0.2	-0.3	0.7
ML	ML	ML	ML	ML	ML	ML	ML	ML	DL	ML	SM
-	-	-	-	-	-	-	-	-	-	-	-
-	-	-	-	-	-	-	-	-	-	-	-
0.156	0.274	0.154	0.182	0.163	0.099	0.220	0.091	0.260	0.104	0.169	0.171
0.035	0.053	0.044	0.043	0.043	0.033	0.045	0.034	0.053	0.037	0.040	0.044
0.173	0.126	0.111	0.115	0.101	0.154	0.081	0.156	0.065	0.060	0.074	0.075
0.037	0.040	0.039	0.035	0.035	0.040	0.030	0.043	0.030	0.028	0.028	0.031
-	-	0.016	0.019	0.080	0.032	-	0.036	0.011	0.075	0.021	0.164
-	-	0.015	0.015	0.031	0.020	-	0.022	0.013	0.031	0.015	0.043
-	-	-	-	-	-	-	0.004	-	-	-	-
-	-	-	-	-	-	-	0.007	-	-	-	-
-	-	-	-	-	-	0.009	0.004	-	-	-	-
-	-	-	-	-	-	0.010	0.007	-	-	-	-
0.057	0.033	0.036	0.019	0.024	0.029	0.012	0.051	0.019	0.030	0.012	0.004
0.023	0.021	0.023	0.015	0.018	0.019	0.012	0.026	0.017	0.020	0.012	0.007
0.002	0.011	0.028	-	-	-	0.012	0.015	0.008	-	0.030	0.018
0.005	0.013	0.020	-	-	-	0.012	0.014	0.011	-	0.018	0.016
-	-	-	-	-	-	-	-	-	-	-	-
-	-	-	-	-	-	-	-	-	-	-	-
0.097	0.067	0.095	0.240	0.177	0.144	0.146	0.167	0.179	0.272	0.124	0.075
0.029	0.030	0.036	0.047	0.044	0.039	0.039	0.044	0.046	0.053	0.035	0.031
0.027	0.007	-	0.058	0.035	0.032	0.006	0.018	0.080	0.060	0.030	0.011
0.016	0.010	-	0.026	0.021	0.020	0.009	0.016	0.033	0.028	0.018	0.012
0.002	-	-	-	0.017	0.003	0.003	-	0.027	0.011	0.003	-
0.005	-	-	-	0.015	0.006	0.006	-	0.020	0.013	0.006	-
0.035	0.119	0.103	0.115	0.094	0.022	0.121	0.033	-	-	0.062	0.007
0.018	0.039	0.037	0.035	0.034	0.016	0.036	0.021	-	-	0.026	0.010
0.022	0.022	0.012	0.006	-	0.006	0.016	0.015	-	-	0.021	-
0.014	0.018	0.013	0.009	-	0.009	0.014	0.014	-	-	0.015	-
0.054	0.015	0.024	0.019	0.014	0.006	0.022	0.033	0.023	0.015	0.012	0.007
0.022	0.014	0.019	0.015	0.014	0.009	0.016	0.021	0.018	0.015	0.012	0.010
-	0.004	-	-	0.014	-	-	-	-	-	0.003	0.007
-	0.007	-	-	0.014	-	-	-	-	-	0.006	0.010
0.277	0.204	0.336	0.188	0.188	0.356	0.258	0.244	0.302	0.332	0.328	0.332
0.044	0.048	0.058	0.043	0.045	0.053	0.048	0.051	0.056	0.056	0.050	0.055
0.005	0.022	0.024	-	0.010	0.006	0.009	0.011	-	0.007	-	0.036
0.007	0.018	0.019	-	0.012	0.009	0.010	0.012	-	0.010	-	0.022
-	-	0.012	-	-	0.006	-	0.007	0.004	-	-	-
-	-	0.013	-	-	0.009	-	0.010	0.007	-	-	-
-	-	-	-	-	-	-	-	-	-	-	-
-	-	-	-	-	-	-	-	-	-	-	-
0.052	0.048	0.051	0.032	0.083	0.083	0.084	0.098	0.023	0.034	0.104	0.079
0.022	0.026	0.027	0.019	0.032	0.031	0.030	0.035	0.018	0.022	0.032	0.032

Table 2.S2 continued...

WP 54	WP 57	WP 59	WP 60	WP 66	WP 70	WP 73	WP 74	WP 76	WP 77	WP 81	WP 83
310	294	308	321	315	249	280	262	427	355	340	348
989	375	1553	1661	1212	1549	1773	232	14	68	539	547
1.7	1.4	1.9	1.9	1.8	2.0	1.8	2.0	1.9	2.3	2.1	2.2
0.9	1.3	0.0	-0.2	3.1	0.7	-1.7	0.3	-2.2	-0.2	-1.7	-1.9
ML	SM	ML	ML	ML	ML	SM	SM	SM	SM	SM	SM
-	-	-	0.020	-	-	0.036	0.020	0.029	0.046	-	-
-	-	-	0.015	-	-	0.021	0.014	0.018	0.019	-	-
0.116	0.206	0.162	0.295	0.140	0.091	0.174	0.118	0.178	0.095	0.313	0.144
0.035	0.045	0.038	0.048	0.039	0.034	0.043	0.031	0.042	0.027	0.047	0.036
0.067	0.186	0.022	0.101	0.310	0.248	-	-	-	-	0.065	0.085
0.027	0.044	0.015	0.032	0.052	0.051	-	-	-	-	0.025	0.028
0.015	0.036	0.062	0.009	-	-	0.441	0.047	0.385	0.071	0.051	0.093
0.013	0.021	0.025	0.010	-	-	0.056	0.021	0.054	0.024	0.022	0.029
-	-	0.003	0.006	-	-	-	0.005	-	0.009	-	-
-	-	0.005	0.008	-	-	-	0.007	-	0.009	-	-
-	-	0.003	0.003	-	-	0.036	0.022	0.140	0.093	0.022	0.008
-	-	0.005	0.006	-	-	0.021	0.014	0.038	0.027	0.015	0.009
0.021	0.010	0.031	-	0.007	0.040	0.030	0.002	-	-	0.019	0.021
0.016	0.011	0.018	-	0.009	0.023	0.019	0.005	-	-	0.014	0.015
0.021	-	0.022	0.006	-	-	-	0.027	-	0.018	-	0.021
0.016	-	0.015	0.008	-	-	-	0.016	-	0.012	-	0.015
-	-	-	-	-	-	-	-	-	-	-	-
-	-	-	-	-	-	-	-	-	-	-	-
0.061	0.007	0.129	0.058	0.163	0.131	0.063	0.103	0.067	0.060	0.081	0.168
0.026	0.009	0.035	0.025	0.042	0.040	0.027	0.030	0.028	0.022	0.028	0.038
0.003	0.007	0.025	0.006	0.007	0.026	0.010	0.017	0.013	0.046	0.065	0.032
0.006	0.009	0.016	0.008	0.009	0.019	0.011	0.013	0.012	0.019	0.025	0.018
-	-	0.006	-	-	-	0.030	0.069	-	0.060	0.013	-
-	-	0.008	-	-	-	0.019	0.025	-	0.022	0.012	-
0.040	0.003	0.064	0.127	0.003	0.011	-	-	-	0.033	0.105	0.032
0.021	0.006	0.025	0.035	0.007	0.012	-	-	-	0.017	0.031	0.018
0.012	-	-	0.009	0.137	0.146	-	-	-	-	-	-
0.012	-	-	0.010	0.039	0.042	-	-	-	-	-	-
0.052	0.007	0.006	0.012	0.120	0.018	0.010	0.015	0.003	-	0.005	0.051
0.024	0.009	0.008	0.011	0.037	0.016	0.011	0.012	0.006	-	0.007	0.022
-	-	-	-	-	-	0.010	0.015	0.016	0.027	0.008	0.008
-	-	-	-	-	-	0.011	0.012	0.014	0.015	0.009	0.009
0.532	0.497	0.328	0.283	0.050	0.157	0.082	0.182	0.092	0.217	0.162	0.243
0.054	0.056	0.049	0.047	0.025	0.043	0.031	0.038	0.032	0.038	0.037	0.043
-	-	-	-	0.010	0.015	-	0.002	0.010	0.011	0.008	-
-	-	-	-	0.011	0.014	-	0.005	0.011	0.010	0.009	-
0.003	0.003	-	-	-	0.004	-	-	-	-	-	-
0.006	0.006	-	-	-	0.007	-	-	-	-	-	-
-	-	-	-	-	-	-	-	-	-	-	0.003
-	-	-	-	-	-	-	-	-	-	-	0.005
0.058	0.039	0.137	0.052	0.003	0.069	0.079	0.355	0.067	0.215	0.084	0.072
0.025	0.022	0.036	0.023	0.007	0.030	0.030	0.047	0.028	0.038	0.028	0.026

Table 2.S2 continued...

WP 95	WP 97	WP 99	WP 100	WP 102	WP 105	WP 106	WP 107	WP 110
352	266	290	255	364	327	383	252	265
552	666	231	25	562	33	1532	638	1658
2.0	2.0	1.9	2.4	2.1	1.5	1.9	2.1	2.1
0.3	1.2	-0.3	0.6	-3.6	2.4	-0.1	-0.2	-0.2
SM	SM	SM	SM	SM	SM	ML	SM	ML
-	0.006	0.019	0.007	0.040	-	-	0.028	0.021
-	0.009	0.015	0.010	0.016	-	-	0.018	0.016
0.194	0.238	0.135	0.158	0.097	0.115	0.137	0.203	0.083
0.039	0.047	0.037	0.042	0.025	0.034	0.033	0.044	0.032
0.020	-	0.016	-	-	0.411	0.042	0.015	0.069
0.014	-	0.014	-	-	0.052	0.019	0.013	0.029
0.071	0.060	0.041	0.109	0.128	-	0.105	0.089	0.024
0.025	0.026	0.022	0.036	0.028	-	0.030	0.031	0.018
-	0.019	-	0.014	0.007	-	0.015	-	-
-	0.015	-	0.014	0.007	-	0.012	-	-
0.018	0.034	0.038	0.243	0.071	-	-	0.012	0.021
0.013	0.020	0.021	0.050	0.022	-	-	0.012	0.016
0.038	0.028	-	0.007	0.004	-	0.017	0.012	0.010
0.019	0.018	-	0.010	0.005	-	0.013	0.012	0.012
-	-	0.003	-	0.042	0.043	-	0.046	0.003
-	-	0.006	-	0.017	0.021	-	0.023	0.007
-	-	-	-	-	-	-	-	-
-	-	-	-	-	-	-	-	-
0.207	0.226	0.150	0.067	0.073	0.011	0.235	0.120	0.118
0.040	0.046	0.039	0.029	0.022	0.011	0.041	0.035	0.037
0.015	0.016	0.003	0.032	0.027	-	0.017	0.034	0.021
0.012	0.014	0.006	0.020	0.014	-	0.013	0.020	0.016
0.005	0.013	0.003	0.011	0.015	-	0.010	0.018	0.007
0.007	0.012	0.006	0.012	0.010	-	0.010	0.015	0.010
0.030	0.003	0.063	-	0.015	0.057	0.017	-	0.087
0.017	0.006	0.027	-	0.010	0.024	0.013	-	0.032
0.010	-	-	-	-	-	-	-	0.010
0.010	-	-	-	-	-	-	-	0.012
0.015	0.028	0.016	0.046	-	-	-	0.018	0.024
0.012	0.018	0.014	0.024	-	-	-	0.015	0.018
0.005	-	-	-	0.016	0.006	-	-	0.010
0.007	-	-	-	0.011	0.008	-	-	0.012
0.247	0.163	0.411	0.173	0.095	0.296	0.337	0.145	0.367
0.043	0.041	0.054	0.044	0.025	0.048	0.046	0.038	0.056
-	-	-	0.025	0.035	-	-	0.034	0.010
-	-	-	0.018	0.015	-	-	0.020	0.012
0.003	-	-	0.004	-	-	-	-	-
0.005	-	-	0.007	-	-	-	-	-
0.010	-	-	-	-	-	-	-	-
0.010	-	-	-	-	-	-	-	-
0.111	0.166	0.091	0.102	0.336	0.060	0.064	0.225	0.083
0.031	0.041	0.032	0.035	0.040	0.025	0.024	0.045	0.032

Sample ID	WP 1	WP 2	WP 3	WP 4	WP 5	WP 7	WP 9
Recent specimens per 1 cc	922	224	216	136	166	3443	604
Fossil specimens per 1 cc	133	22	49	24	15	413	179
Elevation (m.s.l.)	2.1	0.8	0.5	0.2	0.3	0.1	2.7
Taphofacies*	ML	ML	ML	ML	SM	DL	SM
>500µm specimens	-	-	-	-	-	0.001	-
250-500µm specimens	-	-	0.005	0.018	0.180	0.046	0.016
150-250µm specimens	0.075	0.103	0.274	0.242	0.403	0.203	0.188
<150µm specimens	0.925	0.897	0.722	0.740	0.417	0.751	0.797
Modern specimens:							
Minimally corraded	0.266	0.036	0.039	0.050	0.126	0.013	0.307
Moderately corraded	0.004	0.031	0.014	0.007	0.007	0.001	0.038
Maximally corraded	-	-	-	-	-	-	-
0-49% fragment	0.008	0.031	0.020	0.037	0.002	0.013	0.042
50-99% fragment	0.403	0.134	0.142	0.221	0.123	0.264	0.413
Predated	0.123	0.018	0.028	0.088	0.012	0.187	0.148
Unaltered	0.579	0.836	0.915	0.723	0.907	0.687	0.657
Fossil specimens:							
Minimally corraded	-	-	-	-	-	-	-
Moderately corraded	0.090	0.455	0.306	0.208	0.267	0.041	0.145
Maximally corraded	0.910	0.545	0.694	0.792	0.733	0.958	0.855
0-49% fragment	0.090	0.182	-	0.067	0.067	0.010	-
50-99% fragment	0.178	0.136	0.237	0.167	0.187	0.353	0.143
Total fossils	0.126	0.090	0.185	0.150	0.083	0.107	0.229

* DL = Distal Lagoon Basin, ML = Main Lagoon Basin, SM = Shallow Marine Area

Table 2.S3: Taphonomic data (fractional abundances).

Table 2.S3 continued...

WP 10	WP 11	WP 12	WP 13	WP 14	WP 15	WP 17	WP 19	WP 20
3584	3558	3802	1984	1216	2534	8781	8115	2108
1574	955	960	410	491	734	883	717	674
0.4	0.1	0.2	0.7	1.2	1.2	2.2	0.5	0.2
DL	DL	DL	DL	ML	DL	DL	DL	ML
-	-	-	-	-	0.006	-	-	-
0.042	0.047	0.030	0.045	0.076	0.071	0.010	0.049	0.045
0.180	0.383	0.283	0.269	0.335	0.327	0.148	0.327	0.324
0.777	0.570	0.687	0.686	0.588	0.595	0.843	0.623	0.631
0.257	0.248	0.354	0.439	0.530	0.298	0.175	0.287	0.251
0.018	0.022	0.017	0.013	0.010	0.040	0.007	0.007	0.030
-	-	-	-	-	-	-	-	-
0.007	0.016	0.013	0.019	0.023	0.056	0.026	0.025	0.020
0.471	0.350	0.323	0.409	0.421	0.241	0.229	0.347	0.417
0.164	0.216	0.091	0.184	0.084	0.116	0.029	0.057	0.130
0.604	0.619	0.539	0.477	0.414	0.697	0.255	0.203	0.551
-	-	-	-	-	-	-	-	-
0.241	0.088	0.404	0.105	0.094	0.418	0.324	0.263	0.063
0.758	0.912	0.596	0.896	0.907	0.583	0.676	0.737	0.936
0.025	-	0.022	0.005	0.012	0.025	0.028	0.039	0.027
0.165	0.147	0.165	0.063	0.078	0.076	0.348	0.296	0.099
0.305	0.212	0.202	0.171	0.288	0.225	0.091	0.081	0.242

* DL = Distal Lagoon Basin, ML = Main Lagoon Basin, SM = Shallow Marine Area

Table 2.S3 continued...

WP 22	WP 23	WP 25	WP 28	WP 29	WP 30	WP 31	WP 34	WP 36
3750	2415	3354	3110	1690	4902	1316	1536	1939
602	930	730	397	570	355	169	237	154
0.7	0.2	0.2	0.3	0.4	0.3	0.4	0.5	0.3
DL	ML	SM	DL	DL	DL	ML	SM	DL
-	-	0.003	-	-	-	-	-	-
0.031	0.092	0.192	0.014	0.083	0.145	0.012	0.016	0.078
0.031	0.367	0.665	0.171	0.248	0.364	0.079	0.286	0.261
0.938	0.541	0.141	0.816	0.669	0.491	0.909	0.698	0.660
0.416	0.378	0.305	0.311	0.594	0.185	0.713	0.333	0.218
0.017	0.010	0.001	0.015	0.031	0.010	0.026	0.016	0.020
-	-	-	-	-	-	-	-	-
0.007	0.021	0.011	0.009	0.011	0.052	0.032	0.022	0.033
0.352	0.364	0.307	0.301	0.270	0.300	0.443	0.382	0.182
0.201	0.254	0.181	0.037	0.025	0.162	0.032	0.036	0.063
0.573	0.481	0.487	0.332	0.650	0.705	0.524	0.427	0.729
-	-	-	-	-	-	-	-	-
0.327	0.469	0.428	0.426	0.432	0.284	0.438	0.701	0.490
0.673	0.531	0.573	0.575	0.569	0.714	0.562	0.300	0.514
0.027	0.012	0.018	0.010	0.004	0.017	0.053	0.013	0.020
0.213	0.101	0.193	0.282	0.170	0.288	0.148	0.097	0.137
0.138	0.278	0.179	0.113	0.252	0.068	0.114	0.134	0.073

* DL = Distal Lagoon Basin, ML = Main Lagoon Basin, SM = Shallow Marine Area

Table 2.S3 continued...

WP 37	WP 38	WP 40	WP 41	WP 43	WP 44	WP 46	WP 51	WP 54
1690	1830	1888	1587	1638	3315	1939	206	992
147	275	166	198	173	870	237	42	166
0.2	0.4	0.7	0.4	0.3	0.2	-0.3	0.7	0.9
ML	DL	ML	ML	SM	DL	ML	SM	SM
0.005	-	0.004	0.009	-	0.003	-	0.019	-
0.039	0.098	0.092	0.091	0.137	0.033	0.090	0.157	0.115
0.275	0.392	0.307	0.306	0.413	0.244	0.363	0.450	0.344
0.681	0.510	0.596	0.594	0.450	0.720	0.547	0.374	0.541
0.277	0.122	0.081	0.081	0.010	0.409	0.018	0.093	0.052
0.002	0.003	0.007	0.073	0.010	0.012	0.003	0.101	0.007
-	-	-	-	-	-	-	-	-
0.018	0.052	0.124	0.024	0.063	0.068	0.184	0.034	0.024
0.231	0.227	0.303	0.133	0.259	0.169	0.329	0.171	0.440
0.064	0.038	0.036	0.020	0.010	0.013	0.024	0.074	0.036
0.466	0.654	0.302	0.411	0.083	0.057	0.082	0.678	0.262
-	-	-	-	-	-	-	-	-
0.486	0.730	0.325	0.222	0.255	0.577	0.785	0.721	0.643
0.515	0.267	0.673	0.774	0.747	0.423	0.215	0.288	0.355
0.007	0.023	0.024	0.015	0.041	0.003	0.008	0.024	0.006
0.174	0.116	0.126	0.131	0.259	0.132	0.144	0.072	0.090
0.080	0.131	0.081	0.111	0.095	0.208	0.109	0.168	0.144

* DL = Distal Lagoon Basin, ML = Main Lagoon Basin, SM = Shallow Marine Area

Table 2.S3 continued...

WP 57	WP 59	WP 60	WP 66	WP 70	WP 73	WP 74	WP 76	WP 77
376	3942	2099	1276	1632	1792	240	15	71
91	653	134	98	128	1303	332	132	258
1.3	0.0	-0.2	3.1	0.7	-1.7	0.3	-2.2	-0.2
SM	ML	DL	SM	SM	SM	SM	SM	SM
0.006	-	-	-	-	0.012	0.005	0.307	0.052
0.044	0.040	0.030	0.032	0.039	0.166	0.056	0.440	0.184
0.153	0.192	0.315	0.274	0.249	0.541	0.640	0.200	0.464
0.797	0.768	0.655	0.695	0.712	0.281	0.299	0.053	0.300
0.163	0.107	0.267	0.498	0.231	0.643	0.416	0.399	0.014
0.031	0.011	0.013	0.061	0.008	-	0.107	-	-
-	-	-	-	-	-	-	-	-
0.051	0.003	0.011	0.007	0.024	-	0.008	-	-
0.252	0.062	0.063	0.221	0.184	0.032	0.267	0.038	0.014
0.071	0.016	0.041	0.104	0.067	0.071	0.172	0.041	0.014
0.793	0.060	0.125	0.368	0.518	0.289	0.481	0.355	0.183
-	-	-	-	-	-	-	-	-
0.957	0.600	0.513	0.143	0.050	0.799	0.549	0.773	0.636
0.044	0.400	0.484	0.856	0.953	0.201	0.452	0.227	0.364
-	-	-	0.041	0.063	-	-	-	-
0.121	0.002	0.060	0.122	0.336	0.021	0.048	0.053	0.074
0.195	0.142	0.060	0.071	0.073	0.421	0.581	0.900	0.784

* DL = Distal Lagoon Basin, ML = Main Lagoon Basin, SM = Shallow Marine Area

Table 2.S3 continued...

WP 81	WP 83	WP 95	WP 97	WP 99	WP 100	WP 102	WP 105	WP 106
544	557	563	681	232	26	582	33	1226
237	212	244	390	342	29	862	5	828
-1.7	-1.9	0.3	1.2	-0.3	0.6	-3.6	2.4	-0.1
SM	SM	ML	ML	SM	SM	ML	SM	ML
0.038	0.031	-	0.010	0.054	0.251	-	-	-
0.175	0.062	0.042	0.037	0.171	0.401	0.024	-	0.021
0.478	0.299	0.211	0.466	0.163	0.218	0.224	-	0.358
0.310	0.608	0.747	0.487	0.612	0.130	0.752	1.000	0.622
0.318	0.391	0.276	0.120	0.009	0.106	0.005	0.258	0.285
0.038	0.034	0.016	0.016	-	-	-	0.275	0.010
-	-	-	-	-	-	-	-	-
0.006	0.017	0.080	0.062	0.263	0.031	0.003	0.061	0.084
0.376	0.290	0.412	0.350	0.849	0.200	0.010	0.122	0.543
0.079	0.115	0.065	0.045	0.034	0.016	0.002	0.021	0.038
0.665	0.615	0.744	0.752	0.534	0.804	0.043	0.343	0.128
-	-	-	-	-	-	-	-	-
0.963	0.882	0.918	0.892	0.553	0.828	0.839	-	0.728
0.038	0.118	0.082	0.108	0.447	0.172	0.161	1.000	0.272
-	-	-	-	0.006	-	-	-	-
0.054	0.030	0.079	0.031	0.056	0.103	0.028	-	0.077
0.303	0.276	0.302	0.364	0.596	0.532	0.597	0.133	0.403

* DL = Distal Lagoon Basin, ML = Main Lagoon Basin, SM = Shallow Marine Area

Table 2.S3 continued...

WP 107	WP 110
538	1696
413	988
-0.2	-0.2
SM	ML
-	0.005
0.048	0.061
0.494	0.243
0.458	0.692
0.405	0.248
0.079	0.020
-	-
0.022	0.012
0.286	0.149
0.131	0.018
0.357	0.136
-	-
0.813	0.811
0.186	0.189
-	0.004
0.015	0.016
0.435	0.368

* DL = Distal Lagoon Basin, ML = Main Lagoon Basin, SM = Shallow Marine Area

CHAPTER 3

TESTING FORAMINIFERAL TAPHONOMY AS A TSUNAMI INDICATOR IN A SHALLOW ARID SYSTEM LAGOON: SUR, SULTANATE OF OMAN

Jessica E. Pilarczyk*

Eduard G. Reinhardt

School of Geography and Earth Sciences, McMaster University, Hamilton, ON,
Canada, L8S 4K1

*Corresponding author: J.E. Pilarczyk (pilarcje@mcmaster.ca)

Citation: Pilarczyk, J.E., Reinhardt, E.G. Testing foraminiferal taphonomy as a tsunami indicator in a shallow arid system lagoon: Sur, Sultanate of Oman. Prepared for *Marine Geology*.

Status: to be submitted March 2011

ABSTRACT

The tsunami produced by the 1945 Makran Trench earthquake is considered to be the second deadliest in the Indian Ocean after the 26 December 2004 Indonesian event. The tsunami struck Iran, Pakistan, India and Oman; however, historical records outside of India and Pakistan are sparse due to limited populations in those regions and little communication with larger cities. Sur Lagoon, Oman, a small microtidal lagoon, contains stratigraphic evidence of the 1945 tsunami. The goal of this study is to test the utility of foraminiferal provenance and taphonomy as an indicator of the 1945 event and examine its potential in detecting older events in the geologic record. Foraminiferal (taxa and taphonomy) and high resolution particle size analysis show that high abundances of predominantly marine taxa (*Amphistegina* spp., *Ammonia inflata*, and planktics) associated with the tsunami bed indicate an outside marine origin for the sediment. Influxes of large test sizes and fossil specimens support a shallow marine provenance. Findings indicate that foraminiferal analysis, when combined with other proxies (e.g. mollusc taphonomy, particle size distribution), can be used to delineate tsunami units from normal background sedimentation in intertidal systems. This technique holds potential for detecting older events in Sur Lagoon which are documented in historical texts, but have not yet been ‘ground-truthed’.

3.1 INTRODUCTION

Most taphonomic studies of foraminifera focus on time-averaging or lateral transport of tests with only semi-quantitative observations on test condition (e.g. fragmentation, size; Hawkes et al., 2007; Kortekaas and Dawson, 2007). However, recent research has shown that test condition along with provenance assessment may provide useful environmental information and may help determine overwash events in coastal systems (e.g. Pilarczyk et al., 2011). Here we present the second phase of a two part study that firstly examined recent taphonomic trends (test condition and provenance; Pilarczyk et al., submitted) in Sur Lagoon, Oman (Fig. 3.1) and now examines an inferred 1945 Makran Trench tsunami deposit. Documentation of recent events like the 1945 tsunami, often with written or oral accounts, are important for understanding overwash dynamics in coastal settings and interpreting older events in the stratigraphic record (e.g. lagoons or ponds; Satake and Atwater, 2007).

The 1945 tsunami deposit in Sur Lagoon was found to have a lateral, sheet-like geometry with distinctive bivalve shell taphonomy (shell condition and provenance), and with its shallow position in the stratigraphic record, was inferred to be from the 1945 event (Donato et al., 2008). The bivalve taphonomy proved very useful for identifying the event in trench sections where large exposures are possible, but its utility will be limited by sample size in core studies. This study examines the foraminiferal trends within this deposit for eventual application to older deposits deeper in the stratigraphic record within the lagoon.

3.1.1 The 1945 Makran Trench tsunami

On 28 November 1945 a M_w 8.1 subduction zone earthquake located approximately 300 km west of Karachi, Pakistan resulted in a tsunami with wave heights ranging from 2 - 13 m and was reported to have killed over 4000 people (Fig. 1b; Ambraseys and Melville, 1982; Byrne et al., 1992; Pararas-Carayannis, 2006). Debate exists over the exact location of the epicentre of the 1945 tsunamigenic earthquake. Byrne et al. (1992) argue that the rupture occurred on a 5° dipping thrust plane extending 70 - 90 km inland and 10 - 30 km offshore (25.15°N, 63.48°E). Similarly, Ambraseys and Melville (1982) report the epicentre to be located at 25.02°N and 63.47°E. In contrast to the single rupture hypothesis maintained by Byrne et al. (1992) and Ambraseys and Melville (1982), Okal and Synolakis (2008) simulated a multiple simultaneous rupture scenario along three known fault zones within the MSZ and then compared it to a more speculative scenario involving another 450 km of rupture to include a 'probable' fault zone. It

was found that maximum wave amplitude between the two simulations did not vary significantly, however the wave generated by the additional ‘probable’ fault expressed trapping inside the Gulf of Oman. Other models show that the 1945 tsunami propagated to the south (Dominey-Howes et al., 2007) impacting the eastern corner of the Arabian Peninsula (Heidarzadeh et al., 2008b), and suggests that the observed tsunami was too large to be attributed to a single rupture and may have been the result of a submarine landslide (Dominey-Howes, 2007; Ambraseys and Melville, 1982). Bilham et al. (2007) support this idea blaming submarine landslides triggered by the earthquake for damaged underwater phone lines. The apparent discrepancy over the origin of propagation is likely due to a lack of understanding concerning earthquake generation, since it is not known whether single or multiple ruptures occurred. Models for two hypothetical Makran earthquakes (e.g. 1765, 1851) were simulated by Okal and Synolakis (2008) and Ambraseys and Melville (1982), however data regarding the magnitude and locations impacted by these events are scarce. In 1945, most of the Arabian Sea coastline had low populations mostly consisting of isolated villages and survivors of the event are becoming aged and increasingly difficult to find. Recent interviews (2008) of a resident of Sur who was a young boy at the time described tsunami flooding reaching ~3 m at Sur (Donato et al., 2009).

Geological evidence of the 1945 tsunami is also sparse. Compelling evidence of the 1945 tsunami was found in Sur Lagoon (Fig. 3.2) in 2006 and is discussed in detail in Donato et al. (2008, 2009). The inferred tsunami bed (5 - 25 cm thick) has high concentrations of angular shell fragments, articulated bivalves (out of life position) from lagoon and offshore provenance, is laterally extensive and covers an area of at least ~1 km² (Fig. 3.3; Fig. 3.4). The bed thins progressively in a western and southern direction, and becomes finer grained, better sorted and skewed with increased distance from the entrance channel. The sheet-like shell bed was deemed to be tsunamigenic (vs. a storm) due to the unique character of the shells which indicate offshore scour of the substrate with landward transport and deposition inside the lagoon (Morton et al., 2007).

3.2 REGIONAL SETTING

3.2.1 Sur Lagoon physiography

Sur Lagoon, a small (~12 km²) tidally-dominated (mean tidal amplitude ~1.2 m), lagoon, is situated approximately 100 km south of the capital Muscat on the western coast of Oman (Fig. 3.1; Fig. 3.2). The lagoon can be divided into a Distal (average elevation = 0.6 ± 0.5 m.s.l.) and Main Lagoon Basin (average elevation =

0.3 ± 0.6 m.s.l.) and communicates with the Shallow Marine Area (average elevation = -0.8 ± 1.1 m.s.l.; Pilarczyk et al., submitted). Communication with the Gulf of Oman is through a narrow (103 - 209 m wide) entrance channel at its northeastern corner, which connects a 2.5 km network of tidal channels (Fig. 3.2). The lagoon is bordered by Paleocene-Eocene aged highlands and is restricted on its north-eastern margin by a low lying sand spit (~2 - 3 m.s.l.; Fig. 3.2b). The lagoon basin experiences minimal wave action and contains a network of intertidal sand and mudflats which are exposed through diurnal tides. Low density mangrove patches fringe most of the lagoon except along the NE tip of the Distal Lagoon Basin and the SW section of the Main Lagoon Basin where high density mangroves are present. Sand texture within the lagoon becomes finer with increasing elevation and distance from the marine source (see Fig. 3 in Pilarczyk et al., submitted). The high energy Shallow Marine Area outside of the lagoon has a narrow shelf which abruptly drops to depths in excess of 200 m after ~5 km (Szuman et al., 2006).

3.2.2 Recent cyclonic activity

Cyclone activity in the northern Arabian Sea is rare and is generally characterized by small cells that dissipate quickly. For a complete list of cyclone tracks in the northern Arabian Sea see Knapp et al. (2009). Cyclones Gonu (2007) and Phet (2010) are the exception and represent the most 'severe cyclonic storms' to have ever impacted the Arabian Peninsula in recorded history (Fritz et al., 2010). Cyclone Gonu in 2007, the most intense storm on record in the Arabian Sea with a Category 5 rating, resulted in ~50 deaths and \$4 billion in coastal damage (JTWC, 2007; Dube et al., 2009; Fritz et al., 2010). On 1 June 2007, Gonu began as a depression over the eastern Arabian Sea and within hours of it moving west towards Mumbai, India it had intensified into Tropical Storm Gonu. By 4 June 2007 the storm reached Category 5 status with wind speeds in excess of 240 km/hr reported 475 km east of Masirah Island, Oman. As the cyclone tracked northwest towards Oman, cooler sea surface temperatures and drier air caused it to gradually weaken before it made landfall at Ras al-Hadd (easternmost point on the Arabian Peninsula, ~30 km ESE of Sur) on 5 June 2007. Despite the reduction in wind speed (e.g. >240 - 164 km/hr), Cyclone Gonu's strike at Ras al-Hadd marked the most severe storm ever recorded on the Arabian Peninsula. After it made landfall, Gonu tracked to the north-northwest where it downgraded to a tropical storm and made landfall on Iran's Makran Coast on 7 June 2007.

Fritz et al. (2010) reported greatest damage at Ras al-Hadd with a 5 m storm surge that destroyed wall structures 200 m inland, and a marked decrease in high water marks with increasing distance from the initial strike location. Muscat was

impacted by a 3 m storm surge that caused severe coastal erosion and road damage. A field survey at Sur in November 2007 showed that Gonu's intense rain (>610 mm) and resultant flow through Wadi Shamah eroded the small delta and washed away the bridge (Donato et al., 2009). Despite the estimated storm surge of 2.6 m (Dube et al., 2009), a survey of the lagoon after the event found no record of overwash or shells (Donato et al., 2009).

More recently, on 2 June 2010 Cyclone Phet skimmed parallel to Oman's coast. It began as a Category 3 on 2 June 2010 with sustained winds of greater than 210 km/h. It lashed Oman's eastern region with hurricane-strength winds through to 4 June 2010 before moving northeast towards Karachi, Pakistan. Sur was closest to the path of the storm and was hit quite hard. Phet was not expected to make landfall on Oman, however it did hit Ras al-Hadd, Oman dumping 152 mm of rain within 24 hours. Damage from the storm has not been assessed although this storm was less intense than Cyclone Gonu three years earlier, which did not produce a shell accumulation.

3.2.3 Arabian Sea environments as tsunami recorders

Arid Arabian Sea coastlines are difficult to work with, as there is a lack of suitable environments to act as tsunami recorders. Overwash onto terrestrial surfaces has low preservation potential as the sand sheet dries quickly and then is blown away. A body of water is needed to preserve the overwash event, yet there are few coastal lagoons or estuaries that are truly suitable. Most of the previous studies have been in temperate or tropical areas where there are many suitable environments including terrestrial areas, coastal ponds, marshes and estuaries (e.g. Goff et al., 2000; Luque et al., 2002; Cisternas et al., 2005; Rajendran et al., 2006; Kortekaas and Dawson, 2007). However, most of the lagoons or estuaries on the eastern coast of Oman, from Muscat to Sur, are found in barrier choked wadis (khors) that occasionally flood and erode any accumulated sediments. Sur is somewhat unique in that it has one major wadi (Wadi Shamah) that occasionally floods (e.g. during Cyclone Gonu), but most flow appears to by-pass the lagoon basin and is directed out towards sea. A wet or intertidal environment is necessary to preserve any sand or shell sheets and Sur represents one of the better environments.

3.3 METHODS

In 2006, eight trench sections and corresponding short cores were collected

in the Main and Distal Lagoon Basins and are the same cores used by Donato et al. (2008, 2009). A digital elevation model (DEM) was created by walking a Trimble R3 differential GPS unit in north-south transects spaced 100 m apart, and east-west lines at 300 m spacing (Fig. 3.2b; Donato et al. 2008, 2009). Submerged locations of the lagoon and Shallow Marine Area were surveyed using a single-beam echo sounder. Both datasets were processed with Geosoft Oasis TM software to create a DEM and were levelled to a mean sea level datum (see Donato et al., 2008).

Samples were selected based on facies designations derived from the shell taphonomy and particle-size data as described by Donato et al. (2009). Approximately 1 cm³ samples were sieved (>63 µm) and examined using a binocular microscope. A total of 22 foraminiferal taxa (for plates see Pilarczyk et al., submitted) were identified using the taxonomy of Hottinger et al. (1993) and Hayward et al. (2004). Individual specimens were taphonomically categorized using the same criteria developed in Pilarczyk et al. (submitted). These include: unaltered, fragmented, corroded (combined influence of corrosion and abrasion) and sediment in-filled tests (e.g. fossil; see Plate II in Pilarczyk et al., submitted). In addition, specimens were categorized into small (<150 µm), medium (150 - 250 µm) or large (>250 µm) test sizes (Fig. 3.5; Fig.3.6; Online Figs. 3.1 – 3.5).

3.4 RESULTS

3.4.1 Previous shell and particle-size results

Facies were defined through shell bed and particle-size results and are summarized here from Donato et al. (2008, 2009). Pre-1945 lagoon deposition is dominated by structureless fine sands with low abundances of lagoon mollusc taxa typical of intertidal arid environments (e.g. *Hiatula ruppelliana*, *Marcia mamorata*, *Marcia opima*, *Protapes* sp.; Donato et al., 2008). In cores 1 – 8, the unit is ~2 – 15 cm thick and likely extends downward in the substrate.

The tsunami unit ranges in thickness from 10 – 40 cm and is characterized by a slight coarsening to medium sand, which is largely shell material (Fig. 3.4). Particle-size analysis was performed on the <2000 µm fraction, omitting the coarse shells. Differences in the undigested vs. acid digested particle size data illustrate the dominance of shelly material in the sediment (note: in Fig 4 of Donato et al., 2009 digested (D) and undigested (UD) labels are erroneously labelled). The shell concentration consists of abundant offshore (e.g. *Anadara uropigimelana*, *Tellina palatum*, *Glycermeris* sp.) and lagoon mollusc taxa that were taphonomically distinct (i.e. articulation, angular fragmentation). The shell concentrations were

very distinct in the stratigraphy and were used initially to define the tsunami unit, but subsequent particle-size results extended its range to include sandy intervals above the shell (Cores 3 and 8).

Post-1945 lagoon sedimentation is similar in character to the pre-1945 lagoon sedimentation except in some cores there are thinner shell units that do not have the characteristics of the tsunami shell unit. These thinner beds represent erosion and reworking of the shell bed through tidal channel migration observed in several locations in the lagoon. Shells, once eroded, are concentrated at the bottom of tidal channels and subsequently become bioencrusted and bored losing their previous taphonomic character (Fig. 3.4). Sediment texture is similar to the pre-1945 sediments as well, and is reflected by a structureless fine-sand (Donato et al., 2009). Recent debris is also found in the upper sand indicating erosion and re-sedimentation events.

3.4.2 Previous foraminiferal results from surface samples

Foraminiferal analysis of surface samples in Pilarczyk et al. (submitted) found three biofacies within Sur Lagoon that were largely defined by geographic areas: 1) the subtidal Shallow Marine Area (-1.9 to 0.3 m.s.l.) with higher wave energy; 2) the mostly intertidal Main Lagoon Basin (-0.3 to 0.9 m.s.l.) with moderate wave energy, and 3) the dominantly intertidal Distal Lagoon Basin (0.1 to 1.1 m.s.l.) characterized by very low wave energy. However, the biofacies had very similar assemblages and were defined largely by the presence/absence of a few key species that were either low, or moderate in abundance (*Ammonia inflata*, *Amphistegina* spp., *Elphidium advenum* and planktics). The taphonomic characters did not show any strong correlation with position in the lagoon although abundance of fossil specimens and test size did show some trends.

3.4.3 Foraminiferal character of the tsunami unit

Analysis of the cores following the same procedure as Pilarczyk et al. (submitted) was conducted in an effort to determine taphonomic overprinting of the foraminiferal tests within the tsunami unit (Reinhardt et al., 2011). Overall, there is not a great difference in the foraminiferal assemblages within the cores since similar taxa are found in all units. The assemblage is dominated by miliolids and *Ammonia parkinsoniana* with *Ammonia tepida*, *Elphidium craticulatum*, *Elphidium gerthi*, *Peneroplis planatus* and *Porsonion granosa* present in smaller abundances (Fig. 3.5; Online Figs. 3.1 – 3.5). The Shannon Diversity Index (SDI) also does not vary

between the units; pre-tsunami (2.0 ± 0.1), tsunami (2.0 ± 0.1) and post-tsunami (1.8 ± 0.2 ; Online Figs. 3.1 – 3.5) all have similar values.

However, there are some important differences in minor but important taxa in the tsunami unit that are very diagnostic (Pilarczyk et. al, submitted). These include *A. inflata*, *Amphistegina* spp. and planktics, as well as taphonomic characters consistent with the modern Shallow Marine Area (i.e. large specimens, fossil specimens; Fig. 3.5; Fig. 3.6). In all cores *A. inflata* abundances are highest in the tsunami unit (e.g. $4\% \pm 1$); although, small amounts ($<2\%$) are also present in pre-1945 sediments in cores 3, 4, 5 and 6. In post-1945 sediments, abundances of *A. inflata* from cores taken closest to the entrance channel (cores 6, 7 and 3) are high (1%, 1%, 4%), but still less than abundances within the tsunami unit (4%, 3%, 5%). *Amphistegina* spp. follow a similar trend where abundances within the tsunami unit are higher ($4\% \pm 1$) than the other units (pre-1945 is $<3\%$; post-1945 is $<2\%$ except at core 3 where it is 5%); but also, in post-1945 lagoon sediments, abundances show a decrease with distance away from the lagoon entrance (Fig. 3.6a). Planktics are also slightly higher in some tsunami units, but in most cores the abundances are not significantly different from the pre- or post-1945 sediments (Fig. 3.5). Overall, *A. inflata* and *Amphistegina* spp. are the best indicator species since sediments above and below the tsunami unit contain lower abundances and it was a consistent trend.

The tsunami unit also has higher abundances of large ($>250 \mu\text{m}$), and fossil ($31\% \pm 8$) specimens. Large tests and fossil specimens were previously shown to be associated with modern Shallow Marine Areas (Pilarczyk et al., submitted). Fragmented individuals are higher in some of the tsunami units, but the trend is not consistent throughout the cores. Similarly, abundances of total individuals per 1 cm^3 are quite variable and only in cores 1, 3, 6 and 7 do they peak in the tsunami unit (Online Figs. 3.1 – 3.5).

3.5 DISCUSSION

Foraminiferal analysis was able to distinguish the tsunami unit as discerned through shell taphonomy and particle size analysis. This is largely accomplished with two allochthonous species, *Amphistegina* spp. and *Ammonium inflata*, with the number of large specimens and to a lesser extent, fossil taxa also helping define the unit in the cores. However, the abundance of these indicator species is very low ($<5\%$) and the overall taphonomic character was not significantly different in the tsunami unit compared with pre- and post-1945 sediments (Fig. 3.5; Fig. 3.6). There was no, or very little overprinting (fragmentation) of the foraminiferal tests through the process of tsunami transport and deposition vs. the bivalves which showed

distinctive features (Online Figs. 3.1 – 3.5). Only the proportions of large tests and fossil specimens increased in the tsunami unit, which can be explained by probable sorting that occurred with transport and deposition during the event.

3.5.1 Allochthonous tests and size-sorting

Hawkes et al.'s (2007) analysis of deposits from the 2004 Indian Ocean tsunami were able to resolve distinct episodes of deposition by the presence of offshore radiolarians in uprush phases and mangrove foraminifera dominating backwash phases. Donato et al. (2009) alluded to multiple tsunami incursions into the Sur Lagoon, however, there was not enough evidence with shell taphonomic or particle-size data to really support any conclusions. Likewise, there does not seem to be any systematic trend in the foraminiferal data; however, subtle changes may not be evident due to lower sampling resolution. In addition, as pointed out in Pilarczyk et al., (submitted) the biofacies/taphofacies within the lagoon are very homogeneous, and as a result, changes in test characters may be hard to identify.

Changes in test size and planktic foraminifera have also been used to delineate pre- and post-tsunami sedimentation resulting from the 2004 Indian Ocean event (Hawkes et al., 2007). Results indicated that test size was a useful taphonomic characteristic; medium sized tests (<200µm) characterized the pre-tsunami sediment while the tsunami unit tended to have larger tests (>200µm) and test concentrations tended to increase up through the unit (Hawkes et al., 2007). The results from Sur mostly mirror these findings where the 1945 tsunami unit is shown to contain a predominance of larger tests, and in some instances shows increases in planktic foraminifera and concentration of tests, however this is not displayed in all cores. The most important indicators are the robust *Amphistegina* spp., *A. inflata* and in some instances, fossil specimens which indicates a Shallow Marine Area provenance for the sediment. As would be expected, certain taxa will be more useful than others depending upon geographic location, type of coastal recorder and the characteristics of the tsunami itself. As pointed out previously, identifying the useful taxa and their taphonomic trends should be conducted to properly assess the stratigraphic record (Pilarczyk et al, submitted; Mamo et al., 2009).

3.5.2 Fragmentation

The lack of an increase in fragmentation of recent (vs. fossil) specimens in the tsunami unit seems unusual (Online Figs. 3.1 – 3.5). Increased fragmentation is present in some of the cores (e.g. core 2) but it is not a distinctive feature and was

often not different than what was observed in pre- and post-1945 sediments. Kortekaas and Dawson (2007) described increased fragmentation in their tsunami unit in Portugal, but it was documented with qualitative observation, so it is difficult to assess fully. In the case of Sur Lagoon, fragmentation is not a dominant feature, a point which is in direct contrast with bivalve taphonomic results that show extensive angular fragmentation (Donato et al., 2008). However, it is unclear that a tsunami would in fact cause increased foraminiferal fragmentation and we do not seem to have that effect represented here. It is thought that the high degree of angular fragmentation associated with larger shells maybe due to the type of coastline (Reinhardt et al., 2006; Donato et al., 2009; Massari et al., 2009). Rocky shorelines may provide the hard substrate for shell collision and fragmentation vs. soft sediment shorelines where fragmentation might be less. Even though there is a rocky shoreline at Sur which enhanced fragmentation of the bivalves, the 1945 tsunami at Sur does not seem to have taphonomically overprinted the foraminiferal tests (e.g. Reinhardt et al., 2011). However, the tsunami was relatively small (~3 m wave height) and a larger event may have produced a more apparent effect.

3.5.3 Relationships with bed geometry

Mapping the indicator species laterally and vertically in the cores will be important for documenting bed geometry (sheet-like) as well as distinguishing between a tsunami and storm origin (Morton et al., 2007). The foraminiferal results agree well with the shell designation of the tsunami unit (see Fig 4 in Donato et al., 2009), but corresponded better with PSD data (i.e. Cores 1, 2, 4, 5, 8). As discussed in Donato et al. (2009), the PSD data corresponds well with the base of the shell unit, but the upper boundary in several cores extends into the overlying sand (Cores 1, 3, 8; Fig. 3.5). The extension of the boundary is due to abundance of small shell fragments in the sand which have PSDs that are similar to the shell unit. The foraminifera also correspond well with the base of the shell, but better matched the PSD data for the upper boundary. It is unclear whether this upper shell fragment-rich sand is from the tsunami or the reworking of the boundary with subsequent storms or tidal channel migrations (Donato et al., 2009; Fig. 3.5). This blurring of the top boundary (i.e. time-averaging) is expected to be more pronounced with the smaller foraminifera than with the shells themselves (see Fig. 3.3). Contributions to this effect may also be from crab burrowing, which was observed to bring shell material and sediment from the tsunami unit to the surface (McLachlan et al., 1998).

In Donato et al. (2009), core 7 was found to be problematic as there was a lack of thick shell beds to determine the extent of the tsunami unit (Fig. 3.5). In this case, the foraminiferal records better indicate the overwash interval. Based on its

stratigraphic position and correlation with the other taphonomically distinct shell beds (e.g. articulation, fragmentation), a more confident interpretation can be made on its origin (Pilarczyk et al., 2011; Reinhardt et al., 2011). This will be particularly important in future cores studies.

3.5.4 The potential for documenting older events

Historical records mention several tsunamis that have impacted the coastlines of the Northern Arabian Sea (e.g. 325 B. C, 1483, 1851, 1765, etc.; Ambraseys and Melville, 1982; Heidarzadeh et al., 2008a; Heidarzadeh et al., 2008b; Heidarzadeh et al., 2009 and references therein). So far only the most recent 1945 event has been 'ground-truthed' by actual geologic evidence (Donato et al., 2008; Donato et al., 2009). Little is known about these events and details regarding the dates, coastlines impacted, wave heights, number of deaths and earthquake epicentres are often contradicted in the literature (see Heidarzadeh et al., 2008b). Several studies have reported upwards of ten tsunamigenic earthquakes originating from the eastern and western flanks of the Makran Subduction Zone (MSZ) since 325 B.C., however, this number may not be accurate since tsunamis in this region have likely not been properly reported (Quittmeyer and Jacob, 1979; Ambraseys and Melville, 1982; Pararas-Carayannis, 2006; Heidarzadeh et al., 2008a). These records are based on historical texts and until date, only the most recent event in 1945 has been corroborated with geologic evidence (Donato et al., 2008; Donato et al., 2009). While often incomplete, the historical tsunami record for the Northern Arabian Sea documents at least six events that had a magnitude greater than 8.0 (e.g. 325 B.C., May 1008, 18 February 1483; May 1668; 1765; 19 April 1851; 27 November 1945). The oldest tsunami on record is thought to have been responsible for destroying Alexander the Great's fleet on its way back to Mesopotamia in 325 B.C. (Pararas-Carayannis, 2006).

Using the 1945 tsunami deposit as a reference, foraminiferal provenance and taphonomy can be used as a tsunami indicator for older geologic deposits that can only be accessed through core studies where there is little or no shell signature. Previous studies have used foraminifera as tsunami indicators (see Mamo et al., 2009 and references therein); however, the added use of taphofacies analysis could provide better provenance assessment and a comprehensive hydrodynamic interpretation in these studies. At Sur Lagoon, shelly sand sheets containing influxes of predominantly offshore taxa (*Amphistegina* spp., *A. inflata*, and possibly planktics), larger test sizes and fossil specimens are likely to be the result of tsunami deposition rather than storm. Preliminary work shows a series of such beds in long cores taken from the lagoon. Ascribing either a storm or tsunami origin to these

beds will help to qualify risk assessment for the Omani coastline, which to date remains undocumented.

3.6 CONCLUSIONS

The combined use of foraminiferal provenance and taphonomy was effective in identifying the 1945 Makran trench tsunami at Sur Lagoon and will likely be a good indicator of older events at this location. High abundances of predominantly marine taxa (*Amphistegina* spp., *A. inflata*, and possibly planktics) coupled with high abundances of large test sizes, fragments and fossil specimens were found to be associated with tsunami deposition. At Sur Lagoon, most sedimentologic tsunami criteria (e.g. grading) did not apply to the 1945 tsunami bed. Bivalve taphonomic analysis conducted previously however, provided evidence of a tsunami through the presence of articulated bivalves and angular fragments from offshore provenance. Both PSD and foraminiferal analysis support this tsunami interpretation and hold the added benefit of delineating older deposits where shell quantities are limited (e.g. cores). Although successful in detecting the 1945 tsunami deposit, foraminiferal analysis on its own would only be effective in documenting a marine incursion and should be combined with other proxies when ascribing an event origin.

ACKNOWLEDGEMENTS

The authors are indebted to Simon Donato, Richard Rothaus, Tom Vosmer and Barry Jupp for field support and assistance while on site in Oman. Special acknowledgements are given to Simon Donato who provided core samples. We also wish to thank Oman LNG who provided detailed tide gauge data. Funding was provided by a NSERC Discovery research grant to EGR and a Geological Society of America (GSA) student research grant to JEP.

REFERENCES

- Ambraseys, N. N., Melville, C. P., 1982. A history of Persian earthquakes. New York: Cambridge University Press, 219 p.
- Bilham, R., Lodi, S., Hough, S., Bukhary, S., Khan, A. M., Rafeeqi, S. F. A., 2007. Seismic hazard in Karachi, Pakistan: uncertain past, uncertain future. *Seismol. Res. Lett.* 78, 601-613.
- Byrne, D. E., Sykes, L. R., Davis, D. M., 1992. Great thrust earthquakes and seismic slip along the plate boundary of the Makran Subduction Zone. *J.*

- Geophys. Res. 97, 449-478.
- Cisternas, M., Atwater, B. F., Torrejon, F., Sawai, Y., Machuca, G., Lagos, M., Eipert, A., Youlton, C., Salgado, I., Kamataki, T., Shishikura, M., Rajendran, C. P., Malik, J. K., Rizal, Y., and Husni, M., 2005. Predecessors of the giant 1960 Chile earthquake. *Nature* 437, 404-407.
- Dominey-Howes, D., Cummins, P., Burbidge, D., 2007. Historic records of teletsunami in the Indian Ocean and insights from numerical modeling. *Nat. Hazards* 42, 1-17.
- Donato, S. V., Reinhardt, E. G., Boyce, J. I., Rothaus, R., Vosmer, T., 2008. Identifying tsunami deposits using bivalve shell taphonomy. *Geology* 36, 199-202.
- Donato, S. V., Reinhardt, E. G., Boyce, J. I., Pilarczyk, J. E., Jupp, B. P., 2009. Particle-size distribution of inferred tsunami deposits in Sur Lagoon, Sultanate of Oman. *Mar. Geol.* 257, 54-64.
- Dube, S. K., Jain, I., Rao, A. D., Murty, T. S., 2009. Storm surge modelling for the Bay of Bengal and Arabian Sea. *Nat. Hazards* 51, 3-27.
- Fritz, H. M., Blount, C. D., Albusaidi, F. B., Al-Harthy, A. H. M., 2010. Cyclone Gonu storm surge in Oman. *Estuar. Coast. Shelf S.* 86, 102-106.
- Goff, J. R., Rouse, H. L., Jones, S. L., Hayward, B. W., Cochran, U., McLea, W., Dickinson, W. W., Morley, M. S., 2000. Evidence for an earthquake and tsunami about 3100 - 3400 yr ago, and other catastrophic saltwater inundations recorded in a coastal lagoon, New Zealand. *Mar. Geol.* 170, 231-249.
- Hawkes, A. D., Bird, M., Cowie, S., Grundy-Warr, C., Horton, B. P., Tan Shau Hwai, A., Law, L., Macgregor, C., Nott, J., Eong Ong, J., Rigg, J., Robinson, R., Tan-Mullins, M., Tiong, T., Yasin, Z., Wan Aik, L., 2007. Sediments deposited by the 2004 Indian Ocean tsunami along the Malaysia-Thailand Peninsula. *Mar. Geol.* 242, 169-190.
- Hayward, B. W., Holzmann, M., Grenfell, H. R., Pawlowski, J., Triggs, C. M., 2004. Morphological distinction of molecular types in *Ammonia* - towards a taxonomic revision of the world's most commonly misidentified foraminifera. *Mar. Micropaleontol.* 50, 237-271.
- Heidarzadeh, M., Pirooz, M. D., Zaker, N. H., Synolakis, C. E., 2008a. Evaluating tsunami hazard in the northwestern Indian Ocean. *Pure Appl. Geophys.* 165, 2045-2058.
- Heidarzadeh, M., Pirooz, M. D., Zaker, N. H., Yalciner, A. C., Mokhtari, M., Esmaeily, A., 2008b. Historical tsunami in the Makran Subduction Zone off the southern coasts of Iran and Pakistan and results of numerical modeling. *Ocean Eng.* 35, 774-786.
- Heidarzadeh, M., Pirooz, M. D., Zaker, N. H., Yalciner, A. C., 2009. Preliminary estimation of the tsunami hazards associated with the Makran subduction

- zone at the northwestern Indian Ocean. *Nat. Hazards* 48, 229-243.
- Hottinger, L., Halicz, E., Reiss, Z., 1993. Recent foraminifera from the Gulf of Aqaba, Red Sea. *Slovenska Akademija Znanosti in Umenosti (Ljubljana)*, classis IV, dela, 33, 179, 230 pp.
- Joint Typhoon Warning Center (JTWC), 2007. Northern Indian Ocean tropical cyclone best track data, Retrieved on 4 June 2007.
- Knapp, K. R., Kruk, M. C., Levinson, D. H., Gibney, E. J., 2009. Archive compiles new resource for global tropical cyclone research. *EOS* 90, 46.
- Kortekaas, S., Dawson, A. G., 2007. Distinguishing tsunami and storm deposits: an example from Martinhal, SW Portugal. *Sediment. Geol.* 200, 208-221.
- Luque, L., Lario, J., Civis, J., Silva, P. G., Zazo, C., Goy, J. L., Dabrio, C. J., 2002. Sedimentary record of a tsunami during Roman times, Bay of Cadiz, Spain. *J. Quaternary Sci.* 17, 623-631.
- Mamo, B., Strotz, L., Dominey-Howes, D., 2009. Tsunami sediments and their foraminiferal assemblages. *Earth-Sci. Rev.* 96, 263-278.
- Massari, F., D'Alessandro, A., Davaud, E., 2009. A coquinoid tsunamite from the Pliocene of Salento (SE Italy). *Sediment. Geol.* 221, 7-18.
- McLachlan, A., Fisher, M., Al-Habsi, H. Al-Shukairi, S., and Al-Habsi, A., 1998, Ecology of sandy beaches in Oman. *J. Coast. Conservation.* 4: 181-190.
- Morton, R.A., Gelfenbaum, G., Jaffe, B.E., 2007. Physical criteria for distinguishing sandy tsunami and storm deposits using modern examples. In: Tappin, D.R. (Ed.), *Sedimentary Features of Tsunami Deposits—Their Origin, Recognition and Discrimination.* *Sediment. Geol.* 200, 184–207.
- Okal, E. A., Synolakis, C. E., 2008. Far-field tsunami hazard from mega-thrust earthquakes in the Indian Ocean. *Geophys. J. Int.* 172, 995-1015.
- Pararas-Carayannis, G., 2006. The potential of tsunami generation along the Makran Subduction Zone in the northern Arabian Sea. Case study: the earthquake and tsunami of November 28, 1945. *Sci. Tsunami Hazards* 24, 358-384.
- Pilarczyk, J. E., Reinhardt, E. G., 2011. *Homotrema rubrum* (Lamarck) taphonomy as an overwash indicator in marine ponds on Anegada, British Virgin Islands. *Nat. Hazards* doi, 10.1007/s11069-010-9706-3.
- Pilarczyk, J. E., Reinhardt, E. G., Boyce, J. I., Schwarcz, H. P., Donato, S. V., submitted. Foraminiferal taphonomy reveals sediment transport trends in an intertidal lagoon: Sur Lagoon, Sultanate of Oman. *Mar. Micropaleontol.*
- Quittmeyer, R. C., Jacob, K. H., 1979. Historical and modern seismicity of Pakistan, Afghanistan, India, and southeastern Iran. *Bull. Seismol. Soc. Am.* 69, 773-823.
- Rajendran, C. P., Rajendran, K., Machado, T., Satyamurthy, T., Aravazhi, P., Jaiswal, M., 2006. Evidence of ancient sea surges at the Mamallapuram coast of India and implications for previous Indian Ocean tsunami events.

Current Science 91, 1242-1247.

Reinhardt, E. G., Goodman, B. N., Boyce, J. I., Lopez, G., van Hengstum, P., Rink, W. J., Mart, Y., Raban, A., 2006. The tsunami of 13 December A.D. 115 and the destruction of Herod the Great's harbour at Caesarea Maritima, Israel. *Geology* 34, 1061-1064.

Reinhardt, E.G., Pilarczyk, J.E., Brown, A., 2011. Probable tsunami origin for a shell and sand sheet from marine ponds on Anegada, British Virgin Islands. *Nat. Hazards*, doi 10.1007/s11069-011-9730-y

Satake, K., Atwater, B. F., 2007. Long-term perspectives on giant earthquakes and tsunamis at subduction zones. *Annual Review of Earth and Planetary Sciences* 35, 349-374.

Szuman, M., Berndt, C., Jacobs, C., Best, A., 2006. Seabed characterization through a range of high-resolution acoustic systems – a case study offshore Oman. *Mar. Geophys. Res.* 27, 167-180.

CHAPTER 3 FIGURES

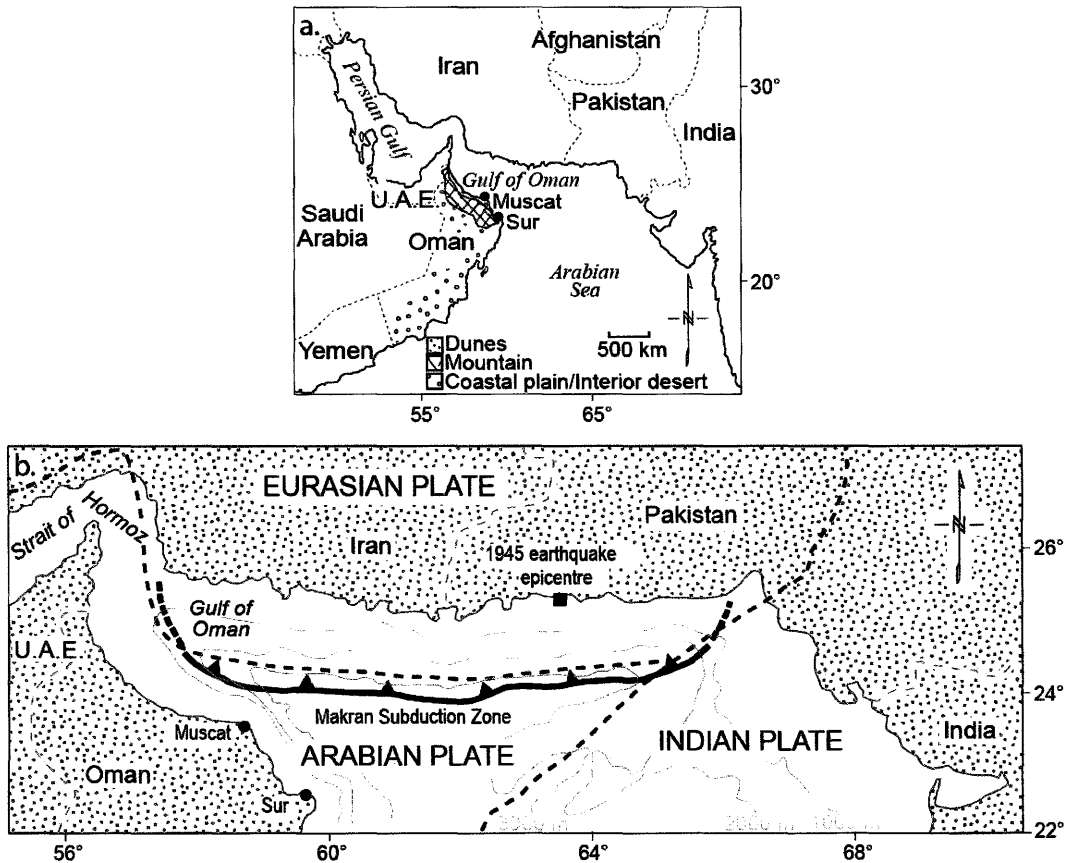


Figure 3.1: a. Location of Sur, Oman. b. Makran Subduction Zone (MSZ), broad-scale plate tectonics and the 1945 earthquake epicentre are indicated (after Donato et al., 2009 and Heidarzadeh et al., 2008).

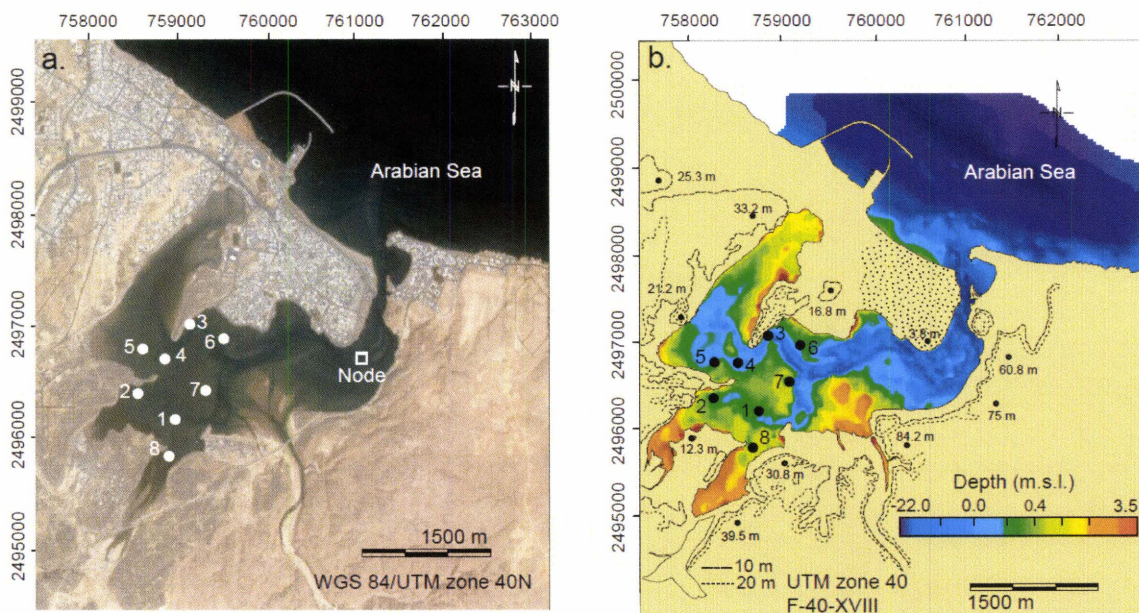
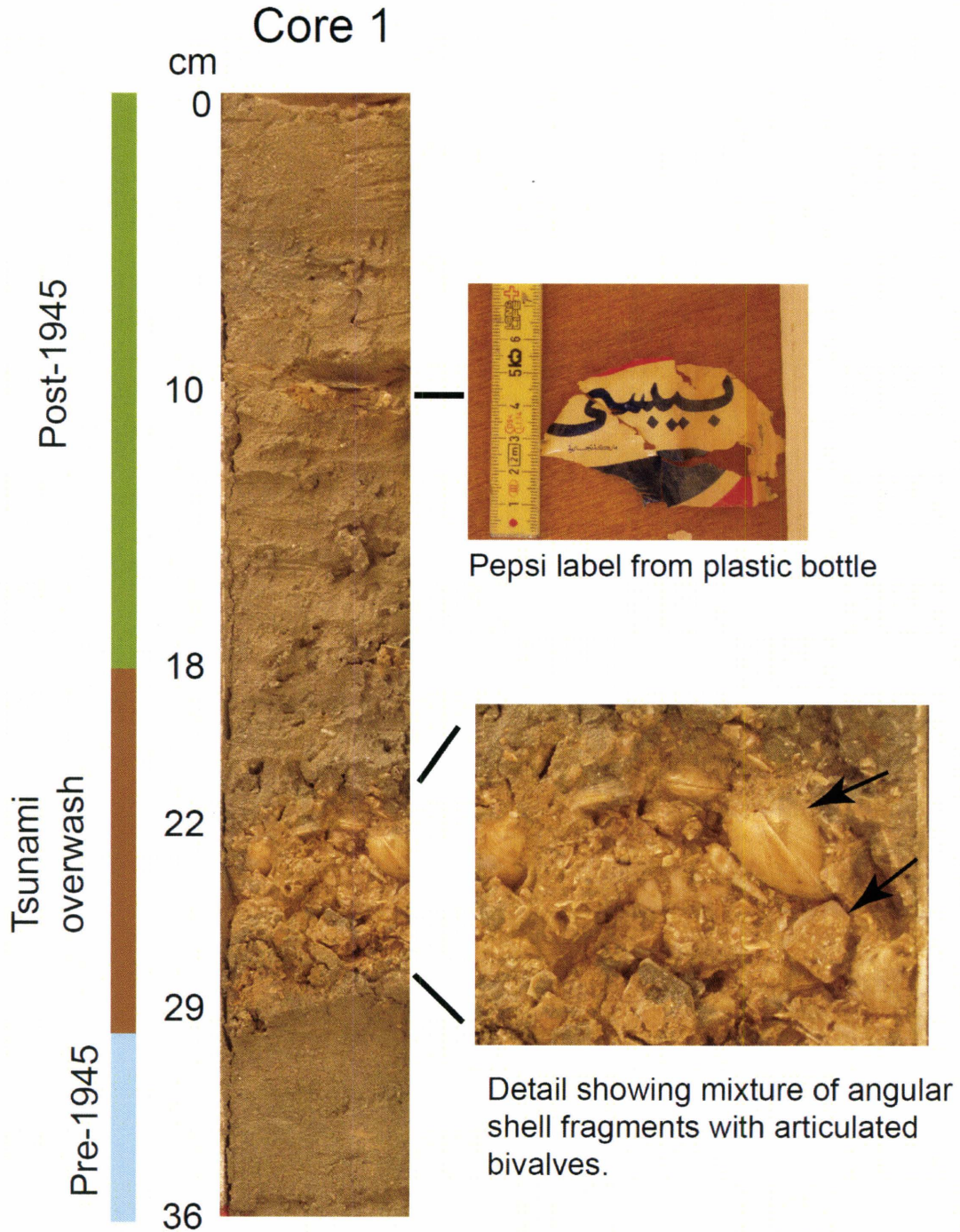


Figure 3.2: a. Google Earth image of Sur Lagoon indicating the lagoon entrance, tidal channels, wadi entrance and location of cores 1 – 8 (circles). b. Digital Elevation Model (DEM) of Sur Lagoon. The node used to measure core distances from the lagoon entrance is indicated by a square (Fig. 3.4).

Figure 3.3: Photographic record of Core 1 showing the stratigraphic units designated by bivalve taphonomy and particle-size data as shown in Donato et al. (2009). Details of the tsunami unit shows articulated bivalves out of life position with angular fragmented shells. Note the red-orange color of the shell unit vs. the sand above and below. Recent pop bottle label which shows reworking of the upper sediments. Compare exposure with trench section in Fig. 4d (*see following page*).



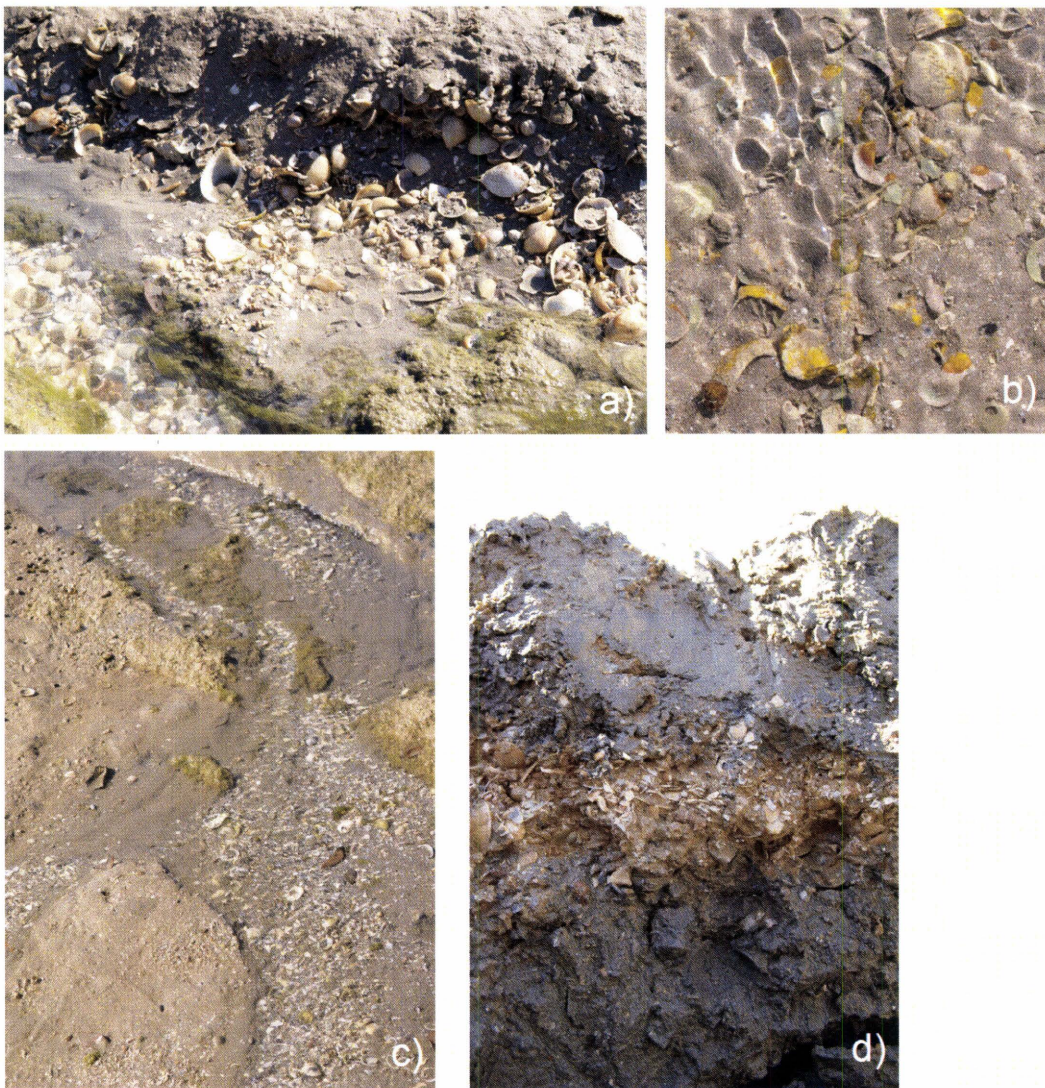
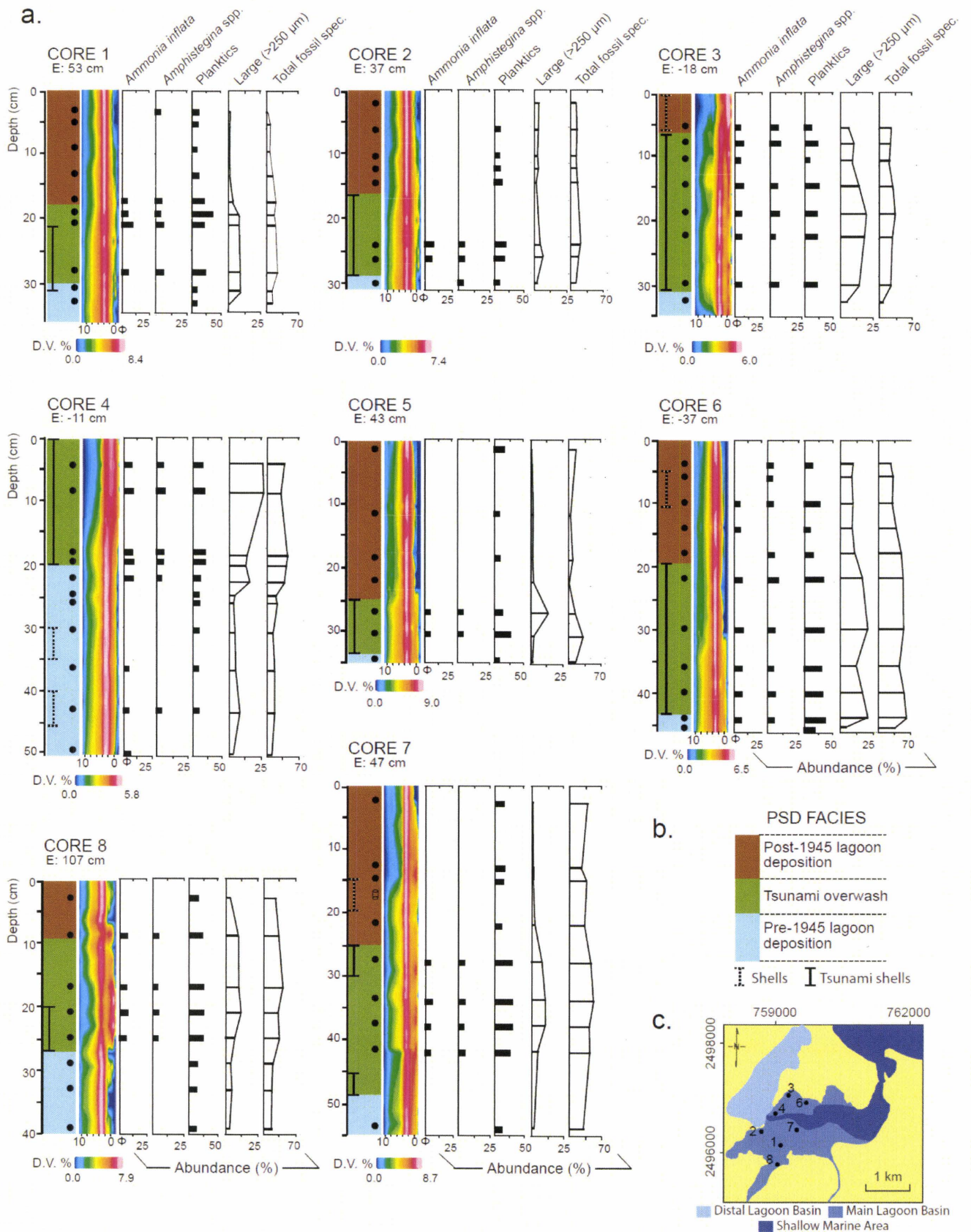


Figure 3.4: **a.** Tidal channel erosion of the tsunami shell unit. **b.** shells exposed in tidal channel become edge rounded, bioeroded (microboring) and encrusted. **c.** accumulation of shells at the bottom of tidal channels. **d.** exposure of the shell unit in a trench section close to core 1.

Figure 3.5: **a.** Lithologic (PSD), shell and foraminiferal data for cores 1 – 8. Foraminifera and taphonomic characters that best reflect tsunami overwash are indicated. For all taxonomic and taphonomic data see Online Figs. 1 - 5. Tsunami and lagoon units are based the PSD and shell taphonomy (Donato et al., 2008; Donato et al., 2009). **b.** PSD facies. **c.** Core locations within Sur Lagoon (*See following page*).



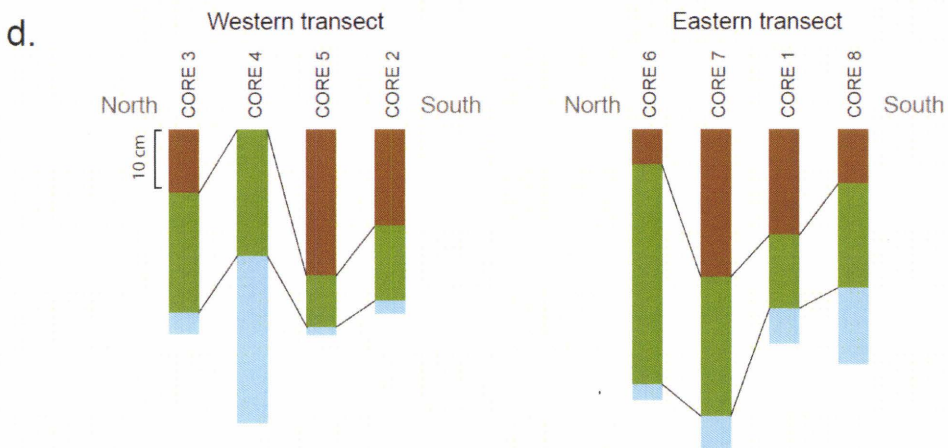
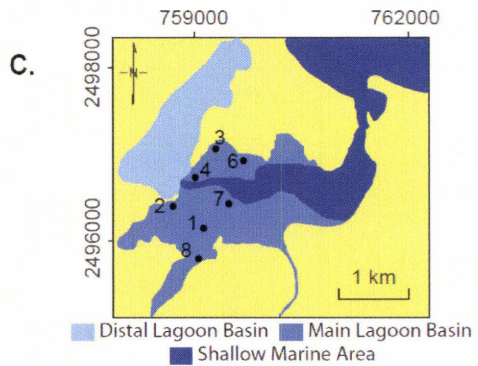
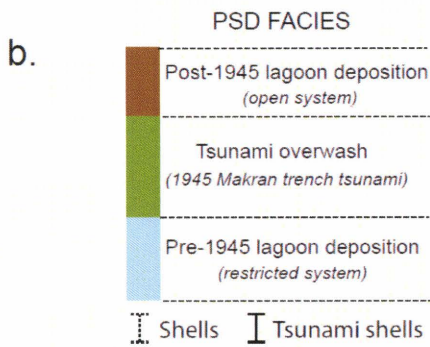
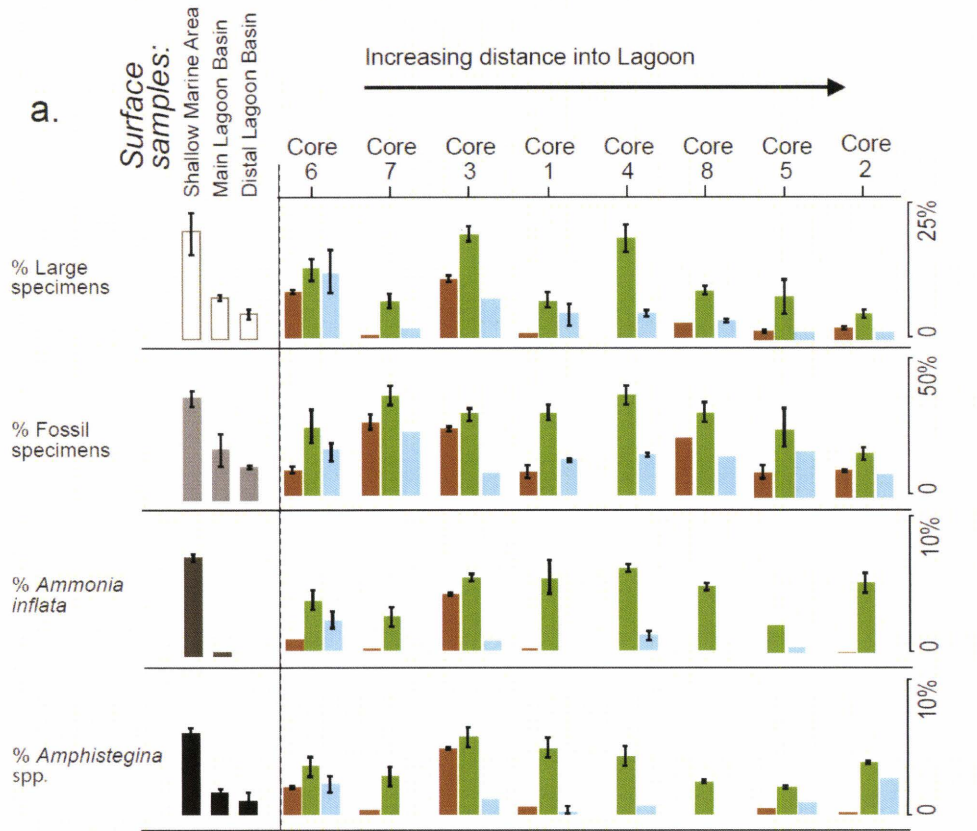


Figure 3.6: **a.** Foraminiferal data from surface samples (after Pilarczyk et al., submitted) and major stratigraphic units in Sur Lagoon. Core locations are arranged in order of increasing distance into the lagoon. Percentages on the y-axis reflect relative abundances. **b.** A generalized stratigraphic section indicating an older more restricted lagoon system evolving into a more open system by way of tsunami inundation. **c.** Core locations within Sur Lagoon. **d.** Correlation of cores through two north-south transect lines (eastern and western) indicating a slight thinning trend in tsunami bed thickness (*See previous page*).

CHAPTER 3 ONLINE SUPPLEMENTARY DATA

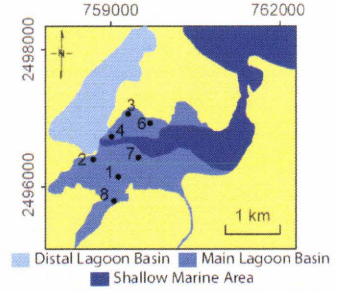
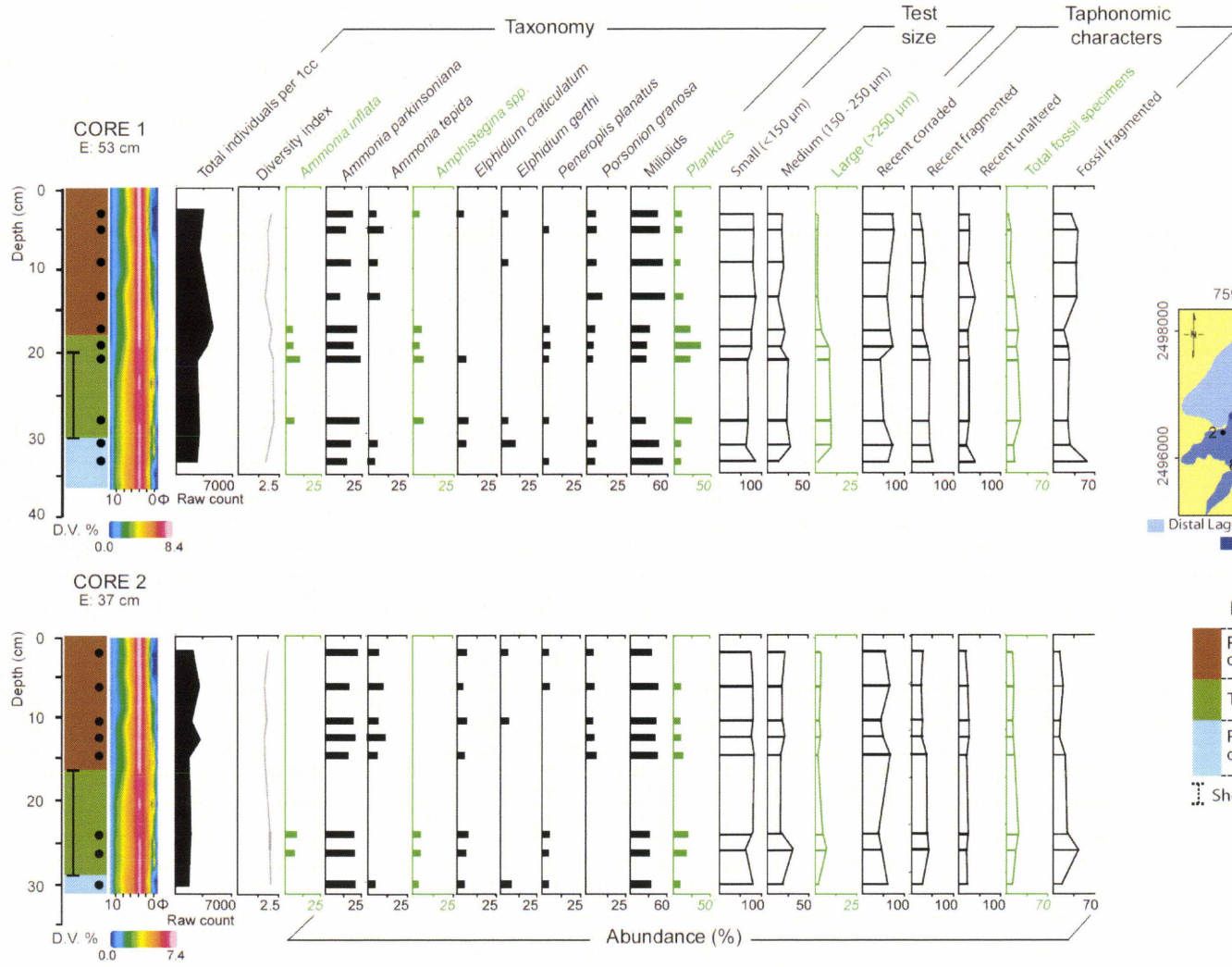
Online Supplementary Figure 3.1: Lithologic, PSD and foraminiferal data for cores 1 and 2. Core elevation (E) is indicated. Total individuals per 1 cm³, Shannon Diversity Index (SDI), foraminiferal taxa, test size (small: <150 µm; medium: 150-250 µm; large: >250 µm), taphonomic characters (modern corroded, modern fragmented, modern unaltered, total fossil specimens and fossil fragments) are indicated. Foraminiferal based tsunami indicators are highlighted in green. Tsunami and lagoon units are based the PSD and shell taphonomy (Donato et al., 2008; Donato et al., 2009). Black circles indicate sampling intervals. *See page 75.*

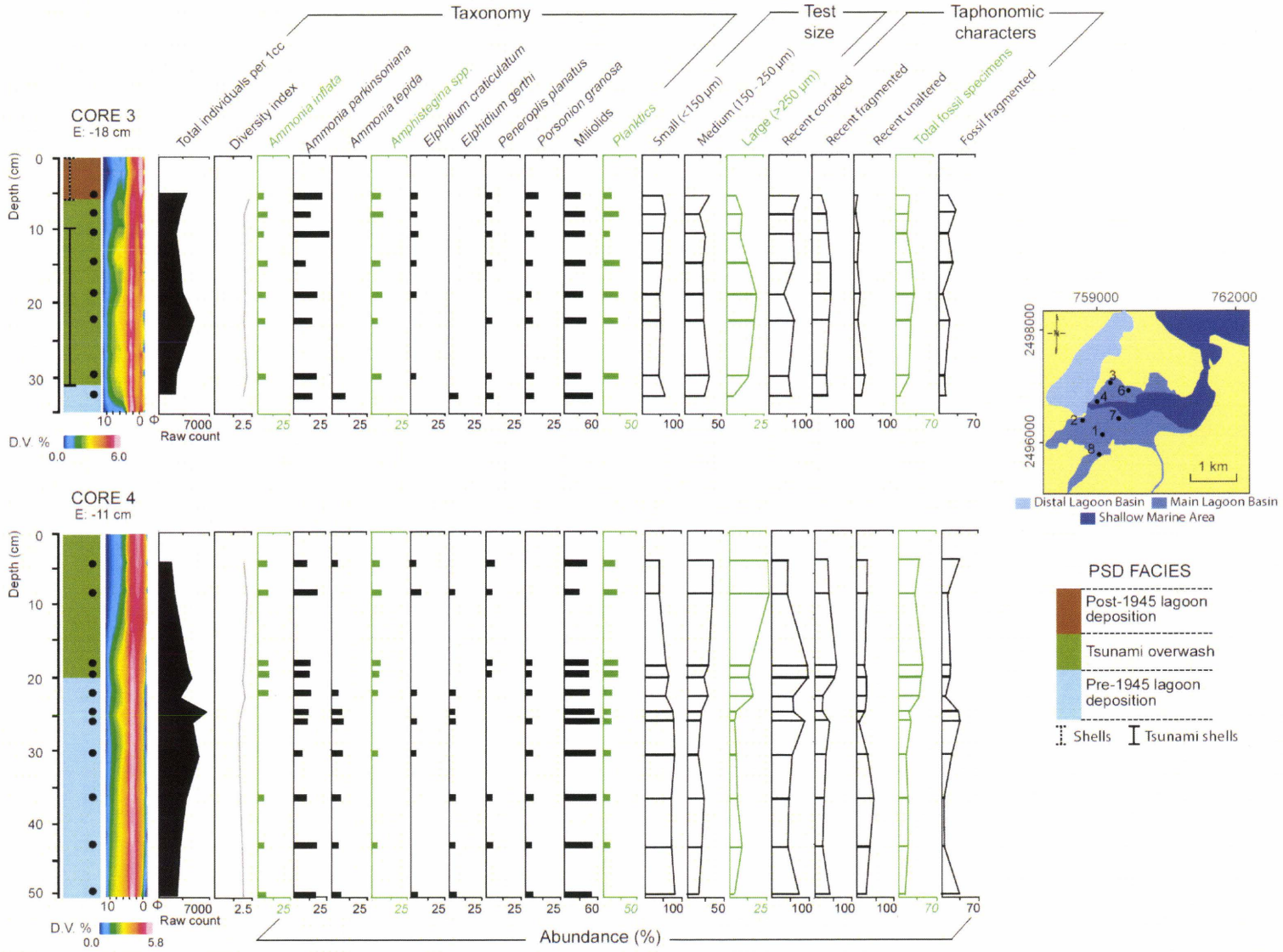
Online Supplementary Figure 3.2: Lithologic, PSD and foraminiferal data for cores 3 and 4. Core elevation (E) is indicated. Total individuals per 1 cm³, Shannon Diversity Index (SDI), foraminiferal taxa, test size (small: <150 μm; medium: 150-250 μm; large: >250 μm), taphonomic characters (modern corroded, modern fragmented, modern unaltered, total fossil specimens and fossil fragments) are indicated. Foraminiferal based tsunami indicators are highlighted in green. Tsunami and lagoon units are based the PSD and shell taphonomy (Donato et al., 2008; Donato et al., 2009). Black circles indicate sampling intervals. *See page 76.*

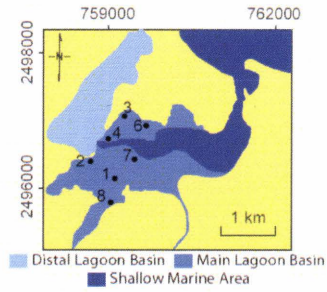
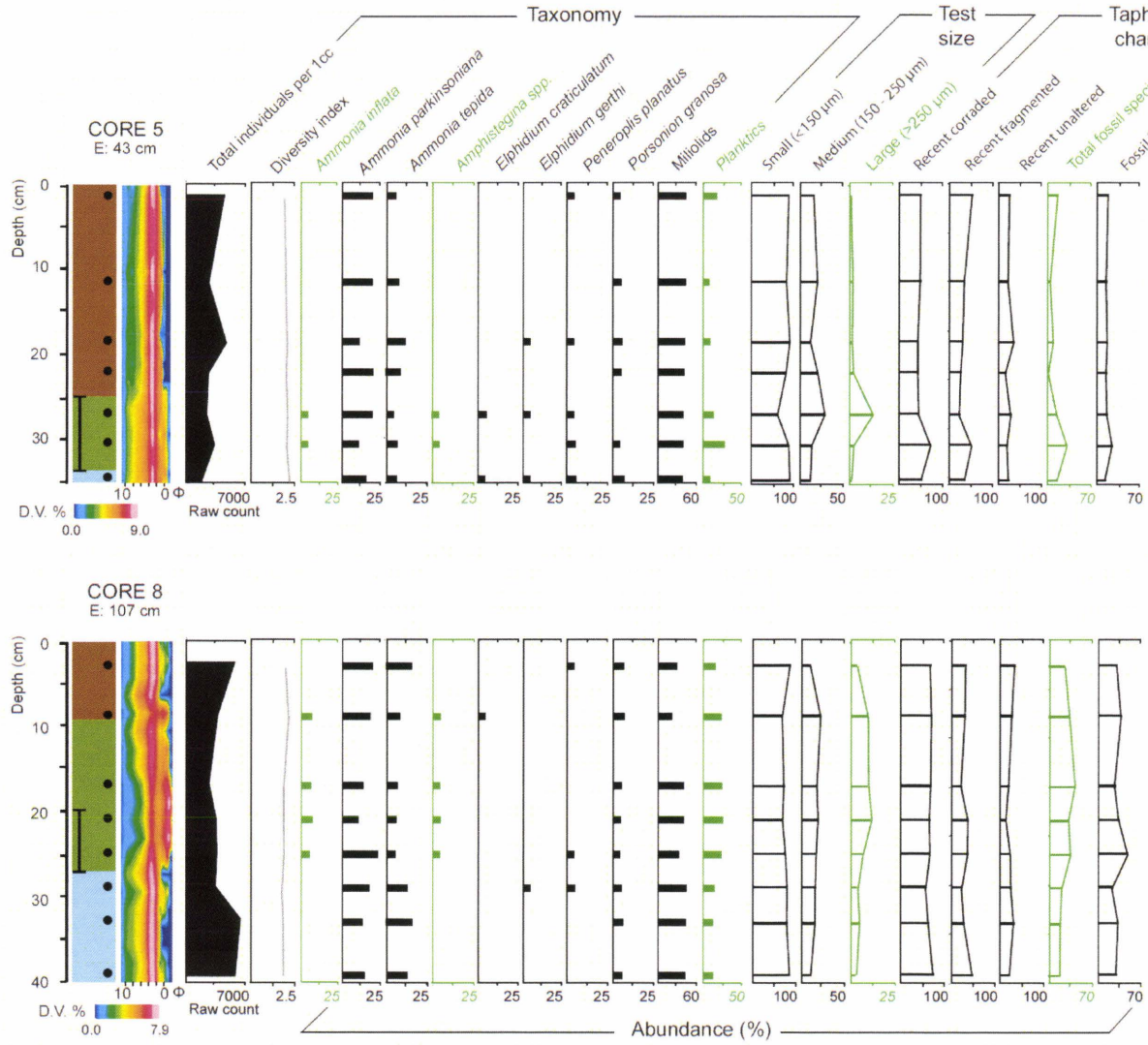
Online Supplementary Figure 3.3: Lithologic, PSD and foraminiferal data for cores 5 and 8. Core elevation (E) is indicated. Total individuals per 1 cm³, Shannon Diversity Index (SDI), foraminiferal taxa, test size (small: <150 μm; medium: 150-250 μm; large: >250 μm), taphonomic characters (modern corroded, modern fragmented, modern unaltered, total fossil specimens and fossil fragments) are indicated. Foraminiferal based tsunami indicators are highlighted in green. Tsunami and lagoon units are based the PSD and shell taphonomy (Donato et al., 2008; Donato et al., 2009). Black circles indicate sampling intervals. *See page 77.*

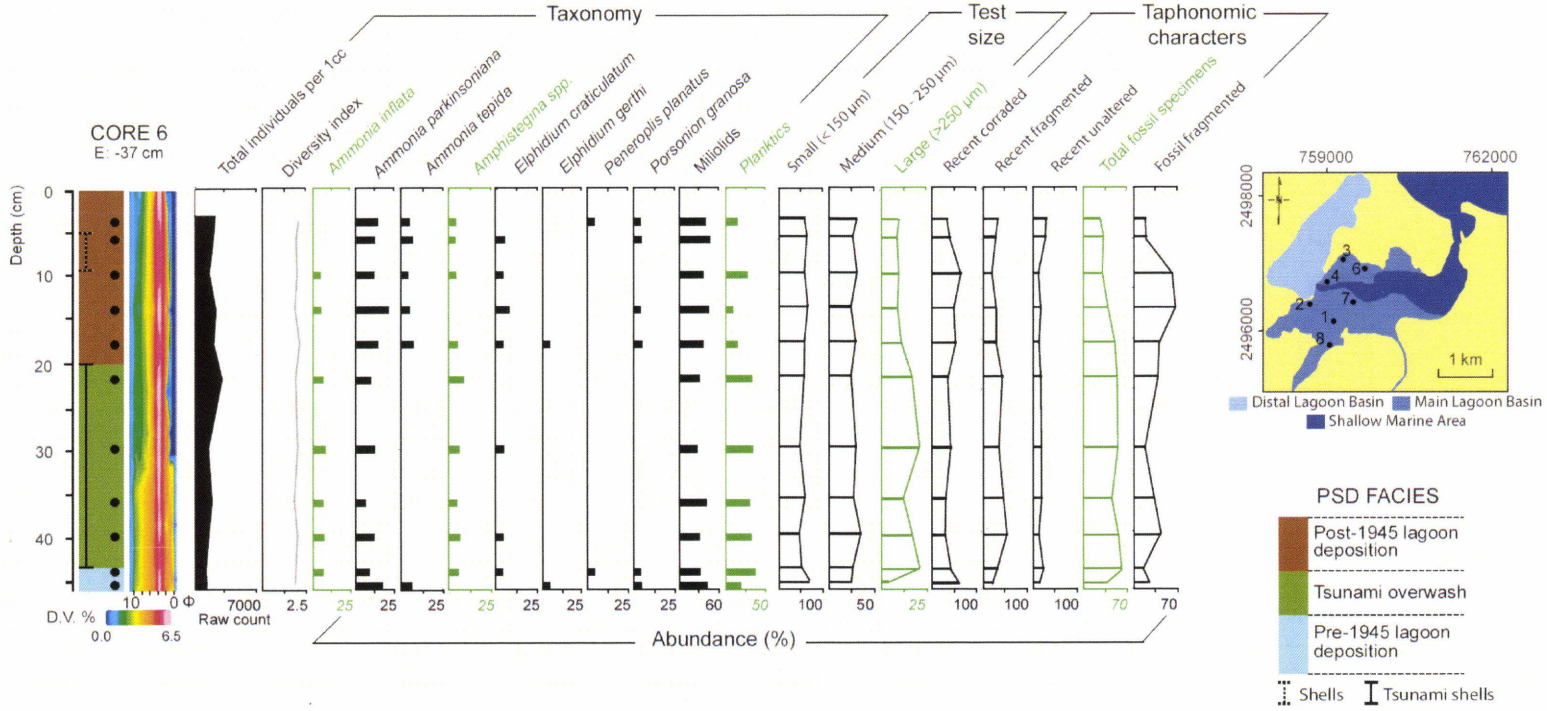
Online Supplementary Figure 3.4: Lithologic, PSD and foraminiferal data for core 6. Core elevation (E) is indicated. Total individuals per 1 cm³, Shannon Diversity Index (SDI), foraminiferal taxa, test size (small: <150 μm; medium: 150-250 μm; large: >250 μm), taphonomic characters (modern corroded, modern fragmented, modern unaltered, total fossil specimens and fossil fragments) are indicated. Foraminiferal based tsunami indicators are highlighted in green. Tsunami and lagoon units are based the PSD and shell taphonomy (Donato et al., 2008; Donato et al., 2009). Black circles indicate sampling intervals. *See page 78.*

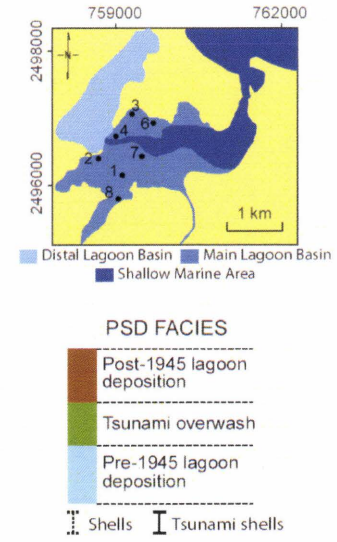
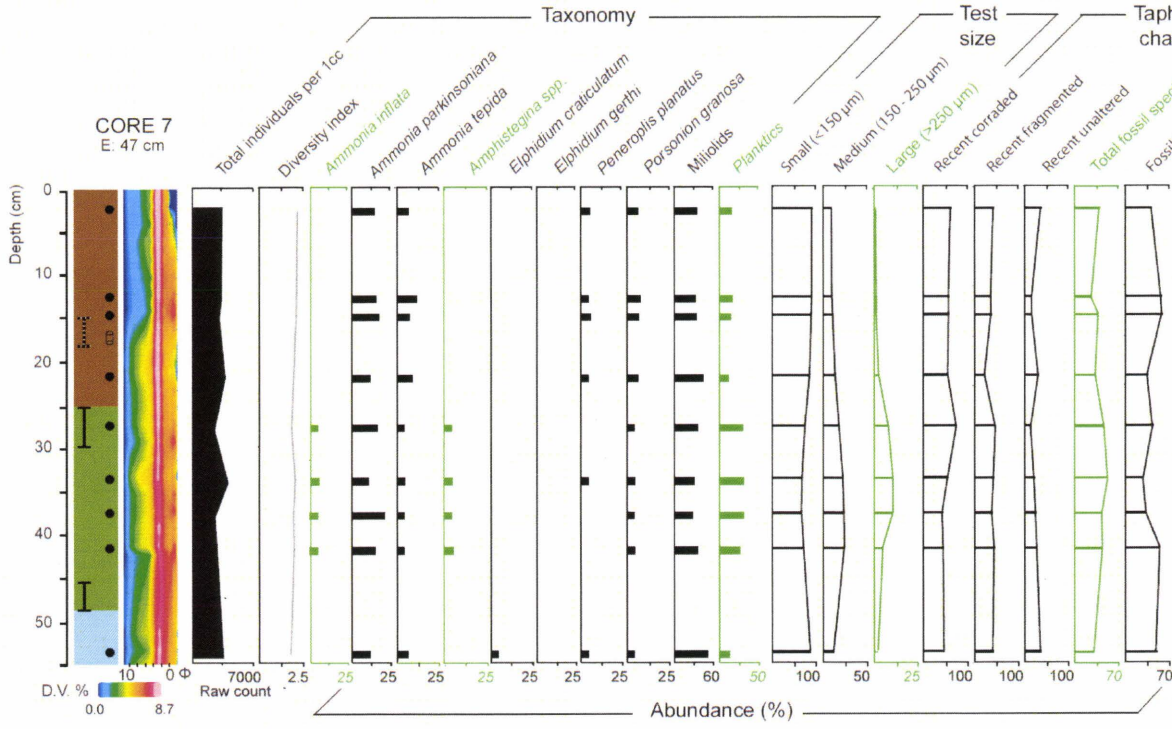
Online Supplementary Figure 3.5: Lithologic, PSD and foraminiferal data for core 7. Core elevation (E) is indicated. Total individuals per 1 cm³, Shannon Diversity Index (SDI), foraminiferal taxa, test size (small: <150 μm; medium: 150-250 μm; large: >250 μm), taphonomic characters (modern corroded, modern fragmented, modern unaltered, total fossil specimens and fossil fragments) are indicated. Foraminiferal based tsunami indicators are highlighted in green. Tsunami and lagoon units are based the PSD and shell taphonomy (Donato et al., 2008; Donato et al., 2009). Black circles indicate sampling intervals. *See page 79.*











CHAPTER 3 TABLES

CORE 1

Sample ID	4-6 cm	6-8 cm	10-12 cm	14-16 cm	18-20 cm	20-22 cm	22-23 cm	29-31 cm	32.5-34 cm	34-36 cm
TAPHONOMY										
>250µm specimens	0.010	0.007	0.006	0.008	0.033	0.080	0.079	0.088	0.089	0.004
150-250µm specimens	0.171	0.167	0.186	0.121	0.202	0.155	0.241	0.223	0.267	0.124
<150µm specimens	0.819	0.825	0.808	0.871	0.765	0.765	0.681	0.689	0.644	0.872
Recent specimens:										
Corraded	0.698	0.730	0.636	0.571	0.643	0.710	0.413	0.488	0.698	0.602
Fragments	0.221	0.288	0.355	0.283	0.297	0.396	0.456	0.438	0.459	0.521
Unaltered	0.201	0.212	0.188	0.349	0.177	0.184	0.203	0.202	0.134	0.342
Fossil specimens:										
Fragments	0.286	0.389	0.360	0.371	0.157	0.229	0.247	0.222	0.256	0.535
Total fossils	0.035	0.086	0.072	0.146	0.208	0.175	0.202	0.243	0.124	0.143
TAXONOMY										
<i>Ammonia inflata</i>	-	-	0.006	-	0.038	0.035	0.089	0.051	-	-
<i>Ammonia parkinsoniana</i>	0.174	0.126	0.164	0.094	0.199	0.175	0.223	0.217	0.164	0.141
<i>Ammonia tepida</i>	0.039	0.102	0.049	0.073	0.004	0.004	0.003	0.006	0.059	0.033
<i>Amphistegina</i> sp.	0.008	0.005	0.009	-	0.041	0.031	0.066	0.057	-	0.004
<i>Brizalina striatula</i>	0.042	0.008	0.022	0.017	-	-	0.003	0.003	0.003	0.004
<i>Cibicides lobatula</i>	0.026	0.005	0.012	0.007	0.030	0.013	0.007	0.039	0.007	0.010
<i>Ephidium advenum</i>	0.047	0.031	0.046	0.024	0.041	0.035	0.030	0.036	0.046	0.041
<i>Ephidium craticulatum</i>	0.016	0.008	0.009	-	0.008	0.002	0.049	0.071	0.043	0.012
<i>Ephidium gerthi</i>	0.049	0.010	0.031	0.005	0.011	0.009	0.010	0.036	0.089	0.010
<i>Ephidium striatopunctulum</i>	0.057	0.107	0.052	0.097	0.109	0.069	0.052	0.030	0.066	0.137
<i>Patinellinella</i> sp.	0.013	-	0.028	-	0.008	-	0.010	-	0.010	0.002
<i>Peneroplis planatus</i>	-	0.013	0.003	0.002	0.011	0.031	0.016	0.015	0.007	0.010
<i>Porsonia granosa</i>	0.034	0.045	0.043	0.077	0.034	0.020	0.020	0.012	0.043	0.035
<i>Rosalina orientalis</i>	0.008	0.003	0.003	-	0.000	0.009	0.007	0.012	-	-
Milioids	0.398	0.442	0.475	0.508	0.274	0.232	0.213	0.202	0.420	0.486
Planktics	0.089	0.094	0.046	0.094	0.192	0.334	0.203	0.214	0.046	0.077

Table 3.1: Taphonomic data (fractional abundances).

Table 3.1 continued...

CORE 2

Sample ID	2-4 cm	6-8 cm	10-12 cm	12-14 cm	14-16 cm	23-25 cm	25-27 cm	29-30.5 cm
TAPHONOMY								
>250µm specimens	0.030	0.027	0.020	0.028	0.011	0.039	0.063	0.016
150-250µm specimens	0.199	0.162	0.165	0.195	0.148	0.146	0.294	0.171
<150µm specimens	0.772	0.810	0.815	0.777	0.841	0.815	0.643	0.814
Recent specimens:								
Corraded	0.593	0.712	0.493	0.561	0.721	0.445	0.527	0.665
Fragments	0.277	0.240	0.267	0.256	0.365	0.380	0.420	0.267
Unaltered	0.153	0.207	0.233	0.239	0.180	0.223	0.180	0.195
Fossil specimens:								
Fragments	0.100	0.156	0.111	0.098	0.194	0.226	0.415	0.136
Total fossils	0.089	0.103	0.091	0.094	0.117	0.185	0.143	0.085
TAXONOMY								
<i>Ammonia inflata</i>	-	-	-	0.003	-	0.063	0.042	-
<i>Ammonia parkinsoniana</i>	0.212	0.149	0.177	0.193	0.134	0.180	0.188	0.193
<i>Ammonia tepida</i>	0.064	0.100	0.064	0.113	0.047	0.008	0.004	0.044
<i>Amphistegina</i> sp.	-	0.005	-	0.003	-	0.039	0.038	0.026
<i>Brizalina striatula</i>	0.035	0.008	0.023	0.008	0.009	0.023	0.025	0.022
<i>Cibicides lobatula</i>	0.029	0.005	0.019	0.005	0.022	0.023	0.025	0.048
<i>Ephidium advenum</i>	0.058	0.023	0.060	0.013	0.034	0.066	0.054	0.035
<i>Ephidium craticulatum</i>	0.006	0.008	0.004	0.018	0.004	0.012	0.038	0.022
<i>Ephidium gerthi</i>	0.042	0.010	0.045	0.015	0.017	0.008	0.004	0.066
<i>Ephidium striatopunctulum</i>	0.151	0.105	0.102	0.138	0.129	0.063	0.079	0.127
<i>Patinellina</i> sp.	0.042	-	0.008	-	-	-	-	0.018
<i>Peneroplis planatus</i>	0.013	0.013	0.008	-	-	0.035	0.033	0.018
<i>Porsonia granosa</i>	0.019	0.044	0.041	0.040	0.069	0.012	0.008	0.009
<i>Rosalina orientalis</i>	0.003	0.003	0.004	-	0.000	0.012	0.013	0.009
Milioids	0.317	0.434	0.398	0.385	0.414	0.289	0.288	0.298
Planktics	0.010	0.093	0.049	0.070	0.121	0.168	0.163	0.066

Table 3.1 continued...

CORE 3								
Sample ID	4-6 cm	6-9 cm	9-11 cm	13-15 cm	17-20 cm	20-23 cm	28-30 cm	30-33 cm
TAPHONOMY								
>250µm specimens	0.089	0.128	0.116	0.174	0.226	0.210	0.169	0.074
150-250µm specimens	0.322	0.209	0.291	0.252	0.264	0.267	0.339	0.279
<150µm specimens	0.589	0.664	0.593	0.575	0.510	0.523	0.492	0.647
Recent specimens:								
Corraded	0.822	0.703	0.690	0.716	0.442	0.713	0.563	0.624
Fragments	0.235	0.365	0.410	0.487	0.485	0.439	0.366	0.400
Unaltered	0.139	0.082	0.175	0.132	0.209	0.146	0.328	0.240
Fossil specimens:								
Fragments	0.143	0.291	0.145	0.230	0.043	0.168	0.074	0.091
Total fossils	0.268	0.249	0.221	0.310	0.352	0.290	0.254	0.081
TAXONOMY								
<i>Ammonia inflata</i>	0.035	0.068	0.022	0.066	0.050	0.048	0.051	0.008
<i>Ammonia parkinsoniana</i>	0.210	0.117	0.273	0.072	0.166	0.127	0.161	0.125
<i>Ammonia tepida</i>	0.009	0.011	0.011	0.006	0.008	0.003	0.007	0.091
<i>Amphistegina</i> sp.	0.061	0.077	0.007	0.057	0.074	0.031	0.066	0.011
<i>Brizalina striatula</i>	0.017	-	0.026	0.012	0.008	0.014	0.004	0.011
<i>Cibicides lobatula</i>	0.026	0.009	0.011	0.009	0.005	0.014	0.007	0.008
<i>Ephidium advenum</i>	0.048	0.046	0.045	0.060	0.026	0.079	0.033	0.023
<i>Ephidium craticulatum</i>	0.048	0.043	0.052	0.030	0.032	0.007	0.033	0.004
<i>Ephidium gerthi</i>	0.004	-	0.015	-	0.005	0.003	0.007	0.065
<i>Ephidium striatopunctulum</i>	0.048	0.014	0.086	0.036	0.066	0.048	0.070	0.057
<i>Patinellinella</i> sp.	0.013	0.003	0.007	0.003	0.005	0.003	0.007	0.015
<i>Peneroplis planatus</i>	0.022	0.028	0.019	0.024	0.008	0.017	0.022	0.046
<i>Porsonion granosa</i>	0.070	0.011	0.037	0.030	0.016	0.027	0.040	0.038
<i>Rosalina orientalis</i>	0.017	0.009	0.004	0.006	0.008	0.003	0.007	0.004
Miliolids	0.253	0.345	0.341	0.360	0.311	0.364	0.271	0.471
Planktics	0.118	0.219	0.041	0.228	0.213	0.210	0.212	0.023

Table 3.1 continued...

CORE 4											
Sample ID	2-7 cm	8-10 cm	18-20 cm	20-21 cm	22-24 cm	24-26 cm	26-27 cm	29-33 cm	36-38 cm	40-47 cm	51-53 cm
TAPHONOMY											
>250µm specimens	0.257	0.265	0.136	0.128	0.158	0.043	0.033	0.044	0.050	0.081	0.032
150-250µm specimens	0.340	0.332	0.275	0.213	0.269	0.184	0.171	0.136	0.218	0.184	0.142
<150µm specimens	0.403	0.403	0.588	0.658	0.573	0.773	0.797	0.821	0.733	0.735	0.826
Recent specimens:											
Corraded	0.442	0.430	0.958	0.973	0.575	0.586	0.880	0.553	0.470	0.437	0.728
Fragments	0.383	0.417	0.620	0.552	0.248	0.232	0.432	0.332	0.281	0.233	0.432
Unaltered	0.288	0.280	0.216	0.276	0.274	0.229	0.065	0.294	0.462	0.354	0.254
Fossil specimens:											
Fragments	0.299	0.084	0.137	0.126	0.040	0.286	0.312	0.156	0.011	0.015	0.300
Total fossils	0.363	0.284	0.430	0.401	0.362	0.173	0.209	0.115	0.153	0.151	0.095
TAXONOMY											
<i>Ammonia inflata</i>	0.053	0.063	0.059	0.067	0.063	-	-	0.003	0.017	0.011	0.037
<i>Ammonia parkinsoniana</i>	0.092	0.171	0.115	0.110	0.117	0.103	0.092	0.055	0.087	0.163	0.154
<i>Ammonia tepida</i>	0.009	-	-	0.004	0.025	0.059	0.065	0.061	0.051	0.033	0.049
<i>Amphistegina</i> sp.	0.048	0.063	0.051	0.039	0.014	0.002	-	0.012	0.002	0.019	0.003
<i>Brizalina striatula</i>	0.013	0.015	0.016	0.018	0.016	0.042	0.031	0.029	0.011	0.014	0.012
<i>Cibicides lobatula</i>	0.009	0.022	0.020	-	0.030	0.027	0.003	0.009	0.011	0.008	0.012
<i>Ephidium advenum</i>	0.110	0.108	0.051	0.046	0.071	0.071	0.038	0.075	0.079	0.060	0.065
<i>Ephidium craticulatum</i>	0.013	0.059	0.008	0.004	0.022	0.002	0.010	0.014	0.004	0.008	0.040
<i>Ephidium gerthi</i>	-	0.011	0.008	0.007	0.030	0.027	0.034	0.003	0.032	0.011	0.034
<i>Ephidium striatopuncticum</i>	0.057	0.078	0.055	0.057	0.044	0.022	0.041	0.075	0.028	0.068	0.052
<i>Patinellinella</i> sp.	-	-	-	0.007	-	0.007	0.007	-	0.002	-	0.018
<i>Peneroplis planatus</i>	0.053	0.022	0.036	0.018	0.008	0.012	0.003	-	0.028	0.038	0.009
<i>Porosion granosa</i>	0.004	0.004	0.020	0.018	0.035	0.037	0.034	0.038	0.045	0.027	0.043
<i>Rosalina orientalis</i>	0.004	-	-	0.007	0.008	0.002	0.003	-	0.002	0.005	0.003
Milfoids	0.382	0.227	0.387	0.415	0.425	0.518	0.558	0.542	0.548	0.467	0.458
Planktics	0.154	0.156	0.174	0.184	0.093	0.068	0.079	0.084	0.055	0.068	0.009

Table 3.1 continued...

CORE 5							
Sample ID	0-3 cm	10-13 cm	17-20 cm	21-23 cm	26-28 cm	27-34 cm	34-35 cm
TAPHONOMY							
>250µm specimens	0.009	0.020	0.016	0.023	0.137	0.026	0.014
150-250µm specimens	0.146	0.190	0.111	0.195	0.277	0.126	0.112
<150µm specimens	0.846	0.791	0.873	0.781	0.586	0.848	0.874
Recent specimens:							
Corraded	0.491	0.479	0.427	0.426	0.452	0.726	0.511
Fragments	0.529	0.355	0.320	0.276	0.242	0.524	0.364
Unaltered	0.239	0.216	0.343	0.153	0.277	0.189	0.225
Fossil specimens:							
Fragments	0.131	0.100	0.118	0.100	0.113	0.200	0.085
Total fossils	0.174	0.056	0.108	0.029	0.167	0.330	0.169
TAXONOMY							
<i>Ammonia inflata</i>	-	-	-	-	0.023	0.019	0.004
<i>Ammonia parkinsoniana</i>	0.194	0.195	0.114	0.198	0.190	0.099	0.160
<i>Ammonia tepida</i>	0.042	0.065	0.118	0.069	0.019	0.057	0.048
<i>Amphistegina</i> sp.	0.010	0.006	-	0.003	0.016	0.024	0.009
<i>Brizalina striatula</i>	0.010	0.038	0.021	0.057	0.032	0.005	0.048
<i>Cibicides lobatula</i>	0.014	0.009	0.007	0.009	0.016	0.028	0.004
<i>Elphidium advenum</i>	0.100	0.071	0.086	0.072	0.055	0.042	0.074
<i>Elphidium craticulatum</i>	0.007	0.012	0.004	0.012	0.035	-	0.017
<i>Elphidium gerthi</i>	0.007	0.006	0.021	0.006	0.013	-	0.026
<i>Elphidium striatopunctulum</i>	0.059	0.130	0.100	0.123	0.113	0.057	0.117
<i>Patinellinella</i> sp.	-	0.006	0.014	0.006	-	0.028	0.009
<i>Peneroplis planatus</i>	0.024	0.018	0.032	0.012	0.019	0.042	0.043
<i>Porsonion granosa</i>	0.021	0.047	0.050	0.042	0.010	0.024	0.061
<i>Rosalina orientalis</i>	-	0.003	-	0.009	0.006	0.005	0.009
Miliolids	0.349	0.355	0.361	0.339	0.329	0.311	0.316
Planktics	0.163	0.038	0.071	0.042	0.123	0.259	0.056

Table 3.1 continued...

CORE 6											
Sample ID	3-5 cm	5-7 cm	9-11 cm	13-15 cm	17-19 cm	21-23 cm	29-31 cm	35-37 cm	39-41 cm	43-45 cm	45-46 cm
TAPHONOMY											
>250µm specimens	0.093	0.080	0.090	0.084	0.103	0.162	0.205	0.116	0.164	0.206	0.038
150-250µm specimens	0.310	0.265	0.313	0.245	0.296	0.246	0.301	0.273	0.356	0.264	0.251
<150µm specimens	0.597	0.654	0.598	0.671	0.601	0.591	0.493	0.611	0.480	0.531	0.710
Recent specimens:											
Corraded	0.361	0.430	0.669	0.515	0.553	0.378	0.443	0.331	0.317	0.448	0.637
Fragments	0.345	0.294	0.211	0.311	0.311	0.449	0.371	0.481	0.556	0.324	0.220
Unaltered	0.294	0.276	0.119	0.174	0.136	0.173	0.186	0.188	0.127	0.228	0.143
Fossil specimens:											
Fragments	0.169	0.177	0.594	0.647	0.385	0.365	0.162	0.309	0.412	0.133	0.229
Total fossils	0.248	0.296	0.279	0.367	0.477	0.516	0.530	0.432	0.540	0.590	0.336
TAXONOMY											
<i>Ammonia inflata</i>	0.008	0.009	0.021	0.015	0.013	0.045	0.060	0.050	0.052	0.045	-
<i>Ammonia parkinsoniana</i>	0.130	0.117	0.109	0.207	0.132	0.084	0.111	0.055	0.111	0.079	0.167
<i>Ammonia tepida</i>	0.042	0.061	0.023	0.038	0.068	-	0.006	0.010	0.006	-	0.052
<i>Amphistegina</i> sp.	0.027	0.013	0.021	-	0.026	0.076	0.047	0.033	0.046	0.041	-
<i>Brizalina striatula</i>	0.008	0.048	0.009	-	-	-	-	0.002	-	-	-
<i>Cibicides lobatula</i>	0.015	0.013	0.029	0.011	0.026	0.017	0.019	0.010	0.012	0.012	0.015
<i>Ephidium advenum</i>	0.095	0.083	0.073	0.045	0.060	0.090	0.060	0.052	0.052	0.037	0.063
<i>Ephidium craticulatum</i>	0.015	0.048	0.041	0.079	0.043	0.011	0.032	0.010	0.031	0.025	0.015
<i>Ephidium gerthi</i>	0.004	-	-	0.008	0.017	-	-	0.002	0.003	-	0.015
<i>Ephidium striatopuncticulum</i>	0.084	0.057	0.023	0.068	0.060	0.034	0.047	0.067	0.031	0.058	0.033
<i>Patinellinella</i> sp.	0.008	-	0.003	-	-	0.003	0.003	0.017	0.022	0.012	0.007
<i>Peneroplis planatus</i>	0.027	0.013	0.015	0.011	0.017	0.017	0.019	0.005	0.012	0.021	0.011
<i>Porosion granosa</i>	0.023	0.030	0.012	0.019	0.038	0.008	0.009	0.005	0.009	0.017	0.026
<i>Rosalina orientalis</i>	-	-	0.006	-	-	-	0.003	-	0.006	-	0.007
Mitoids	0.389	0.474	0.361	0.429	0.370	0.297	0.256	0.393	0.306	0.302	0.415
Planktics	0.126	0.035	0.255	0.071	0.132	0.319	0.326	0.290	0.299	0.351	0.174

Table 3.1 continued...

CORE 7									
Sample ID	2-4 cm	12-14 cm	14-16 cm	21-23 cm	27-29 cm	33-35 cm	37-39 cm	41-43 cm	53-55 cm
TAPHONOMY									
>250µm specimens	0.003	0.007	0.007	0.020	0.075	0.101	0.102	0.045	0.017
150-250µm specimens	0.093	0.097	0.107	0.132	0.175	0.221	0.233	0.239	0.118
<150µm specimens	0.904	0.896	0.886	0.847	0.749	0.678	0.665	0.716	0.865
Recent specimens:									
Corraded	0.607	0.564	0.567	0.545	0.739	0.540	0.419	0.444	0.459
Fragments	0.407	0.349	0.355	0.209	0.454	0.408	0.373	0.427	0.393
Unaltered	0.346	0.147	0.153	0.295	0.129	0.204	0.239	0.263	0.343
Fossil specimens:									
Fragments	0.265	0.412	0.425	0.200	0.284	0.138	0.184	0.395	0.333
Total fossils	0.314	0.190	0.300	0.254	0.394	0.452	0.357	0.370	0.231
TAXONOMY									
<i>Ammonia inflata</i>	0.005	-	-	-	0.025	0.046	0.031	0.028	-
<i>Ammonia parkinsoniana</i>	0.123	0.130	0.147	0.095	0.141	0.088	0.185	0.123	0.093
<i>Ammonia tepida</i>	0.059	0.109	0.062	0.082	0.025	0.038	0.024	0.028	0.055
<i>Amphistegina</i> sp.	0.005	0.005	-	-	0.032	0.038	0.031	0.040	0.000
<i>Brizalina striatula</i>	0.015	0.005	-	0.041	0.007	0.013	0.007	0.019	0.010
<i>Cibicides lobatula</i>	0.039	0.026	0.034	0.027	0.007	0.017	0.024	0.034	0.020
<i>Elphidium advenum</i>	0.074	0.078	0.085	0.050	0.035	0.079	0.062	0.046	0.101
<i>Elphidium craticulatum</i>	0.005	-	0.011	-	0.004	0.004	0.010	0.006	0.018
<i>Elphidium gerthi</i>	0.005	0.016	-	0.014	-	-	0.003	0.006	0.013
<i>Elphidium striatopunctulum</i>	0.079	0.036	0.073	0.064	0.085	0.042	0.010	0.009	0.028
<i>Patinellinella</i> sp.	0.020	0.026	0.023	0.005	-	0.004	0.010	0.022	0.005
<i>Peneroplis planatus</i>	0.044	0.031	0.045	0.032	0.007	0.025	0.014	0.012	0.023
<i>Porsonion granosa</i>	0.054	0.068	0.056	0.055	0.021	0.025	0.027	0.022	0.028
<i>Rosalina orientalis</i>	0.005	0.005	0.011	0.009	-	0.004	-	0.003	0.005
Milioids	0.330	0.328	0.333	0.441	0.353	0.308	0.281	0.364	0.503
Planktics	0.138	0.135	0.119	0.086	0.258	0.271	0.281	0.238	0.101

Table 3.1 continued...

CORE 8								
Sample ID	2-4 cm	8-10 cm	16-18 cm	20-22 cm	24-26 cm	28-30 cm	32-34 cm	38-40 cm
TAPHONOMY								
>250µm specimens	0.027	0.091	0.093	0.112	0.061	0.033	0.041	0.025
150-250µm specimens	0.099	0.219	0.176	0.190	0.169	0.159	0.155	0.107
<150µm specimens	0.874	0.690	0.731	0.698	0.770	0.808	0.804	0.868
Recent specimens:								
Corraded	0.636	0.668	0.647	0.620	0.635	0.539	0.594	0.704
Fragments	0.337	0.319	0.234	0.390	0.383	0.249	0.300	0.493
Unaltered	0.309	0.249	0.179	0.118	0.220	0.232	0.295	0.200
Fossil specimens:								
Fragments	0.221	0.289	0.185	0.250	0.404	0.145	0.242	0.212
Total fossils	0.209	0.282	0.371	0.267	0.297	0.155	0.135	0.128
TAXONOMY								
<i>Ammonia inflata</i>	-	0.053	0.043	0.056	0.039	-	-	-
<i>Ammonia parkinsoniana</i>	0.193	0.177	0.128	0.093	0.227	0.172	0.122	0.142
<i>Ammonia tepida</i>	0.148	0.066	0.052	0.042	0.039	0.115	0.154	0.117
<i>Amphistegina</i> sp.	-	0.027	0.021	0.028	0.020	-	-	-
<i>Brizalina striatula</i>	0.009	0.018	-	-	-	0.007	0.003	0.028
<i>Cibicides lobatula</i>	0.018	0.004	0.006	0.005	0.002	-	0.018	0.003
<i>Ephidium advenum</i>	0.050	0.018	0.034	0.019	0.032	0.029	0.041	0.042
<i>Ephidium craticulatum</i>	-	0.013	-	0.005	0.002	0.005	-	0.008
<i>Ephidium gerthi</i>	0.006	0.004	0.003	0.005	0.002	0.014	0.008	0.011
<i>Ephidium striatopunctulum</i>	0.089	0.133	0.061	0.075	0.048	0.060	0.063	0.081
<i>Patinellina</i> sp.	-	-	0.006	0.005	0.009	-	0.013	-
<i>Peneroplis planatus</i>	0.021	0.018	0.009	0.019	0.027	0.021	0.005	0.017
<i>Porosion granosa</i>	0.056	0.058	0.043	0.033	0.029	0.041	0.056	0.053
<i>Rosalina orientalis</i>	0.003	-	-	-	-	0.002	0.010	-
Milolids	0.291	0.208	0.379	0.388	0.324	0.430	0.418	0.411
Planktics	0.116	0.204	0.214	0.229	0.200	0.105	0.091	0.089

CHAPTER 4

HOMOTREMA RUBRUM (LAMARCK) TAPHONOMY AS AN OVERWASH INDICATOR IN MARINE PONDS ON ANEGADA, BRITISH VIRGIN ISLANDS

Jessica E. Pilarczyk*

Eduard G. Reinhardt

School of Geography and Earth Sciences, McMaster University, Hamilton, ON,
Canada, L8S 4K1

*Corresponding author: J.E. Pilarczyk (pilarcje@mcmaster.ca)

Citation: Pilarczyk, J.E., Reinhardt, E.G., 2011. *Homotrema rubrum* (Lamarck) taphonomy as an overwash indicator in marine ponds on Anegada, British Virgin Islands. *Natural Hazards*, doi: 10.1007/s11069-010-9706-3

Status: received 15 March 2010, accepted 11 December 2010, published online 2 February 2011.

Reprinted with permission from Springer

COPYRIGHT PERMISSION

Springer License Terms and Conditions

License Number: 2661941445350

License date: May 04, 2011

Licensed content publisher: Springer

Licensed content publication: Natural Hazards

Licensed content title: Homotrema rubrum (Lamarck) taphonomy as an overwash indicator in Marine Ponds on Anegada, British Virgin Islands

Licensed content author: Jessica E. Pilarczyk

Licensed content date: Jan 1, 2011

Type of Use: Thesis/Dissertation

Portion: Full text

Number of copies: 6

Author of this Springer article: Yes and you are a contributor of the new work

Title of your thesis / dissertation: Foraminiferal Taphonomy as a Paleo-Tsunami and Overwash Indicator in Coastal Environments - Evidence from Oman and the British Virgin Islands

Expected completion date: May 2011

Estimated size (pages): 170

ABSTRACT

Marine hypersaline ponds on Anegada, British Virgin Islands contain stratigraphic evidence (Shell and Sand Sheet) of a A.D. 1650–1800 overwash event that could have formed through a hurricane or tsunami. Candidates for the deposit include far-field (e.g. 1755 Lisbon tsunami) and local Puerto Rico Trench events (e.g. 1690), but hurricanes cannot be ignored. The goal of this study is to provide additional information to assess the origin of the deposit by examining the taphonomic characters of *Homotrema rubrum*, a common encrusting foraminifer in Caribbean reef settings. Surface samples (n = 12) from major sub-environments (reef-flat, beach, storm wrack, and dune) and pond sections (n = 6; 20–80 cm thick) were analyzed for their *Homotrema* concentration (specimens/cm³) and taphonomic character. Particle-size analysis was conducted on the same sections and samples. Highly Preserved (red colored, angular, intact chambers) *Homotrema* dominate the beach, storm wrack, and reef-flat deposits relative to the dune sand, but the beach and storm wrack contain the largest specimens. The Shell and Sand Sheet in the pond has Highly Preserved and abundant *Homotrema* (specimens/cm³) versus other sedimentary units in the ponds (e.g. Mud Cap and Shelly Mud). Its taphonomic character is most similar (test size and condition) to the storm wrack deposit on the beach indicating an outside provenance for the sand. Concentration of *Homotrema* in the Shell and Sand Sheet declined southward indicating a northerly reef-flat provenance for the overwash, although it does not preclude a southern inundation as well. It is unclear whether *Homotrema* individuals originated from the reef itself or were eroded from older beach ridge deposits during the overwash event. Conclusions from *Homotrema* taphonomic analysis were limited by the lack of comparative data from known hurricane and tsunami deposits in other Caribbean regions.

4.1 INTRODUCTION

Marine ponds have proven to be excellent recorders of overwash events, with sandy deposits often ascribed to major storm events, although tsunamis are also a possibility (e.g. Donnelly 2005; Park et al. 2009). In the Caribbean, most overwash deposits are considered to be formed by hurricanes rather than tsunamis due to their frequency. However, there are several historical accounts of tsunamis affecting the Caribbean (e.g. 1755 Lisbon tsunami). These accounts are sparse and there are few comparative geological studies to assess the records (e.g. Atwater et al. 2010; Jones and Hunter 1992). Anegada, British Virgin Islands, due to its position relative to the Atlantic Ocean and the Puerto Rico Trench, may be a good tsunami recorder of local (e.g. 1690, 1867; Reid and Taber 1920; Zahibo et al. 2003) and trans-oceanic events (e.g. 1755 Lisbon; O’Loughlin and Lander 2003). However, potential tsunami overwash events are expected to be intermingled with hurricane deposits and discerning between the two may be difficult. Modern hypersaline ponds on Anegada show a distinctive Shell and Sand Sheet that is laterally extensive and contains abundant foraminifera including *Homotrema rubrum* (Lamarck; Fig. 4.1). The origin of the overwash is not known as the chronologic (e.g. between A.D. 1650 and 1800) and stratigraphic evidence could not provide the necessary resolution to ascribe it to a known hurricane or tsunami (Atwater et al. 2010). The goal of this study is to provide additional data for assessing the deposit by determining the sand provenance using the taphonomy of *Homotrema* fragments.

Foraminiferal provenance is used extensively to document overwash events from both tsunamis and hurricanes (e.g. Hippensteel and Martin 1999; Scott et al. 2003; Hawkes et al. 2007; Mamo et al. 2009). However, there are few studies using taphonomic condition to help refine this data which could prove useful (e.g. Hawkes et al. 2007; Kortekaas and Dawson 2007). Taphonomic condition of the reef-dwelling *Homotrema rubrum* (Lamarck) has been shown to be an indicator of transport direction in reefal settings but has never been applied to overwash deposits (MacKenzie et al. 1965; Machado and Moraes 2002). It has great potential in this regard, as its encrusting habit in the reef provides a defined source for judging overwash dynamics.

4.1.1 *Homotrema rubrum* taphonomy

Homotrema rubrum (Lamarck) are red (bleaches to whitish-pink following death; Emiliani 1951), sessile foraminifera that grow attached to the lower surfaces of shells, corals, and reef detritus. The colored test consists of pronounced chambers that hollow after death (Fig. 4.2). *Homotrema* is restricted to latitudes between

30°N and 30°S, has a distribution similar to hermatypic corals, and is widely found in reef cryptic space, submarine caves and on non-growing areas of corals, reef rubble, shells, and calcareous algae (MacKenzie et al. 1965; Elliott et al. 1996 and references therein). Five test morphologies (hemispherical, globose, knobby, encrusting, and columnar) were initially related to environmental factors (Emiliani 1951) but later considered to be a result of both ontogeny and environment. Elliott et al. (1996) noted that test morphology was most affected by sedimentation, wave energy, light intensity, reproduction, competition, and predation, whereas knobby (branching) and globose tests dominated protected, less energetic habitats, and hemispherical and encrusting tests persisted in more energetic conditions.

MacKenzie et al. (1965) showed that *Homotrema* becomes detached with large waves and currents in the nearshore environment which disperses them over short distances from the reef. It was shown that the percentage of *Homotrema* decreased rapidly along a transect from the reefal zone inland toward the coastline. Beaches and more quiescent areas like open lagoons, often contained negligible abundances of *Homotrema*. Two of the three beaches analyzed by MacKenzie et al. (1965) contained small and well-rounded specimens of *Homotrema* compared to the larger more red specimens from the reef zone. Overall, the highest concentration of *Homotrema* occurred in the high-energy reef zone and decreased significantly closer to shore. It was concluded that *Homotrema* is a reliable indicator of sand transport dynamics in the reef system.

In a similar study, Machado and Moraes (2002) compared *Homotrema* from two reefal contexts with differing hydrodynamic settings. They found that well preserved, reddish specimens with angular edges were an indicator of proximity to their initial reefal context, whereas polished (rounded) specimens were evidence of sediment transport and/or energetic hydrological conditions.

4.2 SITE DESCRIPTION

Anegada, a small (54 km²) island part of the British Virgin Islands (BVI), is situated on the easternmost edge of the Caribbean unobstructed by the nearby islands to the north and east, making it ideal for detecting storm and tsunami overwash deposits (Fig. 4.1a). The Puerto Rico Trench, running parallel to Anegada's northern shore, is situated along the western side of a 1,300 km long subduction zone, where the North American plate is subducting under the Caribbean plate at a rate of 2 m per century (Lopez et al. 2006). The close proximity of the island to the trench (125 km away) and the open Atlantic make the island a potential

recorder of local (e.g. 1867) and trans-oceanic tsunamis (e.g. 1755 Lisbon tsunami) as well as hurricanes.

A low-lying island, Anegada reaches maximum heights of 8 m above MSL (Mean Sea Level) on its western half (Atwater et al. 2010). Its northern windward coastline has a fringing reef that extends for 15 km to the southeast, while the leeward side of the island has a smaller system of patch reefs. An open lagoon extending ~1,000 m between the reef and Anegada's northern shore is characterized by a sandy reef flat with water depths ranging from 2–4 m. The ponds, located on the western side of the island, are confined by beach ridges that reach greater heights (2–4 m above MSL) on the windward side than they do on the leeward side. Numerous breaches of the beach ridges were recorded in aerial photographs and are interpreted in Atwater et al. (2010; Fig. 4.1a).

The hypersaline ponds (93–250 ppt; Jarecki and Walkey 2006), bounded by Pleistocene limestone highlands and beach ridges, are present on the western side of Anegada (Fig. 4.1a). Red pond is a small rounded basin that is situated closest to the windward side of the island. Bumber Well is elongate and contains an ephemerally flooded section along its northernmost tip. Point Peter is the smallest basin and is connected to Red Pond in the southeast. All 3 ponds have shallow water depths (~20 cm) and are capped with a microbial-mat peat that is dominated by cyanobacteria, diatoms, and sulphur bacteria in deeper layers (Jarecki and Walkey 2006).

4.3 EVENT HISTORY

Many Caribbean islands are hit annually by hurricanes but have unknown risks for local Puerto Rico Trench and trans-oceanic tsunamis (Atwater et al. 2010). Some known events include the tsunamis of 1690 and 1867 generated on the Puerto Rico Trench, although the precise epicentre remains unknown (Reid and Taber 1920; Stein 1982; McCann et al. 1984; Zahibo et al. 2003). Knowledge of these events is limited, but it was noted that the 1867 event would have reached Anegada from the south and resulted in wave heights ~1.5 m in Tortola, BVI (O'Loughlin and Lander 2003). Wave heights associated with the 1755 Lisbon tsunami were reported to reach 2–6 m at Hispaniola, Dominican Republic which is ~700 km to the west of Anegada, and on Cuba's coastline which is ~1,000 km WNW. However, there are no reports from Anegada as it was sparsely populated at the time (O'Loughlin and Lander 2003; Atwater et al. 2010).

Westward tracking hurricanes from the Atlantic Ocean were documented in the British Virgin Islands in 1713 (Pickering 1983), 1819 (Milla's and Pardue 1968; Pickering 1983) and Hurricane Donna in 1960 (Dunn 1961). Donna was one of the largest (Category 3) hurricanes in the region in the last 50 years and attained wind speeds of 55 m/s. The eye of the storm came within 15 km of Anegada's southern shore, but eyewitness accounts report that the storm surge only caused minor flooding in southern areas (Dunn 1961; Atwater et al. 2010).

4.4 METHODOLOGY

4.4.1 Sample collection

Seven trench sections were recorded in Bumber Well, Red and Point Peter Ponds with gutter cores from sidewalls collected for detailed sampling (Fig. 4.1a, b). Surface samples were collected for comparative purposes from sub-environments: shallow reef-flat ($n = 4$), beach ($n = 3$), storm wrack deposits on beach ($n = 3$), and dune sand on beach ridges ($n = 2$; Fig. 4.1b). Radiocarbon dates from terrestrial organic matter and shells were performed at Woods Hole (NOSAMS; Fig. 4.3). Radiocarbon ages were calibrated using Calib (v 5.01, IntCal04 calibration data; Reimer et al. 2004) for terrestrial material and Marine04 (Hughen et al. 2004) for shells. Only calibrated ages (2 SD) are reported with further details provided in Atwater et al. (2010).

4.4.2 Taphonomic analysis

Approximately 1 cm³ samples ($n = 89$) were sieved ($>63 \mu\text{m}$) and dried for taphonomic analysis (Fig. 4.3). Samples were subdivided with a dry splitter to provide specimen counts of ~ 300 *Homotrema* and were identified and quantified using a binocular dissecting microscope ($\times 60$). The number of *Homotrema* specimens per unit volume (specimens/cm³) was calculated for all samples. Scanning Electron Microscope (SEM) images of diagnostic specimens were taken using a Nikon Neoscope desktop SEM (Fig. 4.2).

Taphonomic preservation (Exceptionally Preserved, Well Preserved, Moderately Preserved or Highly Altered) and test size ($>500 \mu\text{m}$, 250–500 μm , 150–250 μm or $<150 \mu\text{m}$) were recorded (Fig. 4.3; Table 4.1; Table 4.2). Tests that were red, angular, and contained a complete chamber structure were categorized as 'Exceptionally Preserved', while 'Well Preserved' tests were pink, angular, and had hollowed chambers. Rounded specimens that were pink with hollowed chambers

were classified as ‘Moderately Preserved’, and those that were pink to white were classified as ‘Highly Altered’ (Figs. 4.1, 4.3). For summary purposes in Fig. 4.1, the Exceptionally and Well-Preserved categories are grouped into ‘Highly Preserved Specimens’ and specimens $>250\ \mu\text{m}$ are grouped into the ‘Large Specimens’ category.

4.4.3 Particle-size analysis (PSD)

Particle-size analysis was conducted on 6 cores using a Beckman Coulter LS230 laser diffraction particle size analyzer. Gutter cores were sampled at 1 cm resolution except Site 11 which was sampled at 1–2 cm. Samples were sieved ($1,800\ \mu\text{m}$) before introduction into the LS230 as the instrument cannot analyze particle sizes $>2,000\ \mu\text{m}$. Therefore, much of the shell material is not analyzed since many whole specimens are removed through sieving. Samples were homogenized by stirring as a moist paste before analysis and ultrasonically disaggregated with hexametaphosphate (NaPO_3)₆ added to reduce flocculation. The Fraunhofer optical model was used to calculate particle-size distributions (Figs. 4.3, 4.4, 4.5). The particle-sizes were log transformed to the Wentworth Phi Scale, interpolated, and gridded using a triangular irregular network (TIN) algorithm (Sambridge et al. 1995) and plotted as color surface plots using Geosoft Oasis TM software (Donato et al. 2009; van Hengstum et al. 2007; Table 4.3).

4.5 RESULTS

4.5.1 Stratigraphy and particle-size distributions (PSDs)

Four distinct sedimentary units are found in the ponds as documented in Atwater et al. (2010). All trenches had basal limestone (likely Pleistocene; Howard 1970; Horsfield 1975) with overlying units of Shelly Mud, a Shell and Sand Sheet, and a Mud Cap that sharply or gradationally transitioned to a microbial-mat peat (Figs. 4.4, 4.5). This stratigraphic succession was repeatedly found in trenches throughout the ponds (see Atwater et al. 2010), but it did vary somewhat from location to location (e.g. texture and thickness; Fig. 4.4c). Field descriptions of the units were largely defined through the shell concentration and relative proportions of sand and lime mud.

The basal Shelly Mud is a 10–40 cm thick, massive, silty-clay sized, limey mud which was found in all three ponds (mean = $4.6\ \phi$; mode = $4.4\ \phi$; SD = $4.7\ \phi$; Figs. 4.3, 4.4, 4.5). Shell material in this mud was relatively low at 2 clasts/cm³ and

includes *Anomalocardia* spp. and cerithid gastropods, indicating a marine to hypersaline pond environment (Reinhardt et al. 2011). The foraminifera from this unit are predominately miliolids (~70% *Quinqueloculina* spp. and *Triloculina* spp.), which also typify coastal lagoons and marine ponds (Poag 1981; Murray 1991; Brewster-Wingard and Ishman 1999). The Shelly Mud is a well-defined stratigraphic unit in the ponds with characters that are found in all sections except Site 15. The PSD is skewed towards finer particle sizes, and the mode has two distinct peaks with an additional small peak in the fine tail of the PSD (Sites 13, 14, 16, 19). Very little sand is present suggesting isolation from outside reef-flat sources. The boundary between the overlying Shell and Sand Sheet does not always correspond with stratigraphic boundaries identified in the field (e.g. Site 14 could be 10 cm lower).

The Shell and Sand Sheet is heterogeneous in its composition. Although analyzed sites are predominantly from shallow margins of the ponds and contain shells and *Homotrema* sand, the sand was also found in central regions of each pond (Atwater et al. 2010). The unit (2–19 cm thick) is not well defined in the PSD data due to its variable characteristics in the pond and the removal of large shell material for analysis. It was well defined in the field sections due to the high concentration of clasts (shell and lithoclasts) and/or distinctive pink-colored sand (Atwater et al. 2010). Based on PSD data, the unit is (except Site 15) sand-sized but often contains a significant mud matrix (mean = 1.7 ϕ ; mode = 2.0 ϕ ; SD = 2.2 ϕ ; Figs. 4.3, 4.4, 4.5). The high bio-lithoclast concentration (6 clasts/cm³) includes shells, *Anomalocardia* spp. (bivalve) and cerithids (gastropod), with lithoclasts (pebbles). The clasts were derived from scour or winnowing of underlying Shelly Mud (Reinhardt et al. 2011). The fine to medium bioclastic sand contains abundant *Homotrema* and is generally well sorted but also contains a muddy matrix in many areas (Figs. 4.4, 4.5). In locations where small shell fragments and sand (<2 mm) are present, the PSD data corresponds well with the Shell and Sand sheet identified in the field (e.g. Site 14; Fig. 4.4); however, in units that contain larger shell material with muddy matrix, the correspondence was poor (e.g. Site 13; Fig. 4.4). The PSD distributions are not peaked compared to the other units likely reflecting a combination of pond and outside sourced sediment (Fig. 4.4). Trends in the PSD within the Shell and Sand Sheet are not well defined perhaps due to the missing >2 mm clasts in the analysis; however, slight trends are present in the field defined intervals but vary from normal to reverse grading.

The Mud Cap is a lime mud that transitions to a Microbial-Mat Peat, which presently covers the modern pond surface. The unit ranges in thickness from 1–30 cm as defined by field logging of trench sections. Particle sizes are variable in the unit, but typically are mud to sandy mud (mean = 3.8 ϕ ; mode = 3.9 ϕ ; SD = 3.7 ϕ ;

e.g. Site 14 vs. Site 16) and contain interspersed sandy laminae (e.g. Site 19). The PSD of this unit is most similar to the Muddy Shell of the former marine pond; however, the PSDs are not entirely consistent (Figs. 4.4c, 4.5) suggesting that it was deposited under different conditions. Often there is little PSD distinction between what is defined as the Shell and Sand Sheet and the Mud Cap (Fig. 4.3). Atwater et al. (2010) considers the Shell and Sand Sheet and the Mud Cap to be from the same event that may explain the poorly defined boundaries. The difference between the two is largely in the concentration of >2 mm clasts which is lower in the Mud Cap at 2 clasts/cm³ versus 6 clasts/cm³ in the Shell and Sand Sheet (Reinhardt et al. 2011). The clast composition is very similar to the Shelly Mud and the Shell and Sand Sheet (i.e. all *Anomalocardia* and cerithids; Reinhardt et al. 2011).

The transition to the microbial-mat peat is either distinct with a carbonate crust (Atwater et al. 2010), or gradual and hard to define. It ranges in thickness from 1 – 22 cm and contains the largest particle-sizes of any unit (mean = 1.6 ϕ ; mode = 1.6 ϕ ; SD = 1.4 ϕ), a reflection of the presence of evaporate crystals in the mats. However, the PSD analyses also include particles of algal mats so the values are not entirely accurate.

4.5.2 *Homotrema* taphonomy

The modern surface samples collected from various sub-environments have distinctly different characteristics. The highest concentration of *Homotrema* is in the dune sand (3,503 \pm 1,414 specimens/cm³), followed by the reef-flat (2,710 \pm 966), beach (1,060 \pm 950), storm wrack deposit (848 \pm 50) and hypersaline pond (354 \pm 393; Fig. 4.1b). The most altered *Homotrema* are found in the dune sand with only 24 \pm 3% Highly Preserved specimens which are small (21 \pm 15% in large size fraction). The largest and the best preserved specimens are found in the storm wrack deposits (75 \pm 17%; 66 \pm 10%), the beach (63 \pm 44%; 37 \pm 24%) and the reef-flat (32 \pm 10%; 34 \pm 20%).

In all the analyzed pond sections, there is a prominent peak in *Homotrema* concentration (specimens/cm³) that generally coincides with the Shell and Sand Sheet from the field observations. The exception was in Sites 13 and 16 where there is a peak in the Mud Cap (Figs. 4.1b, 4.3). Atwater et al. (2010) associates the Mud Cap with the overwash event itself, which may explain the *Homotrema* peak in the mud. The specimens associated with the *Homotrema* peak are predominantly large (i.e. >250 μ m), Highly Preserved (i.e. exceptionally to well preserved) with red to dark-pink color and many intact chambers (Figs. 4.1b, 4.2, 4.3). They closely match the modern beach, reef-flat, and storm wrack deposits and therefore are indicative of

overwash. Above and below this peak, large and Highly Preserved *Homotrema* specimens are absent at most sites (e.g. 5, 11, 13, 16 and 19). The lack of Highly Preserved specimens in the Shelly Mud indicates it is not a source for the *Homotrema* in the Shell and Sand Sheet like it is for the >2 mm clasts (Reinhardt et al. 2011). Smaller (<150–250 μm), moderately to highly altered specimens are found (10–90%) in low concentrations in both the underlying Shelly Mud and also the overlying Mud Cap, but not in all instances (e.g. Site 16 vs. Site 14; Fig. 4.3). These specimens are likely aeolian sand inputs from surrounding dunes as the taphonomic condition is a close match.

The concentration of *Homotrema* tests (specimens/cm³) in the Shell and Sand Sheet decreases markedly in the pond transects indicating a southerly trending overwash direction (Fig. 4.1b). The western transect through Red and Point Peter Ponds shows a southward decrease from $2,714 \pm 59$ specimens/cm³ at Site 15, to $1,182 \pm 138$, 284 ± 51 and 264 ± 34 at Sites 19, 13 and 11, respectively. This southward decline likely represents a distance to source relationship with production of *Homotrema* occurring on the northern fringing reef, while the smaller patch reefs to the south would not produce as many individuals. It therefore does not preclude an additional inundation from the south (Reinhardt et al. 2011). Trends in other taphonomic characters are less prominent with proportions of large and Highly Preserved specimens showing taphonomic uniformity across the sheet deposit (Fig. 4.1b).

4.6 DISCUSSION

Based on the stratigraphic data presented in Atwater et al. (2010), the Shell and Sand Sheet formed during an overwash event between A.D. 1650–1800, although the exact cause (tsunami vs. hurricane) is uncertain. The sheet-like geometry of the overwash deposit can be indicative of a tsunami (e.g. Morton et al. 2007) and the *Homotrema* data supports an outside provenance for the sand, which would strengthen this interpretation, but the lack of large (>2 mm) reef-flat clasts needs to be considered (Reinhardt et al. 2011).

The Shell and Sand Sheet has distinctive *Homotrema* taphonomy and closely matches outside sources (beach, storm wrack, and reef-flat). The storm wrack is an important deposit as its taphonomic signature is what might be expected from sorting and transport of reef-flat sediment during an overwash into the ponds. It contains high concentrations of Highly Preserved specimens, which is very similar to the Shell and Sand Sheet with abundant, large and Highly Preserved *Homotrema*. The decreasing concentration of *Homotrema* in the transects also indicates overwash

from the north. However, the Shell and Sand Sheet is missing the coarse (>2 mm) reef-flat shell material that was a dominant component in the storm wrack deposit (Reinhardt et al. 2011). The lack of coarse reef-flat clasts suggests that the overwash sand originated from a combination of previously sorted deposits (i.e. beach) and/or reef-flat material that was sorted during the event itself.

Hydrodynamic modelling of possible tsunami scenarios and hurricanes (Category 5) indicates that only Lisbon (1775—Mw 9.0) or a Puerto Rico Trench (Mw 8.7, Mw 8.0) tsunami could cause the necessary inundation with a 2.25 m beach ridge elevation (Wei et al. 2010). The models show that hurricane waves tend to dissipate on the fringing reef and do not produce the necessary inundation. Buckley et al. (2011) model transport of boulders associated with the Shell and Sand Sheet and found that only a near-field Mw 8.0 Puerto Rico Trench outer-rise tsunami could move the boulders. The modeled tsunami inundations barely overtop the 2.25 m high beach ridges and if correct, may explain the lack of large reef-flat clasts in the Shell and Sand Sheet. A probable scenario involves entrainment of reef-flat and beach sediments with the coarse clasts left behind due to reducing flow competence as the inundation overtops the beach ridges. Plunge pools on the inner edge of the ponds may have also been a source of *Homotrema* as the scour may have eroded older beach deposits (Atwater et al. 2010).

Sandy overwash is a characteristic feature of hurricane deposits, but the sand bodies tend to be lobate in shape rather than sheet-like (e.g. Morton et al. 2007). Other studies of sandy overwash from Caribbean hurricanes only report sand and do not mention coarser reef clasts or *Homotrema* and therefore may not have been significant in those contexts (e.g. Donnelly 2005). However, this lack of comparative data makes it difficult to assess the results from Anegada. Anegada's ponds, with their close proximity to reef source regions and their low-lying topography, make it difficult to distinguish hurricane versus tsunami deposits. Here, we present plausible evidence that seems to support a tsunami interpretation, but further research is needed to constrain *Homotrema* taphonomic processes. Further analysis of other known hurricane and tsunami deposits is also required to better constrain differences in their signatures (e.g. MacKenzie et al. 1965; Machado and Moraes 2002).

4.7 CONCLUSIONS

Homotrema taphonomy shows promise as an overwash indicator for Caribbean reef environments. *Homotrema* are small (sand-sized), readily transported and have high productivities, so are abundant in the sediment record

(100–1,000/cm³). They have a defined provenance in the reef with known life-habits (attached) and quickly inherit taphonomic characteristics after death (e.g. bleaching of color). They are also visible in field observations due to their distinctive pink color and can be efficiently analyzed for high-resolution studies.

Homotrema taphonomy indicated overwash into Anegada's ponds that occurred from A.D. 1650–1800; however, it alone could not determine whether it formed from a tsunami or hurricane. Additional evidence from hydrodynamic modelling of the overwash event and boulder transport in the ponds suggests that it was from a tsunami rather than a hurricane. Conclusions from the *Homotrema* taphonomy were limited by the lack of comparative data from known hurricane and tsunami deposits. However, with future research, it may allow us to better understand the hydrodynamics of these events.

ACKNOWLEDGEMENTS

The government of the British Virgin Islands permitted access to Anegada's salt ponds, use of airphotos, and guidance from its specialists in disaster management, surveying, and natural science. Among them, we especially thank Cynthia Rolli, Rondell Smith, Shannon Gore, and Dylan Penn. Lianna Jarecki shared her comprehensive knowledge of Anegada's salt ponds, Alejandra Rodriguez assisted with field work and Alyson Brown helped with laboratory work. Insightful comments from Brian Atwater and two anonymous reviewers greatly improved this manuscript. The work was supported in part by the Nuclear Regulatory Commission under its project N6480, a tsunami-hazard assessment for the eastern United States and an NSERC Discovery grant to ER.

REFERENCES

- Atwater, B.F., ten Brink, U.S., Buckley, M., Halley, R.S., Jaffe, B.E., Lopez-Venegas, A.M., Reinhardt, E.G., Tuttle, M.P., Watt, S., Wei, Y., 2010. Geomorphic and stratigraphic evidence for an unusual tsunami or storm a few centuries ago at Anegada, British Virgin Islands. *Natural Hazards*, doi 10.1007/s11069-010-9622-6
- Brewster-Wingard, G.L., Ishman, S.E., 1999. Historical Trends in Salinity and Substrate in Central Florida Bay: A Paleoecological Reconstruction Using Modern Analogue Data. *Estuaries*, 22: 369-383
- Buckley, M., Wei, Y., Jaffe, J., Watt, S., 2011. Inverse modeling of velocities and inferred cause of overwash that emplaced inland fields of boulders at Anegada, British Virgin Islands. *Natural Hazards*, doi 10.1007/s11069-011-

9725-8

- Donato, S.V., Reinhardt, E.G., Boyce, J.I., Pilarczyk, J.E., Jupp, B.P., 2009. Particle-size distribution of inferred tsunami deposits in Sur Lagoon, Sultanate of Oman. *Marine Geology*, 257: 54-64
- Donnelly, J., 2005. Evidence of past intense tropical cyclones from backbarrier salt pond sediments: a case study from Isla de Culebrita, Puerto Rico, USA. *Journal of Coastal Research*, 42: 201-210
- Dunn, G.E., 1961. The hurricane season of 1960. *Monthly Weather Review*, 89: 99-108
- Elliott, J.M., Logan, A., Thomas, M.L.H., 1996. Morphotypes of the foraminiferan *Homotrema rubrum* (Lamarck): Distribution and relative abundance on reefs in Bermuda. *Bulletin of Marine Science*, 58: 261-276
- Emiliani, C., 1951. On the species *Homotrema rubrum* (Lamarck). *Cushman Foundation for Foraminiferal Research Special Contribution*, 2: 143-147
- Hawkes, A.D., Bird, M., Cowie, S., Grundy-Warr, C., Horton, B.P., Tan Shau Hwai, A., Law, L., Macgregor, C., Nott, J., Eong Ong, J., Rigg, J., Robinson, R., Tan-Mullins, M., Tiong, T., Yasin, Z., Wan Aik, L., 2007. Sediments deposited by the 2004 Indian Ocean tsunami along the Malaysia-Thailand Peninsula. *Marine Geology*, 242: 169-190
- Hippensteel, S.P., Martin, R.E., 1999. Foraminifera as an indicator of overwash deposits, barrier island sediment supply, and barrier island evolution, Folly Island, South Carolina. *Palaeogeography, Palaeoclimatology, Palaeoecology*, 149: 115-125
- Horsfield, W.T., 1975. Quaternary vertical movements in the Greater Antilles. *Geological Society of America Bulletin*, 86: 933-938
- Howard, J., 1970. Reconnaissance geology of Anegada Island. *Caribbean Research Institute, St. Thomas*, pp 18
- Hughen, K.A., Baillie, M.G.L., Bard, E., Beck, J.W., Bertrand, C.J.H., Blackwell, P.G., Buck, C.E., Burr, G.S., Cutler, K.B., Damon, P.E., Edwards, R.L., Fairbanks, R.G., Friedrich, M., Guilderson, T.P., Kromer, B., McCormac, G., Manning, S., Ramsey, C.B., Reimer, P.J., Reimer, R.W., Remmele, S., Southon, J.R., Stuiver, M., Talamo, S., Taylor, F.W., van der Plicht, J., Weyhenmeyer, C.E., 2004. Marine04 marine radiocarbon age calibration, 0-26 cal kyr BP; IntCal04; calibration. *Radiocarbon*, 46: 1059-1086
- Jarecki, L., Walkey, M., 2006. Variable hydrology and salinity of salt ponds in the British Virgin Islands. *Saline Systems* 2, doi 10.1186/1746-1448-2-2
- Jones, B., Hunter, I.G., 1992. Very Large Boulders on the Coast of Grand Cayman: The Effects of Giant Waves on Rocky Coastlines. *Journal of Coastal Research*, 8: 763-774
- Kortekaas, S., Dawson, A.G., 2007. Distinguishing tsunami and storm deposits: an example from Martinhal, SW Portugal. *Sedimentary Geology*, 200: 208-221

- Lopez, A.M., Stein, S., Dixon, T., Sella, G., Calais, E., Jansma, P., Weber, J., LaFemina, P., 2006. Is there a northern Lesser Antilles forearc block? *Geophysical Research Letters*, 33 doi:10.1029/2005GL025293
- Machado, A.J., Moraes, S.S., 2002. A note on the occurrence of the encrusting foraminifera *Homotrema rubrum* in reef sediments from two distinctive hydrodynamic settings. *Annals of the Brazilian Academy of Science*, 74: 727-735
- MacKenzie, F.T., Kulm, L.D., Cooley, R.L., Barnhart, J.T., 1965. *Homotrema rubrum* (Lamarck), a sediment transport indicator. *Journal of Sedimentary Research*, 35: 265-272
- Mamo, B., Strotz, L., Dominey-Howes, D., 2009. Tsunami sediments and their foraminiferal assemblages. *Earth Science Reviews*, 96: 263-278
- McCann, W., Feldman, L., McCann, M., 1984. Catalogue of felt earthquakes for Puerto Rico and neighboring islands 1492-1899 with additional information for some 20th century earthquakes. Unpublished material provided as a pdf by the lead author. pp 122
- Millás, J.C., Pardue, L., 1968. Hurricanes of the Caribbean and adjacent regions, 1492 – 1800. *Academy of the Arts and Sciences of the Americas*, Miami, Fla.
- Morton, R.A., Gelfenbaum, G., Jaffe, B.E., 2007. Physical criteria for distinguishing sandy tsunami and storm deposits using modern examples. *Sedimentary Geology*, 200: 184-207
- Murray, J.W., 1991. *Ecology and Palaeoecology of Benthic Foraminifera*. Longman, Harlow pp. 397
- O'Loughlin, K.F., Lander, J.F., 2003. Caribbean tsunamis: A 500-year history from 1498 – 1998. *Kluwer Academic*, Dordrecht, Boston, pp 263
- Park, L.E., Siewers, F.D., Metzger, T., Sipahioglu, S., 2009. After the hurricane hits: Recovery and response to large storm events in a saline lake, San Salvador Island, Bahamas. *Quaternary International*, 195: 98-105
- Pickering, V.W., 1983. Early history of the British Virgin Islands: from Columbus to emancipation. *Falcon Publications International*, pp 248
- Poag, C.W., 1981. *Ecologic Atlas of Benthic Foraminifera of the Gulf of Mexico*. Marine Science International, Woods Hole, Massachusetts
- Reid, H.F., Taber, S., 1920. The Virgin Islands earthquakes of 1867-1868. *Bulletin of the Seismological Society of America*, 10: 9-20
- Reimer, P.J., Baille, M.G.L., Bard, E., Bayliss, A., Beck, J.W., Bertrand, C.J.H., Blackwell, P.G., Buck, C.E., Burr, G.S., Cutler, K.B., Damon, P.E., Edwards, R.L., Fairbanks, R.G., Friedrich, M., Guilderson, T.P., Hogg, A.G., Hughen, K.A., Kromer, B., McCormac, G., Manning, S., Ramsey, C.B., Reimer, R.W., Remmele, S., Southon, J.R., Stuiver, M., Talamo, S., Taylor, F.W., van der Plicht, J., Weyhenmeyer, C.E., 2004. IntCal04 terrestrial

- radiocarbon age calibration, 0-26 cal kyr BP; IntCal04; calibration.
Radiocarbon, 46: 1029-1058
- Reinhardt, E.G., Pilarczyk, J.E., Brown, A., 2011. Probable tsunami origin for a shell and sand sheet from marine ponds on Anegada, British Virgin Islands. *Natural Hazards*, doi 10.1007/s11069-011-9730-y
- Sambridge, M., Braun, J., McQueen, H., 1995. Geophysical parametrization and interpolation of irregular data using natural neighbors. *Geophysical Journal International*, 122: 837-857
- Scott, D.B., Collins, E.S., Gayes, P.T., Wright, E., 2003. Records of prehistoric hurricanes on the South Carolina coast based on micropaleontological and sedimentological evidence, with comparison to other Atlantic Coast records. *Geological Society of America Bulletin*, 115: 1027-1039
- Stein, S., 1982. Subduction seismicity and tectonics in the Lesser Antilles Arc. *Journal of Geophysical Research*, 87: 8642-8664
- van Hengstum, P.J., Reinhardt, E.G., Boyce, J.I., Clark, C., 2007. Changing sedimentation patterns due to historical land-use change in Frenchman's Bay, Pickering, Canada: evidence from high-resolution textural analysis. *Journal of Paleolimnology*, 37: 603-618
- Wei, Y., ten Brink, U.S., Atwater, B.F., 2010. Modeling of tsunamis and hurricanes as causes of the catastrophic overwash of Anegada, British Virgin Islands, between 1650 and 1800: Abstract OS42B-03. Presented at 2010 Fall meeting, American Geophysical Union, San Francisco, California, 13–17 December 2010
- Zahibo, N., Pelinovsky, E., Yalciner, A.C., Kurkin, A., Koselkov, A., Zaitsev, A., 2003. The 1867 Virgin Island Tsunami. *Natural Hazards and Earth System Sciences*, 3: 367-376

CHAPTER 4 FIGURES

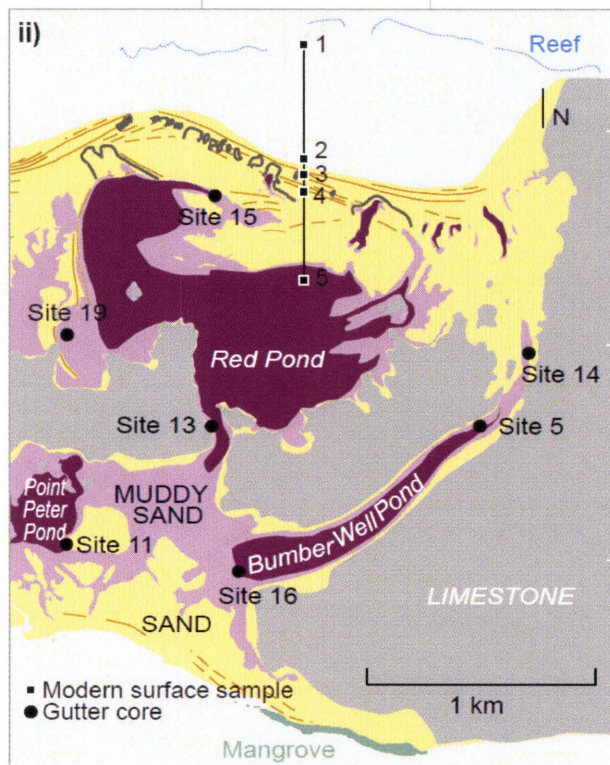
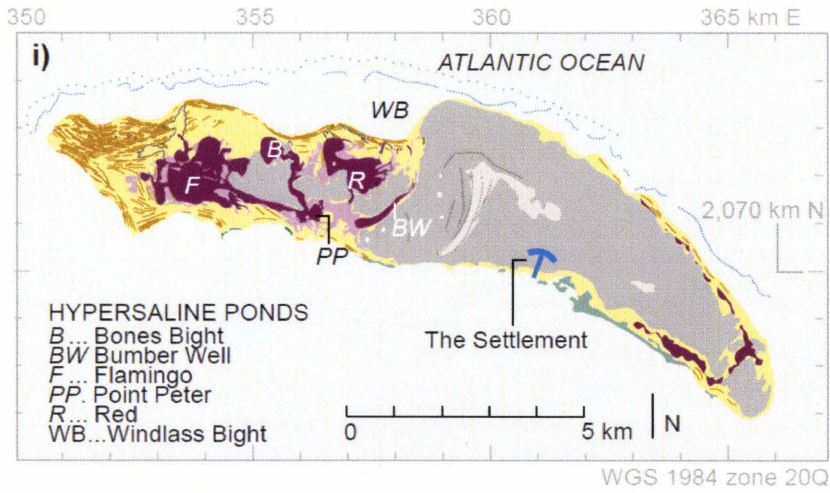


Figure 4.1a: **a)** Map of Anegada showing major geomorphic features (modified from Atwater et al. 2010). **b)** Detailed map of study area showing site locations of trenches (sites 5, 11, 13, 14, 15, 16, 19) and surface samples (1–5) depicted in (c).

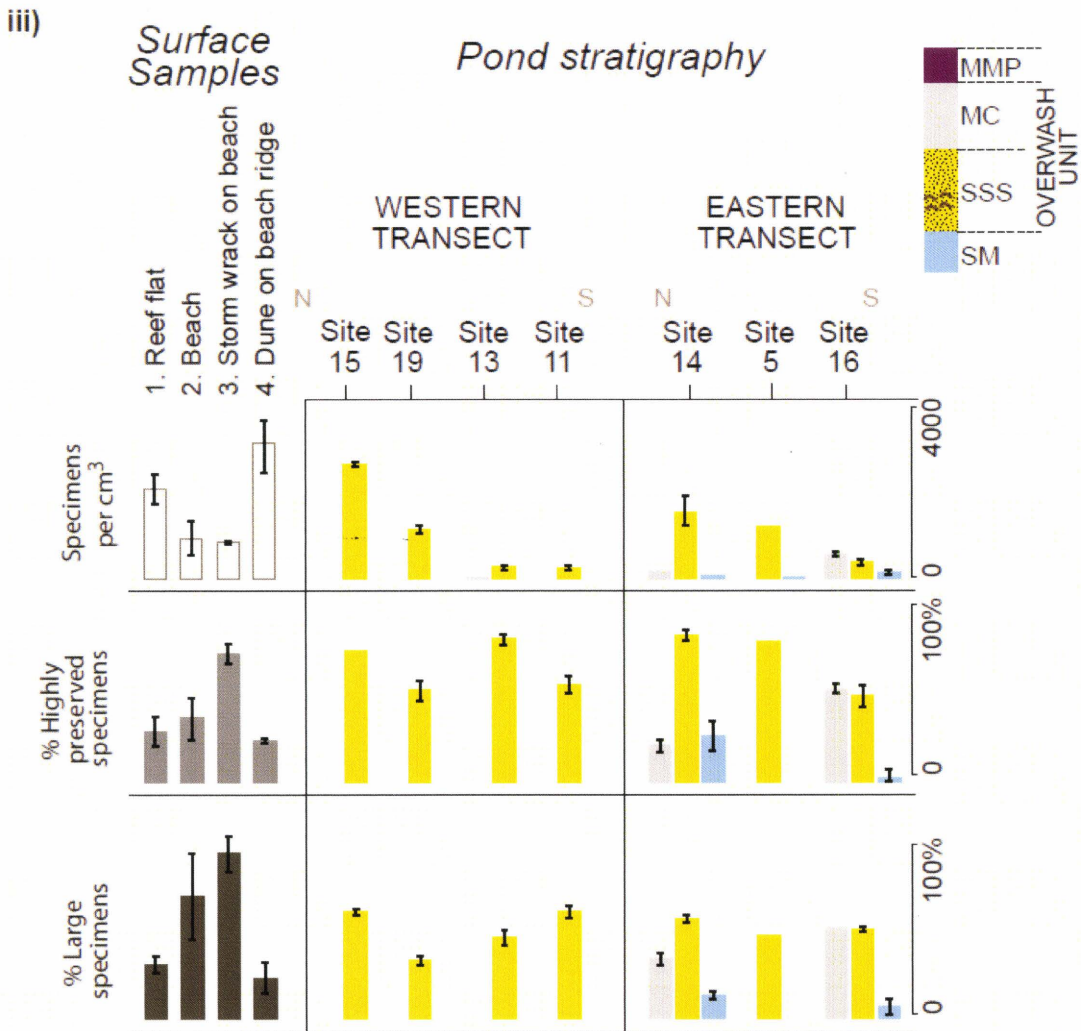


Figure 4.1b: **c)** *Homotrema* taphonomic data from surface samples and major stratigraphic units in the ponds. Two north–south transects (western and eastern) are compared. The western transect runs through Red and Point Peter Ponds, while the eastern transect encompasses Bumber Well Pond. A generalized stratigraphic section based on all trench sections is indicated at the top right. *MMP* Microbial-Mat Peat, *MC* Mud Cap, *SSS* Shell and Sand Sheet, *SM* Shelly Mud.

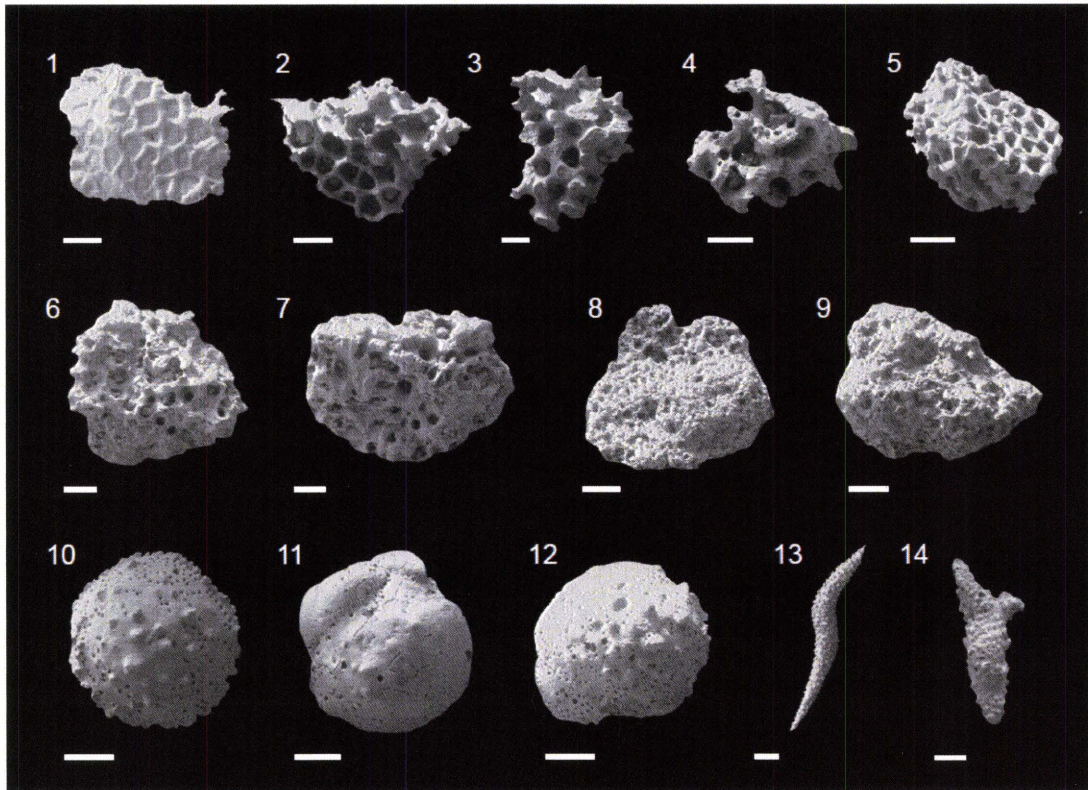
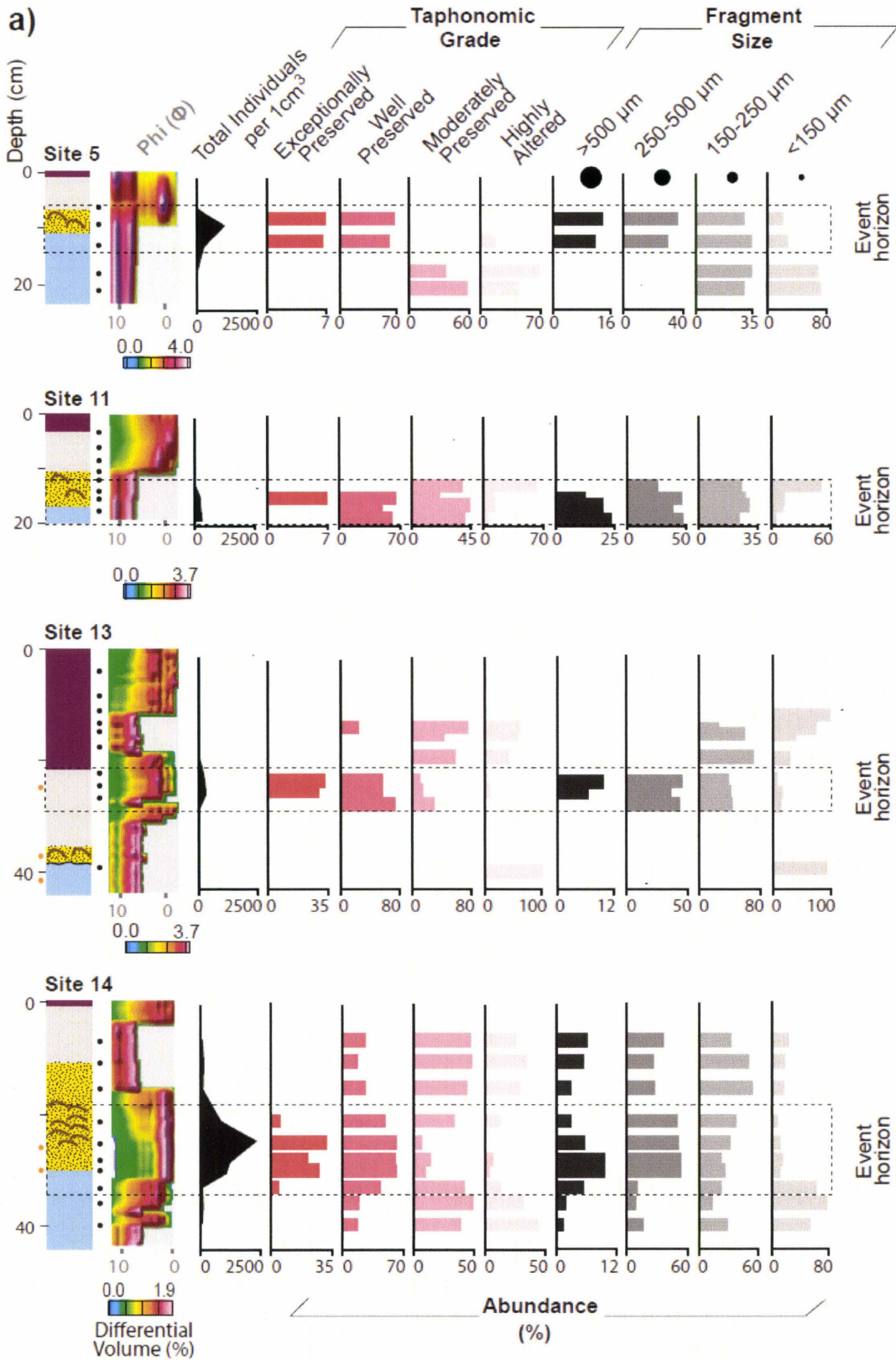


Figure 4.2: Taphonomic condition of *Homotrema* specimens. (1) Exceptionally preserved (red, angular, well preserved chambers); (2–5) Well preserved (pink, angular, hollowed chambers); (6–8) Moderately preserved (pink, rounded, hollowed chambers); (9) Highly altered (whitish, rounded, hollowed chambers); (10–12) *Homotrema* encrusted on *Ammonia beccari*, (10) Exceptionally preserved, (11) Well preserved (12) Moderately preserved; (13) Unaltered holothuridian spicule; (14) *Homotrema* encrusted holothuridian. Scale bars represent 100 μm .

Figure 4.3: **a)** Detailed lithological, PSD, and *Homotrema* taphonomic data for core sites 5, 11, 13, 14, 15, 16, c and 19. Event horizon designation is based on *Homotrema* concentration peak. Circles indicate sampling intervals (black) and radiocarbon dating intervals (orange; see Atwater et al. 2010 for details on radiocarbon dates). **b)** Trench site locations for gutter cores. **c)** Generalized stratigraphic section based on all trench sections. (see following page)



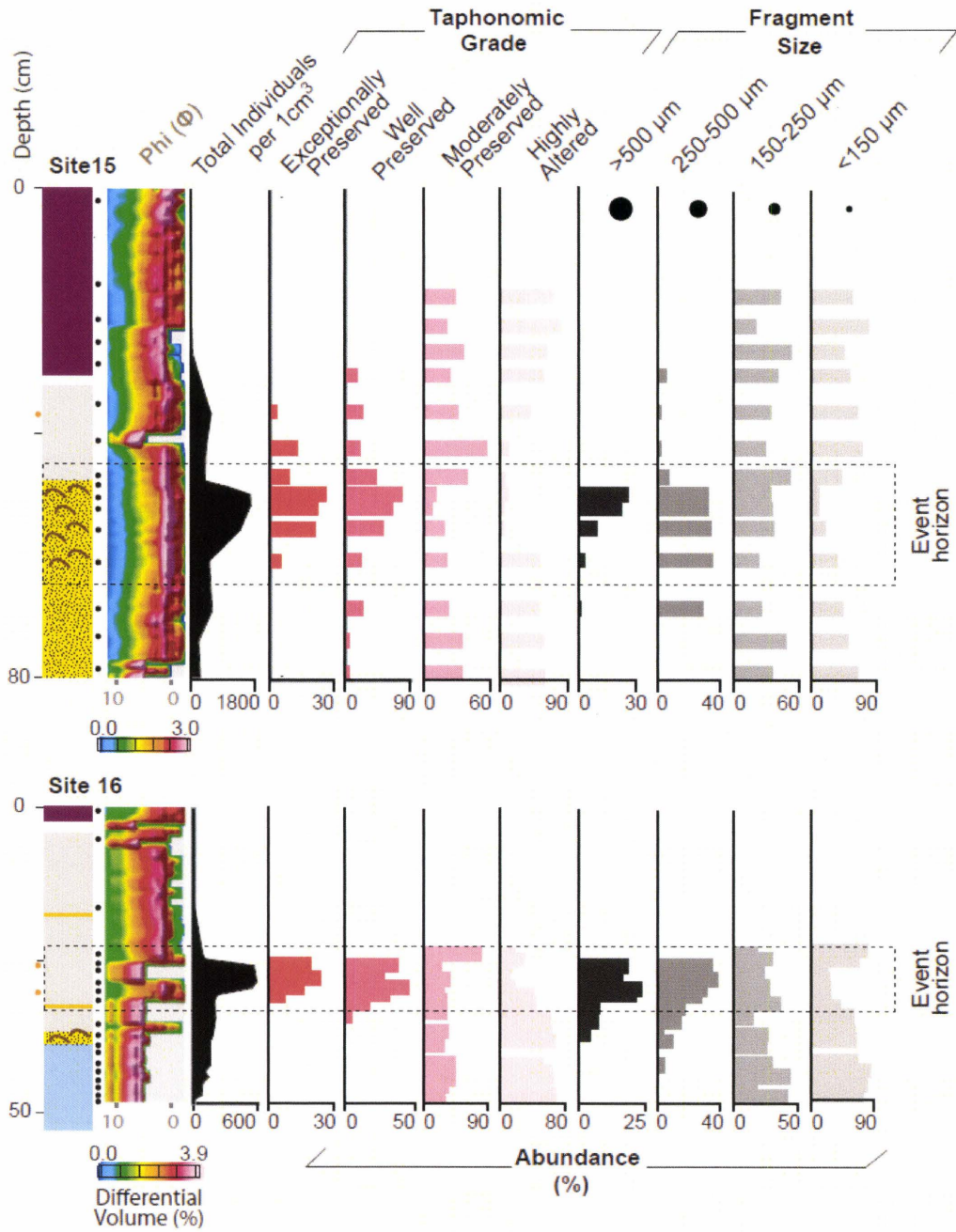


Figure 4.3: continued

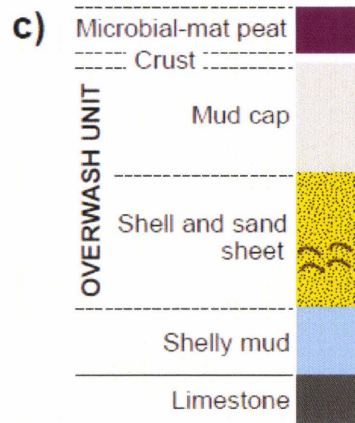
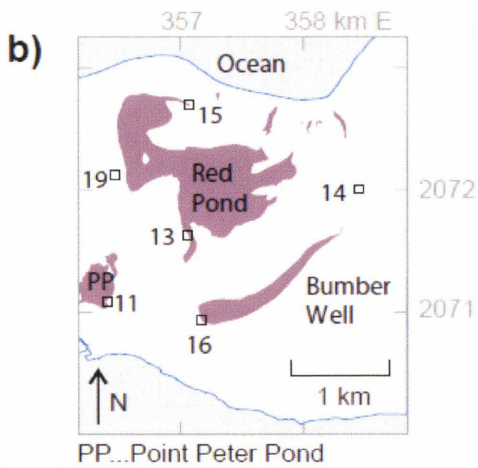
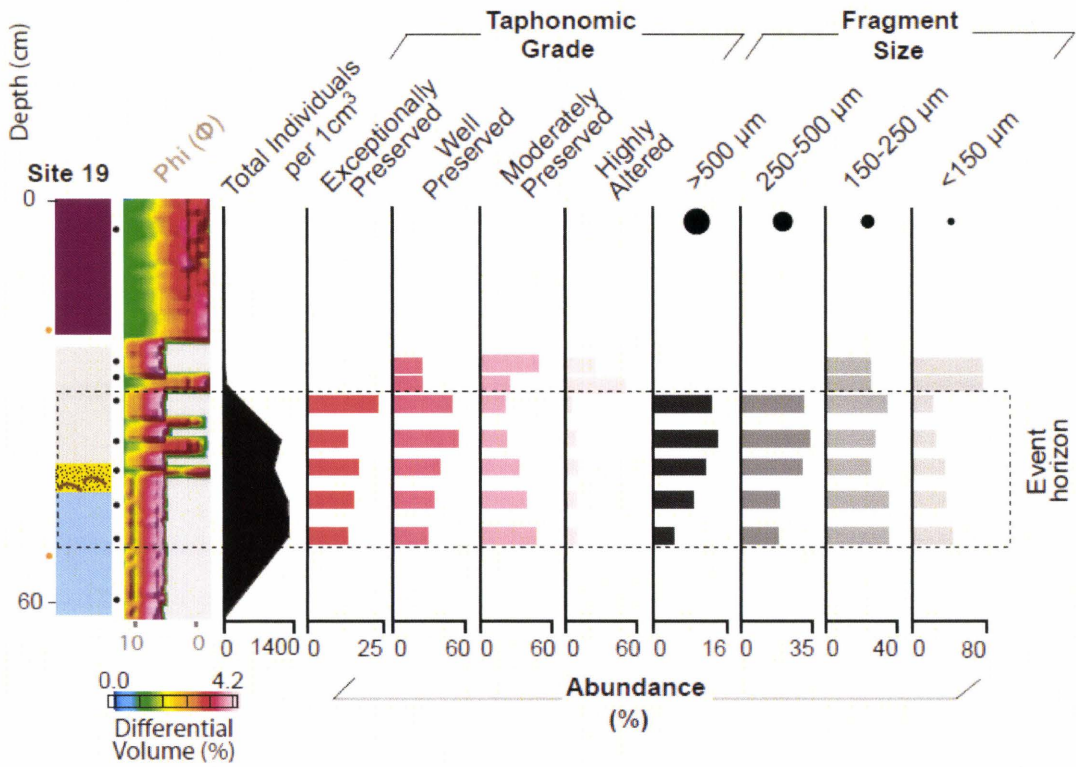


Figure 4.3: continued

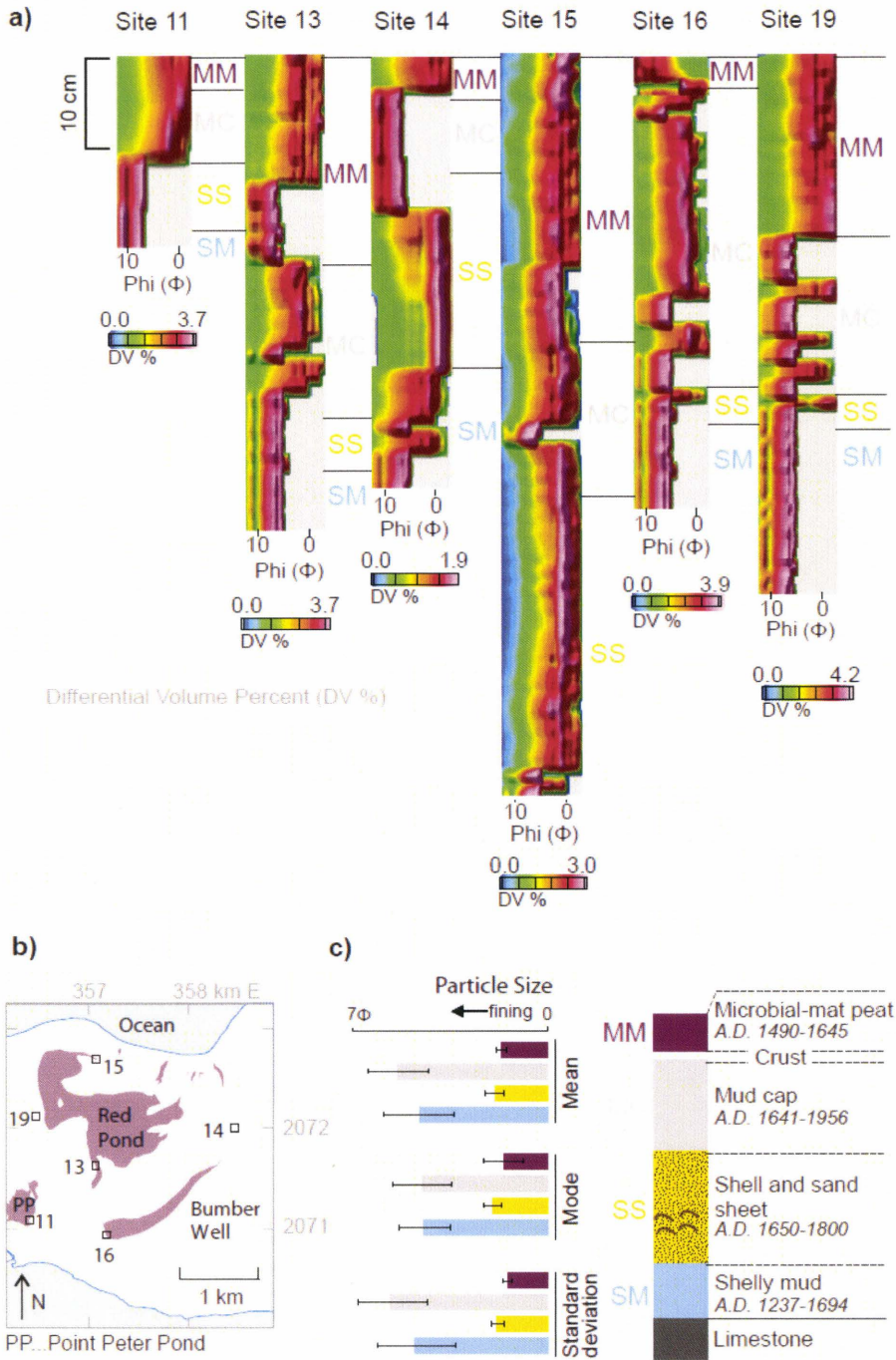


Figure 4.4: **a)** Core PSD plots for pond sections (gutter cores). Facies designations are based on field observations (see Fig. 4.3). **b)** Location of core sites (adapted from Atwater et al. 2010). **c)** Average PSD statistical data for facies.

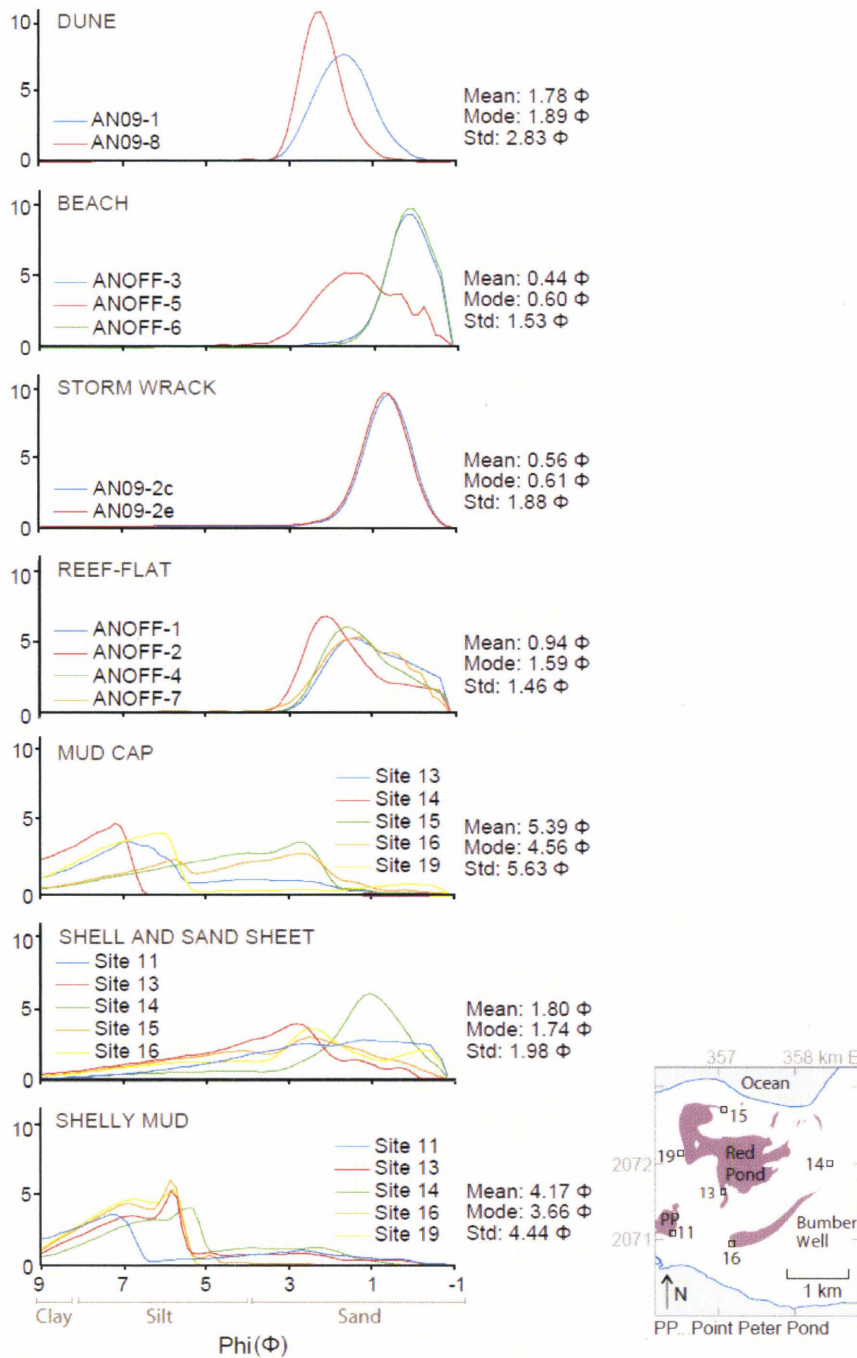


Figure 4.5: PSD plots of modern environments for comparison with the Mud Cap, Shell and Sand Sheet and Shelly Mud from pond stratigraphy. Statistical data (mean, mode, and SD) of each environment (modern samples) and unit (core samples) is indicated.

CHAPTER 4 TABLES

Core ID	Sample Interval	Total Spec.	Spec. per 1 cc	Taphonomic condition				Fragment size			
				Excep. Pres.	Well Pres.	Mod. Pres.	Highly Altered	>500 um	250-500 um	150-250 um	<150 um
AN09-5	6-7 cm	0	0	-	-	-	-	-	-	-	-
AN09-5	10-11 cm	153	1224	0.085	0.732	0.105	0.078	0.137	0.353	0.288	0.222
AN09-5	15-16 cm	45	360	0.067	0.600	-	0.177	0.111	0.288	0.333	0.266
AN09-5	20-21 cm	6	48	-	-	0.333	0.666	-	-	0.333	0.666
AN09-5	24-25 cm	7	56	-	-	0.571	0.428	-	-	0.288	0.714
AN09-13	3-4 cm	0	0	-	-	-	-	-	-	-	-
AN09-13	7-8 cm	0	0	-	-	-	-	-	-	-	-
AN09-13	10-11 cm	0	0	-	-	-	-	-	-	-	1.000
AN09-13	12-13 cm	4	32	-	0.250	0.750	-	-	-	0.250	0.750
AN09-13	13-14 cm	5	40	-	-	0.400	0.600	-	-	0.600	0.400
AN09-13	17-18 cm	7	56	-	-	0.571	0.429	-	-	0.714	0.286
AN09-13	21-22 cm	31	248	0.323	0.548	0.097	0.032	0.097	0.452	0.387	0.065
AN09-13	23-24 cm	40	320	0.275	0.525	0.125	0.075	0.065	0.355	0.419	0.161
AN09-13	25-26 cm	7	56	-	0.714	0.286	-	-	0.429	0.429	0.143
AN09-13	37-38 cm	1	8	-	-	-	1.000	-	-	-	1.000
AN09-14	6-7 cm	38	152	-	0.263	0.474	0.263	0.061	0.359	0.328	0.252
AN09-14	10-11 cm	46	184	-	0.174	0.478	0.348	0.053	0.255	0.500	0.191
AN09-14	15-16 cm	41	164	-	0.268	0.439	0.293	0.030	0.274	0.536	0.161
AN09-14	21-22 cm	217	868	0.046	0.493	0.341	0.120	0.030	0.499	0.382	0.089
AN09-14	25-26 cm	585	2340	0.318	0.614	0.065	0.003	0.057	0.507	0.316	0.120
AN09-14	28-29 cm	311	1244	0.196	0.601	0.135	0.068	0.098	0.526	0.226	0.150
AN09-14	30-31 cm	272	1088	0.268	0.618	0.092	0.022	0.096	0.528	0.254	0.122
AN09-14	33-34 cm	26	104	0.038	0.423	0.423	0.115	0.054	0.100	0.223	0.623
AN09-14	36-37 cm	22	88	-	0.182	0.500	0.318	0.018	0.081	0.135	0.766
AN09-14	40-41 cm	18	72	-	0.167	0.389	0.444	0.014	0.164	0.288	0.534
AN09-15	3-4 cm	-	-	-	-	-	-	-	-	-	-
AN09-15	17-18 cm	7	28	-	-	0.286	0.714	-	-	0.429	0.571
AN09-15	22-23 cm	5	20	-	-	0.200	0.800	-	-	0.200	0.800
AN09-15	26-27 cm	11	44	-	-	0.364	0.636	-	-	0.545	0.455
AN09-15	30-31 cm	51	204	-	0.176	0.235	0.588	-	0.059	0.412	0.529
AN09-15	36-37 cm	141	564	0.035	0.248	0.319	0.397	-	0.007	0.348	0.645
AN09-15	42-43 cm	106	424	0.132	0.208	0.575	0.085	-	0.009	0.292	0.698
AN09-15	47-48 cm	98	392	0.092	0.429	0.398	0.082	-	0.082	0.520	0.398
AN09-15	48-49 cm	249	996	0.269	0.779	0.084	0.108	0.269	0.313	0.333	0.084
AN09-15	49-50 cm	423	1692	0.208	0.617	0.109	0.066	0.213	0.329	0.350	0.109
AN09-15	51-52 cm	427	1708	0.220	0.649	0.070	0.061	0.225	0.321	0.354	0.101
AN09-15	55-56 cm	347	1388	0.213	0.539	0.196	0.052	0.098	0.337	0.372	0.193
AN09-15	60-61 cm	131	524	0.053	0.221	0.214	0.511	0.038	0.351	0.237	0.374
AN09-15	68-69 cm	150	600	-	0.253	0.227	0.520	0.007	0.287	0.260	0.447
AN09-15	73-74 cm	54	216	-	0.074	0.352	0.574	-	-	0.481	0.519
AN09-15	79-80 cm	66	264	-	0.061	0.348	0.591	-	-	0.348	0.652
AN09-16	0-1 cm	0	0	-	-	-	-	-	-	-	-
AN09-16	8-9 cm	0	0	-	-	-	-	-	-	-	-
AN09-16	15-16 cm	0	0	-	-	-	-	-	-	-	-
AN09-16	24-25 cm	11	88	-	-	0.818	0.182	-	-	0.182	0.818
AN09-16	25-26 cm	13	104	-	-	0.692	0.308	-	-	0.308	0.692

Table 4.1: *Homotrema* taphonomic data for cores

Table 4.1 continued...

Core ID	Sample Interval	Total Spec.	Spec. per 1 cc	Taphonomic condition				Fragment size			
				Excep. Pres.	Well Pres.	Mod. Pres.	Highly Altered	>500 µm	250-500 µm	150-250 µm	<150 µm
AN09-16	26-27 cm	71	568	0.197	0.380	0.268	0.155	0.183	0.352	0.239	0.225
AN09-16	29-30 cm	74	592	0.243	0.270	0.365	0.122	0.162	0.378	0.230	0.230
AN09-16	30-31 cm	68	544	0.162	0.456	0.309	0.074	0.235	0.324	0.206	0.235
AN09-16	31-32 cm	28	224	0.071	0.321	0.179	0.429	0.214	0.286	0.214	0.286
AN09-16	32-33 cm	25	200	-	0.200	0.360	0.440	0.080	0.160	0.360	0.400
AN09-16	35-36 cm	26	208	-	0.038	0.346	0.615	0.077	0.154	0.154	0.615
AN09-16	38-39 cm	23	184	-	-	0.348	0.652	0.043	0.043	0.261	0.652
AN09-16	39-40 cm	20	160	-	-	0.300	0.700	-	0.100	0.250	0.650
AN09-16	43-44 cm	20	160	-	-	0.450	0.550	-	0.050	0.300	0.650
AN09-16	44-45 cm	14	112	-	-	0.357	0.643	-	-	0.143	0.857
AN09-16	45-46 cm	18	144	-	-	0.333	0.667	-	-	0.444	0.556
AN09-16	46-47 cm	11	88	-	-	0.364	0.636	-	-	0.182	0.818
AN09-16	48-49 cm	10	80	-	-	0.300	0.700	-	-	0.300	0.700
AN09-16	49-50 cm	0	0	-	-	-	-	-	-	-	-
AN09-19	7-8 cm	0	0	-	-	-	-	-	-	-	-
AN09-19	22-23 cm	4	32	-	0.250	0.500	0.250	-	-	0.250	0.750
AN09-19	25-26 cm	8	64	-	0.250	0.250	0.500	-	-	0.250	0.750
AN09-19	28-29 cm	56	448	0.232	0.500	0.214	0.054	0.125	0.304	0.339	0.232
AN09-19	33-34 cm	144	1152	0.132	0.549	0.222	0.097	0.139	0.333	0.271	0.257
AN09-19	37-38 cm	125	1000	0.168	0.392	0.328	0.112	0.112	0.296	0.248	0.344
AN09-19	42-43 cm	160	1280	0.150	0.344	0.406	0.100	0.088	0.194	0.356	0.363
AN09-19	47-48 cm	162	1296	0.130	0.302	0.475	0.093	0.043	0.179	0.352	0.426
AN09-19	59-60 cm	0	0	-	-	-	-	-	-	-	-

Sample No.	Specimens per 1 cc	Taphonomic condition				Fragmentsize				Environment
		Exceptionally preserved	Well preserved	Moderately preserved	Highly altered	>500 μm	250-500 μm	150-250 μm	<150 μm	
AN09-1	2503	0.005	0.214	0.388	0.393	0.000	0.316	0.514	0.169	Dune on beach ridge
ANOFF-8	4502	0.015	0.249	0.419	0.317	0.000	0.102	0.706	0.191	Dune on beach ridge
ANOFF-3	308	0.091	0.558	0.208	0.143	0.692	0.211	0.068	0.029	Beach
ANOFF-5	2128	0.092	0.122	0.697	0.088	0.023	0.100	0.451	0.426	Beach
ANOFF-6	744	0.054	0.204	0.462	0.280	0.280	0.589	0.125	0.670	Beach
AN09-2a	809	0.125	0.434	0.345	0.094	0.152	0.662	0.126	0.059	Storm wrack
AN09-2c	904	0.248	0.434	0.221	0.097	0.190	0.696	0.106	0.008	Storm wrack
AN09-2e	832	0.135	0.615	0.173	0.077	0.197	0.358	0.279	0.166	Storm wrack
ANOFF-1	1768	0.088	0.201	0.597	0.113	0.019	0.420	0.522	0.038	Offshore
ANOFF-2	4060	0.103	0.532	0.263	0.101	0.005	0.192	0.644	0.158	Offshore
ANOFF-4	2556	0.066	0.156	0.670	0.108	0.023	0.330	0.464	0.183	Offshore
ANOFF-7	2456	0.094	0.127	0.674	0.104	0.043	0.252	0.331	0.373	Offshore

Table 4.2: *Homotrema* taphonomic data for surface samples

Core ID	Sample Interval	Particle size			Core ID	Sample Interval	Particle size		
		Mean (μm)	Mode (μm)	σ (μm)			Mean (μm)	Mode (μm)	σ (μm)
AN09-13	0-1 cm	1.98	3.24	1.48	AN09-14	0-1 cm	1.84	2.57	1.52
AN09-13	1-2 cm	1.51	2.84	1.25	AN09-14	1-2 cm	1.71	2.57	1.26
AN09-13	2-3 cm	1.72	2.84	1.31	AN09-14	2-3 cm	1.52	1.36	1.38
AN09-13	3-4 cm	1.93	3.64	1.52	AN09-14	3-4 cm	8.07	6.87	8.42
AN09-13	4-5 cm	1.63	2.97	1.22	AN09-14	4-5 cm	8.33	7.14	8.70
AN09-13	5-6 cm	1.81	0.01	1.48	AN09-14	5-6 cm	7.99	6.87	8.39
AN09-13	6-7 cm	0.87	-0.53	0.90	AN09-14	6-7 cm	7.88	6.87	8.38
AN09-13	7-8 cm	2.08	0.14	1.79	AN09-14	7-8 cm	7.97	6.87	8.40
AN09-13	8-9 cm	2.33	3.78	1.91	AN09-14	8-9 cm	8.01	6.87	8.41
AN09-13	9-10 cm	2.36	2.70	1.97	AN09-14	9-10 cm	8.00	6.87	8.40
AN09-13	10-11 cm	2.30	2.57	1.92	AN09-14	10-11 cm	7.56	6.74	8.06
AN09-13	11-12 cm	2.05	0.28	1.76	AN09-14	11-12 cm	7.51	6.60	8.04
AN09-13	12-13 cm	7.59	6.60	8.03	AN09-14	12-13 cm	7.52	6.60	8.04
AN09-13	13-14 cm	7.87	6.87	8.36	AN09-14	13-14 cm	7.56	6.74	8.06
AN09-13	14-15 cm	7.29	6.33	7.86	AN09-14	14-15 cm	7.21	6.20	9.97
AN09-13	15-16 cm	7.37	6.33	7.87	AN09-14	15-16 cm	2.18	1.36	1.88
AN09-13	16-17 cm	6.75	5.80	7.28	AN09-14	16-17 cm	1.63	1.22	1.57
AN09-13	17-18 cm	7.80	6.87	8.37	AN09-14	17-18 cm	1.66	1.22	1.58
AN09-13	18-19 cm	6.83	5.93	7.44	AN09-14	18-19 cm	1.20	1.09	1.45
AN09-13	19-20 cm	3.22	2.84	2.91	AN09-14	19-20 cm	1.06	1.09	1.41
AN09-13	20-21 cm	3.80	3.91	3.72	AN09-14	20-21 cm	0.73	0.95	1.16
AN09-13	21-22 cm	3.14	4.05	2.61	AN09-14	21-22 cm	1.00	1.09	1.40
AN09-13	22-23 cm	2.76	2.70	2.26	AN09-14	22-23 cm	1.08	1.09	1.55
AN09-13	23-24 cm	2.80	2.70	2.60	AN09-14	23-24 cm	1.02	1.09	1.57
AN09-13	24-25 cm	2.73	2.70	2.36	AN09-14	24-25 cm	0.83	0.95	1.57
AN09-13	25-26 cm	2.49	2.70	2.14	AN09-14	25-26 cm	0.76	0.95	1.53
AN09-13	26-27 cm	3.77	4.05	3.75	AN09-14	26-27 cm	0.69	0.82	1.50
AN09-13	27-28 cm	6.62	5.66	7.28	AN09-14	27-28 cm	0.76	0.82	1.62
AN09-13	28-29 cm	1.65	2.57	1.28	AN09-14	28-29 cm	0.81	0.95	1.68
AN09-13	29-30 cm	2.15	0.14	1.84	AN09-14	29-30 cm	0.79	0.82	1.73
AN09-13	30-31 cm	3.71	3.78	3.69	AN09-14	30-31 cm	0.77	0.82	1.63
AN09-13	31-32 cm	6.73	5.66	7.30	AN09-14	31-32 cm	3.09	2.57	2.91
AN09-13	32-33 cm	6.33	5.66	6.77	AN09-14	32-33 cm	3.18	2.43	2.94
AN09-13	33-34 cm	6.71	5.66	7.31	AN09-14	33-34 cm	2.94	2.57	2.68
AN09-13	34-35 cm	6.86	5.80	7.45	AN09-14	34-35 cm	3.20	2.57	2.94
AN09-13	35-36 cm	6.64	5.66	7.29	AN09-14	35-36 cm	3.88	2.30	3.78
AN09-13	36-37 cm	6.90	5.80	7.47	AN09-14	36-37 cm	6.66	5.80	7.31
AN09-13	37-38 cm	6.24	5.66	6.61	AN09-14	37-38 cm	3.28	2.57	2.93
AN09-13	38-39 cm	6.82	5.80	7.44	AN09-14	38-39 cm	3.22	2.57	2.82
AN09-13	39-40 cm	6.87	5.80	7.46	AN09-14	39-40 cm	6.72	5.66	7.31
AN09-13	40-41 cm	6.78	5.66	7.32	AN09-14	40-41 cm	6.62	5.66	7.17
AN09-13	41-42 cm	6.91	5.80	7.46	AN09-14	41-42 cm	6.71	5.66	7.30
AN09-13	42-43 cm	6.73	5.66	7.32	AN09-14	42-43 cm	7.19	6.06	7.79
AN09-13	43-44 cm	6.77	5.66	7.34					

Table 4.3: Textural data

Table 4.3 continued...

Core ID	Sample Interval	Particle size			Core ID	Sample Interval	Particle size		
		Mean (μm)	Mode (μm)	σ (μm)			Mean (μm)	Mode (μm)	σ (μm)
AN09-15	0-1 cm	1.05	0.28	1.20	AN09-15	48-49 cm	1.87	2.43	1.67
AN09-15	1-2 cm	2.02	1.76	2.18	AN09-15	49-50 cm	1.63	2.16	1.47
AN09-15	2-3 cm	1.41	1.22	1.36	AN09-15	50-51 cm	1.33	2.03	1.23
AN09-15	3-4 cm	2.14	2.30	1.96	AN09-15	51-52 cm	1.60	2.03	1.48
AN09-15	4-5 cm	2.45	2.57	2.32	AN09-15	52-53 cm	1.54	2.03	1.49
AN09-15	5-6 cm	2.07	2.16	1.99	AN09-15	53-54 cm	1.45	1.89	1.44
AN09-15	6-7 cm	1.62	2.57	1.39	AN09-15	54-55 cm	1.46	2.03	1.52
AN09-15	7-8 cm	1.84	2.70	1.39	AN09-15	55-56 cm	1.73	2.16	1.54
AN09-15	8-9 cm	1.73	1.22	1.50	AN09-15	56-57 cm	1.57	2.16	1.51
AN09-15	9-10 cm	2.10	1.36	1.76	AN09-15	57-58 cm	1.72	2.30	1.46
AN09-15	10-11 cm	2.09	2.57	1.63	AN09-15	58-59 cm	1.63	2.16	1.59
AN09-15	11-12 cm	1.59	2.57	1.28	AN09-15	59-60 cm	1.69	2.16	1.62
AN09-15	12-13 cm	1.90	2.57	1.45	AN09-15	60-61 cm	1.55	2.16	1.54
AN09-15	13-14 cm	2.12	3.78	1.62	AN09-15	61-62 cm	1.56	2.16	1.57
AN09-15	14-15 cm	1.82	2.70	1.37	AN09-15	62-63 cm	1.75	2.16	1.72
AN09-15	15-16 cm	2.20	3.91	1.65	AN09-15	63-64 cm	1.40	2.16	1.27
AN09-15	16-17 cm	1.87	3.78	1.38	AN09-15	64-65 cm	1.49	2.16	1.27
AN09-15	17-18 cm	1.60	2.57	1.32	AN09-15	65-66 cm	1.29	2.03	1.20
AN09-15	18-19 cm	1.85	2.70	1.41	AN09-15	66-67 cm	1.77	2.43	1.43
AN09-15	19-20 cm	2.01	2.84	1.56	AN09-15	67-68 cm	2.06	2.43	1.68
AN09-15	20-21 cm	1.71	2.70	1.35	AN09-15	68-69 cm	1.64	2.57	1.35
AN09-15	21-22 cm	1.46	-0.53	1.14	AN09-15	69-70 cm	2.56	2.57	2.17
AN09-15	22-23 cm	1.38	2.57	1.18	AN09-15	70-71 cm	3.00	3.91	2.56
AN09-15	23-24 cm	3.77	2.57	3.88	AN09-15	71-72 cm	2.12	2.57	1.69
AN09-15	24-25 cm	3.83	3.91	3.88	AN09-15	72-73 cm	1.85	2.57	1.39
AN09-15	25-26 cm	3.83	2.70	3.92	AN09-15	73-74 cm	1.59	2.43	1.34
AN09-15	26-27 cm	3.37	2.57	3.23	AN09-15	74-75 cm	1.61	2.43	1.28
AN09-15	27-28 cm	3.91	2.57	3.92	AN09-15	75-76 cm	1.95	2.57	1.51
AN09-15	28-29 cm	3.45	2.70	3.18	AN09-15	76-77 cm	1.89	2.43	1.57
AN09-15	29-30 cm	3.34	2.57	2.95	AN09-15	77-78 cm	6.55	5.66	7.20
AN09-15	30-31 cm	3.14	2.57	2.88	AN09-15	78-79 cm	3.87	4.18	3.73
AN09-15	31-32 cm	2.99	2.57	2.74	AN09-15	79-80 cm	6.68	5.66	7.30
AN09-15	32-33 cm	2.11	1.89	1.90					
AN09-15	33-34 cm	1.77	2.16	1.50					
AN09-15	34-35 cm	1.62	2.03	1.39					
AN09-15	35-36 cm	2.34	2.43	2.07					
AN09-15	36-37 cm	2.03	2.43	1.68					
AN09-15	37-38 cm	2.03	2.30	1.66					
AN09-15	38-39 cm	2.27	2.57	1.78					
AN09-15	39-40 cm	2.97	4.32	2.56					
AN09-15	40-41 cm	6.55	5.66	7.17					
AN09-15	41-42 cm	7.13	6.20	7.78					
AN09-15	42-43 cm	2.66	2.43	2.30					
AN09-15	43-44 cm	2.36	2.43	2.08					
AN09-15	44-45 cm	2.00	2.43	1.81					
AN09-15	45-46 cm	2.09	2.43	1.77					
AN09-15	46-47 cm	1.76	2.43	1.49					
AN09-15	47-48 cm	2.15	2.43	1.93					

Table 4.3 continued...

Core ID	Sample Interval	Particle size			Core ID	Sample Interval	Particle size		
		Mean (μm)	Mode (μm)	σ (μm)			Mean (μm)	Mode (μm)	σ (μm)
AN09-19	0-1 cm	1.20	-0.53	1.05	AN09-19	47-48 cm	6.71	5.66	7.30
AN09-19	1-2 cm	1.29	1.22	1.18	AN09-19	48-49 cm	6.82	5.80	7.44
AN09-19	2-3 cm	1.58	2.70	1.22	AN09-19	49-50 cm	6.61	5.66	7.22
AN09-19	3-4 cm	1.76	2.70	1.50	AN09-19	50-51 cm	6.72	5.66	7.21
AN09-19	4-5 cm	1.81	2.70	1.64	AN09-19	51-52 cm	6.74	5.80	7.34
AN09-19	5-6 cm	1.37	1.22	1.27	AN09-19	52-53 cm	6.87	5.80	7.46
AN09-19	6-7 cm	1.56	2.70	1.21	AN09-19	53-54 cm	6.66	5.66	7.19
AN09-19	7-8 cm	1.67	2.57	1.31	AN09-19	54-55 cm	6.90	5.80	7.45
AN09-19	8-9 cm	2.09	2.57	1.67	AN09-19	55-56 cm	7.18	6.74	7.81
AN09-19	9-10 cm	1.84	2.43	1.67	AN09-19	56-57 cm	6.68	5.66	7.19
AN09-19	10-11 cm	1.48	2.57	1.24	AN09-19	57-58 cm	7.31	6.47	7.98
AN09-19	11-12 cm	1.21	-0.53	1.08	AN09-19	58-59 cm	7.24	6.87	7.85
AN09-19	12-13 cm	1.48	2.57	1.24	AN09-19	59-60 cm	7.24	7.28	7.73
AN09-19	13-14 cm	1.21	1.09	1.15					
AN09-19	14-15 cm	0.94	-0.53	0.98	AN09-5	2-3 cm	8.79	10.37	9.01
AN09-19	15-16 cm	1.09	-0.53	1.07	AN09-5	6-7 cm	2.51	2.43	2.57
AN09-19	16-17 cm	0.76	-0.53	0.96	AN09-5	9-10 cm	8.59	10.37	8.92
AN09-19	17-18 cm	0.75	-0.53	0.99	AN09-5	13-14 cm	8.69	10.37	8.96
AN09-19	18-19 cm	0.88	-0.53	1.00	AN09-5	20-21 cm	8.89	10.37	9.26
AN09-19	19-20 cm	0.85	-0.53	0.97					
AN09-19	20-21 cm	6.90	5.80	7.31	AN09-11	4-5 cm	1.39	-0.53	1.12
AN09-19	21-22 cm	7.31	6.47	7.91	AN09-11	5-6 cm	1.31	1.22	1.17
AN09-19	22-23 cm	6.90	5.93	7.47	AN09-11	6-7 cm	1.19	0.95	1.17
AN09-19	23-24 cm	7.15	6.20	7.81	AN09-11	7-8 cm	1.14	0.55	1.21
AN09-19	24-25 cm	6.66	5.66	7.23	AN09-11	9-10 cm	2.01	2.57	1.71
AN09-19	25-26 cm	1.07	-0.13	0.99	AN09-11	10-11 cm	2.47	2.70	2.11
AN09-19	26-27 cm	1.10	0.14	1.03	AN09-11	11-12 cm	7.98	6.87	8.40
AN09-19	27-28 cm	6.66	5.66	7.23	AN09-11	12-13 cm	7.94	6.87	8.38
AN09-19	28-29 cm	6.81	5.93	7.45	AN09-11	13-14 cm	7.90	6.87	8.36
AN09-19	29-30 cm	6.88	5.93	7.48	AN09-11	14-15 cm	8.58	10.37	8.88
AN09-19	30-31 cm	6.73	5.80	7.29	AN09-11	16-18 cm	8.45	7.28	8.84
AN09-19	31-32 cm	3.08	4.05	2.58					
AN09-19	32-33 cm	6.22	5.53	6.72					
AN09-19	33-34 cm	6.66	5.80	7.29					
AN09-19	34-35 cm	2.88	2.57	2.49					
AN09-19	35-36 cm	2.97	2.70	2.54					
AN09-19	36-37 cm	6.71	5.80	7.34					
AN09-19	37-38 cm	6.60	5.66	7.22					
AN09-19	38-39 cm	1.13	0.55	1.08					
AN09-19	39-40 cm	6.66	5.66	7.29					
AN09-19	40-41 cm	6.57	5.66	7.17					
AN09-19	41-42 cm	6.86	5.80	7.43					
AN09-19	42-43 cm	6.72	5.66	7.25					
AN09-19	43-44 cm	6.88	5.80	7.45					
AN09-19	44-45 cm	6.54	5.66	7.10					
AN09-19	45-46 cm	7.06	5.93	7.66					
AN09-19	46-47 cm	6.66	5.66	7.30					

CHAPTER 5

PROBABLE TSUNAMI ORIGIN FOR A SHELL AND SAND SHEET FROM MARINE PONDS ON ANEGADA, BRITISH VIRGIN ISLANDS

Eduard G. Reinhardt*

Jessica E. Pilarczyk

Alyson Brown

School of Geography and Earth Sciences, McMaster University, Hamilton, ON,
Canada, L8S 4K1

*Corresponding author: E.G. Reinhardt (ereinhar@mcmaster.ca)

Citation: Reinhardt, E.G., Pilarczyk, J.E., Brown, A., 2011. Probable tsunami origin for a shell and sand sheet from marine ponds on Anegada, British Virgin Islands. *Natural Hazards*, doi: 10.1007/s11069-011-9730-y

Status: received 8 March 2010, accepted 16 January 2011, published online 4 February 2011.

Reprinted with permission from Springer

COPYRIGHT PERMISSION

Springer License Terms and Conditions

License Number: 2661950789788

License date: May 04, 2011

Licensed content publisher: Springer

Licensed content publication: Natural Hazards

Licensed content title: Probable tsunami origin for a Shell and Sand Sheet from marine ponds on Anegada, British Virgin Islands

Licensed content author: Eduard G. Reinhardt

Licensed content date: Jan 1, 2011

Type of Use: Thesis/Dissertation

Portion: Full text

Number of copies: 6

Author of this Springer article: Yes and you are a contributor of the new work

Title of your thesis / dissertation: Foraminiferal Taphonomy as a Paleo-Tsunami and Overwash Indicator in Coastal Environments - Evidence from Oman and the British Virgin Islands

Expected completion date: May 2011

Estimated size (pages): 170

ABSTRACT

A distinctive Shell and Sand Sheet found beneath the marine ponds of Anegada, British Virgin Islands, was formed by a post-1650 AD overwash event, but its origin (tsunami or hurricane) was unclear. This study assesses the taphonomic characters of the shell and large clast material (>2 mm) to determine its provenance and origin. Pond-wide stratigraphic units (Shelly Mud, Shell and Sand Sheet, Mud Cap) were analyzed (12 samples) at four sites in Bumber Well and Red Pond along with eight samples from the Shell and Sand Sheet in a 2 km transect of Bumber Well. Mollusks in the pond muds include *Anomalocardia* spp. and cerithids with no allochthonous shells from the offshore reef-flat. Results show that the shells and clasts (>2 mm) are derived from the erosion and winnowing of the underlying Shelly Mud of the former marine pond, forming a distinctive sheet-like deposit with *Homotrema* sand. The Shell and Sand Sheet contains articulated *Anomalocardia* bivalves and moderate numbers of angular fragments (approximately 35%) that are likely from crab predation. Radiocarbon dates of articulated *Anomalocardia* specimens from the Shell and Sand Sheet range widely (approximately 4000 years), with shell condition (pristine to variably preserved) showing no correlation with age. The articulated condition of the bivalves with the wide-ranging dates suggests erosion and winnowing of the underlying Shelly Mud but minimal transport of the bivalves. The Shell and Sand Sheet has taphonomic characteristics indicative of a widespread tsunami overwash (sheet-like extent and articulated specimens) but lacks allochthonous reef-flat shells. Reef-flat shell material may not have penetrated the pond, as a tsunami would have to cross the reef-flat and overtop high dunes (2.2 m) hindering transport of larger shell material but allowing the *Homotrema* sand to penetrate. Processes including hurricane overwash, pond wave action, or tidal channel opening and closure are not favored interpretations as they would not produce extensive sheet-like deposits. Taphonomic analysis is hampered by the limited (400–500 years BP) depositional history from Anegada's ponds and the lack of comparative data from other Caribbean locations.

5.1 INTRODUCTION

A central question when considering the origin of event beds in coastal settings is whether they formed by storms or tsunamis, a question that is particularly important in active seismic settings. In the Caribbean with its prevalence of hurricanes, storm beds would be expected to be more frequent in the depositional record of coastal areas, however, a local or transoceanic tsunami origin cannot always be dismissed (e.g. Donnelly 2005). The 1755 Lisbon tsunami is a prominent example with reported effects in the Caribbean with estimated heights of 2–6 m east of Anegada, Hispaniola, and Cuba (Fig. 1; O’Loughlin and Lander 2003). However, although there are scattered written accounts of the 1755 Lisbon event in the Caribbean (2.6 m east of Anegada, west in Hispaniola and Cuba; O’Loughlin and Lander 2003), there is little geological evidence documenting its effects on the coastline and there are no reports for the US Atlantic seaboard (Barkan et al. 2009). Local Caribbean Plate boundaries have also produced tsunamis yet little is known about them (e.g. 1867 earthquake likely in Anegada Passage; Reid and Taber 1920; Zahibo 2003; Fig. 5.1; see Atwater et al. (2010) for full discussion).

Discerning between a storm or tsunami event bed is not always easy, and in Caribbean reef settings with their abundance of shelly material, shells can be significant components of these beds (e.g., Parsons-Hubbard 2005). However, most shell bed studies focus on the taphonomic effects of hurricanes and storms but few consider tsunamis (e.g. Miller et al. 1992; Martin and Henderson 2003; Parsons-Hubbard 2005). Unless transport has occurred over great distances (e.g., Morales et al. 2008) or the coastal setting allows separation of storm surges with elevation, there can be doubt on the origin of an event bed (e.g., Jones and Hunter 1992; Donnelly 2005; Park et al. 2009). In many Caribbean islands, coastal lagoons and ponds are often very close to sea level and not far from the coast making it difficult to vet these deposits.

Stratigraphic information from ponds on Anegada, British Virgin Islands, shows a distinctive sheet-like shell and sand bed that post-dates A.D. 1650 and may coincide with the 1755 Lisbon event or other local tsunamis (e.g., Antilles 1690; Atwater et al. 2011). However, several known hurricanes (e.g., 1780, 1819) are also a possibility, and the goal of this study is to document and assess the taphonomic characters of the shelly material to determine its provenance and origin. Previous work (Reinhardt et al. 2006; Donato et al. 2008; Morales et al. 2008; Massari et al. 2009) has shown that shell taphonomic characters may be instructive for distinguishing a tsunami event but the approach has never been applied in a reef setting.

5.2 SETTING

Most seismicity in the Caribbean is concentrated on the Antilles arc from Hispanola to Trinidad where the Caribbean Plate is overriding the North American and South American Plates (Fig. 5.1; Tanner and Shedlock 2004). Anegada, British Virgin Islands, is 125 km south of the Puerto Rico trench that demarcates the North American and Caribbean Plate boundary with plate motions (2 m/100 years) nearly parallel to the trench (Fig. 5.1; ten Brink et al. 2004; Grindlay et al. 2005; Lopez et al. 2006). Expectations are that a Puerto Rico trench or trans-oceanic tsunami would leave an overwash record in the ponds of Anegada. There are several historical references for tsunamis generated by seismic activity near Puerto Rico and the Virgin Islands. Two of these were prominent, the Virgin Island tsunami of 1867 and the Puerto Rico tsunami of 1918 that caused extensive coastal inundations (see Atwater et al. (2011) for details).

Hurricanes would also be expected to leave overwash beds in the low-lying ponds of Anegada. Hurricane Donna (Fig. 5.1; Category 3; 1960; Dunn 1961) as a recent example passed Anegada 15 km to the south, but the storm surge did not cause widespread inundation of the island (wave heights close to 2.5 m above MSL; Atwater et al. 2011). However, a larger hurricane might cause more extensive incursions. Notable historic events include the 1780 hurricane that is considered one of the most disastrous Caribbean hurricanes on record, and specifically for Anegada, a hurricane that struck nearby Tortola in 1713, and one that hit the island in 1819 closing an inlet (Milla's and Pardue 1968; Pickering 1983).

Most of the British Virgin Islands are volcanic with high topographic relief while Anegada is small (54 km²), low-lying (maximum 8 m, but mostly 2–3 m above MSL) and composed of limestone (Fig. 5.1, 5.2). The island is approximately 2–3 km wide and 17 km long with a long axis orientation approximately west to southeast. The northern windward side faces the Atlantic Ocean and has a fringing reef and a shallow reef-flat area that is wide (1.5 km) and shallow (1–2 m) at Windlass Bight (Fig. 5.2; Dunne and Brown 1979). The island core is reefal limestone likely Pleistocene in age (Howard 1970; Horsfield 1975) with a recent covering of carbonate sand (beach ridges) and mud deposits. Extensive hypersaline ponds (93–250 ppt measured in 1995; Jarecki and Walkey 2006) exist in the western half of the island confined by beach ridges (2–3 m in height) and contain extensive microbial mats on the bottom (Fig. 5.2). Water depths are shallow <20 cm as measured in Red Pond (1995), and the pond tidal ranges are considerably less (<3.5 cm) than the astronomical ocean tidal range that is approximately 40 cm. Evidence of less-restricted conditions are evidenced by tidal notches [Approximately 15–20 cm high; see Fig. 5.3g; Atwater et al. (2011)] in exposed limestone that surrounds

the ponds and possible remanent tidal channels in the beach ridge topography (Atwater et al. 2011).

5.3 SHELL TAPHONOMY

Shell beds, lags, or concentrations can be a common feature of shelf and coastal areas, and considerable research has been devoted to understanding their formation through taphonomic analysis (e.g., see Brett 2003). Shell beds can form through storm transport or winnowing of the substrate concentrating and amalgamating shelly deposits into a concentrated bed (e.g., Anderson and McBride 1996; Davies et al. 1989). Recent research has shown that shell beds may also form during a tsunami and may have distinctive shell taphonomy, bed geometry, and structure (e.g. Reinhardt et al. 2006; Donato et al. 2008). The premise of shell bed taphonomy and its utility for event stratigraphy (i.e. distinguishing storms versus tsunamis) is that large-scale processes will overprint background taphonomic characters providing information on the event. The amount of overprinting may relate to the magnitude or type of event and may be significant, or may leave little trace on the shell assemblage (e.g. Miller et al. 1992; Davies et al. 1989). For example, previous studies (e.g. Reinhardt et al. 2006; Donato et al. 2008) have shown tsunami shell beds to contain high concentrations of shells, articulated bivalves, and angular fragments with many allochthonous taxa; while background taphonomic processes do not produce these characters. Not all of these characters might be present in a tsunami unit, which is highlighted by recent research from Pliocene shell beds in Italy (Massari et al. 2009) which found articulated specimens but low angular fragmentation. The amount of fragmentation may depend on the availability of hard-grounds or presence of rocky shorelines which is the case in Reinhardt et al. (2006) and Donato et al. (2008). As discussed in Donato et al. (2008, 2009), it is a collective of taphonomic indices that is important for a tsunami determination (e.g. articulation, high angular fragmentation, provenance, and sheet-like geometry of shell bed). The lack of certain characters does not preclude a tsunami interpretation (e.g. Massari et al. 2009), but their presence may strengthen it. The overall bed geometry and extent has proven important (Massari et al. 2009; Donato et al. 2008) with sheet-like beds contrasting the more localized or lens-shaped storm shell concentrations (Meldahl and Cutler 1992). Characteristics of storm shell concentrations are itemized in Table 3 in Anderson and McBride (1996).

Recognition of a singular tsunami or storm event bed depends on taphonomic overprinting of the shells and preservation of the bed without subsequent exhumation and alteration. In ideal settings, deep scour of the substrate followed by rapid sediment infilling aids preservation of the event bed (Reinhardt et

al. 2006; Donato et al. 2008; Goodman-Tchernov et al. 2009). Deep scour and subsequent burial aids preservation as background processes (i.e. seasonal storms or tidal currents) may not be significant enough to re-expose and alter the beds. However, in settings where these processes are more significant or where large events are frequent, singular beds may be amalgams of event beds with mixtures of taphonomic characters.

5.4 METHODS

For the taphonomic analysis, samples were collected from ten trench sections from Bumber Well and Red Pond ($n = 21$) with two surface samples from a storm wrack-line deposit on the reef-flat beach at Windlass Bight (see map insets Fig. 5.4, 6). Detailed trench stratigraphy is provided in Atwater et al. (2010). Stratigraphic sections are predominantly from the pond margins where trenches could be excavated and sampled above pond water levels. Gouge cores were retrieved from the flooded central portions of Red pond. Geomorphic features were documented using air photos, maps, differential GPS (Watt et al. 2011) and survey level with elevations related to an approximate mean sea level (MSL) datum (Fig. 5.6). Shell and Sand Sheet samples were collected along the length of Bumber Well Pond to determine taphonomic trends along the suspected overwash path (see map inset Fig. 5.6). Two stratigraphic sections from Bumber Well (14 and 16) and Red Pond (13, 15) were also sampled to provide shell and clast data for all major stratigraphic units [Fig. 5.4; Atwater et al. (2010)]. Sediment sample size was large, at approximately 1.2 L providing representative quantities of shells and clasts for analysis. Samples were sieved using a 2 mm screen to quantify the mollusks and their taphonomic condition along with other clast material (e.g. carbonate crusts, wood fragments, pebbles; Fig. 5.3, 5.4, 5.6). Large samples were randomly split with shell and clast counts ranging from 1,000 to 8,000. Storm wrack-line samples on Windlass Bight provide comparative reef-flat data for assessing provenance of the shells and clasts in the Shell and Sand Sheet from the pond (probable overwash unit).

Species identification followed Mikkelsen and Bieler (2007) and Warmke and Abbott (1961). Bivalve taphonomic analysis used similar characters as Reinhardt et al. (2006) and Donato et al. (2008; Fig. 5.3; articulated, whole valve, angular and rounded fragmentation, bored, encrusted, and dissolved). Gastropod taphonomic characters were also quantified (Fig. 5.3; Table 5.1; whole shell, dissolved, angular and rounded fragmentation, missing apex, bored, encrusted). Additional clast identification included, quantities of limestone pebbles (lithoclasts), terrestrial gastropods (undifferentiated), the foraminifer *Homotrema rubrum* (>2 mm), carbonate crusts (intraclasts), and fragments of coral, sea urchin, *Halimeda*

(calcareous green alga), branching coralline algae, and wood. The relative abundance of large clasts and shells (>2 mm) per unit volume of sediment was tabulated to document stratigraphic trends. The <2 mm fraction was analyzed for foraminiferal taphonomy and also particle size, which is described and discussed in Pilarczyk and Reinhardt (2011).

Radiocarbon analyses (AMS) for the stratigraphic sections (Sites 13–16) were performed at Woods Hole (NOSAMS) on plant and shell material selected from stratigraphic units (Fig. 5.4, 5.5). Dates from all sections are provided in Atwater et al. (2010). Sample selection focussed on constraining the age of the Shell and Sand Sheet using terrestrial organic matter (e.g. leaves) and articulated shells (*Anomalocardia*). Radiocarbon ages were calibrated using Calib (v 5.01, IntCal04 calibration data; Reimer et al. 2004) for the terrestrial material and Marine04 (Hughen et al. 2004) for the shells. Only calibrated ages (2σ) are reported with further details provided in Atwater et al. (2010).

5.5 RESULTS

5.5.1 Stratigraphy and molluskan ecology

The stratigraphic sections (approx. 30) as documented in Atwater et al. (2010) show sedimentary units that are found throughout the extent of the ponds (Fig. 5.4). The base of the sections is defined by Neogene (likely Pleistocene; Howard 1970) reefal limestone ranging from approximately 0.5–0.75 m below MSL in the ponds but extends up to 8 m above MSL in western portions of the island. The basal stratigraphic unit (Shelly Mud) consists of lime mud with lower amounts of shells and clasts (2 clasts/cm³) which is overlain by a Shell and Sand Sheet [6 clasts/cm³; fine to medium sand; Pilarczyk and Reinhardt (2011)]. The Shell and Sand Sheet is variable in composition and consists of well-sorted *Homotrema* bioclastic sand and/or shell with some units consisting of more poorly sorted muddy shell (Atwater et al. 2010; Pilarczyk and Reinhardt 2011). The shell concentrations are found mainly on the shallow margins of the ponds, while the *Homotrema* sand is found in the central portions of the ponds. Above this unit is a lime Mud Cap (mostly ~10 cm) with a lower shell and clast concentration of 2 clasts/cm³ which grades or sharply transitions (with a carbonate crust) to a Microbial Mat Peat (mostly 10–15 cm) which extends to the surface (Fig. 5.4). The Microbial Mat Peat variably contains sand and minor shell and evaporites.

Molluskan assemblages in the stratigraphic sections consist of variable amounts of cerithids (*Cerithium variabile*, *Cerithidea beattyi*, *Cerithium eburneum*,

and *Batillaria minima*) and *Anomalocardia* spp. (*Anomalocardia cunimeris* and *Anomalocardia brasiliiana*) indicative of a marine to hypersaline pond or lagoon environment (Figs. 5.3, 5.4). All sedimentary units have mollusk assemblages that are similar (except the Microbial Mat Peat), with variation only in their concentrations (2 vs. 6 clasts/cm³; Fig. 5.4). *Anomalocardia* spp. are facultatively mobile infaunal (3–5 cm) suspension feeders found in marine ponds, mangroves, and lagoons throughout the Caribbean and are known to withstand high salinities (80 ppt; Britton and Morton 1989; Read 1964; Parker 1959; Emery et al. 1957). In Florida Bay, they have been found in lower salinity regimes ranging from 15 to 40 ppt (Brewster-Wingard and Ishman 1999). Similarly, cerithid gastropods (epifaunal vagile detritivores) are found in similar environments (15–40 ppt in Florida Bay; Brewster-Wingard and Ishman 1999) but often in high numbers with large accumulations on the bottom and margins of lagoons, ponds, and mangroves. The distribution of these taxa in the basal Shelly Mud, Shell and Sand Sheet, and overlying Mud Cap is consistent with a marine to hypersaline pond environment which is also evidenced with the foraminiferal data (dominantly miliolids—*Triloculina* sp., *Quinqueloculina* sp.) presented in Pilarczyk and Reinhardt (2011). The predominance of mud-sized sediment also indicates a restricted setting.

5.5.2 Former marine pond shell bed and reef-flat storm wrack comparisons

The reef-flat storm wrack deposit shares no common mollusk taxa with the Shell and Sand Sheet from the ponds (Fig. 5.3). The only common species is *Cerithium variabile* that is present in minor proportions in one of the samples and may be reworked from older pond deposits on the reef-flat. The main component (66%) of the Shell and Sand Sheet is cerithid gastropods (*Cerithium variabile*, *Cerithidea beattyi*, and *Cerithium eburneum*) with minor amounts of *Batillaria minima* (6%), all of which are common pond and lagoon taxa. This contrasts with the storm wrack deposit assemblage with its predominance of limpets (including false limpets). There are also no common bivalve taxa, the lagoonal *Anomalocardia* spp. (27%) dominates the Shell and Sand Sheet while the storm wrack deposit has a variety of reef dwelling taxa (Fig. 5.3).

The taphonomy is very different, with bivalves in the Shell and Sand Sheet predominantly preserved as whole shells and angular fragments, while the storm wrack deposit contains many encrusted and bored specimens. The Shell and Sand Sheet also contains articulated specimens, albeit in low proportions, but noteworthy due to their importance in previous tsunami studies (e.g. Donato et al. 2008; Reinhardt et al. 2006; Morales et al. 2008; Massari et al. 2009). Similarly, with the gastropods, there is a lack of encrusted specimens in the Shell and Sand Sheet but it

contains higher amounts of angular shell fragments and dissolved shell. The high amounts of gastropod fragments is also dominant in the reef-flat environment, although likely from different processes (crab fragmentation vs. transport—see 5.5.3).

Likewise, other clast material shows little correspondence between the pond and reef-flat deposits. The Shell and Sand Sheet contains abundant angular to subrounded limestone pebbles and fragments of carbonate crusts (~0.25 cm thick) which are not present in the storm wrack deposit. In contrast, the storm wrack deposit contains abundant algae fragments (*Halimeda* and branching coralline algae) and coral fragments (Fig. 5.3). Large specimens (>2 mm) of *Hometrema rubrum* are not found in the Shell and Sand Sheet, but are abundant in the sand-sized fraction (<2 mm; see Pilarczyk and Reinhardt 2011).

5.5.3 Pond taphonomic and stratigraphic trends

The taphonomic and clast data are similar in all pond units, but there are some differences worth noting (Fig. 5.4). The Shell and Sand Sheet contains the same proportions of shells and clasts as the underlying Shelly Mud of the former marine pond, although the concentration of clasts is much higher at 6 versus 2 clasts/cm³ and there are higher proportions of carbonate crust fragments (15 vs. 40%; Fig 5.4). The overlying Mud Cap is different than the underlying units as it has higher proportions of whole *Anomalocardia* valves, apex broken cerithids and contains few pebbles but many wood fragments. However, the concentration of shells and clasts (clasts/cm³) is similar to that of the Shelly Mud.

Previous taphonomic studies placed importance on angular fragmentation and the presence of articulated bivalves (e.g. Donato et al. 2008) as a tsunami indicator. In Anegada's ponds, the Shell and Sand Sheet did not contain higher proportions of angular fragmentation or articulated bivalves although the concentration of these characters is higher (clasts/cm³). In this case, the fragmentation is likely due to crab or bird predation (see Zuschin et al. 2003) rather than physical fragmentation during an extreme event.

Taphonomic and petrographic characters of the Shell and Sand Sheet in Bumber Well pond (NE-SW oriented; Fig. 5.6) increase or decrease toward the central portion of pond. The concentration of shells and clasts (clasts/cm³) generally decreases into the central pond, likely reflecting decelerating overwash flow entering from the northern and southern margins. The proportions of cerithids increase and likely reflect preferential entrainment and concentration of the

epifaunal cerithids through transport. Cerithids would have been concentrated on the surface and margins of the ponds where dissolution would be high with fluctuating pond water levels. These specimens would be more readily transported versus the infaunal and larger size *Anomalocardia* (Fig. 5.6). Bivalve fragments also tend to have higher proportions in the central sections relative to the larger whole valves suggesting sorting with transport. Limestone pebbles (lithoclasts) tend to be more dominant in the central area of Bumber Well which may reflect a source effect. Exposed limestone is more prominent in the middle of the pond rather than at the northern and southern extremities (Fig. 5.2).

The lack of coarse (>2 mm) allochthonous reef-flat shells in the Shell and Sand Sheet is perhaps the most significant observation. There are some reef-flat *Halimeda* fragments present in the pond muds, but these could have been windblown as the segments are very light (Fig. 5.4). The marine pond provenance for the shells and clasts (>2 mm) is in contrast with the sand-sized *Homotrema rubrum* that originated from the beach or reef-flat (Pilarczyk and Reinhardt 2011).

5.5.4 Radiocarbon dates

Radiocarbon dates on both terrestrial and shell remains show some similarities but also some important differences; particularly with the shell material (Figs. 5.4c, 5.5). A full discussion of the dates is provided in Atwater et al. (2010); here, the focus is the taphonomic significance. The dates for the articulated *Anomalocardia* shells show a large range but many of them date to the sixteenth to seventeenth century A.D. The dates in Site 14 show the greatest range at ~4000 years even though they have good color and show little taphonomic alteration (Fig. 5.5). In contrast, the shells from Site 16 have the worst taphonomic condition (grade) with loss of color and a thin carbonate crust but have a narrow age range at ~500 years. Similarly, Site 13 dates have a narrow range (~300 years) but have better preserved color (Fig. 5.5). The wide range in dates at Site 14 indicates significant time averaging of articulated *Anomalocardia* shells. This finding is not unusual when radiocarbon dating individual valves (e.g. Flessa et al. 1993), but it is unusual to have such a range of dates for articulated bivalves. The articulated specimens of *Anomalocardia* were difficult to separate for radiocarbon dating and required use of a dissecting knife to separate the valves. It was unclear what caused the valves to adhere so strongly, but this may have allowed dead articulated specimens to be eroded and transported in lower current regimes. Crab or bird burrowing may have exhumed older articulated bivalves (and other shell material) which may have been available for transport on the surface (Flessa et al. 1993). Articulated bivalves are often selected for radiocarbon dating versus individual

valves that may be thousands of years too old (e.g. Simms et al. 2009; Kidwell et al. 2005). However, in low-energy conditions, and perhaps only with *Anomalocardia*, this assumption may not always be valid.

The dominant sixteenth to seventeenth century A.D. age range for the articulated *Anomalocardia* is consistent with the terrestrial organic matter dates. The two radiocarbon dates from the Shelly Mud below the Shell and Sand Sheet (mangrove roots) have a slightly earlier age range from the mid-fifteenth to mid-seventeenth century A.D., while the overlying Mud Cap dates from plant leaves range from the mid-seventeenth to twentieth century A.D. (narrowed to 1650–1800 with the collection of dates; Atwater et al. (2010); Fig. 5.4c). Dates from other trench sections have similar age relationships and are discussed in Atwater et al. (2010).

5.6 DISCUSSION

5.6.1 Pond taphonomic processes

In Anegada's shallow ponds, the background taphonomic processes would include dissolution of shells exposed on the surface, abrasion due to wave action and fragmentation from crab and bird predation (Zuschin et al. 2003). Individual articulated bivalves might be expected to be scattered in the pond muds but not in a concentrated bed. Concentration of shells into beds would not be a dominant process in the restricted pond environment as seasonal currents would be wind driven which would be minimal considering the small fetch distances. Storms and/or tsunamis in the past might have overprinted these background taphonomic characters, by sorting and concentrating the shells into beds or concentrations, and transporting shells from an outside provenance through overwash (e.g. a reef-flat source). Shells might also be concentrated through winnowing wave action in the shallow waters of the ponds with high winds during a hurricane (e.g. Martin and Henderson 2003) or may become concentrated due to lower sediment inputs or higher biological productivity (storm winnowing versus episodic starvation models; Dattilo et al. 2008). This may have been more pronounced in the past if tidal channel connections with the open ocean allowed currents to remove muds.

5.6.2 Does the Shell and Sand Sheet represent an event bed?

The preliminary consideration is whether the Shell and Sand Sheet in Anegada's ponds represents an event deposit. A large-scale event (hurricane or

tsunami) that erodes beach ridges opening older relict tidal channels and/or causes widespread overwash across beach ridges would be expected to contain reef-flat shells. The lack of reef-flat shells in the Shell and Sand Sheet is problematic for an event bed interpretation. However, the stratigraphic association of the shells with the *Homotrema* sand and its probable reef-flat/beach provenance does suggest a large overwash event (Pilarczyk and Reinhardt 2011) rather than reduced sedimentation rates or increased biological productivity in the ponds (Dattilo et al. 2008).

The radiocarbon dates indicate that the stratigraphic sequence in the ponds formed over a relatively short time period, with deposition occurring at similar times in both Bumber Well and Red Pond suggestive of one large event rather than multiple. At Site 13 (Red Pond), the deposition of the Shelly Mud, Shell and Sand Sheet, and the Mud Cap all span several 100 years with similar ages found in Site 16 (Bumber Well) for the Shell and Sand Sheet and the Mud Cap. The large range in radiocarbon dates (2701 B.C.–1436 A.D.) from Site 14 (Bumber Well) may reflect erosion or burrowing of older pond deposits under the beach ridges, but the youngest age (1319–1436 A.D.) from the articulated shells is similar to the ages obtained from Site 13 and 16. It is possible that the Shell and Sand Sheet at Site 14 represents an amalgam of event beds or a continuously deposited sequence (condensed bed) spanning approximately 4000 years, but in context with the other data this does not seem plausible. The presence of *Homotrema* sand with common stratigraphic position and extent within the individual ponds along with the timing of deposition from the radiocarbon dates (Site 13 and 16) suggest one large event rather than multiple amalgamated beds.

5.6.3 Shell and Sand Sheet characteristics and a tsunami origin

The Shell and Sand Sheet from Anegada's ponds shares some of the previously documented characteristics of a tsunami deposit, but there is not yet a criterion for recognizing tsunami versus storm deposits in all settings (Goff et al. 2004; Morton et al. 2007). In previous shell bed research, articulated bivalves, abundant angular fragmentation, allochthonous shells from an outside provenance, and sheet-like geometry were found to be important for determining tsunami versus storm deposition. The mixture of angular fragments and articulated bivalves are judged to be important indicators of substrate scour and live transport of bivalves with angular fragmentation indicating large-scale currents and turbulence (Reinhardt et al. 2006; Donato et al. 2008, 2009; Morales et al. 2008; Massari et al. 2009). However, in the case of Anegada's restrictive ponds, the presence of articulated specimens does not necessarily indicate live transport, although it does likely

indicate minor scour of the substrate. Currents concentrating the shells must have been high enough to erode older shells from the substrate, but not high enough to disarticulate the shells or cause fragmentation. Older shells may have been available in the shallow subsurface, brought there through burrowing crabs and birds and may have remained articulated. The angular fragmentation in this case could not be confidently associated with transport and is likely from predation by crabs and birds in the ponds. The shells did not originate from outside areas (i.e., reef-flat), and all shells and clasts came from scour (and/or winnowing) of the Shelly Mud of the former marine pond. Trends in taphonomic and petrographic characters along Bumber Well reinforce this, indicating possible transport directions from northern and southern margins which may explain the shell and sand stratigraphy (see Atwater et al. 2010).

The pond-specific origin for the >2 mm shells and clasts is in contrast with the finer fraction (<2 mm) that shows a possible reef-flat or beach source for the *Homotrema rubrum* (Pilarczyk and Reinhardt 2011). The *Homotrema rubrum* from the Shell and Sand Sheet are large with well-preserved color compared to the underlying Shelly Mud and the overlying Mud Cap. The source of the larger and better preserved specimens is the beach or reef-flat, but they could have originated from older sediments underlying the existing beach ridges defining the ponds (Pilarczyk and Reinhardt 2011). The lack of coarser reef-flat clasts (and *Homotrema*; Pilarczyk and Reinhardt 2011) in the Shelly Mud indicates no large tidal channel connection with the reef-flat in the former marine pond. The former marine pond as represented by the Shelly Mud was a marine to hypersaline environment based on the molluscan and foraminiferal data, so there was some connection, but it was likely very limited [probably from the south—see Atwater et al. (2010)]. This may explain the lack of coarser clasts from the reef-flat in the Shell and Sand Sheet, as with tsunami overwash, water crossing the reef-flat and overtopping the beach ridges may have prevented the coarser fraction from making its way into the pond during the event (Wei et al. 2010). Erosion may have occurred in plunge pools (and relict tidal channels) behind the ridges as documented in the aerial photos (Atwater et al. 2010). This may have eroded older underlying beach sands and *Homotrema rubrum* transporting it into the pond (Pilarczyk and Reinhardt 2011).

The widespread distribution of the Shell and Sand Sheet throughout the ponds and the consistent dates to the mid-seventeenth to nineteenth century A.D. suggest one widespread event (tsunami) rather than a hurricane that would produce more limited overwash lobes or wedges on the pond margins (see below). The proposed tsunami scenario would cause instantaneous and widespread overwash across the beach ridges creating pond-wide flows, which is consistent with the

taphonomic data showing a winnowing and concentration effect (see Atwater et al. 2010). The suspended mud would then accumulate after the event which is consistent with the Mud Cap (mostly 10–15 cm thick) seen throughout the ponds. The radiocarbon dates on leaves have very consistent ages (see Fig. 5.4) suggesting a pond-wide accumulation rather than isolated scour and fill. If this is correct, it also indicates that much of the mud was not exported from the ponds, suggesting that there were no significant openings created during the event.

5.6.4 Hurricane considerations

Sustained hurricane wave action (versus a tsunami) might erode and reactivate choked tidal channels with storm surge transporting sand from older underlying beach deposits into the pond. Storm surge and wave action in the ponds may have eroded and transported shells and clasts from the Shelly Mud substrate onto the margins of the ponds. Winnowing and export of muds would continue after the event, but beach ridge accretion would cause renewed restriction and mud deposition (Mud Cap). However, hurricane Donna (1960, Category 3; Dunn 1961) with its maximum sustained wind speeds of 110 knots produced no breaches through the beach ridges of Windlass Bight as evidenced with air photos taken in 1945 and 1969. Obviously, larger events are possible and may have had a greater effect on the ponds and cannot be dismissed. Hurricane deposits from other Caribbean locations show some similarities but also some significant differences with the Anegada deposits. Hurricane Floyd (1999) produced shell concentrations (30 cm thick) consisting of articulated *Anomalocardia* and abundant cerithids on the margin of Osprey Pond, San Salvador, Bahamas (Martin and Henderson 2003). The extent of the shell bed, and whether it formed a sheet-like deposit in the pond was not reported, but the concentration was formed through wave-generated currents in the pond rather than an overwash event. Other ponds in the Bahamas and Puerto Rico have evidence of sandy overwash and shell concentrations (mainly cerithids) which have been attributed to hurricanes and possibly tsunamis (Dix et al. 1999; Parks et al. 2009; Donnelly 2005). No articulated bivalves or any large allochthonous reef-flat clasts were noted in the shell/sand concentrations but this may be a sampling bias as the core barrels were narrow (estimated at 3–7 cm in diameter) and there were only 1–3 cores recovered. In the Salt Pond (San Salvador, Bahamas) example, hurricane Frances (2004) produced surge heights of 4.8–5.5 m which overtopped a low-lying sand ridge forming a sand wedge in the pond with foraminifera, mollusks (unidentified), and seeds (McCabe and Niemi 2008; Parks et al. 2009). In the ponds of Anegada, Wei et al. (2010) conclude, based on hydrodynamic modeling, that a hurricane could not cause significant overwash (versus a tsunami) with the broad reef-flat and the 2.2 m beach ridge elevation at

Windlass Bight. So although the Shell and Sand Sheet in the ponds of Anegada do share some similar characters as these other hurricane examples, it does not appear to be wedge or lobate in shape (e.g. see Fig. 5.2 in Liu and Fearn 2000). This bed geometry combined with the hydrodynamic modeling and boulder results suggest a tsunami origin rather than a hurricane (Wei et al. 2010; Buckley et al. 2011; Watt et al. 2011).

5.6.5 Stratigraphic comparisons

Interestingly, the age of the stratigraphic sequence is skewed to the last 400–500 years [approximately 50–60 cm of accumulation see Fig. 5.8, Atwater et al. (2010)] suggesting rapid deposition and large-scale events that have eroded the western side of the island where the ponds are situated. By 500 years BP, the platform should have been flooded by rising sea level and should contain earlier deposits (Toscano and Macintyre 2003). The reworked *Anomalocardia* radiocarbon ages and cerithid dates (Atwater et al. 2010) indicate that the ponds existed for several 1000 years or more (oldest ages are 2400–2700 B.C.), which corresponds with the sea level record for the Caribbean (Toscano and Macintyre 2003). The lack of older deposits makes comparisons difficult, as there were no significant shell beds found in the sections that could be directly attributed to a storm or hurricane. Similar environments (ponds) in the Bahamas have higher accumulation thicknesses and their basal dates are much older. Dune Pass Bay Pond has approximately 130 cm of accumulation with basal ages at ~3000 years BP (uncorrected reservoir age versus corrected age at ~1500 years BP; Dix et al. 1999). The Salt Pond from San Salvador Island has approximately 65 cm of accumulation since ~3800 years BP (Parks et al. 2009) and Isla de Culebrita, Puerto Rico has approximately 200 cm with a basal age of ~2200 years BP (Donnelly 2005). The short sedimentary record in Anegada ponds does seem unusual based on these comparative examples.

5.7 CONCLUSIONS

The resolution of the radiocarbon dating cannot constrain the age of the Shell and Sand Sheet to a particular tsunami (e.g. Antilles 1690; Lisbon 1755) or a hurricane event in Anegada's history, and there is no strong taphonomic indicator to narrow the determination. Characteristics of the deposit suggest a widespread overwash event in the pond involving erosion and winnowing of the former marine pond's substrate into a sheet-like geometry. The event eroded and concentrated articulated bivalves and gastropods along with other clasts from areas on the pond margins (e.g. pebbles). The stratigraphic sections found in the ponds were relatively

young in age (approximately last 400–500 years) indicating that there may have been previous events that have eroded the western half of the island. This lack of temporal stratigraphic data hampered the analysis, as it did not provide any prior events for comparison. Although limited in extent, other pond studies from Bahamas show different characteristics for a hurricane deposit that does not seem to match those from Anegada, but these results are difficult to assess due to the lower sampling resolution (cores).

Making a firm conclusion on the Anegada deposit is difficult as some of the established taphonomic characters for a tsunami are not present (e.g. provenance). Further research on event beds in Caribbean ponds coupled with better eyewitness accounts of known events may establish better criteria for assessing shell bed origins in reef settings. However, based on the balance of data from the other studies (boulders and hydrodynamic modeling), the Shell and Sand Sheet does appear tsunamigenic in origin.

ACKNOWLEDGEMENTS

The government of the British Virgin Islands permitted access to Anegada's salt ponds, use of airphotos, and guidance from its specialists in disaster management, surveying, and natural science. Among them, we especially thank Cynthia Rolli, Rondell Smith, Shannon Gore, and Dylan Penn. Lianna Jarecki shared her comprehensive knowledge of Anegada's salt ponds, Alejandra Rodriguez assisted with field work and Alyson Brown helped with laboratory work. Brian Atwater provided comments on early drafts of the manuscript. The work was supported in part by the Nuclear Regulatory Commission under its project N6480, a tsunami-hazard assessment for the eastern United States and an NSERC Discovery grant to ER.

REFERENCES

- Anderson, L.C., McBride, R.A., 1996. Taphonomic and paleoenvironmental evidence of Holocene shell-bed genesis and history on the northeastern Gulf of Mexico shelf. *Palaios*, 11: 532-549
- Atwater, B.F., ten Brink, U.S., Buckley, M., Halley, R.S., Jaffe, B.E., Lopez-Venegas, A.M., Reinhardt, E.G., Tuttle, M.P., Watt, S., Wei, Y., 2010. Geomorphic and stratigraphic evidence for an unusual tsunami or storm a few centuries ago at Anegada, British Virgin Islands. *Natural Hazards*, doi 10.1007/s11069-010-9622-6

-
- Barkan, R., ten Brink, U.S., Lin, J., 2009. Far field tsunami simulations of the 1755 Lisbon earthquake: Implications for tsunami hazard to the U.S. East Coast and the Caribbean. *Marine Geology*, 264:109-122
- Brett, C.E., 2003. Taphonomy: sedimentological implications of fossil preservation. In: Middleton G V (Ed.), *Encyclopedia of Sediments and Sedimentary Rocks*. Springer, Dordrecht pp 723–729
- Brewster-Wingard, G.L., Ishman, S.E., 1999. Historical Trends in Salinity and Substrate in Central Florida Bay: A Paleoecological Reconstruction Using Modern Analogue Data. *Estuaries*, 22: 369-383
- Britton, J. C., Morton, B., 1989. *Shore Ecology of the Gulf of Mexico*. University of Texas Press, Austin pp 387pp.
- Buckley, M., Wei, Y., Jaffe, J., Watt, S., 2011. Inverse modeling of velocities and inferred cause of overwash that emplaced inland fields of boulders at Anegada, British Virgin Islands. *Natural Hazards*, doi 10.1007/s11069-011-9725-8
- Dattilo, B.F., Brett, C.E., Tsujita, C.J., Fairhurst, R., 2008. Sediment supply versus storm winnowing in the development of muddy and shelly interbeds from the Upper Ordovician of the Cincinnati region, USA. *Canadian Journal of Earth Sciences*, 45: 243(23)
- Davies, D.J., Powell, E.N., Stanton, R.J. Jr., 1989. Taphonomic signature as a function of environmental process: shells and shell beds in a hurricane-influenced inlet on the Texas coast. *Palaeogeography Palaeoclimatology Palaeoecology*, 72: 317– 356
- Dix, G.R., Patterson, R.T., Parks, L.E., 1999. Marine saline ponds as sedimentary archives of late Holocene climate and sea-level variation along a carbonate platform margin; Lee Stocking Island, Bahamas. *Palaeogeography Palaeoclimatology Palaeoecology*, 150: 223-246
- Donato, S.V., Reinhardt, E.G., Boyce, J.I., Pilarczyk, J.E., Jupp, B.P., 2009. Particle-size distribution of inferred tsunami deposits in Sur Lagoon, Sultanate of Oman. *Marine Geology*, 257: 54-64
- Donato, S.V., Reinhardt, E.G., Boyce, J.I., Rothaus, R., Vosmer, T., 2008. Identifying tsunami deposits using bivalve shell taphonomy. *Geology*, 36: 199-202
- Donnelly, J.P., 2005. Evidence of past intense tropical cyclones from backbarrier salt pond sediments: A case study from Isla de Culebrita, Puerto Rico, USA. *Journal of Coastal Research*, 142: 201–210
- Dunn, G.E., 1961. The hurricane season of 1960. *Monthly Weather Review* 89: 99-108
- Dunne, R.P., Brown, B.E., 1979. Some aspects of the ecology of reefs surrounding Anegada, British Virgin Islands. *Atoll Research Bulletin* 236. The Smithsonian Institution, Washington, D.C., pp 80
-

- Emery, K.O., Stevenson, R.E., Hedgpeth, J.W., 1957. Estuaries and lagoons. In Hedgpeth J W (Ed.) Geological Society of America Memoir 67: Treatise on Marine Ecology and Paleoecology. Geological Society of America, Boulder, CO, pp 73–750
- Flessa, K.W., Cutler, A.H., Meldahl, K.H., 1993. Time and taphonomy: quantitative estimates of time-averaging and stratigraphic disorder in a shallow marine habitat. *Paleobiology*, 19: 266-286
- Goff, J., McFadgen, B.G., Chagué-Goff, C., 2004. Sedimentary differences between the 2002 Easter storm and the 15th-century Okoropunga tsunami, southeastern North Island, New Zealand. *Marine Geology*, 204: 235-250
- Goodman-Tchernov, B.N., Dey, H.W., Reinhardt, E.G., McCoy, F., Mart, Y., 2009. Tsunami waves generated by the Santorini eruption reached Eastern Mediterranean shores. *Geology*, 37: 943-946
- Grindlay, N.R., Mann, P., Dolan, J.F., van Gestel, J., 2005. Neotectonics and subsidence of the northern Puerto Rico - Virgin Islands margin in response to the oblique subduction of high-standing ridges. *Geological Society of America Special Publication*, 385: 31-60
- Horsfield, W.T., 1975. Quaternary vertical movements in the Greater Antilles. *Geological Society of America Bulletin*, 86: 933-938
- Howard, J., 1970. Reconnaissance geology of Anegada Island. Caribbean Research Institute, St. Thomas, pp 18
- Hughen, K.A., Baillie, M.G.L., Bard, E., Beck, J.W., Bertrand, C.J.H., Blackwell, P.G., Buck, C.E., Burr, G.S., Cutler, K.B., Damon, P.E., Edwards, R.L., Fairbanks, R.G., Friedrich, M., Guilderson, T.P., Kromer, B., McCormac, G., Manning, S., Ramsey, C.B., Reimer, P.J., Reimer, R.W., Remmele, S., Southon, J.R., Stuiver, M., Talamo, S., Taylor, F.W., van der Plicht, J., Weyhenmeyer, C.E., 2004. Marine04 marine radiocarbon age calibration, 0-26 cal kyr BP; IntCal04; calibration. *Radiocarbon*, 46: 1059-1086
- Jarecki, L., Walkey, M., 2006. Variable hydrology and salinity of salt ponds in the British Virgin Islands. *Saline Systems* 2, doi 10.1186/1746-1448-2-2
- Jones, B., Hunter, I.G., 1992. Very large boulders on the coast of Grand Cayman: the effects of giant waves on rocky coastlines. *Journal of Coastal Research*, 8: 763-774
- Kidwell, S.M., Best, M.M.R., Kaufman, D.S., 2005. Taphonomic trade-offs in tropical marine death assemblages: Differential time averaging, shell loss, and probable bias in siliciclastic vs. carbonate facies. *Geology*, 33: 729-732
- López, A.M., Stein, S., Dixon, T., Sella, G., Calais, E., Jansma, P., Weber, J., LaFemina, P., 2006. Is there a northern Lesser Antilles forearc block? *Geophysical Research Letters*, 33, doi 10.1029/2005GL025293
- Liu, K., Fearn, M.L., 2000. Reconstruction of prehistoric landfall frequencies of catastrophic hurricanes in northwestern Florida from lake sediment records.

- Quaternary Research, 54: 238–245
- Martin, A.J., Henderson, S.W., 2003. When does a taphocoenose become a biocoenose? A storm-generated inland molluscan assemblage, San Salvador Island, Bahamas. Abstracts with Programs, Geological Society of America, 35: 1: 64
- Massari, F., D'Alessandro, A., Davaud, E., 2009. A coquinoid tsunamite from the Pliocene of Salento (SE Italy). *Sedimentary Geology*, 221: 7
- McCabe, J.M., Niemi, T.M., 2008. The 2004 Hurricane Frances overwash deposition indeposition in Salt Pond, San Salvador, the Bahamas. In: Park, L.E., Freile, D. (Eds.), *The 13th Symposium on the Geology of the Bahamas and other Carbonate Regions*, Gerace Research Centre, San Salvador, Bahamas pp 25–42
- Morton, R.A., Gelfenbaum, G., Jaffe, B.E., 2007. Physical criteria for distinguishing sandy tsunami and storm deposits using modern examples. *Sedimentary Geology*, 200: 184-207
- Meldahl, K.H., Cutler, A.H., 1992. Neotectonics and taphonomy: Pleistocene molluscan shell accumulations in the northern Gulf of California. *Palaios*, 7: 187-197
- Mikkelsen, P.M., Bieler, R., 2007. Seashells of southern Florida: living marine mollusks of the Florida Keys and adjacent regions: bivalves, pp 496
- Millás, J.C., Pardue, L., 1968. Hurricanes of the Caribbean and adjacent regions, 1492-1800. Academy of the Arts and Sciences of the Americas, Miami, FL.
- Miller, A.I., Parsons, K.M., Cummins, H., Boardman, M.R., Greenstein, B.J., Jacobs, D.K., 1992. Effect of Hurricane Hugo on molluscan skeletal distributions, Salt River Bay, St. Croix, U.S. Virgin Islands. *Geology*, 20: 23–26
- Morales, J.A., Borrego, J., San Miguel, E.G., López-González, N., Carro, B., 2008. Sedimentary record of recent tsunamis in the Huelva Estuary (southwestern Spain). *Quaternary Science Reviews*, 27: 734-746
- O'Loughlin, K.F., Lander, J.F., 2003. Caribbean tsunamis: A 500-year history from 1498 – 1998. Kluwer Academic, Dordrecht, Boston, pp 263
- Parker, R.H., 1959. Macro-invertebrate assemblages of central Texas coastal bays and Laguna Madre. *American Association of Petroleum Geologists Bulletin*, 43: 2100-2166
- Park, L.E., Siewers, F.D., Metzger, T., Sipahioglu, S., 2009. After the hurricane hits: Recovery and response to large storm events in a saline lake, San Salvador Island, Bahamas. *Quaternary International*, 195: 98-105
- Parsons-Hubbard, K., 2005. Molluscan taphofacies in recent carbonate reef/lagoon systems and their application to sub-fossil samples from reef cores. *Palaios*, 20: 175-191
- Pickering, V.W., 1983. Early history of the British Virgin Islands: from Columbus

- to emancipation. Falcon Publications International, pp 248
- Read, R.H., 1964. Ecology and environmental physiology of some Puerto Rican bivalve molluscs and a comparison with boreal forms. *Caribbean Journal of Science*, 4: 459-465
- Reid, H.F., Taber, S., 1920. The Virgin Islands earthquakes of 1867-1868. *Bulletin of the Seismological Society of America*, 10: 9-20
- Reimer, P.J., Baille, M.G.L., Bard, E., Bayliss, A., Beck, J.W., Bertrand, C.J.H., Blackwell, P.G., Buck, C.E., Burr, G.S., Cutler, K.B., Damon, P.E., Edwards, R.L., Fairbanks, R.G., Friedrich, M., Guilderson, T.P., Hogg, A.G., Hughen, K.A., Kromer, B., McCormac, G., Manning, S., Ramsey, C.B., Reimer, R.W., Remmele, S., Southon, J.R., Stuiver, M., Talamo, S., Taylor, F.W., van der Plicht, J., Weyhenmeyer, C.E., 2004. IntCal04 terrestrial radiocarbon age calibration, 0-26 cal kyr BP; IntCal04; calibration. *Radiocarbon*, 46: 1029-1058
- Reinhardt, E.G., Goodman, B.N., Boyce, J. I., Lopez, G., van Hengstum, P., Rink, W. J., Mart, Y., Raban, A., 2006. The tsunami of 13 December A.D. 115 and the destruction of Herod the Great's harbor at Caesarea Maritima, Israel. *Geology*, 34: 1061-1064
- Simms, A.R., Aryal, N., Yokoyama, Y., Matsuzaki, H., Dewitt, R., 2009. Insights on a proposed Mid-Holocene highstand along the northwestern Gulf of Mexico from the evolution of small coastal ponds. *Journal of Sedimentary Research*, 79: 757-772
- Tanner, J.G., Shedlock, K.M., 2004. Seismic hazard maps of Mexico, the Caribbean, and Central and South America. *Tectonophysics*, 390: 159
- ten Brink, U.S., Danforth, W.W., Polloni, C.F., Andrews, B., Llanes, P., Smith, S., Parker, E., Uozumi, T., 2004. New seafloor map of the Puerto Rico trench helps assess earthquake and tsunami hazards. *EOS Transaction of the American Geophysical Union*, 85: 349
- Toscano, M.A., Macintyre, I.G., 2003. Corrected western Atlantic sea-level curve for the last 11,000 years based on calibrated ^{14}C dates from *Acropora palmata* framework and intertidal mangrove peat. *Coral Reefs*, 22: 257-270
- Warmke, G.L., Abbott, R.T., 1961. *Caribbean Seashells; a guide to the marine mollusks of Puerto Rico and other West Indian Islands, Bermuda and the Lower Florida Keys*. Livingston Pub. Co., pp 348
- Wei, Y., ten Brink, U.S., Atwater, B.F., 2010. Modeling of tsunamis and hurricanes as causes of the catastrophic overwash of Anegada, British Virgin Islands, between 1650 and 1800: Abstract OS42B-03. Presented at 2010 Fall meeting, American Geophysical Union, San Francisco, California, 13–17 December 2010
- Zahibo, N., 2003. The 1867 Virgin Island tsunami; observations and modeling. *Oceanologica Acta*, 26: 609-621

Zuschin, M., Stachowitsch, M., Stanton Jr., R.J., 2003. Patterns and processes of shell fragmentation in modern and ancient marine environments. *Earth Science Reviews*, 63: 33-82

CHAPTER 5 FIGURES

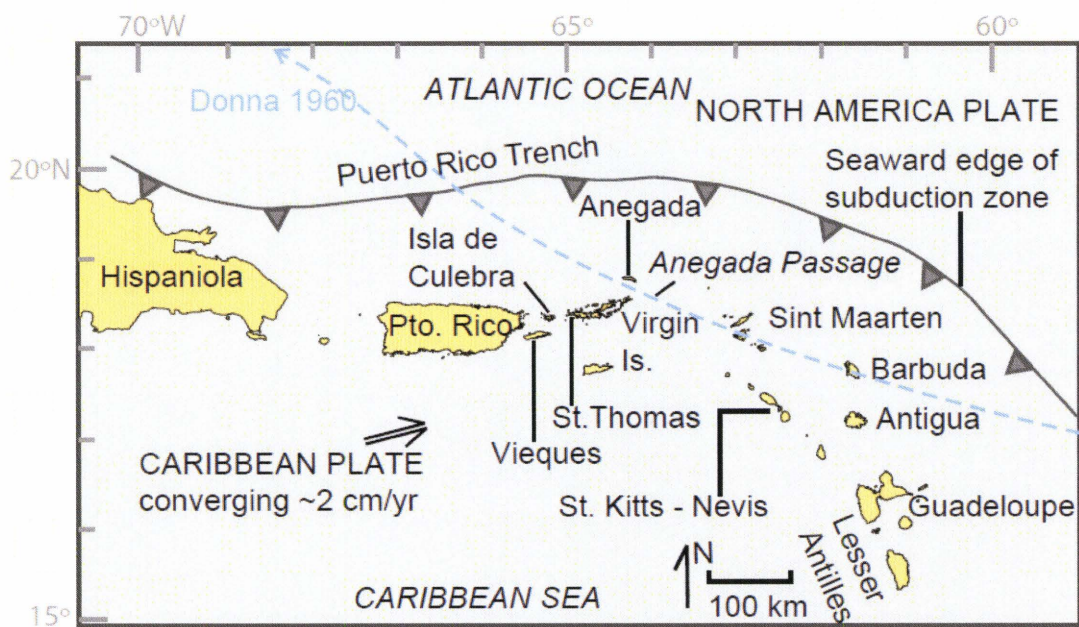
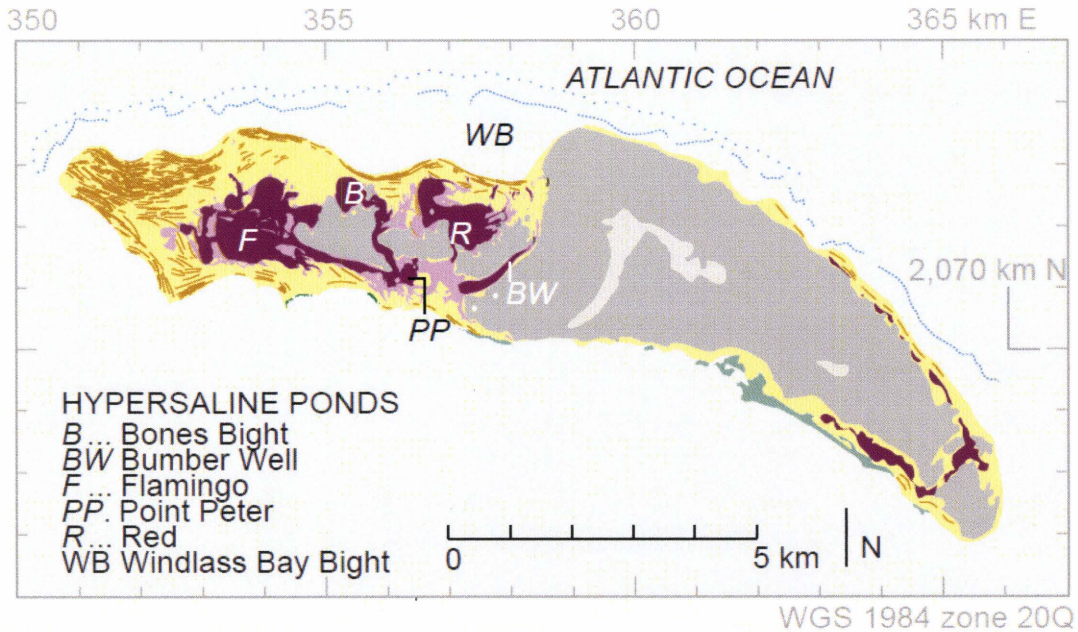


Figure 5.1: Physiography of the northeastern Caribbean showing tectonic plates and the path of Hurricane Donna in 1960 (Modified from Fig. 1 from Atwater et al. 2010; Lopez et al. 2006; Dunn 1961).












-  Mangrove
-  Sand - above seasonal high water of salt ponds
-  Muddy sand
-  Microbial mats and evaporite crusts
-  Limestone (Neogene, probably Pleistocene)
-  Edge of spur-and-groove
-  Reef crest
-  Beach ridge crest (Holocene) - Line dashed where ridge is indistinct
-  Highest parts of island—About 7-8 m above modern sea level.

Figure 5.2: Map showing geomorphic and geological features of Anegada (Modified from Fig. 2, Atwater et al. 2010).

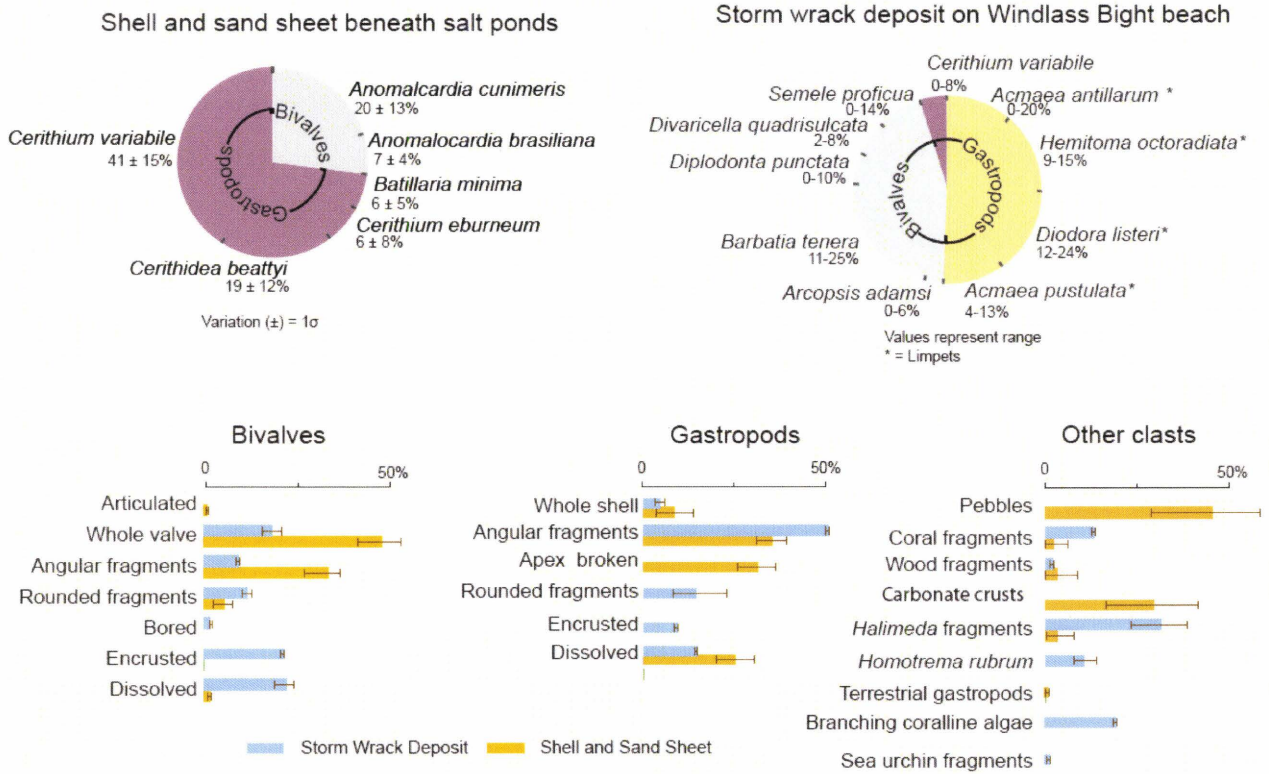
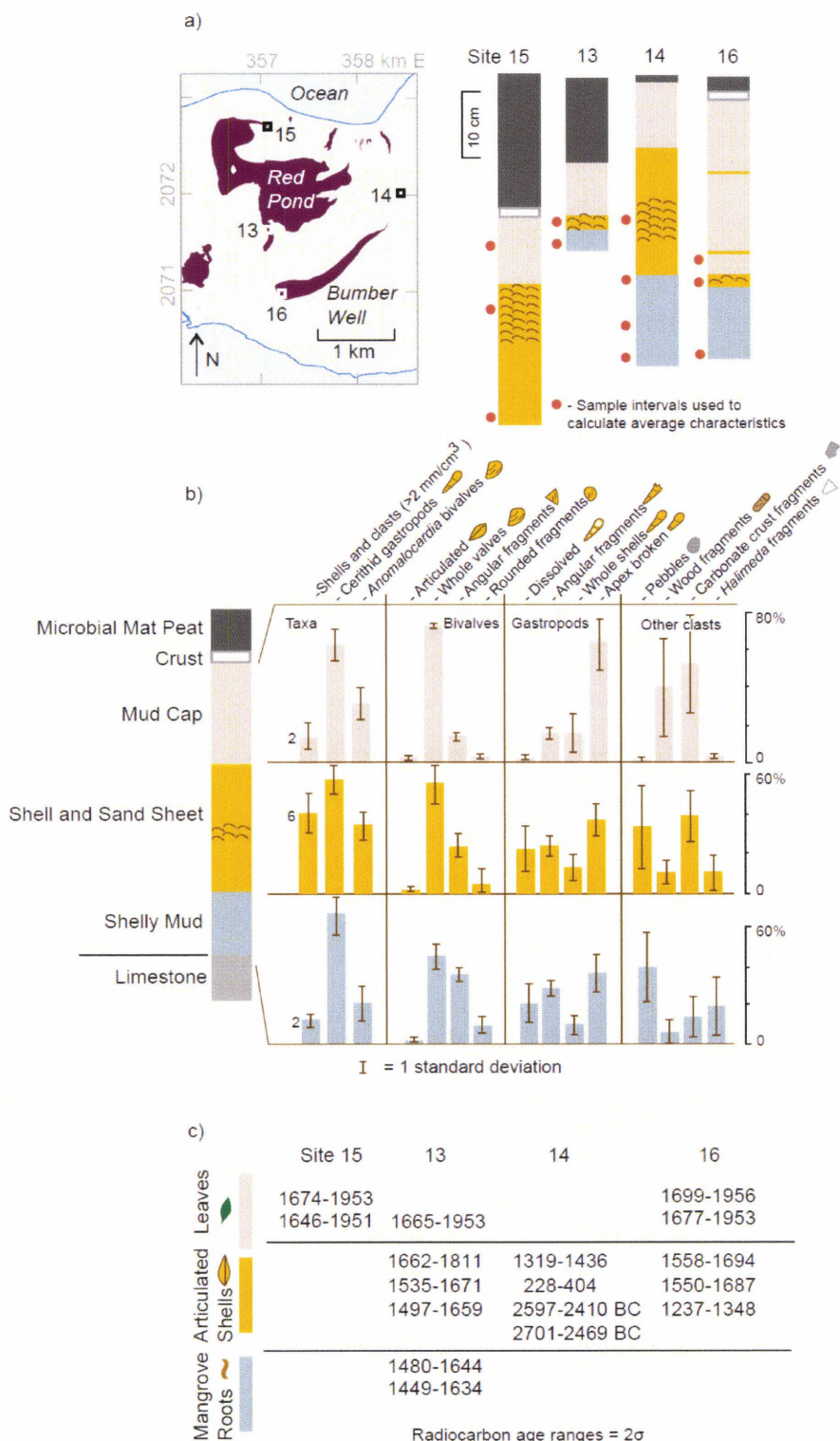


Figure 5.3: Molluskan species, taphonomic and clast data from the Shell and Sand Sheet and the storm wrack deposit on Windlass Bight Beach. Eleven samples were analyzed from the Shell and Sand Sheet and two samples from the storm wrack deposit—average values are reported with 1 σ and the range of values. For the clast data, bars represent 1 σ.

Figure 5.4: a) Location of trenches in Bumber Well and Red Pond and their stratigraphic logs showing sample resolution. b) Mean values of dominant taphonomic and petrographic characters for the idealized stratigraphic section. c) Distribution of radiocarbon dates in the analyzed stratigraphic sections (for details see Atwater et al. 2010; See following page).



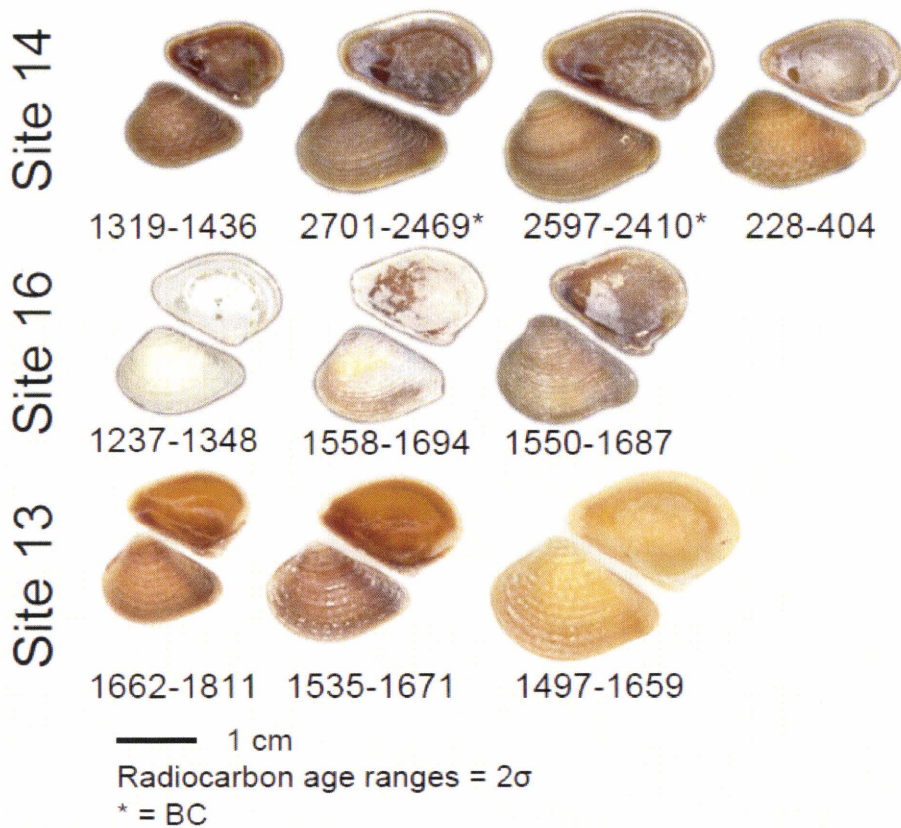
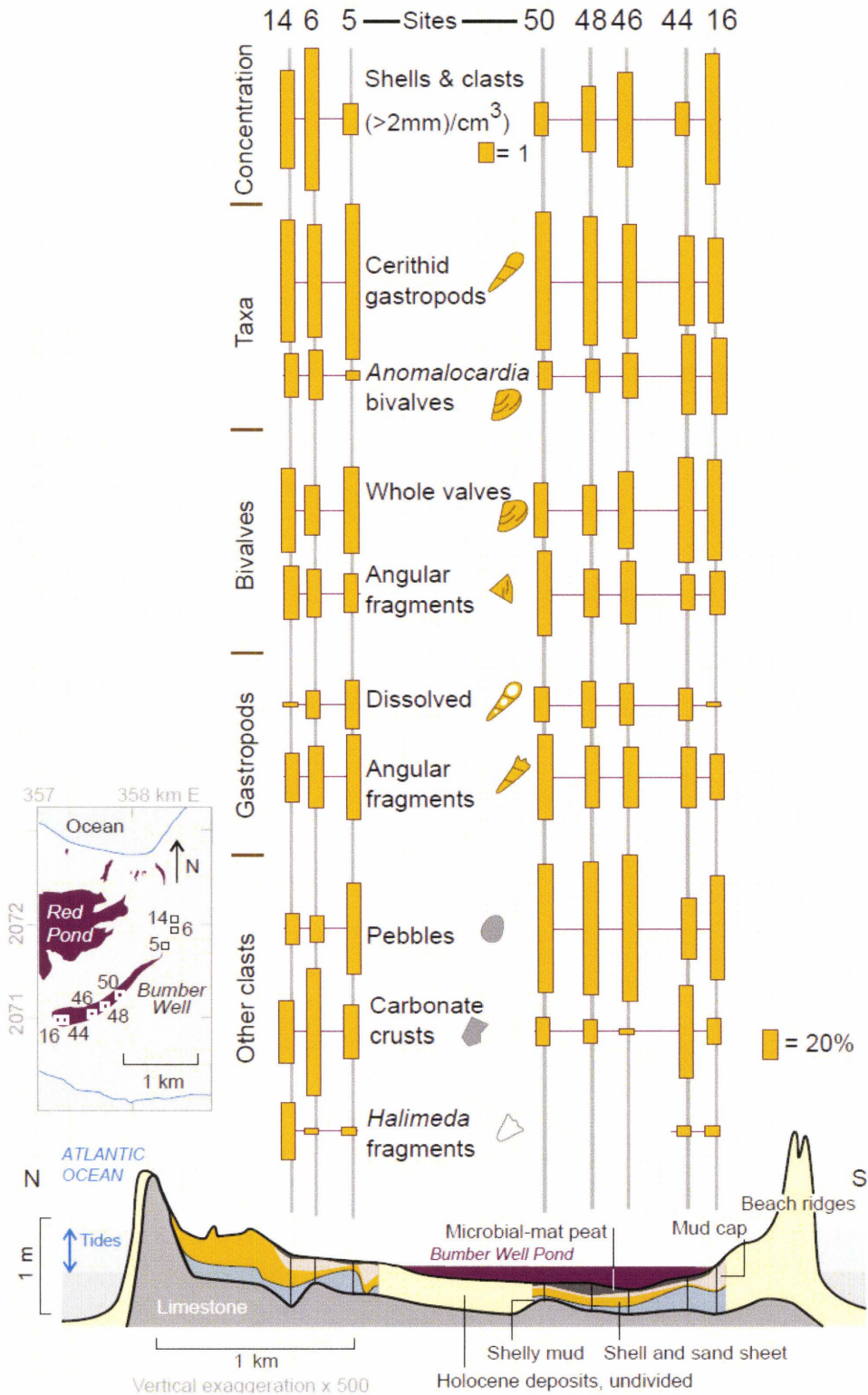


Figure 5.5: Articulated *Anomalocardia* radiocarbon dates for the Shell and Sand Sheet illustrating the range in dates and the lack of taphonomic correlation.

Figure 5.6: Distribution of the dominant taphonomic and petrographic characters of the Sand and Shell Sheet in Bumber Well Pond showing spatial trends. Stratigraphic cross-section from Atwater et al. (2010; See following page).



CHAPTER 5 TABLES

	AN09-13 21-24 cm	AN09-13 21-24 cm	AN09-16 24-29 cm	AN09-16 30-32 cm	AN09-16 32-37 cm	AN09-16 40-45 cm	AN09-14 18-24 cm	AN09-14 30-34 cm
Species:								
<i>Anomalocardia cunimeris</i>	0.610	0.176	0.204	0.390	0.074	0.037	0.229	0.323
<i>Anomalocardia brasiliana</i>	0.035	0.059	0.026	0.070	0.144	0.158	0.022	0.228
<i>Batillaria minima</i>	0.019	0.353	0.016	0.042	0.043	0.072	0.019	0.005
<i>Bulla stiata</i>	0.005	-	0.001	0.004	0.006	0.019	-	0.005
<i>Cerithium eburneum</i>	0.051	0.118	0.008	0.022	0.054	0.081	0.004	-
<i>Cerithidea beattyi</i>	0.103	-	0.659	0.133	0.090	0.074	0.440	0.349
<i>Cerithium variable</i>	0.176	0.294	0.085	0.340	0.586	0.557	0.285	0.090
Cerithids	0.349	0.765	0.768	0.536	0.773	0.784	0.749	0.444
Bivalves	0.646	0.235	0.231	0.460	0.219	0.195	0.251	0.550
Bivalves:								
Articulated	0.006	-	0.004	0.012	0.022	0.006	0.010	0.006
Whole valve	0.530	0.267	0.770	0.667	0.603	0.614	0.571	0.593
Angular fragment	0.178	0.467	0.169	0.290	0.306	0.330	0.362	0.315
Rounded fragment	0.048	0.267	0.027	0.024	0.061	0.025	0.056	0.068
Bored	-	-	-	-	-	-	-	-
Encrusted	-	-	0.011	-	-	0.006	-	-
Dissoluted	0.011	-	0.019	0.006	0.009	0.019	0.001	0.006
Gastropods:								
Dissoluted	0.456	0.467	0.018	0.365	0.343	0.425	0.088	0.109
Large angular fragment	0.238	0.422	0.205	0.222	0.394	0.317	0.277	0.275
Missing apex	0.288	0.111	0.493	0.366	0.239	0.170	0.451	0.536
Small angular fragment	-	-	-	-	-	-	-	-
Rounded fragment	-	-	-	-	-	-	-	-
Bored	-	-	-	-	-	-	-	-
Whole shell	0.018	-	0.284	0.046	0.024	0.084	0.183	0.080
Encrusted	-	-	-	-	-	0.002	-	-
Petrography:								
Pebbles	0.481	0.889	-	0.667	0.741	0.742	0.196	0.071
Coral fragments	0.039	-	-	0.030	-	0.004	-	-
Wood fragments	0.065	0.111	0.050	0.015	-	0.013	0.036	-
Crust	0.377	-	0.875	0.163	0.099	0.026	0.411	0.238
Halimeda fragment	0.013	-	0.025	0.037	0.025	0.017	0.357	0.119
Large foraminifera	-	-	-	-	-	-	-	0.524
<i>Homotrema rubrum</i>	-	-	-	-	-	-	-	0.048
Bone	-	-	-	0.052	0.086	0.105	-	-
Terrestrial gastropod	0.026	-	0.050	0.037	0.049	0.092	-	-

Table 5.1: Mollusc and petrographic data.

Table 5.1 continued...

	AN09-14 34-39 cm	AN09-14 40-454 cm	AN09-15 25-304 cm	AN09-15 36-38 cm	AN09-15 50-55 cm
Species:					
<i>Anomalocardia cunimeris</i>	0.043	0.031	0.312	0.103	0.296
<i>Anomalocardia brasilliana</i>	0.025	0.023	0.146	0.023	-
<i>Batillaria minima</i>	0.009	0.012	0.004	0.008	-
<i>Bulla stiata</i>	-	-	-	0.002	-
<i>Cerithium eburneum</i>	0.005	0.010	-	0.005	0.522
<i>Cerithidea beattyi</i>	0.392	0.355	0.490	0.058	0.021
<i>Cerithium variable</i>	0.526	0.569	0.047	0.801	-
Cerithids	0.932	0.946	0.542	0.872	0.544
Bivalves	0.068	0.054	0.458	0.126	0.296
Bivalves:					
Articulated	-	-	0.021	-	0.030
Whole valve	0.578	0.482	0.788	0.685	0.390
Angular fragment	0.356	0.393	0.144	0.212	0.487
Rounded fragment	0.067	0.089	0.048	0.048	0.037
Bored	-	-	-	-	0.002
Encrusted	-	0.018	-	0.003	0.001
Dissoluted	-	-	-	0.031	0.012
Gastropods:					
Dissoluted	0.065	0.090	0.014	0.046	0.065
Large angular fragment	0.261	0.246	0.122	0.281	0.201
Missing apex	0.537	0.566	0.865	0.301	0.377
Small angular fragment	-	-	-	0.052	0.007
Rounded fragment	-	-	-	-	0.005
Bored	-	-	-	-	0.007
Whole shell	0.131	0.097	-	0.307	0.338
Encrusted	0.006	-	-	0.013	-
Petrography:					
Pebbles	0.182	0.263	0.030	0.006	0.035
Coral fragments	0.273	0.053	-	0.088	0.051
Wood fragments	-	-	0.758	0.263	0.286
Crust	0.091	-	0.152	0.547	0.529
Halimeda fragment	0.455	0.684	0.045	0.073	0.071
Large foraminifera	-	-	-	0.003	-
<i>Homotrema rubrum</i>	-	-	-	0.003	0.008
Bone	-	-	-	-	-
Terrestrial gastropod	-	-	0.015	0.018	0.020

CHAPTER 6

SUMMARY AND CONCLUSIONS

To improve overwash detection, particularly in arid systems where a well developed suite of proxies is lacking, foraminiferal taphonomy was investigated. Studies of this nature are imperative in furthering predictive models, understanding plate movement and estimating tsunami related damage in areas where little to no historical documentation is available. The lack of properly constrained geologic evidence at Sur, Sultanate of Oman and Anegada, British Virgin Islands has hindered the accuracy of prediction models, and subsequently, the assessment of seismic and tsunami hazards.

6.1 ADDRESSING THE CENTRAL RESEARCH QUESTIONS

The central research questions addressed in this dissertation are based on the assessment of foraminiferal taphonomy, not only as an overwash indicator, but also its usefulness in distinguishing between storm and tsunami overwash. Several indicators have previously been used in overwash studies (e.g. lithology, grain size, molluscs, boulders, etc.); however, a well developed set of proxies for detecting overwash in arid systems such as Oman were lacking. In addition, several studies argue the need for a multi-proxy approach to overwash detection (e.g. Morton et al., 2007; Donato et al., 2008; Reinhardt et al., 2011). This dissertation shows that foraminiferal taphonomy can be used as a useful indicator in overwash studies based on the fact that test condition is a reflection of transport history (e.g. exposure, residence time, water energy, etc.) and provides important information regarding sediment provenance. To assess its usefulness, the following three central research questions were considered.

What are the modern spatial distributions and controls on foraminiferal taphonomy in a marine-influenced arid system lagoon?

Chapter 2 illustrates the importance of baseline surface studies in understanding sediment transport dynamics in order to assess overwash deposits and determine where the best sediment records can be sought. This is the first time a comprehensive multi-proxy baseline characterization has been studied extensively in the context of a tsunami. While taphonomic analysis was of limited value in Sur

Lagoon, the enumeration of sediment in-filled fossil specimens proved useful in defining lagoon boundaries: Shallow Marine Basin, Main Lagoon Basin and Distal Lagoon Basin. Findings from a complete surface characterization of the lagoon indicated that overwash events at this location are expected to contain poorly sorted, heterogenous sand with relatively high abundances of *A. inflata*, *Amphistegina* spp., *E. advenum* and planktics, as well as large specimen sizes (>250 µm) and high proportions of fossil specimens. Although of limited value overall, taphonomic results identified the inner areas of the lagoon as the best location to detect overwash deposits in future core studies based on the low representation of fossil specimens.

Can foraminiferal taphonomy be used to document overwash in an arid siliciclastic (Sultanate of Oman) and a semi-tropical carbonate (British Virgin Islands) coastal setting?

Most tsunami overwash studies are conducted in temperate coastal regions where sedimentological and microfossil differences between the contrasting marine and non-marine realms are easily distinguished (e.g. inland lakes, marshes; Clague et al., 1999; Hutchinson et al., 2000; Cisternas et al., 2005). However, overwash studies in arid and tropical settings (e.g. Sultanate of Oman, British Virgin Islands) need to be approached differently due to the lower preservation potential associated with these systems. Coastlines in arid and tropical settings, which lack the contrast between fresh- and salt-water realms, require the use of marginal marine settings (e.g. lagoons, beaches, salt ponds and nearshore zones) where identifying tsunami deposits amongst more frequent background geologic processes is more difficult (Mandic et al., 2004).

Donato et al. (2008, 2009) were among the first to show that tsunami overwash could be detected in arid coastal settings, despite the previous thought that deflation in these settings was too extreme to preserve overwash. Donato et al. (2008) used bivalve taphonomy to ascribe a tsunami origin to the deposit in Sur Lagoon; which proved useful in large-scale trench studies but could not be applied in core studies. Dissertation chapter 3 reports on whether the taphonomic character of foraminifera was similar to that of larger molluscs, and whether taphofacies analysis using these smaller microfossils could be used as a potential overwash indicator for older events. The combined use of foraminiferal provenance and taphonomy was effective in identifying the 1945 Makran trench tsunami at Sur Lagoon and will likely be a good indicator of older events at this location. High abundances of predominantly marine taxa (*Amphistegina* spp., *A. inflata*, and planktics) coupled with high abundances of large test sizes, fragments and fossil specimens were found to be associated with tsunami deposition. At Sur Lagoon, most sedimentologic tsunami criteria (e.g. grading) did not apply to the 1945

tsunami bed. Bivalve taphonomic analysis conducted previously however, provided evidence of a tsunami through the presence of articulated bivalves and angular fragments from offshore provenance. Both PSD and foraminiferal analysis support this tsunami interpretation and hold the added benefit of delineating older deposits where shell quantities are limited (e.g. cores). Although successful in detecting the 1945 tsunami deposit, foraminiferal analysis on its own would only be effective in documenting a marine incursion and should be combined with other proxies when ascribing an event origin.

As a result of the limited success taphofacies analysis had on the 1945 Makran Trench tsunami deposit, a different approach was applied to marine pond cores from Anegada, BVI. Chapter 4 documents the use of *Homotrema rubrum*, a common encrusting foraminifer with a defined provenance in reef settings. *Homotrema* taphonomy was a useful overwash indicator in a Caribbean reef environment by indicating that an overwash deposit within marine pond stratigraphy was emplaced by a southerly trending event. Due to their small size, ability to be transported, high productivity, defined provenance in the reef, attached life mode and quickly inherited taphonomic characteristics after death (e.g. bleaching of color), *Homotrema* are an excellent candidate for high-resolution overwash studies. *Homotrema* taphonomy indicated overwash into Anegada's ponds that occurred from A.D. 1650–1800; however, it alone could not determine whether it formed from a tsunami or hurricane. Chapter 5 describes the taphonomy of molluscs from the same overwash unit and further strengthens a tsunami interpretation since evidence of erosion and winnowing of the former marine pond's substrate into a sheet-like geometry was noted. Although on its own mollusc taphonomy was not a strong overwash indicator at this location, combined with other data (e.g. *Homotrema*, boulders, hydrologic modelling) from other studies it does favour a tsunami interpretation.

Does foraminiferal taphonomic analysis provide insight into the origin of overwash deposits and can it be used to infer hydrodynamic regimes? Does it match up with other proxies?

On its own, taphofacies analysis conducted in Sur Lagoon was not a strong indicator of depositional origin. When combined with taxonomic and sedimentologic data, foraminiferal taphonomy documents a laterally extensive sheet-like deposit with distinctive taphonomic character (e.g. articulated bivalves, large foraminifera and fossil specimens). A tsunamigenic origin for this deposit was strengthened after two severe cyclones (Gonu 2007; Phet 2010) struck the coastline of Oman but left no overwash deposit.

The greatest contribution of foraminiferal taphonomic analysis was observed in cores from Anegada, BVI. The marked decrease in *Homotrema* concentration from north to south along two transects indicates an unusually large event from the north. Since storm overwash is associated with lobate sand lenses and potentially a higher degree of homogenization, it is unlikely that the Shell and Sand Sheet at Anegada is a result of a hurricane. Evidence from mollusc taphonomy (see Chapter 5), transported boulders (Buckley et al., 2011) and hydrological modelling (Wei et al., 2010) also support a tsunami interpretation although this interpretation is limited by the lack of comparative data from known hurricane and tsunami deposits in the Caribbean.

Homotrema taphonomic analysis shows great promise in distinguishing between tsunami and storm deposition in carbonate settings. Several studies have documented overwash deposits in other Caribbean locations, but did not consider a tsunami origin due to the frequency of storms in the geologic record (e.g. Donnelly et al. 2005). In this regard, records of hurricane frequency are potentially skewed, which poses a problem for future risk assessment. Future work needs to focus on the impact of Hurricane Earl which struck Anegada in 2010. Communication with several residents suggests that although flooding occurred, no deposit was left. Through the characterization of modern hurricane deposits, depositional origin interpretations of older deposits may be strengthened.

REFERENCES

- Buckley, M., Wei, Y., Jaffe, J., Watt, S., 2011. Inverse modeling of velocities and inferred cause of overwash that emplaced inland fields of boulders at Anegada, British Virgin Islands. *Natural Hazards*, doi 10.1007/s11069-011-9725-8
- Cisternas, M., Atwater, B. F., Torrejon, F., Sawai, Y., Machuca, G., Lagos, M., Eipert, A., Youlton, C., Salgado, I., Kamataki, T., Shishikura, M., Rajendran, C. P., Malik, J. K., Rizal, Y., and Husni, M., 2005. Predecessors of the giant 1960 Chile earthquake. *Nature* 437, 404-407.
- Clague, J. I., Hutchinson, I., Mathewes, R. W., Patterson, R. T., 1999. Evidence for late Holocene tsunamis at Catala Lake, British Columbia. *Journal of Coastal Research* 15, 45-60.
- Donato, S.V., Reinhardt, E.G., Boyce, J.I., Pilarczyk, J.E., Jupp, B.P., 2009. Particle-size distribution of inferred tsunami deposits in Sur Lagoon, Sultanate of Oman. *Marine Geology*, 257: 54-64
- Donato, S.V., Reinhardt, E.G., Boyce, J.I., Rothaus, R., Vosmer, T., 2008. Identifying tsunami deposits using bivalve shell taphonomy. *Geology*, 36:

199-202

- Donnelly, J.P., 2005. Evidence of past intense tropical cyclones from backbarrier salt pond sediments: A case study from Isla de Culebrita, Puerto Rico, USA. *Journal of Coastal Research*, 142: 201–210
- Hutchinson, I., Guibault, J. P., Clague, J. J., Bobrowsky, 2000. Tsunamis and tectonic deformation at the northern Cascadia margin: a 3000-year record from Deserted Lake, Vancouver Island, British Columbia, Canada. *The Holocene* 10, 429-439.
- Mandic, O., Harzhauser, M., Roetzel, R., 2004. Taphonomy and sequence stratigraphy of spectacular shell accumulations from the type stratum of the Central Paratethys stage Eggenburgian (Lower Miocene, NE Austria). *Cour. Forsch.-Inst. Senckenberg* 246, 69-88.
- Morton, R.A., Gelfenbaum, G., Jaffe, B.E., 2007. Physical criteria for distinguishing sandy tsunami and storm deposits using modern examples. *Sedimentary Geology*, 200: 184-207
- Reinhardt, E.G., Pilarczyk, J.E., Brown, A., 2011. Probable tsunami origin for a shell and sand sheet from marine ponds on Anegada, British Virgin Islands. *Natural Hazards*, doi 10.1007/s11069-011-9730-y
- Wei, Y., ten Brink, U.S., Atwater, B.F., 2010. Modeling of tsunamis and hurricanes as causes of the catastrophic overwash of Anegada, British Virgin Islands, between 1650 and 1800: Abstract OS42B-03. Presented at 2010 Fall meeting, American Geophysical Union, San Francisco, California, 13–17 December 2010